

## N O T I C E

THIS DOCUMENT HAS BEEN REPRODUCED FROM  
MICROFICHE. ALTHOUGH IT IS RECOGNIZED THAT  
CERTAIN PORTIONS ARE ILLEGIBLE, IT IS BEING RELEASED  
IN THE INTEREST OF MAKING AVAILABLE AS MUCH  
INFORMATION AS POSSIBLE

9950-355

(NASA-CR-163038) PRELIMINARY DESIGN DATA  
PACKAGE, APPENDIX C (South Coast Technology,  
Inc.) 239 p HC A11/MF A01 CSCL 13F

N80-27226

G3/85 27873  
Unclas



**SOUTH COAST  
TECHNOLOGY, INC.**  
Santa Barbara, California

A P P E N D I X   C

PRELIMINARY DESIGN DATA PACKAGE

PREPARED FOR:

JET PROPULSION LABORATORIES

CONTRACT NUMBER 955189

PREPARED BY:

SOUTH COAST TECHNOLOGY, INC.

P. O. BOX 3265

SANTA BARBARA, CALIFORNIA 93105

JULY 25, 1979

# HYBRID BY SCT

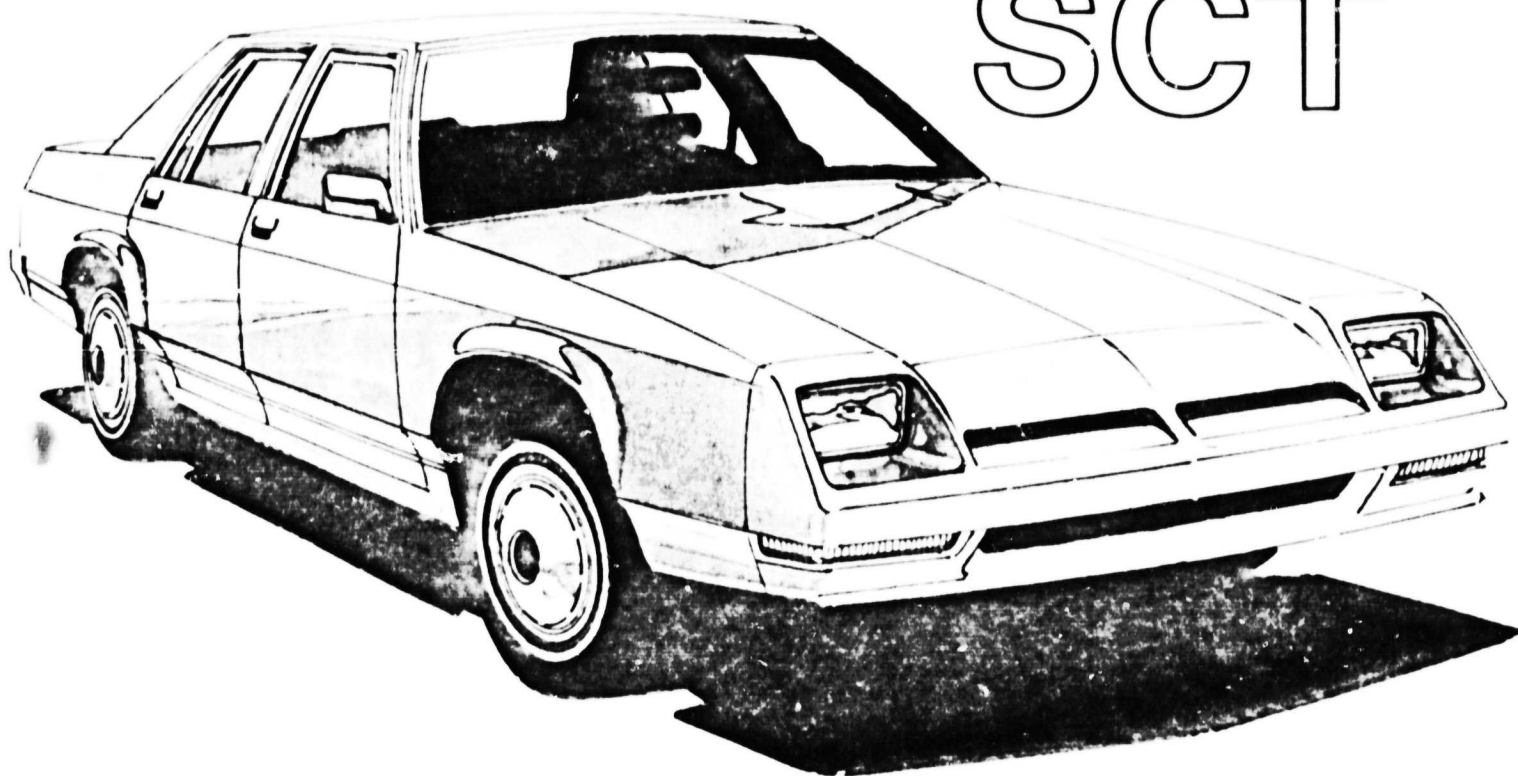




## TABLE OF CONTENTS

	<u>Page</u>
1. INTRODUCTION . . . . .	1
2. DESIGN METHODOLOGY AND ASSUMPTIONS . . . . .	2
2.1 Design Philosophy . . . . .	2
2.2 Propulsion System . . . . .	5
2.3 Chassis Systems . . . . .	16
2.4 Body/Structure . . . . .	19
3. DEVELOPMENT REQUIREMENTS . . . . .	28
3.1 Major Areas of Technology Development . . . . .	28
3.2 Controls . . . . .	29
3.3 Heat Engine . . . . .	32
3.4 Batteries . . . . .	38
4. DESCRIPTION OF NTHV PRELIMINARY DESIGN . . . . .	41
4.1 Propulsion System . . . . .	53
4.1.1 System Description . . . . .	53
4.1.2 System Controller . . . . .	57
4.1.3 Heat Engine and Controls . . . . .	145
4.1.4 Motor and Motor Controls . . . . .	159
4.1.5 Batteries and Battery Charger . . . . .	174
4.1.6 Transmission and Rear Axle . . . . .	187
4.1.7 Accessory Power . . . . .	192
4.2 Chassis Systems . . . . .	195
4.3 Body . . . . .	199
4.4 Vehicle System Characteristics . . . . .	206

## TABLE OF CONTENTS

	<u>Page</u>
4.5 Drawing Package . . . . .	231
5. LIST OF REFERENCES . . . . .	234

### APPENDICES

#### C1. Computer Program Documentation

C1.1 HYBRID2 . . . . .	C- 1
C1.2 VSYS & VSYS2 . . . . .	C- 67
C1.3 CRASH . . . . .	C- 108
C1.4 Handling Programs . . . . .	C- 132
C1.5 Life Cycle Costs . . . . .	C- 175
C2. Drawing Package - In Separate Envelope	
C3. Energy and Materials . . . . .	C- 182

## **1. INTRODUCTION**

This report presents the results of Task 3 - Preliminary Design of the Near Term Hybrid Vehicle Development Program, Phase I. Included are the data and documentation required to define the preliminary design of the South Coast Technology (SCT) Near Term Hybrid Vehicle and quantify its operational characteristics, together with the assumptions and rationale behind the design decisions.

In addition to the paper studies as specified, a first phase design mockup was built to identify and solve any packaging problems. Copies of the photos made from the mockup are included in this report, and the mockup vehicle is available for review at our Santa Barbara facilities.

The work on this task was performed by South Coast Technology, Inc., with assistance from our key subcontractors and consultants, who include:

C. E. Burke Engineering Services - Propulsion system design  
and cost studies

EHV Systems, Inc. - Motor control, charger, and central  
control microprocessor

The Brubaker Group - Body design

Sheller-Globe - Body materials/weight reduction

ESB, Inc. - Lead-acid batteries

Eagle Picher - Nickel-iron batteries

B. T. Andren - Automotive engineering

## 2. DESIGN METHODOLOGY AND ASSUMPTIONS

In this section, the analytical tools and design methods used in the preliminary design of the Near Term Hybrid Vehicle (NTHV) are described. Before proceeding to a discussion of the methodology for specific systems, however, discussion of the overall design philosophy and how it relates to the two worlds of government sponsored research and development, and auto industry product planning, would be useful.

### 2.1 Design Philosophy

The design approach taken by SCT for the NTHV is based on the vehicle requirements defined in Task 1 of this program and on the design tradeoff studies conducted in Task 2. In addition, the approach was heavily influenced by considerations of technology development and transfer in the time frame relevant to this near term program. The subject of the hybrid system development requirements will be discussed in greater detail in Section 3; it suffices at this point to outline the thinking which underlies the relationship between SCT's design approach and the task of developing a hybrid vehicle which maximizes the return on the investment in the NTHV program.

It is as follows:

- a) There is a basic program requirement that the technology and development requirements of the NTHV must be such that it would be capable of being mass produced in the mid-1980's.
- b) Large scale production of hybrid vehicles (or electric vehicles, for that matter) will only happen if one of the major auto manufacturers undertakes it; it will not happen within, or as a result of growth within, the EV industry.

- c) Because of these two factors, the technology developed for the NTHV must be transferable to the auto industry in the same mid-1980's time frame. Such technology transfer is most likely to occur if the hybrid vehicle presents a viable alternative for bringing the fuel consumption of full-sized six passenger automobiles into line with the federally mandated corporate average fuel economy (CAFE).
- d) Relative to a conventional automobile which utilizes comparable technology in vehicle design (transmissions, tires, aerodynamics, structures, etc.), the largest single reduction in fuel consumption comes from the conversion to a hybrid system and the implementation of a control strategy in which the heat engine runs only under selected conditions (high power demand, high speed cruise, or a low battery state of charge). Once the basic conversion to a hybrid system is made, additional refinements at the component or subsystem level result in relatively small additional reductions in fuel consumption.
- e) The biggest development task associated with the NTHV will be the implementation of the type of control strategy just described, in such a way that the transitions from engine-off to engine-on and back again are handled smoothly, with no more discomfort to the occupants than the shifting of an automatic transmission, and in such a way that emissions requirements are met.

- f) Since the biggest payoff in terms of reduced fuel consumption, as well as the biggest development task, is associated with the implementation of an optimum control strategy, that is the place to put the emphasis in a near term program. The less this task is diluted by efforts to make unrelated component or subsystem refinements, the better the chances of success in terms of demonstrating a vehicle with greatly reduced fuel consumption and acceptable driveability and performance.
- g) This, together with the requirement for near term transferability of technology to the auto industry, led us to the conclusion that component designs should be as close to state-of-the-art as possible in order to provide adequate time for system level development. Component level development should be, in general, limited to those areas which are critical to implementation of the control strategy.

Based on these considerations, SCT developed a design philosophy characterized by the following:

- a) The hybrid system is viewed as a means for enabling a major manufacturer to meet CAFE requirements in the year 1985 and beyond, while maintaining a product mix which still possesses a substantial fraction of roomy six-passenger automobiles.
- b) Consequently, the vehicle in which the hybrid propulsion system is to be incorporated is viewed as an evolutionary development of an existing six-passenger vehicle, incorporating those improvements in transmission design, tires, aerodynamics, and materials which can be projected to occur



between now and 1985. It is not a radically different vehicle designed uniquely for hybrid propulsion.

- c) Designs requiring extensive development at the component level are avoided. In general, we have tried to utilize production, or pre-production hardware, incorporating the best current technology. Developmental hardware is utilized only in the event that it would result in a large advantage in system performance, and the development status is such that production by the mid-80's is a good possibility.

## 2.2 Propulsion System

In this area, we include the heat engine, motor and motor controls, system controller and interface electronics, battery charger, battery, transmission (including heat engine startup clutch), and differential.

### 2.2.1 Analytical Methods

The principal tool used in the analytical design of the propulsion system is an improved version of the computer simulation program HYBRID2. The principal elements of the vehicle simulation are shown in Figure 2-1. This program, and its simpler predecessor HYBRID, are described in Section 2.1 of the Task 2 report.<sup>(1)</sup> The changes which have been made in HYBRID2 since the writing of that report include the following:

- a) Improved battery modelling.
- b) Greater flexibility in programming transmission shift points.

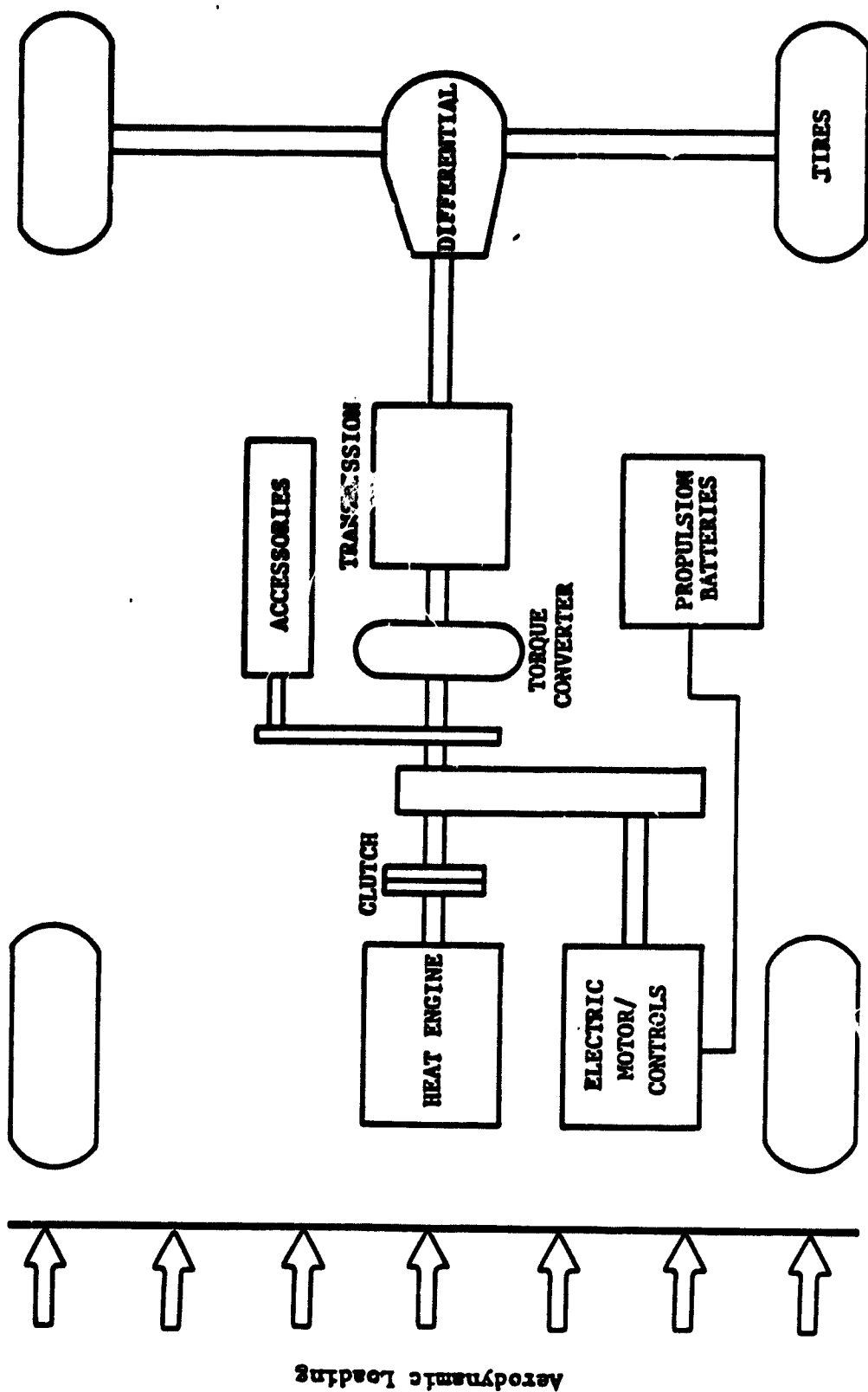


Figure 2-1 Hybrid Vehicle Simulation

c) Incorporation of a warmup period.

A discussion of each of these areas follows.

### Battery Modelling

The version of HYBRID2 which was used for Task 2 computes an average battery specific power over each of the composite driving cycles for Mode 1 operation and determines the corresponding available specific energy from a plot of specific energy vs. specific power (Ragone plot). This provides an estimate of available specific energy which is somewhat optimistic. An alternative model which also uses a Ragone plot is the fractional utilization model. With this technique, it is assumed that, if the battery spends an increment of time  $\Delta t$  at a specific power  $\bar{P}$ , the fraction of the battery capacity which is used up in that time increment is given by

$$\Delta x = \frac{\bar{P} \Delta t}{\bar{E}(\bar{P})} ,$$

where  $\bar{E}$  is the available specific energy at the specific power  $\bar{P}$ .

Passing to the limit and integrating gives the following expression for the fractional depletion  $x$  of the battery at time  $t$ :

$$x(t) = \int_0^t \frac{\bar{P}(T) dT}{\bar{E}(\bar{P}(T))} \quad (1)$$

This approach has a problem opposite to that of the approach used in HYBRID2 in that it tends to overestimate the rate at which the battery is depleted.

The battery model incorporated in the latest version of HYBRID2 is simply a more general form of both of the above two. Instead of using the instantaneous value of specific power in expression (1),

it uses a value which is the average of the specific power over a time interval of width  $2 \Delta t_f$ . Thus, as  $\Delta t_f$  approaches 0, this model approaches the fractional utilization model; and as  $\Delta t_f$  approaches one half of the period of the driving cycle, it approaches the first model used in HYBRID2. The Ragone plot is applicable only for positive values of  $\bar{P}$ ; the method is extended to include regeneration by the expression  $\bar{E}(\bar{P}) = \bar{E}_{c3} \mu_{RG}$ , where  $\bar{E}_{c3}$  is the rated 3-hr specific capacity of the battery in WH/KG, and  $\mu_{RG}$  is a regenerative charge efficiency.

To obtain an estimate of the appropriate value for the averaging half-interval  $\Delta t_f$ , test results on the Electric by SCT were used. The variation in range over the J227a(C) cycle as predicted by the new battery model, as a function of  $\Delta t_f$ , is shown in Figure 2-2. The predicted range equals the actual test range at a value of  $\Delta t_f$  of about eight seconds, and this is the value being used with HYBRID2. In using this particular value of  $\Delta t_f$ , we are making the following assumptions:

- a) The characteristics of the EV-106 batteries used in the test were well represented by the Ragone plot obtained from data supplied by ESB for the EV-106. (In other words, the batteries used in the test were the same ones used in the simulation.)
- b) The appropriate time interval for use with this battery model is independent of the discharge profile, battery type (lead-acid, nickel-iron, etc.), battery age, and so forth.

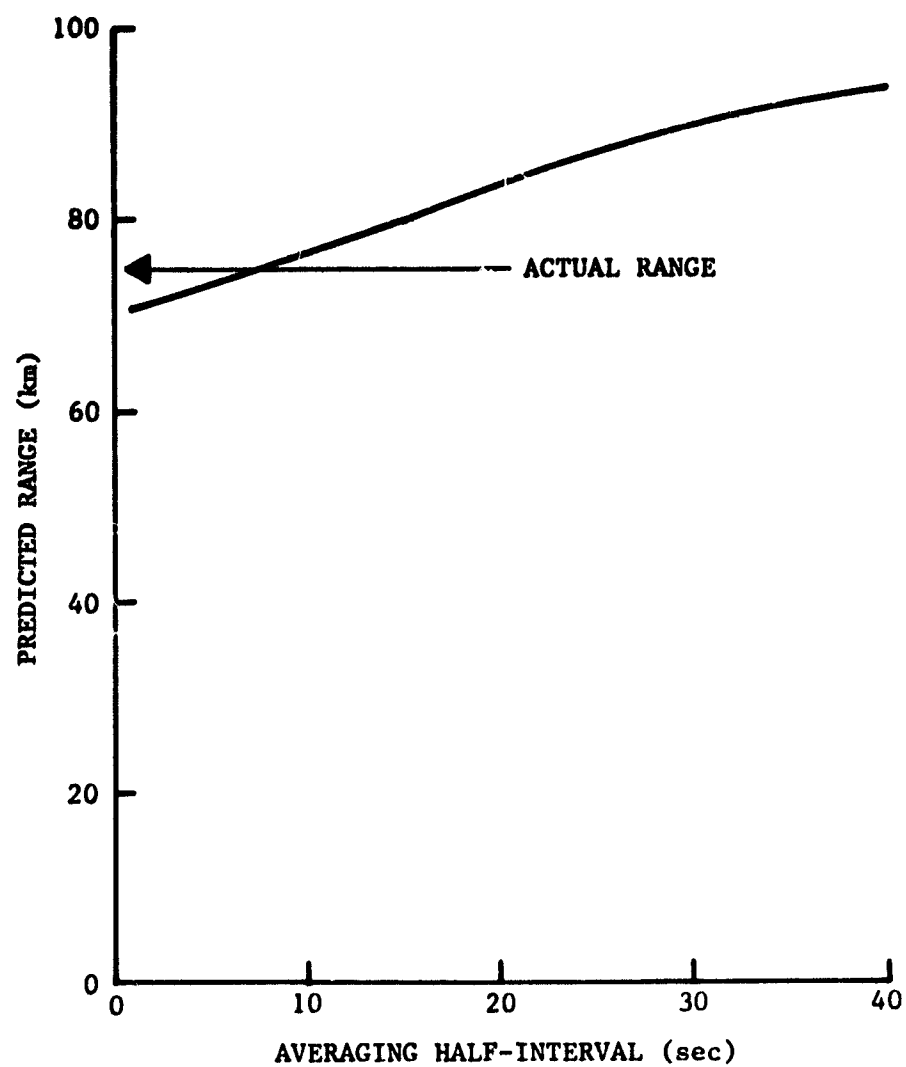


Figure 2-2 Variation of Predicted Range with Averaging Period

The first of these assumptions is probably a pretty good one, since the same battery pack used in the road test came within 3% of the nominal EV-106 capacity in a separate constant current (75A) discharge test. The validity of the second assumption is open to question; however, until somebody has a chance to correlate a great deal of test data on various vehicles under various driving cycles, with the constant current discharge characteristics of the same batteries used in the vehicle tests, we shall continue to make it.

#### Transmission Shift Logic

The shift logic used in the older version of HYBRID2 defined the speeds at which shifts were made as functions of the driver's input to the accelerator pedal. In other words, the transmission was just a conventional automatic with accelerator pedal (rather than vacuum) modulation of the shift points. The newer version of HYBRID2 has a more flexible shift strategy in which an upshift (engine) speed and a downshift speed are defined as functions of engine power. This shift strategy is used as long as the heat engine is operating; when the heat engine is off, the strategy switches to one which is suitable for the electric motor. Shifting when only the electric motor is operating is somewhat simpler because the efficiency of the motor is quite constant over a wide speed and load range. The shift points are defined only on the basis of motor speed.

#### Heat Engine Warmup Period

In actual operation, the heat engine would probably be permitted to run after a cold start long enough to reach an acceptable



operating temperature. To simulate such a condition, HYBRID2 assumes that the system operates on Mode 2 immediately after start-up (since on Mode 2, the engine operates steadily except during deceleration and idling), and then reverts to Mode 1 after warmup. A certain distance each day is assumed to be spent in such warmup driving. This distance is highly dependent on the number of trips made during the day, the ambient temperature, and the amount the engine has cooled down since it was last run. Moreover, the operating temperature at which the reversion to Mode 1 occurs is an unknown until tests are run; this may depend more on the catalytic converter characteristics than the engine characteristics. Because of the large number of unknowns here, we have looked at the question of the impact of such warmup periods on fuel economy parametrically; in other words, we have estimated the reduction in fuel economy as a function of the total amount of warmup driving during the day, rather than trying to estimate the amount of warmup driving required.

#### Engine Start Transients

HYBRID2 assumes that the engine and motor respond instantaneously to the command signals. The transients involved in the engine startup problem were investigated separately with two programs, VSYS and VSYS2. VSYS simulates the engine start transient when the torque converter is active, and VSYS2 simulates it when the torque converter is locked up. Consequently, VSYS uses a 3 mass model, with the masses corresponding to the engine inertia, motor and torque converter pump inertia, and the inertia of the remainder of the drive train and vehicle. VSYS2 uses a 2 mass model, with the engine being one mass and

the combined inertia of the motor drive train and vehicle constituting the other. A detailed description of these programs are found in Appendix A.

#### 2.2.2 Design Methods

##### Control Strategy Optimization

The basic methodology used to optimize the control strategy followed this pattern:

- (1) Optimize shift strategy to keep heat engine operating as close as possible to its minimum bsfc area whenever it is operating.
- (2) Starting with the strategy developed in Task 2 adjust each control parameter until a minimum in fuel consumption is attained (either in the interior, or at either end, of the practical range of values for the control parameter)
- (3) Inspect the simulation results on a detailed level (looking at peak values of battery output power, heat engine bsfc, etc.) to determine whether any basic changes or additions to the structure of the control strategy might offer improvements.
- (4) Evaluate the effect of such structural changes through simulation.
- (5) If improvements do result, optimize any new parameters introduced and re-optimize any old ones whose optimum values may have been shifted by the structural change. (Obviously, if a structural change effects only the mode 2 strategy, it would be pointless to re-optimize another parameter which only affects mode 1.)

Throughout the control strategy development, the structure of the strategy was kept at a level of complexity which would be consistent with the capacity and speed of available microprocessors, and the effects of the strategy were visualized in terms of the operation of the actual propulsion system hardware. The general route was to start with the simplest possible strategy and introduce changes in the direction of increased complexity only if there was a clear benefit in terms of fuel economy or some aspect of system operation.

### System Controller

Implementation of the control strategy is most economically accomplished via a general purpose microprocessor-based system. Microprocessors and their peripheral circuits have seen a steady erosion in price while their computing power has been continually increasing. Since a microprocessor system design can take on an almost endless variety of forms, it is first necessary to set down some guidelines governing the design evolution. The design of a control system for a hybrid vehicle primarily intended for test purposes will by its very nature be governed by a different set of rules than if a large production run was the intent.

The most important parameters in the choice of hardware design should be flexibility and expansion capability. Price should be of secondary importance at this stage of the hybrid vehicle development. The system should be flexible enough to allow easy modifications of the control programs. This generally implies that the processing system should be operating at a fraction of its computing capacity so as not to run into timing problems if additional software is required in critical timing loops. The system should also allow for program and data expansion as that becomes necessary. Additions and modifications should be easily accomplished so that the bulk of engineering time is spent in the optimization of the vehicle's characteristics rather than devising ways to get around the processing systems hardware limitations.

Software design should follow a modularized approach. A

software routine which implements a particular function should be capable of standing on its own with little interaction with other portions of the program. This will allow for easy modifications to sections of code with minimum impact on the rest of the program. Although this approach will tend to produce a longer overall program than if the various sections were highly interrelated, it will allow for much easier testing and optimization of the various vehicle subsystems. As with the hardware system design, the software should be designed with flexibility and expansion in mind.

One of the most important tasks in a microprocessor system design is the hardware/software tradeoff. This is basically a set of decisions as to how to implement the various required functions: which ones are to be done totally in software (low implementation costs) and which are to be done with external hardware or a combination of both. An effective hardware/software tradeoff requires an intimate knowledge of both hardware and software as well as a good understanding of the design goals. Very low cost high volume systems generally tend towards an all software solution unless that is beyond the physical capability of the processing system. Calculator products are a good example. An all software solution, however, often develops a very fine tuned, tightly coupled software/hardware combination not very easily modified without destroying the total systems operating balance. A more modification tolerant (flexible) system is achieved by implementing time-critical functions with external hardware. The design of the hybrid vehicle's control system should make

judicious tradeoffs in this area so as to achieve the utmost in flexibility. Time-critical functions should be very carefully considered for hardware implementation even if software implementation is feasible so as not to impact the overall systems flexibility.

Last but certainly one of the more important requirements of the control system is the ability to easily modify the vehicle's operating parameters and to be able to collect significant data during a test sequence. Operating parameters such as transmission shift points, points at which mode switchover occurs, etc., should be capable of being modified via a calculator type device simply by punching in a few numbers. This will allow the vehicle to be quickly optimized for the correct "feel" as well as to allow experimentation as to the impact a change in one parameter has on another. Data collection is an absolute must if correct use is to be made of the test results. As a minimum, all pertinent internal control system parameters should be output to an external connector. Parameters such as motor RPM, armature current, battery voltage, state of charge etc. should be output each time the control system goes through its cycle. The data output should conform to standard interface specifications so that practically any digital recording device can be used. The recorded data can eventually be played back into a computer for analysis and reduction.

### 2.3 Chassis Systems

Under this heading, we include steering, suspension, brakes, wheels, and tires.



### 2.3.1 Analytic Methods

The design of chassis systems is heavily dependent on the vehicle mass and its distribution. Because of the substantial effect on the mass properties of the incorporation of a battery pack, some means of estimating the effect of such changes in mass properties on vehicle handling characteristics was deemed necessary. Two computer programs were developed by SCT to assist in making such estimates. The programs are called HYSSG and HYSIM; documentation for both is provided in Appendix C1 of this report.

HYSSG computes the steady-state gain of yaw rate to steer angle, and produces a plot of this gain as a function of forward speed. It also plots the Ackermann(neutral steer) line for the vehicle; comparison of these two plots provides an indication of the understeer/oversteer behavior of the car.

HYSIM, on the other hand, simulates the time response of the vehicle to a step input in steer angle at a given forward speed. This permits an assessment to be made of the differences in transient response and obstacle avoidance performance between the reference and hybrid vehicles.

Both HYSSG and HYSIM are based on a very simple mathematical model of the vehicle, which represents it as a single mass with the following degrees of freedom:

- . Lateral displacement
- . Yaw
- . Roll

Gyroscopic effects of the rotating mass of the wheels and tires are taken into account. Pitch is normally small compared to roll in any constant speed maneuvers, so it is neglected.

The model is linear, and does not take into account the following:

- . Change in roll axis with roll angle
- . Tire camber thrust forces and aligning torques
- . Tire compliance (vertical and lateral)
- . Roll steer effects
- . Steering compliance

The model is therefore useful primarily in evaluating the effects of mass distribution and tire cornering coefficients on handling, within the linear range. It is best used by comparing the program results with the results it gives for a baseline of known characteristics; in other words, its usefulness as a predictive model is confined to situations in which there is a baseline configuration available which does not differ too much from the configurations under study, and where the handling characteristics are known. Consequently, in evaluating the hybrid's handling characteristics, the first step was to exercise the model for the Ford LTD. The transient response and oversteer/understeer characteristics obtained for the hybrid were then evaluated relative to this baseline.

Input data to the program consists of the vehicle mass and geometrical properties, location of the roll axis, front and rear roll stiffness and damping, and front and rear tire lateral force

cornering coefficients. Output consists of yaw rate gain as a function of forward speed for HYSSG, and yaw rate, lateral acceleration, and vehicle roll angle as functions of time for HYSIM. More detailed discussion will be found in Appendix A.

### 2.3.2 Design Methods

The chassis design requirements for the Near Term Hybrid Vehicle are limited to packaging changes, the verification of structural attachment points of the propulsion system, and the tuning of front and rear suspension and tires.

The analytical approach described in Section 2.3.1 will be used as the primary basis for system design work. At best, such analysis can narrow the range of final vehicle specifications. The task is primarily going to be an iterative design, test and development effort. Adjustable shock absorbers will be used, variations in spring rates will be obtained and in vehicle testing will be done to subjectively and analytically evaluate the vehicle with revised suspension and tires.

Development testing, using chassis design personnel, will be conducted on an objective basis by comparing ride and handling against the reference Ford LTD vehicle.

The process described is that used by all of the major automotive manufacturers when they carry out chassis changes such as those involved on the NTHV.

### 2.4 Body/Structure

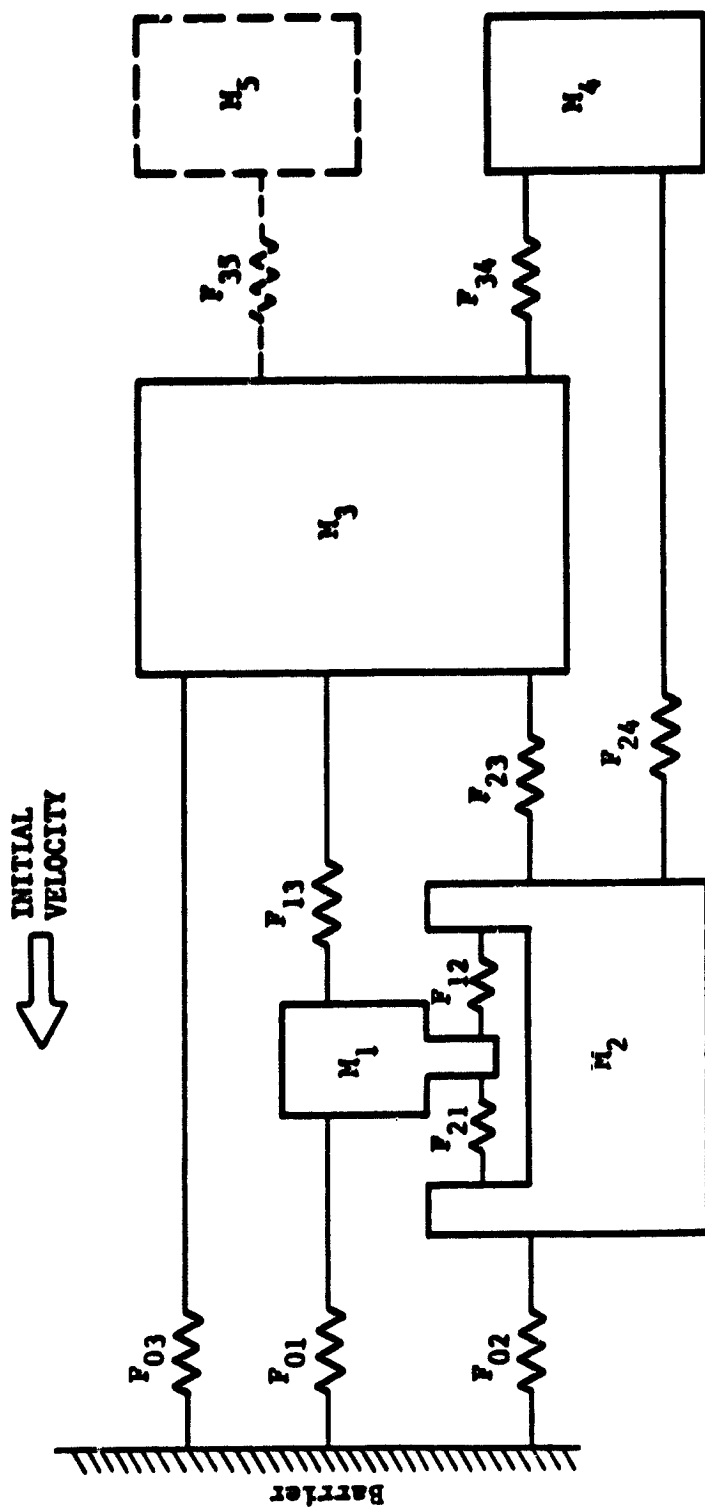
This category includes the frame and body, including battery support structure, bumpers and EA units, interior seats and trim

and sound insulation.

#### 2.4.1 Analytical Methods

The location of the batteries, which constitute the major increment in static load for the hybrid vehicle over the LTD-based reference vehicle, is adjacent to the rear axle. With this location, the additional bending movements in the vehicle frame and body should be small. Since the SCT hybrid uses the same frame and basic body structure as the LTD, a full scale structural analysis of the frame and body under operational loads was not considered necessary at this stage of the design. However, the effect of the additional battery weight on crash loading could be significant; consequently, an analysis was carried out to estimate the probable change in crash performance and determine whether additional energy absorption capacity might be required. The primary tool used in this analysis was the CRASH computer simulation, which is documented in Appendix A of this report.

This program simulates the vehicle as a collection of masses interconnected by crushable elements (generalized springs). The representation used for the reference and hybrid vehicles is shown in Figure 2-3. Each of the crushable elements in Figure 2-3 is represented by a non-linear force vs. deformation characteristics, together with an unloading slope. That is, as long as the deformation velocity for a crushable element is positive, the crush force follows the force deflection characteristic; however, if the deformation velocity goes negative, the force drops off along a straight line passing through the point on the force



CRUSH ELEMENTS:		MASSES:	
F <sub>01</sub>	Front Frame	M <sub>1</sub>	Front Cross-Member/ Suspension/Wheels
F <sub>02</sub>	Radiator/Grille	M <sub>2</sub>	Engine/Motor/Transmission
F <sub>03</sub>	Hood/Fenders/Wheels	M <sub>3</sub>	Body
F <sub>12,21</sub>	Motor/Engine Mounts	M <sub>4</sub>	Rear Axle/Wheels
F <sub>13</sub>	Rear Frame/Torque Box	M <sub>5</sub>	Battery pack (Hybrid Only)
F <sub>23</sub>	Transmission Mount/Firewall		
F <sub>24</sub>	Drive Shaft		
F <sub>34</sub>	Rear Suspension/Wheels		
F <sub>35</sub>	Battery Pack Support (Hybrid Only)		

Figure 2-3 Hybrid/Reference Vehicle Crash Model

deflection characteristic at which the deformation velocity reversed sign.

The force-deflection characteristics of the crushable elements are estimated based on the physical dimensions of the element and its material. This estimation requires, of course, considerable knowledge of the behavior of materials and structural elements in the plastic range. However, even with such experience, unless actual test data is available on the crush characteristics of the individual elements, it is unlikely that the simulation will give very accurate results. Consequently, in the absence of such data, the best approach is to make the best estimate of the crush characteristics on the basis of geometry and materials, and then adjust these estimates (within the bounds dictated by prior experience with the types of crush elements used) to obtain a total vehicle crush which is reasonable for this class of vehicle (about 20 in., or .5 m.). The increment in crush when the battery pack is added may then be estimated from the results of the computer simulation with and without the battery pack.

#### 2.4.2 Design Methods

The basic body design requirements for the Hybrid vehicle are essentially determined by the packaging of the propulsion system components, the location of the batteries and a determination as to which components should change in design or material in order to reduce aerodynamic drag and vehicle weight.

#### Vehicle Packaging

The propulsion system and battery compartment layouts were



accomplished in the procedure used by auto manufacturers. First, a full scale layout was made of the key propulsion system components that were to be installed in the base Ford LTD. Layout drawings of the LTD were obtained from Ford Motor Co. and preliminary component packaging was determined. Following this, a mockup of the actual components in a Ford LTD was done to verify in three dimensions what was shown on the layouts.

Through an iterative process a solution to the packaging was worked out and a preliminary mockup completed. Photos of the mockups are shown in Figures 2-4 through 2-6 . The in-vehicle installation is also reflected on the drawing package which is also part of Appendix B.

A three dimensional mockup is essential in the complex packaging of a hybrid propulsion system as it avoids later discovery of design problems and interferences. This mockup will be upgraded and kept up to date throughout the Phase II design and development effort to provide a continuing control over the detailed aspects of vehicle packaging. In addition to the design tool aspects the mockup will also be used to evaluate serviceability and maintainability aspects of the design as it is in process, thus avoiding difficulties that would be found at a time when costly changes would be necessary.

#### Aerodynamic Drag

Preliminary design studies were completed to select a representative approach to the front end design that would reduce aerodynamic drag. An artist's rendering of design alternatives are included as Figures 4-3 through 4-5.

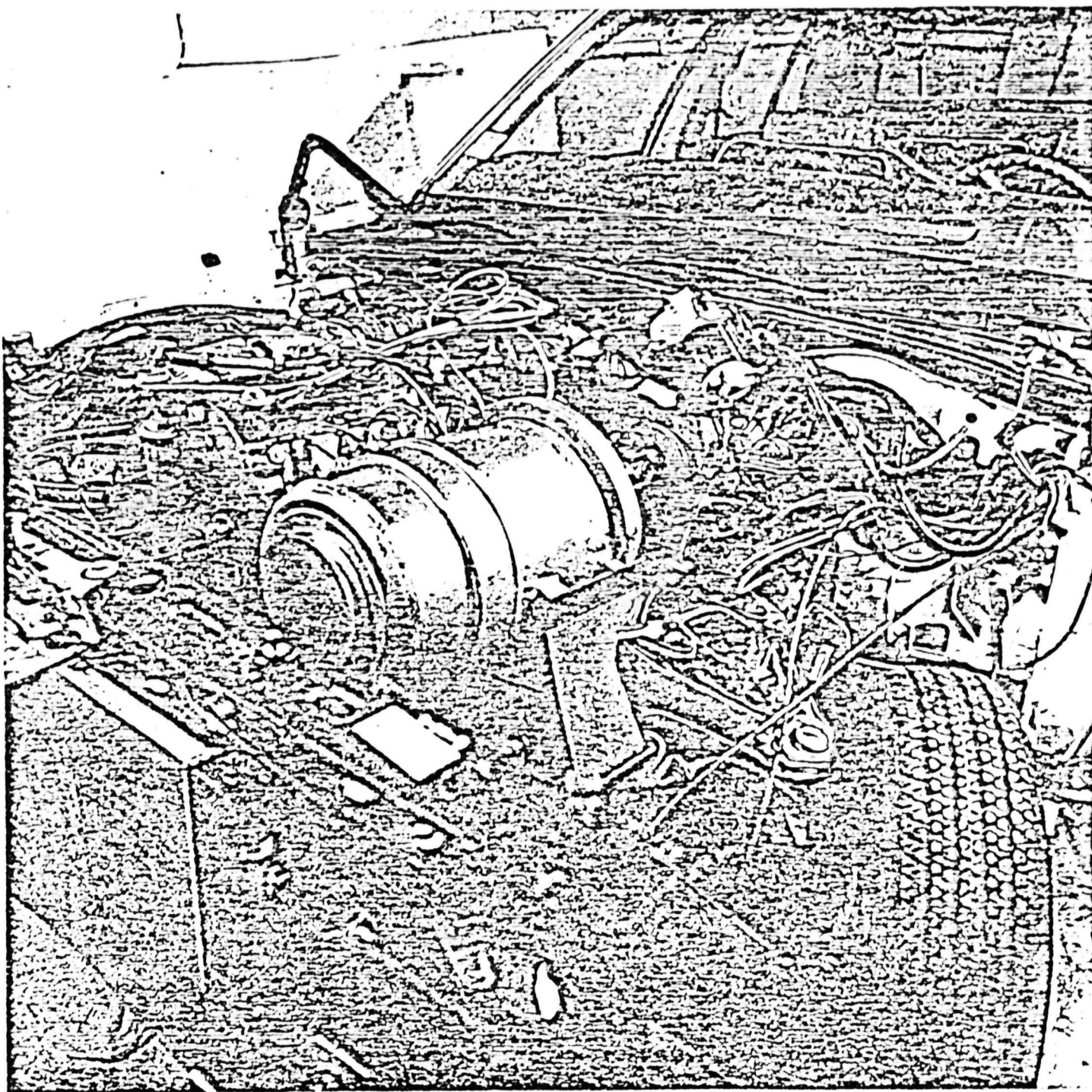


Figure 2-4 Gasoline-Electric Hybrid propulsion system mock up installation in an engine compartment of a six-passenger automobile.

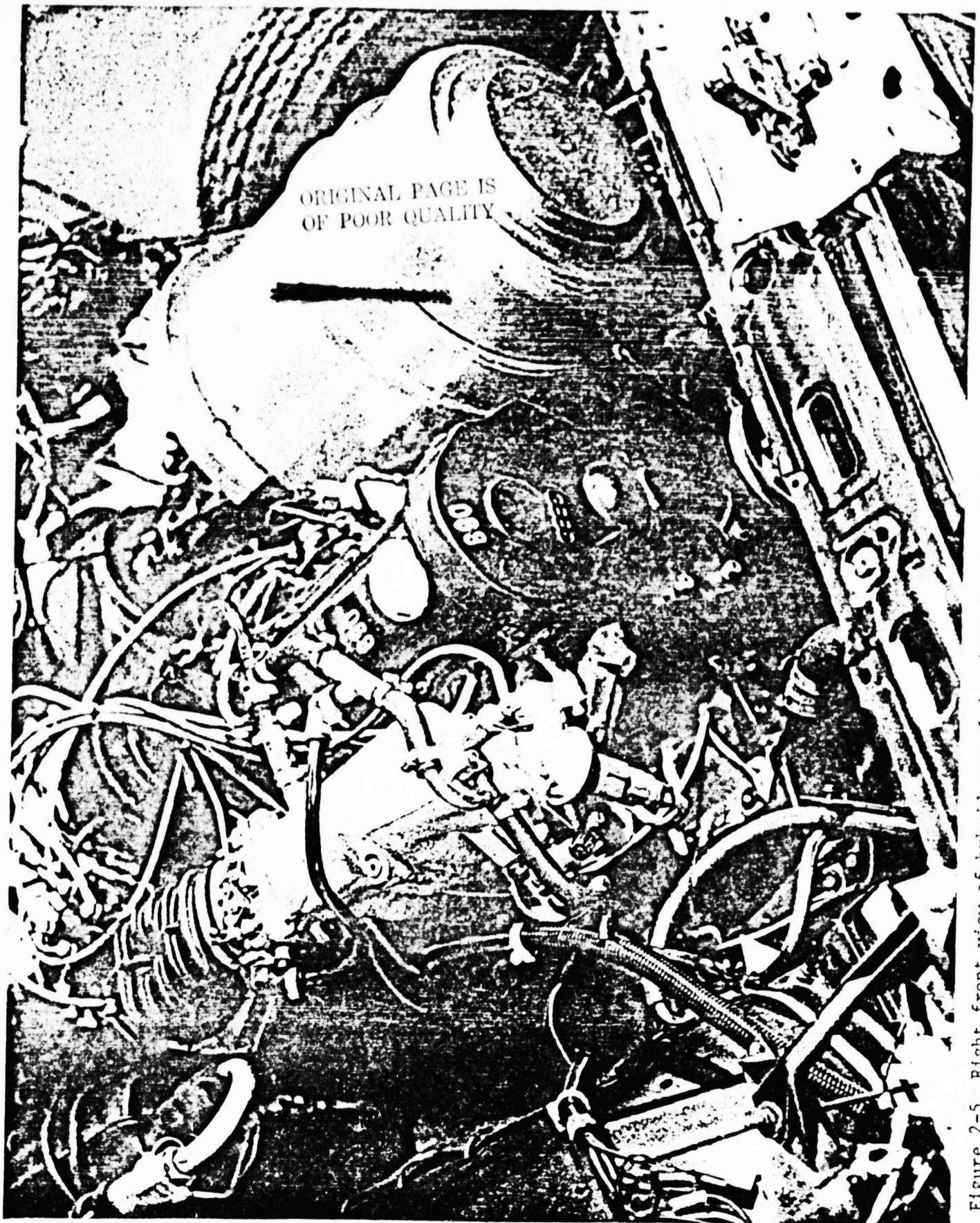


Figure 2-5 Right front view of hybrid propulsion installation showing VE engine and Siemens electric motor.



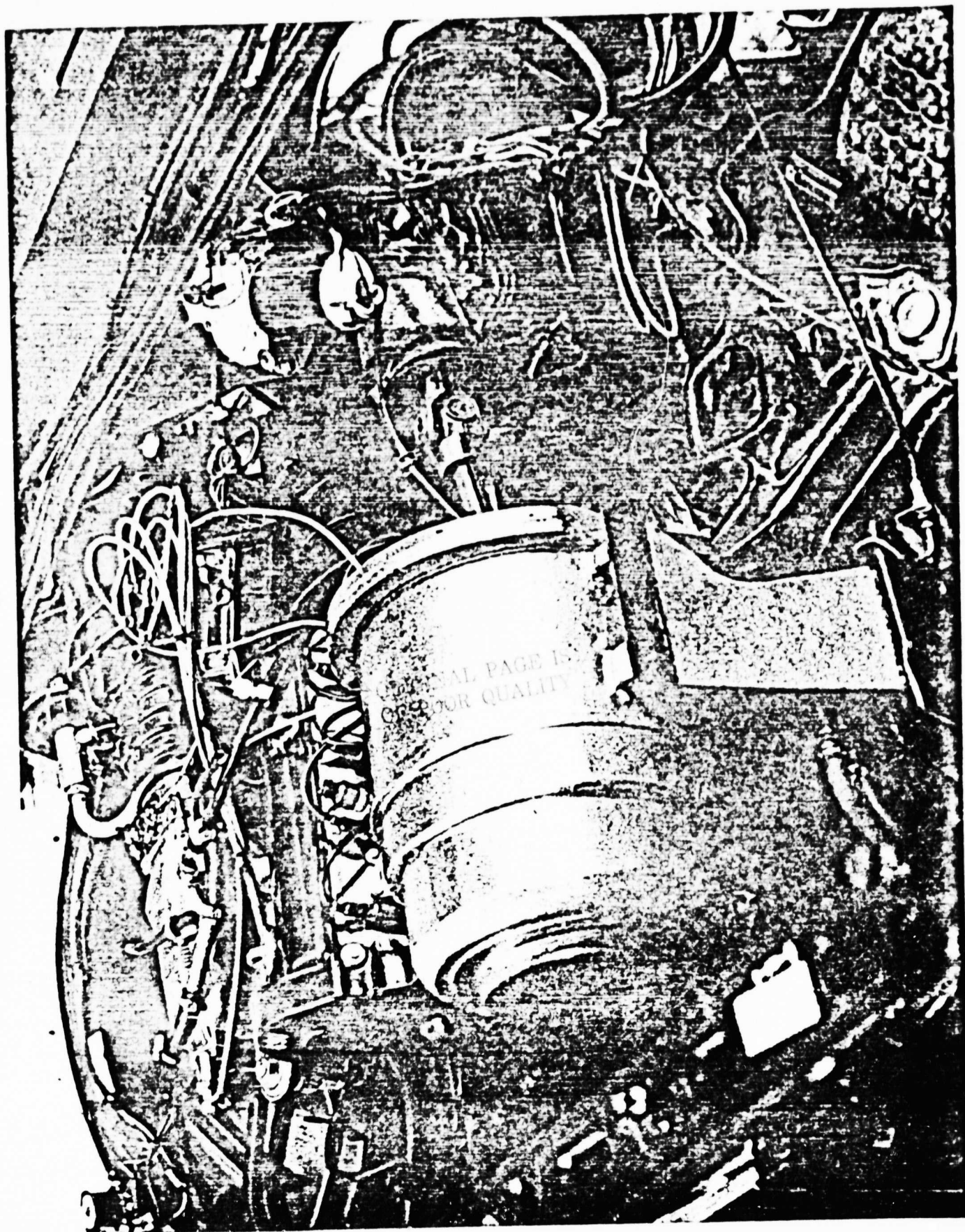


Figure 2-6 Left front view of hybrid propulsion installation showing Siemens electric motor and VW engine.

We believe these studies establish the fact that the LTD front end can be redesigned within the constraints of the hybrid propulsion system and achieve an improvement in aerodynamic drag.

Analysis and wind tunnel testing planned for the Phase II program will be used to insure the achievement of a maximum reduction in drag.

#### Materials Substitution - Vehicle Weight Reduction

A basic groundrule was established for the program which was to achieve weight reduction without costly engineering, prototype tooling and prototype parts cost. To accomplish this, no change for the sake of weight reduction will be made to the body structure and central body portions of the Ford LTD. This does not rule out weight savings that may be incorporated by Ford in the LTD vehicles to be used for mule and ITV build purposes

Having identified a shopping list of components that could change, an analysis was made of the applicable alternate material and the weight savings that could be achieved. After developing a preliminary list the next step was to review this with Sheller-Globe Corporation, our body material design and prototype fabrication source. The results of this review and analysis will be found in Section 4.3 of this report.

### 3. DEVELOPMENT REQUIREMENTS

#### 3.1 Major Areas of Technology Development

The aspect of the SCT Near-Term Hybrid Vehicle which makes it fundamentally different from either a conventional electric vehicle or a conventional I.C.E. vehicle is the systems control strategy; the manner in which the load is shared between the heat engine and the electric motor. This involves on-off operation of the heat engine, with the heat engine being loaded as soon as it is up to speed and firing. As discussed in the Task 2 report, this type of operation has the potential of achieving far lower fuel consumption than running the heat engine continuously. There are two major development areas associated with this approach. The first involves the development of the system control system to the point at which the vehicle's driveability is not inferior to a conventional car's. This is a large task, but one which we are confident is possible with the exertion of enough engineering pressure. The second area involves meeting emission standards. This is a gray area in which there is not even enough data to predict the magnitude of the task. There is simply no data on the emission characteristics of engines operating in this mode, and one of the first tasks in a development program will be to generate enough data so that the magnitude of the task can be assessed. These two areas, controls and emissions, will be discussed in more detail in subsequent sections.

Another subsystem which will require substantial development is the propulsion battery. As pointed out in the Task 2 report, the

requirements for a hybrid vehicle battery are different than those for an electric vehicle battery. Consequently, unique cell and module designs will be required; also, additional characterization and test data will be required before a final assessment can be made of the relative merits of nickel-iron and lead-acid batteries for the hybrid application. Again, this area will be discussed further in a subsequent section.

### 3.2 Controls

#### 3.2.1 System Controller

The system controls development task will not involve the development of new hardware at the component level. It will involve the integration of available hardware, including microprocessor, into a system which implements a fuel efficient control strategy in a vehicle of acceptable driveability. Specifically, it will include the following:

- 1) Continued development of the control strategy on a computer simulation, incorporating updated information on the heat engine, batteries, and so forth, as this data becomes available.
- 2) Dynamometer testing of the heat engine and motor combination, with vehicle inertia being simulated, to evaluate the dynamics of the engine startup/shutdown transients as a function of equivalent vehicle inertia, clutch engagement rate, engine throttle setting, engine temperature, initial system operating point, and so forth.

- 3) Re-evaluation of the microprocessor requirements, selection of a microprocessor, and design, breadboarding, and checkout with the  $\mu$ P development system of the system controller.
- 4) Incorporation of the system controller on the dyno test rig; development testing to adjust control parameters, and evaluate startup dynamics with controller operational.
- 5) Incorporation of the complete system in a test bed vehicle; development testing to modify and fine tune the control parameters to obtain acceptable driveability and performance. The dyno test rig would be retained throughout the vehicle testing and development program to provide a means for doing preliminary checkout and evaluation of system changes under more controlled conditions than is possible in a vehicle.

The in-vehicle phase will occupy the largest part of the system controls development program. It will tie in to the emissions control development program in that, as soon as the control system is developed to a point where the vehicle is operating satisfactorily, the vehicle will be tested on a chassis dyno for emissions in both operating modes.

### 3.2.2 Motor Controls

The development requirements of the motor field controller are minimal. The power circuitry and components will be identical to those in use in the controller for the SCT electric vehicle, with the logic circuits modified to interface with the hybrid's system controller. The armature controller, however, is new; and a certain amount of development will be required. The major problem here is



that the power transistor field is changing rapidly, and the new high power transistors which are becoming available are in many cases not completely characterized. Thus, if a selection is made of a basic power transistor and a controller is designed and breadboarded around it, a substantial amount of bench testing will be required to ascertain what the real limits of the device are in this particular application. As a consequence, a few iterations of device selection and circuit design can be anticipated.

### 3.2.3 Engine Controls

This area is discussed in the next section, largely in the context of emission controls. It is appropriate at this point, however, to discuss the development requirements of the engine clutching arrangement. A preliminary selection of a clutch has been made, and this would be used on the dyno test rig discussed earlier. The tests on this rig will provide an opportunity to evaluate the clutch capacity, stability of engagement characteristics, whether any temperature problems exist with frequent engagement and disengagement, drag when disengaged, and so forth. Based on these tests, a second iteration of clutch selection and/or design modifications is anticipated.

### 3.3 Heat Engine

#### 3.3.1 Emissions

As we have discussed in the Task 2 report, attempting to project the emissions of the hybrid vehicle, based on available steady-state emission maps, would be an exercise in futility, simply because the data is not relevant to the problem. Stating the matter as baldly as possible, the magnitude of the emissions problem with the hybrid vehicle is unknown and will not be known until test data is obtained to characterize emissions in on-off operation. The only thing we can offer right now is our suspicions as to where problems may occur. These are:

- . Higher raw (engine-out) HC and CO emissions as a result of startup transients.
- . Higher raw  $\text{NO}_x$  emissions as a result of operation at higher average engine loading.
- . Greater difficulty in control of HC and CO emissions (also  $\text{NO}_x$ , since a 3-way catalyst will undoubtedly be standard for 1985 production) as a result of a lower average catalyst temperature.

The argument could be made that, because the heat engine operates only a fraction of the time, and then at a high load factor, emissions will not be a problem. This, however, is more wishful thinking than sound engineering. Our projection is that the hybrid will burn about one half of the fuel that the reference vehicle does; in other words, the hybrid is a full sized vehicle with the fuel economy of a sub- or mini-compact. The argument

just stated is consequently worth about as much as the statement that one does not have to worry about emissions from a mini-compact because the engine is small.

Therefore, the emissions problem is one that must be faced squarely and an understanding must be gained early in the development program of the magnitude of the problem. This requires characterizing the emissions in normal operation. The steps in doing this are as follows:

- . Obtain specific emissions maps of the engine, both raw and with catalyst.
- . Define typical engine on and off times for mode 1 and mode 2 operation on the basis of computer simulation results.
- . Operate the engine at various fixed throttle settings, with the dynamometer running at constant speed, but clutching and de-clutching and starting and stopping the engine at the proper times and measure emissions under these conditions. This will require the equivalent of either bag-sampling or continuous sampling, which are procedures not normally used in conjunction with engine dynamometer testing.
- . From this data, specific emissions maps for on-off operation can be obtained. These maps would have to be obtained for on and off times representative of both mode 1 and mode 2 operation. Both raw and treated emissions should also be measured to get an idea of the decrease in catalyst efficiency which results from the on-off operation.

Comparison of the steady-state and on-off emissions maps will provide a method of gauging the magnitude of the emissions control problem.

At this point a judgment will have to be made as to whether or not the problem is workable within the time frame of concern to this program and within the resources which could be allocated to solving it by a major automobile manufacturer. Note that we did not say "within the resources of this program", because it is quite possible that the funding available in the Phase II NTHV would not cover the costs involved in developing a system to meet the relevant emission standards. However, it would be a mistake not to pursue the development of the hybrid system with the most fuel-efficient control strategy simply because of budget limitations of this particular program, unless there is reason to believe that getting the system to comply with emission standards would also be out of reach for a major manufacturer. This is why it is so essential to get a good characterization of engine emissions under operating conditions similar to the hybrid, and to exercise good engineering judgment in assessing the magnitude of the emission control problem.

Assuming that such judgment results in the conclusion that this problem is workable (again, not necessarily within the budget constraints of this program!) without the necessity of a radical overhaul of the overall system control strategy, then the development of the emission control system would proceed as follows:

- . Identification of operating regimes in which emissions are high.
- . Re-calibration of engine parameters to reduce emissions in these areas. In addition to the engine parameters (mixture ratio, spark timing, EGR rate, etc.), it may be necessary to adjust other parameters associated with the engine startup process. These include the point at which fuel is turned on, the rate of clutch engagement, throttle opening when fuel is turned on, and so forth.
- . Running of emission tests on a chassis dynamometer to ascertain compliance with the relevant emission standards. In the event that compliance is not obtained, a modal analysis would be performed to determine what portions of the driving cycle are giving a problem, and what are the possible means for correcting it.
- . Modifying engine and control parameters to reduce emissions on the problem parts of the cycle, re-running chassis dynamometer and engine dynamometer tests as required.

Obviously this is an iterative procedure which could get quite lengthy and expensive. It would be pursued, in this program, to an extent which is consistent with schedule and budget limitations.

We have tacitly assumed in the above discussion that the fuel injected VW Rabbit engine would be used, with (possibly) additional fuel shutoff controls. Because the development on this system was done in Germany, it may be difficult to obtain the variety of parts needed to facilitate the engine re-calibration process.

Consequently, it may turn out to be preferable to use the carbureted Chrysler version of this engine, which has about the same power but higher displacement (1.7 l vs. 1.5 l) and higher torque. The only problem foreseen with the carbureted engine is the lack of ability to shut off fuel to the cylinders while the engine is turning. (For example, on a startup, it may be preferable from an emissions standpoint to keep the fuel off until the engine speed has been brought up to a certain level). Again, resolution of this question will have to wait until dynamometer tests are run with the engine cycled on and off, since we have at this point no way of knowing how much of a problem will be presented by the emissions during the startup and shutdown transients.

Not to be overlooked is the possibility that an examination of the engine emissions in on-off operation will lead to the conclusion that the present system control strategy, with its frequent engine starts and stops, is totally unworkable from an emission control standpoint. In this case, it would be wise to have a backup control strategy available for which the probability of being able to meet emission standards is higher. Such a strategy, along with its implications regarding fuel and energy consumption, is discussed in Section 4.1.4.

One question which has so far been left out of this discussion of emission control development is that of the test procedures to be used on the chassis dynamometer tests. Obviously, the composite cycle constructed in Task 1, while perhaps more representative of normal driving patterns than the urban driving cycle, is not usable

as a test procedure. As discussed in the Task 2 report, the best assumption that can be made is that EPA would make the minimum possible modification to the test procedure which would take into account the bimodal operation of a hybrid, but which would leave the current FTP for emissions for conventional cars unchanged. Such a procedure might go as follows:

- Starting with the batteries fully charged, run the vehicle according to the normal FTP, and note the distance at which the vehicle switches from Mode 1 to Mode 2 operation.  
(Test 1) If the vehicle did not switch from Mode 1 to Mode 2 during the test, continue running after completion of the test until the switchover occurs, and note the distance at which this happens.
- Rerun the vehicle according to the FTP, this time on Mode 2, omitting the cold start. (Test 2)

The average vehicle emissions may then be computed as follows: Suppose  $\bar{d}$  is the average distance driven on those days in which the vehicle is operated.\* If  $d_{FTP}$  is the total 'distance' travelled in performing the FTP, and  $d_1$  is the distance at which the switchover from Mode 1 to Mode 2 occurs, then the average emissions can be estimated by  $\bar{x} = x_1 \cdot \max(d_1, d_{FTP}) + x_2 \cdot (\bar{d} - \max(d_1, d_{FTP}))$  where  $x_1$  and  $x_2$  are the emission rates in grams/mile on Tests 1 and 2, respectively, and  $\bar{x}$  is the average emission rate. A somewhat more elaborate version of this procedure could also be developed, using a distribution

---

\* If we use the JPL projections for annual vehicle travel in the 1985-1995 time span, this would be 55.8 km/day of use. This takes into account 14 days per year when the car is not used.

of daily driving distance in the computation of  $\bar{x}$  rather than just an average driving distance; the test procedure would, however, be the same as that just described. The point is that we should not expect the driving cycle to be changed for hybrid vehicles; the test procedure would have to be an extension of the current FTP using the same driving cycle.

### 3.4 Batteries

The fundamental problem faced by the vehicle and propulsion system designer is the non-existence of the data which would be required to make an incontrovertible, rational decision as to the best type of batteries to use in a 1985 production hybrid vehicle. The safe choice, of course, is lead-acid; improved production batteries approaching the ISOA performance goals will clearly be available in this time frame. In terms of cost, this battery may be in some trouble, however, if lead prices continue to behave as they have recently. The nickel-iron system, as discussed in the Task 2 report, has a number of potential advantages in terms of lower life cycle cost, cleaner accommodation in the vehicle, and higher fuel economy. There are a large number of unknowns associated with it, however, since the ANL program on this battery system has been a lot 'lighter' than those for the lead-acid and nickel-zinc systems. Whether it can achieve production status by 1985 is, of course, dependent on resolution of some of the unknowns and the subsequent level of development effort. Finally, the nickel-zinc system still does not appear to us to have a potential cost/life quotient which is low enough to make it



competitive in the hybrid application. In addition, other problems appear to be cropping up which would severely hamper it in the hybrid application, like the presence of a 'pseudo-memory' effect.

In light of this situation, it appears to us that the most reasonable (if not demonstrably correct) approach is to pursue development of both nickel-iron and lead-acid designs for the hybrid application to a point at which some of the unknowns, particularly with regard to the nickel-iron system, can be resolved to the extent that a more rational selection can be made. The activities which would be pursued in the initial phase of such a program would be the following:

- Design and fabrication of cells of a size appropriate for the 120 V hybrid system.
- Cell testing, at the battery developer, to characterize system performance over the complete range of specific power demands to be made on the battery.
- Design and fabrication of the battery system. This will involve tooling design and procurement in the lead-acid case, and possibly also in the nickel-iron case, with a lead time of about six months.
- Preliminary battery testing at the battery developer to verify performance at nominal conditions.
- Bench testing of the battery systems at SCT, in cooperation with the battery developer, to characterize battery performance under both constant discharge rate conditions and load profiles representative of operation in the hybrid vehicle.

- In-vehicle testing of the selected system.
- Development of thermal management and a single point watering/venting system for the final vehicle.

#### 4. DESCRIPTION OF NTHV PRELIMINARY DESIGN

As discussed in Section 2 of this report, the NTHV is conceived by SCT to be a roomy, six-passenger vehicle in which the hybrid propulsion system would be incorporated by the manufacturer to allow the retention of the high profitability of this class of vehicle while meeting CAFE requirements for 1985 and beyond. As such, apart from the propulsion system, it is an evolutionary development of an existing weight efficient six-passenger vehicle, the Ford LTD, into the 1985 time frame. A summary of the design features and vehicle characteristics is given in Table 4-1. The numbers given in this table are based on the use of nickel-iron batteries. The effects of using alternative battery types will be discussed in Section 4.1 (Propulsion System Description).

Propulsion system layouts are shown in Figures 4-1 and 4-2 and renderings of possible styling treatments in Figures 4-3 to 4-5. A complete drawing package is included as Appendix B to this report.

The passenger compartment and frame are identical to the existing Ford LTD; shape changes have been made at the front and rear for improved aerodynamics. The motor and engine can be accommodated nicely in the space formerly occupied by the V-8; however, there is not much room left under the hood for electronics or batteries. Consequently, the motor controls, battery charger, and system controller (microprocessor) are located under the seats, which is a more favorable environment in terms of temperature than under-hood in any case. Motor controls (armature, field chopper, contactors, and associated logic circuitry) are shown under the front

Table 4-1 - NTHV Summary Description

1. General

Passenger Capacity	6
Layout	Front Engine - Rear Drive
Curb Weight	1864 kg
Distribution	47.6% F, 52.4% R
GVW	2384 kg
Distribution	43.8% F, 56.2% R
Wheelbase mm	2903
Track mm	1581 F, 1575 R
Length mm	5309
Width mm	1968
Height mm	1385
Ground Clearance mm	123.7
Trunk Space cu.m.	.59
Fuel Capacity	40 liters

2. Propulsion System

Engine	VW Rabbit S.I.
Displacement	1.5 l
Peak power	53.3 kw @ 5800 RPM
Peak torque	99 N-M @ 3500 RPM
Motor	Siemens IGV1, separately excited
Rated power	17 kw
Battery	Nickel-Iron
Rated capacity (3 hr rate, 100% DOD)	14.5 kw-hr (54 w-hr/kg)
Nominal voltage	120

<b>Motor Controls</b>	<b>Transistor Choppers</b>
Field chopper	10 AMP
Armature chopper	140 AMP
<b>Transmission</b>	<b>4 Speed Auto., Lockup on 3rd &amp; 4th</b>
Torque Converter mm	276
Stall Torque Ratio	2.1
Ratios 1st	2.45
2nd	1.45
3rd	1.0
4th	.75
Rev.	2.22
<b>Final Drive</b>	
Ratio	5.12

### 3. Chassis Systems

Front Suspension - Unequal length A-arms, coil springs.

Rear Suspension - Live axle located by radius rods and panhard rod, coil springs.

Steering - Recirc. ball and roller, power assisted.

Brakes - Hydraulically assisted (hydroboost)

Front - Disc 11.03" DIA. Vented rotor

Rear - Drum 10"

Wheels - 365 x 165 - Composite

Tires - 205/75R14

### 4. Body and Structure

Construction - Separate frame and body.

Materials - Steel structure, aluminum and plastic front

and including fenders, hood,  
bumper systems, plastic deck lid  
and plastic door outers. Other  
skin panels steel.

FOLDOUT FRAME

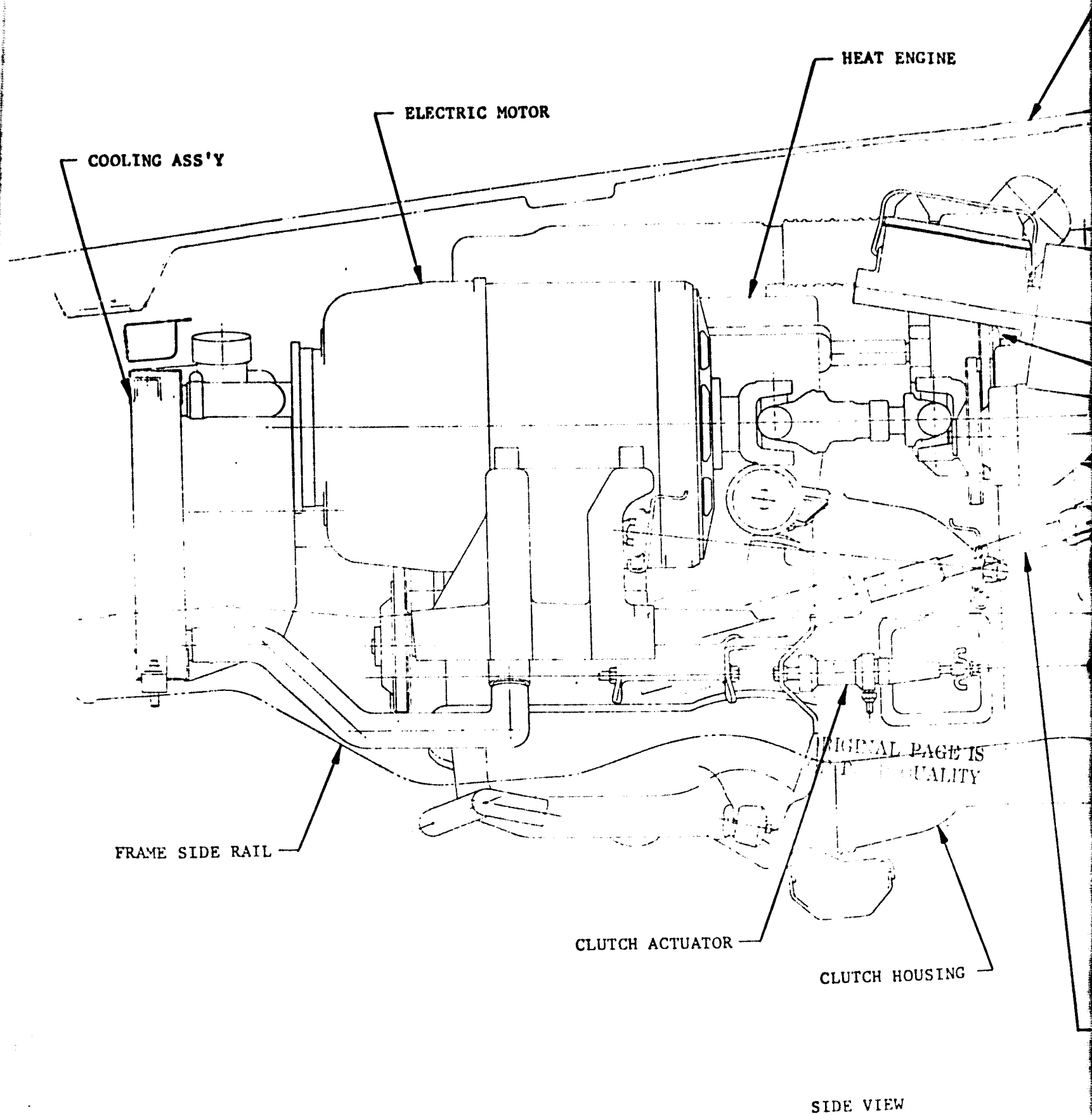
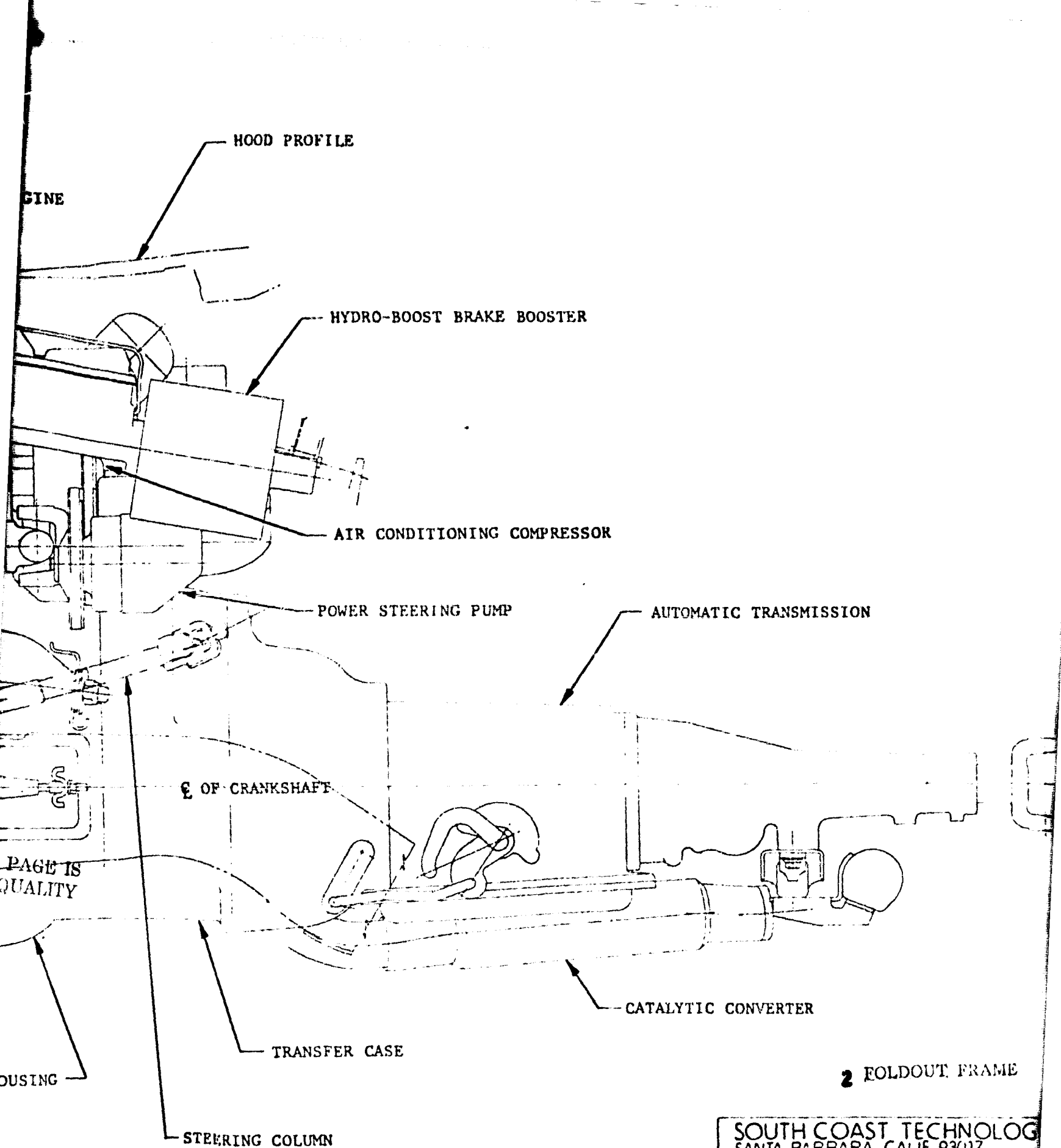
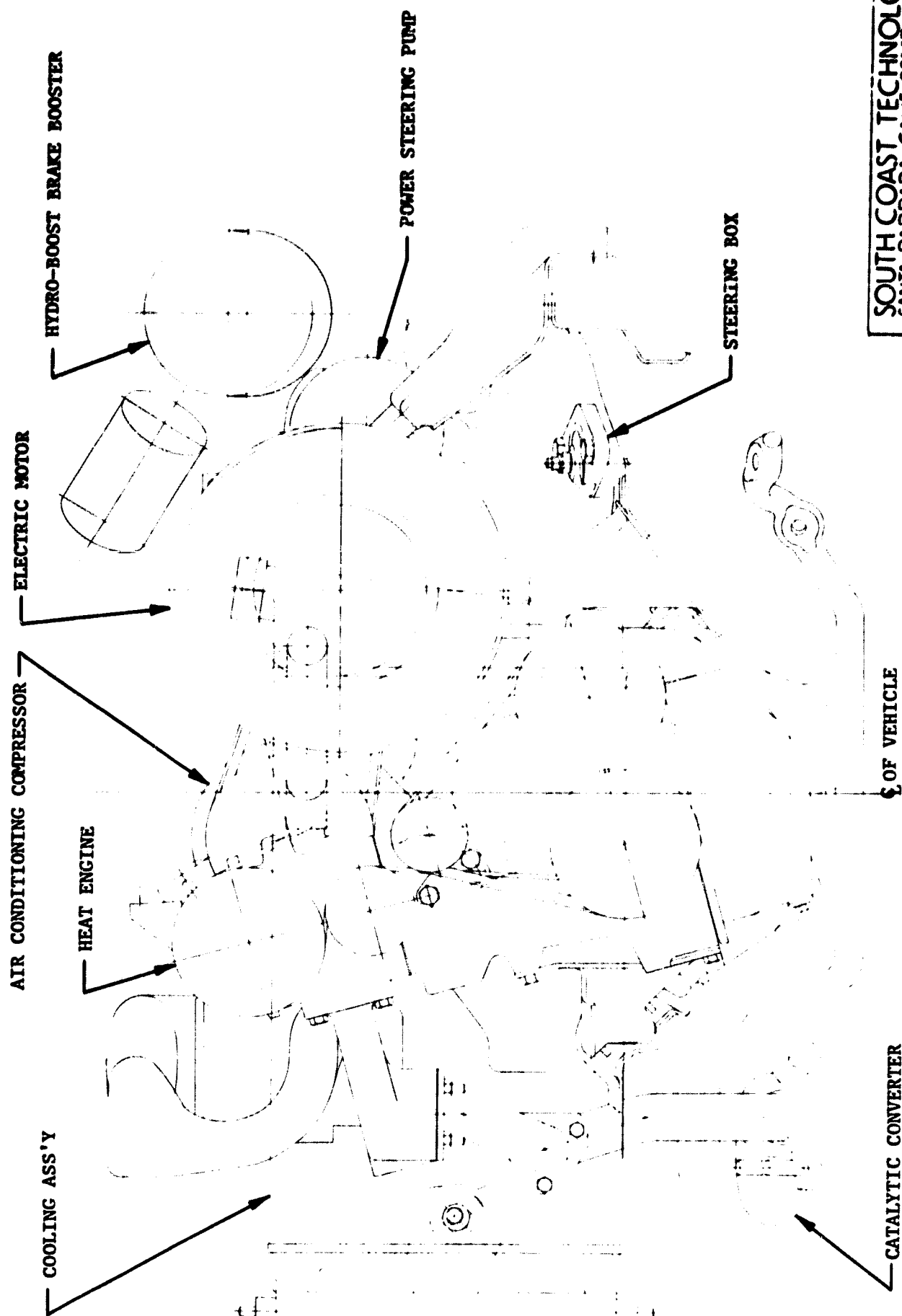


Figure 4-1. PROPULSION SYSTEM PACKAGE



SOUTH COAST TECHNOLOG	
SANTA BARBARA CALIF 93017	
HYBRID PROPULSION SYSTEM	
HYBRID-1979 LTD PACKAGE	
APPROVED	SHT 1 of 2
DRAWN BY	





FRONT VIEW

Figure 4-2. PROPULSION SYSTEM PACKAGE

SOUTH COAST TECHNOLOGY SANTA BARBARA CALIF 93017	
HYBRID PROPULSION SYSTEM	
HYBRID-1979 LTD PACKAGE	
APPROVED	SHT 2 of 2
DESIGNED BY J. J. J. J.	

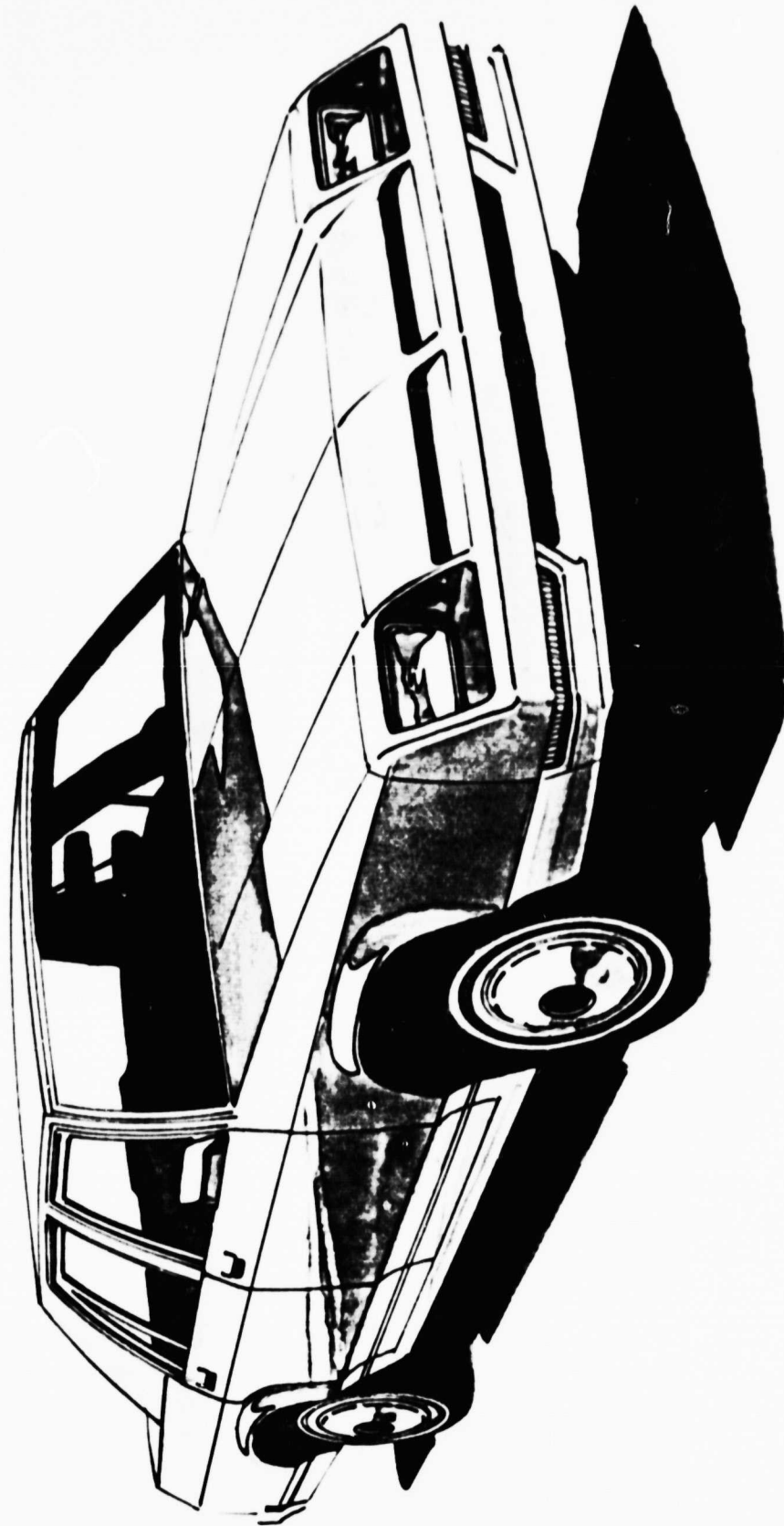


Figure 4-3. FRONT END - REDESIGN EXAMPLE

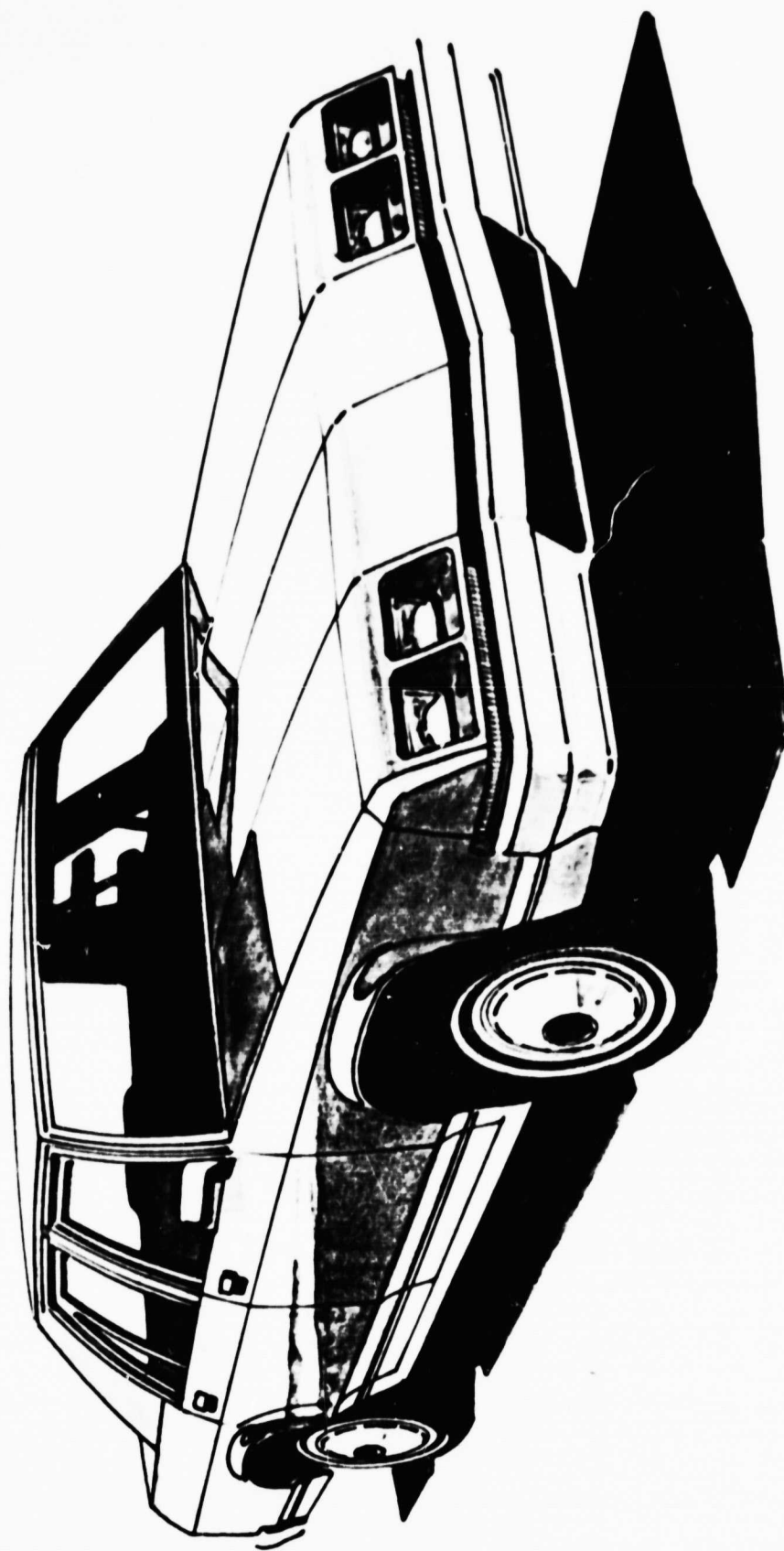


Figure 4-4. FRONT END - REDESIGN EXAMPLE



Figure 4-5. REAR END - TREATMENT EXAMPLE

seat in two modules of equal size. The battery charger and system controller are located under the rear seat, along with the fuel tank. This would limit the fuel tank to about 40 litres capacity; however, there appears to be a good possibility that with more optimum electronics packaging, both the motor controls and the charger could be located under the front seat. This, together with relocation of the system controller to an underdash or trunk location, would allow the area under the rear seat to be devoted entirely to fuel storage, in two interconnected modules providing a more liberal capacity of about 60 litres. The nickel-iron battery is located just aft of the rear axle. This reduces the trunk capacity by about  $.07 \text{ m}^3$ , from  $.66 \text{ m}^3$  down to  $.59 \text{ m}^3$ . This is close enough for practical purposes to our recommended specification of  $.6 \text{ m}^3$ , and well in excess of the minimum requirement of  $.5 \text{ m}^3$ .

Discussion of the design for the various vehicle subsystems, including rationales for major design decisions and design alternatives which require testing for complete evaluation, is given in subsequent sections. Before proceeding to this discussion, however, it would be best to provide a description of the updated reference vehicle in order to have a basis for comparison.

#### Reference Vehicle Description

As a result of a detailed analysis of possible weight savings on the current Ford LTD, discussed in Section 4-3, it was concluded that the 1985 'LTD' could use a 4.26 l ( $260 \text{ in}^3$ ) displacement engine instead of the current 5.0 l engine. This would still provide adequate performance (0-90 kph in 12 sec). Although there is a

possibility that Ford will go to four-speed (overdrive) automatic with full lockup on overdrive, and partial lockup on third, we continued to hypothesize a three-speed with 2.26 final gearing and full lockup on third. We did, however, change the shift strategy to a highly optimized one similar to the one used in the NTHV (Section 4.1), and used a slightly 'tighter' torque converter than is the current practice. In reality, with a 4.26 l engine, the final gearing used with the three-speed is nearly as low (numerically) as the overall gearing (in overdrive) which would be practical with the four-speed. Consequently, the benefits of the four-speed for the reference vehicle would probably be in slightly higher performance in the lower gears rather than in significantly better fuel economy; and we feel that the fuel economy estimates made for the reference vehicle are also representative of what would be obtained with a four-speed.

It was assumed that the reference vehicle would share the same improvements in aerodynamics, tire rolling resistance, lubricants, and so forth, envisioned for the hybrid. The 'people package' for both vehicles remains identical to the current Ford LTD.

Using these assumptions, operation of the reference vehicle was simulated with a slightly modified version of HYBRID2. In this simulation, a fuel map which is equivalent to the one used for the hybrid vehicle heat engine was used; that is, the hybrid's fuel map was compressed horizontally and vertically to account for the fact that the 4.26 l engine would be a lower speed, lower bmep engine. The current LTD was also simulated to provide a baseline. The simulation results were as follows:

<u>Driving Cycle</u>	<u>Uncorrected Fuel Economy</u>	
	<u>Reference Vehicle</u>	<u>LTD</u>
SAEJ227a(B)	5.31 km/l (12.5 mpg)	4.50 (10.6)
Urban	7.41 km/l (17.4 mpg)	6.16 (14.5)
Highway	11.60 km/l (27.3 mpg)	8.72 (20.5)
Yearly composite	8.70 km/l (20.5 mpg)	7.07 (16.6)

The 'yearly composite' driving cycle referred to is the cycle constructed in Task 1 and detailed in Section 3 of the Task 1 report.<sup>(2)</sup> By the term uncorrected fuel economy, we mean the results as computed by the simulation. The LTD's urban cycle fuel economy as measured by EPA is 14 mpg; consequently, the simulation appears to be giving quite accurate results. Since the fuel map used in HYBRID2 is a representative one based on data from a number of pre-1978 engines, some improvement can be expected in the reference vehicle area by 1985. (See discussion on p. 30 of the Task 1 report.<sup>(2)</sup>) Thus, a reasonable estimate for the urban cycle for the reference vehicle would be 18 mpg. Although one can play games with percentages, a meaningful estimate is to just take this urban cycle fuel economy and use that as the probable in-use fuel economy, just as is done currently; i.e., our best estimate is that the 1985 reference vehicle is, in the real world, an 18 mpg car. This agrees with the 18 mpg estimated in Task 1. Now, there should be a meaningful correlation between the yearly composite driving cycle and the way a vehicle is driven over the course of a year's driving, in view of the way in which the yearly composite cycle was constructed. (See (2) for details.) We shall assume such a correlation exists. Hence, for purposes of

estimating the in-use economy of the hybrid vehicle, we can assume that is about 12% lower than the yearly composite value computed by HYBRID2.

Having identified the salient characteristics of our 1985 six-passenger, conventional vehicle, we can proceed with describing the hybrid.

#### 4.1 Propulsion System

##### 4.1.1 System Description

A block diagram of the NTHV propulsion system is shown in Figure 4.6 . It utilizes a 53 kw VW gasoline engine which drives through a hydraulically actuated clutch. This clutch, in conjunction with an ignition on/off switch, and the throttle valve, is the means for starting the heat engine and bringing it on line when it is required and disengaging it when it is not. A dynamic analysis of the process of starting the engine while bringing it on line will be discussed in Section 4.1.2. The clutch output is coupled to one end of the output shaft of a transfer case; the other end of the transfer case output shaft drives the torque converter. The input shaft of the transfer case is driven by the electric motor, and the transfer case input and output shafts are coupled by a HY-V0 chain and sprockets with a 1:1 ratio. The transfer case thus serves as a summing junction for the heat engine and electric motor output torques.

The electric motor is thus always coupled to the torque converter input, and the heat engine also drives the torque converter





input when it is required. The torque converter is of the lockup variety; it drives a four-speed overdrive automatic transmission which is of conventional design, except for the modifications and interface hardware required to accept external shift commands from the system central controller.

The electric motor is of the separately excited type, with a peak power rating of 27 kw when used in conjunction with a 120 V nickel-iron battery pack. A rating of 30 kw is required for the heavier lead-acid system. Below base speed, motor speed and torque are controlled by a transistor armature chopper. This chopper is used only at very low vehicle speeds, in first gear. Under these conditions, maximum motor power is not required for adequate performance; consequently, the armature chopper is rated at only about 50% of the peak motor rating. Over most of the driving speed range, motor speed and torque control is by field weakening, utilizing a transistor chopper.

Input power to the motor comes from the main propulsion battery. Based on the presently available data, the preferred battery system is nickel-iron. However, as indicated previously, a lead-acid battery system will be carried along in the program as an option until such time as an evaluation can be made based on test data of the performance of these two battery systems under operating conditions representative of the hybrid vehicle.

The central controller, incorporating a microprocessor, is the key to efficient operation of the hybrid system. It starts with the driver's input to the accelerator and brake pedals, together

with information on the current operating conditions of the major system components. It processes this information to determine how the system power demand should be split up between the heat engine and electric motor, and translates this data into command signals for the devices which control heat engine and electric motor. These control devices include the ignition on/off relay, throttle valve, and clutch actuation valve for the heat engine, and a field chopper and armature chopper for the electric motor. In addition, the central controller determines whether or not the transmission should be shifted to meet the system power demand most efficiently. While the vehicle is being recharged from the wall plug, the central controller may also be used to control the battery charger.

The input signals to the central controller include accelerator pedal position ( $x^+$ ), brake pedal position ( $x^-$ ), vehicle speed ( $N_2$ ), torque converter input (or motor output) speed ( $N_1$ ), battery voltage ( $V_B$ ), battery current ( $I_B$ ), battery temperature ( $T_B$ ), and heat engine temperature ( $T_E$ ). Other system variables which may be required by the central controller are motor armature current ( $I_A$ ), heat engine manifold vacuum ( $P_M$ ), and motor temperature ( $T_{MO}$ ). All these are indicated as inputs in Figure 4-6, although some may be determined to be unnecessary in the course of system development.

The power supply for the microprocessor and logic portions of the two choppers is an accessory battery which is a normal automotive 12 V battery whose charge is maintained by a DC/DC converter operating off the main battery pack. The accessory battery also supplies the ignition, lights, radio, and power accessories such as windows

and seats. Because the propulsion battery state-of-charge is always maintained above a minimum level, there is always power available to keep the accessory battery charged; consequently, the usual engine-driven alternator is deleted. For the same reasons, the electric drive motor is also always available to start the heat engine; consequently, the usual 12 V starter motor is also deleted.

The only mechanically driven accessories are the air conditioning compressor and power steering pump, which are not shown in Figure 4-6 , to avoid crowding. The power steering pump also supplies the hydraulic assist unit for the brakes (Hydroboost), and hydraulic supply for clutch actuation. The compressor and pump are driven off the input to the transfer case (motor output). A detailed discussion of the accessory drive arrangement will be found in Section 4.1.6.

#### 4.1.2 System Controller

##### Basic Control Strategy

The final version of the control strategy developed during Task 3 for the NTHV incorporates two operating modes, like the strategy discussed in the Task 2 report. It differs from the earlier strategy primarily in the use of a more sophisticated,  $\mu$ P controlled transmission shift strategy, incorporation of a warmup phase, and further optimization of the control parameters. The two operating modes are, of course, distinguished by whether or not a net withdrawal of stored energy is allowed. On Mode 1, such a withdrawal is made; on Mode 2, it is not.

The specifics of what happens on these two modes, and how a combination of effective utilization of battery energy and highly efficient fuel utilization is obtained, are best explained by referring to a set of power curves for the heat engine, electric motor, and the combination of the two. The basic curves we are working with are shown in Figure 4-7. Note that the electric motor maximum power takes a jump at the transition from armature to field control due to the use of a limited power armature chopper. Power is then constant over the field weakening range up to about 4000 RPM, at which point we begin to run into limitations on the current which can be commutated. Power then drops off. In addition to the heat engine maximum power curve, Figure 4-7 shows the lines of constant brake specific fuel consumption in g/kw-hr. Different shift strategies are used depending on whether or not the heat engine is operating. If it is, then it dictates the shift strategy, indicated on Figure 4-7 by upshift and downshift lines; heat engine operation will normally be between these two lines. If the heat engine is off (during deceleration and low power operation), the shift strategy changes so that the upshift always occurs at 4000 RPM and a downshift at 2200 RPM. The efficiency of the electric motor varies so little over this speed range and a reasonable load range, that additional sophistication does not appear to be necessary at this time.

Now, the first two control parameters we shall introduce, in relation to Figure 4-7, are a nominal maximum motor operating power level,  $P_{NOM}$ , and a vehicle transition speed. Both these

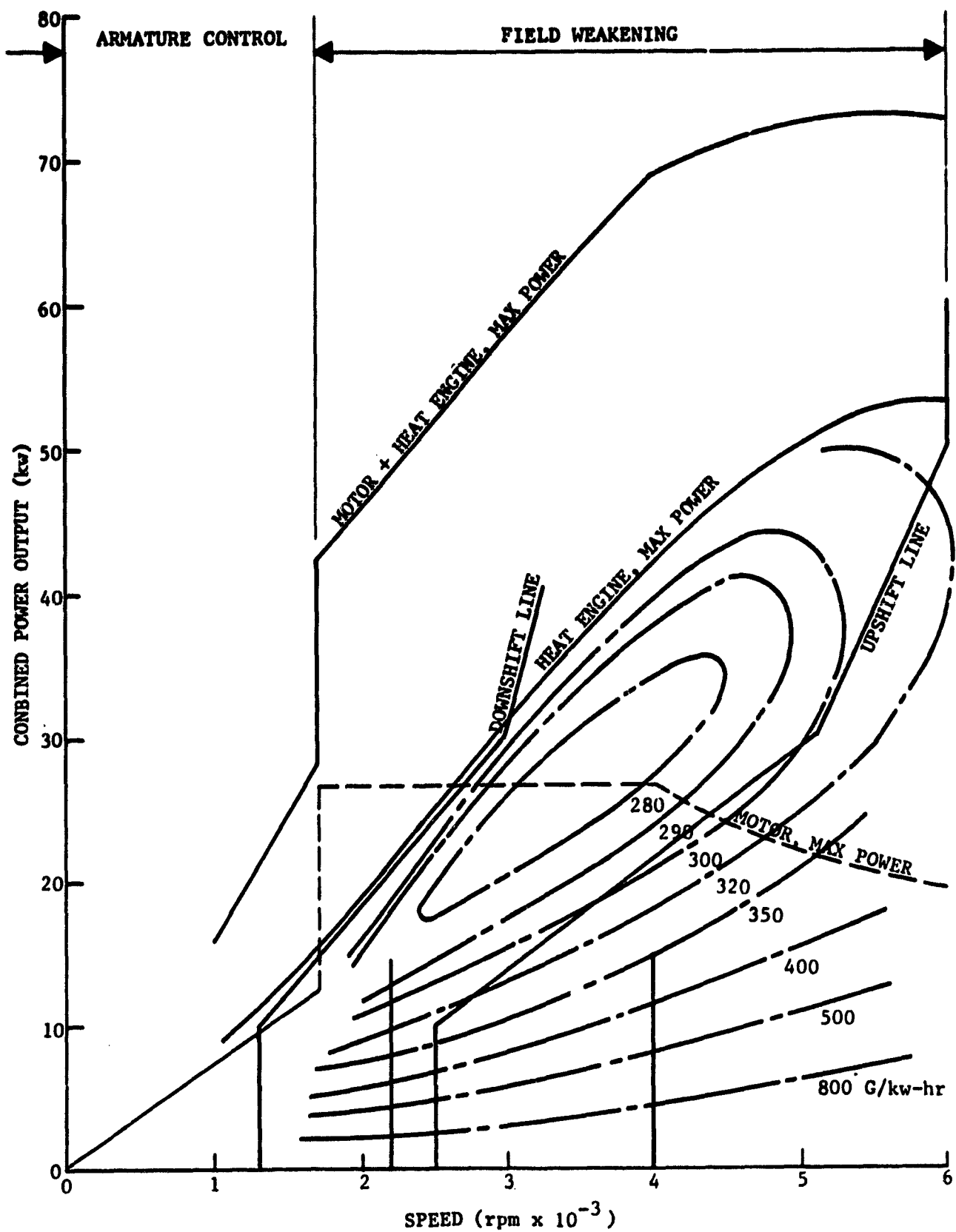


Figure 4-7 Hybrid Propulsion System Power Curves

parameters relate to Mode 1 operation, and their proper selection keeps the battery discharge rates down to levels which provide the most effective utilization of stored energy. In Figure 4-8 ,  $P_{NOM}$  is shown as following the motor maximum power curve until it reaches 18 kw, then being constant at 18 kw. As long as the system power command  $P_{COM}$  is below  $P_{NOM}$ , and the vehicle speed is below the transition speed (72 kph, or about 45 mph), the heat engine remains off and the system operates only on stored energy. Typical operating points are indicated by P (system) and  $P_M$  (motor). Unless the transmission is in first gear (downshift not possible) or fourth gear (upshift not possible), the motor will operate between 2200 and 4000 RPM.

The motor power output of 18 kw corresponds to a battery specific output of about 87 w/kg for the nickel-iron battery pack. This is well within the peak power capabilities; however, sustaining this power level for extended periods would result in rapid depletion of the battery and not very effective utilization of stored energy. To minimize this, the heat engine is cut in and allowed to take over the load if the vehicle speeds exceeds the 72 kph transition speed, as illustrated in Figure 4-9 . In this case, the motor idles at the same speed the engine is running at, and the field is controlled to maintain essentially zero output and the heat engine picks up the entire load. Since the power output required at 72 kph is about 10.5kw, this means that the heat engine will generally be operating in the heavily shaded region shown in Figure 4-9 . In this region, the bsfc remains below 350 g/kw-hr

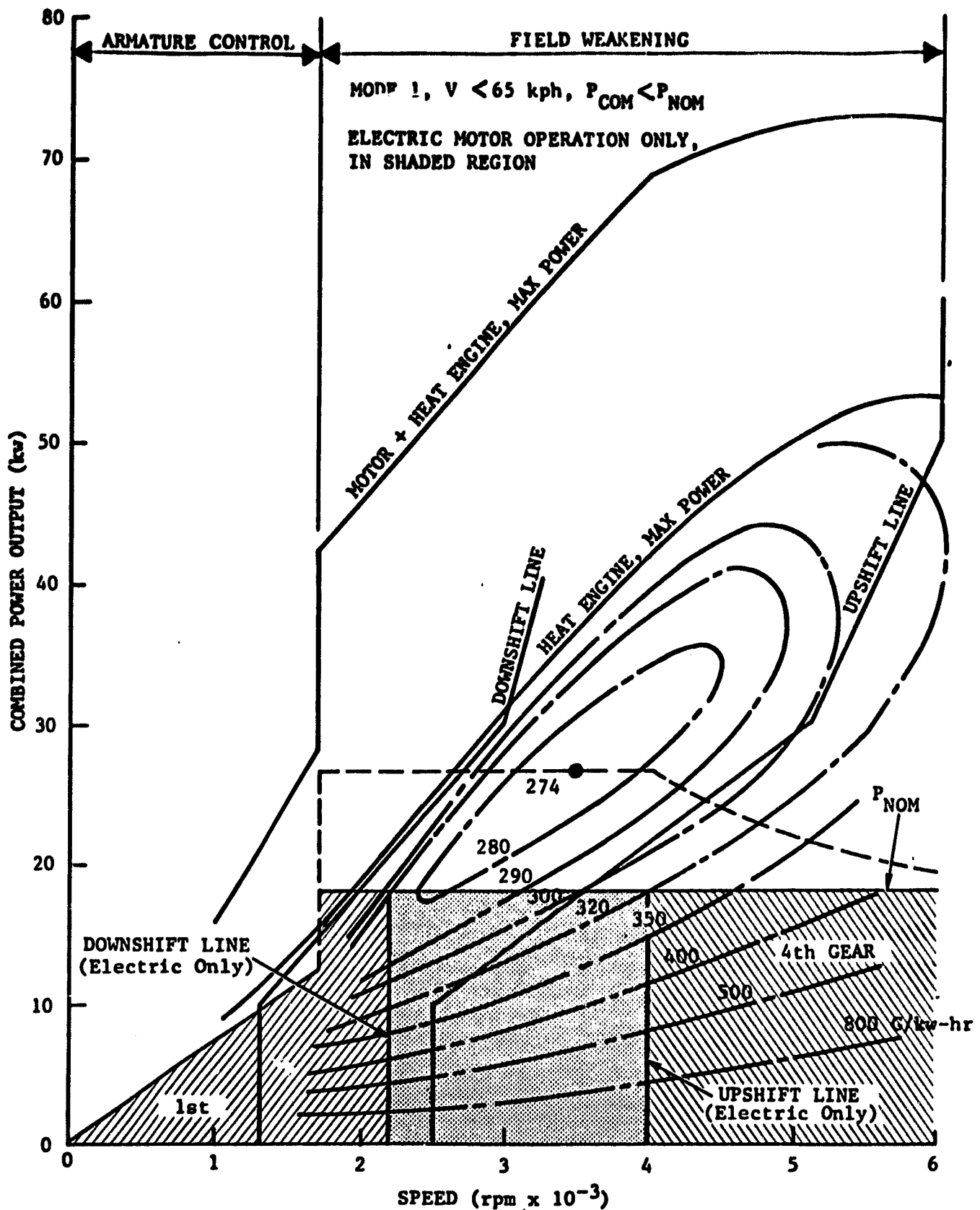


Figure 4-8 Hybrid Control Strategy (1)



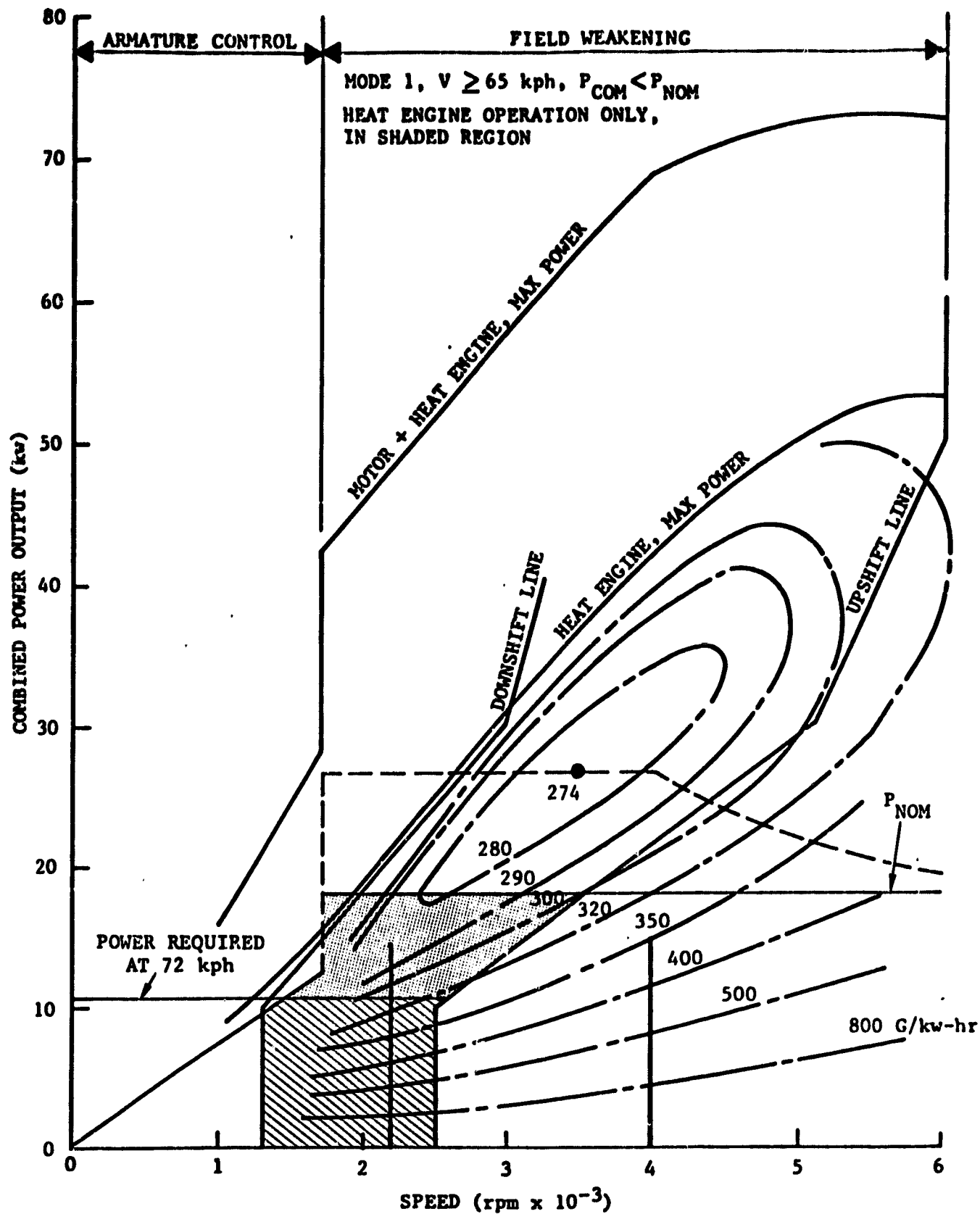


Figure 4-9 Hybrid Control Strategy (2)

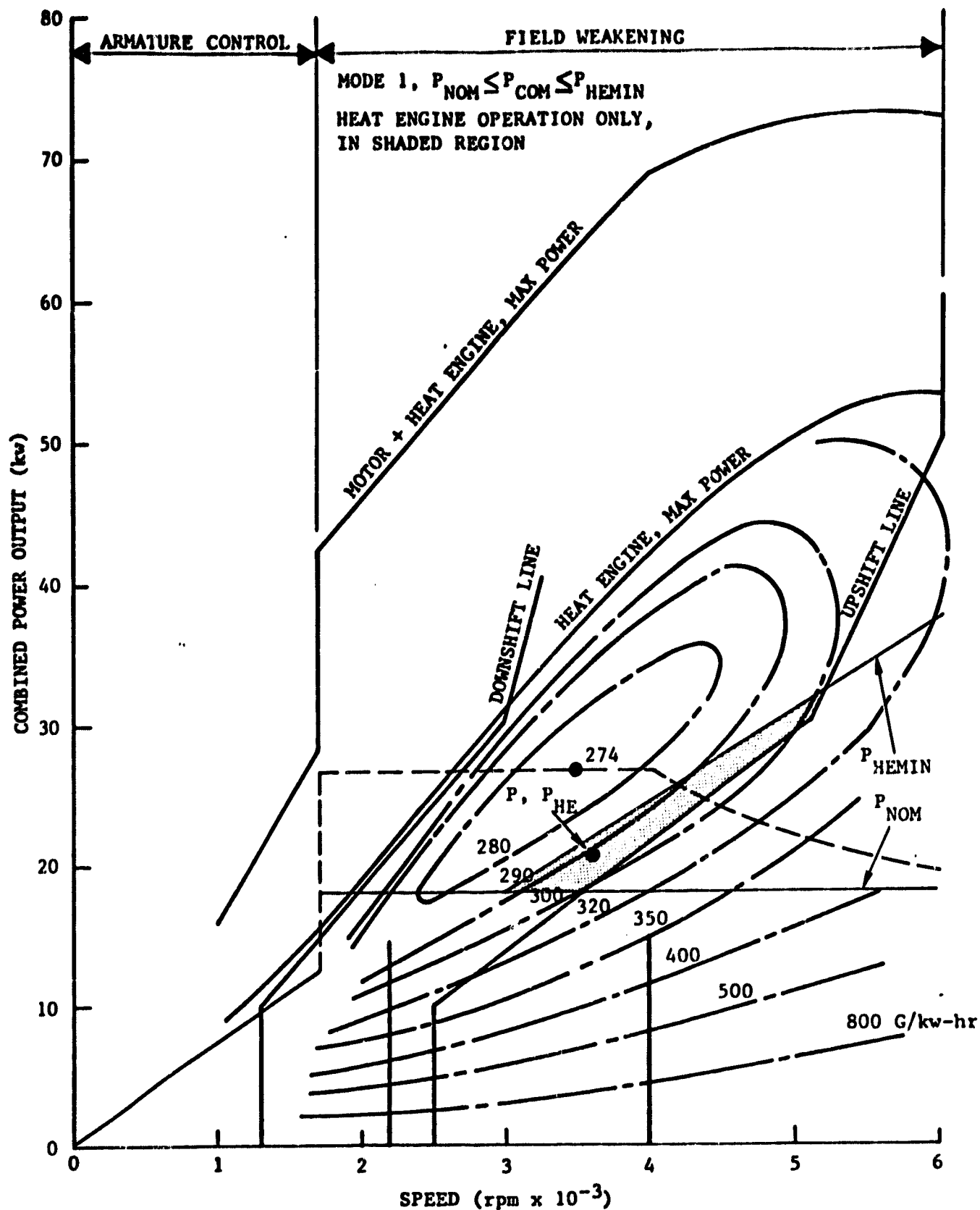


Figure 4-10 Hybrid Control Strategy (3)

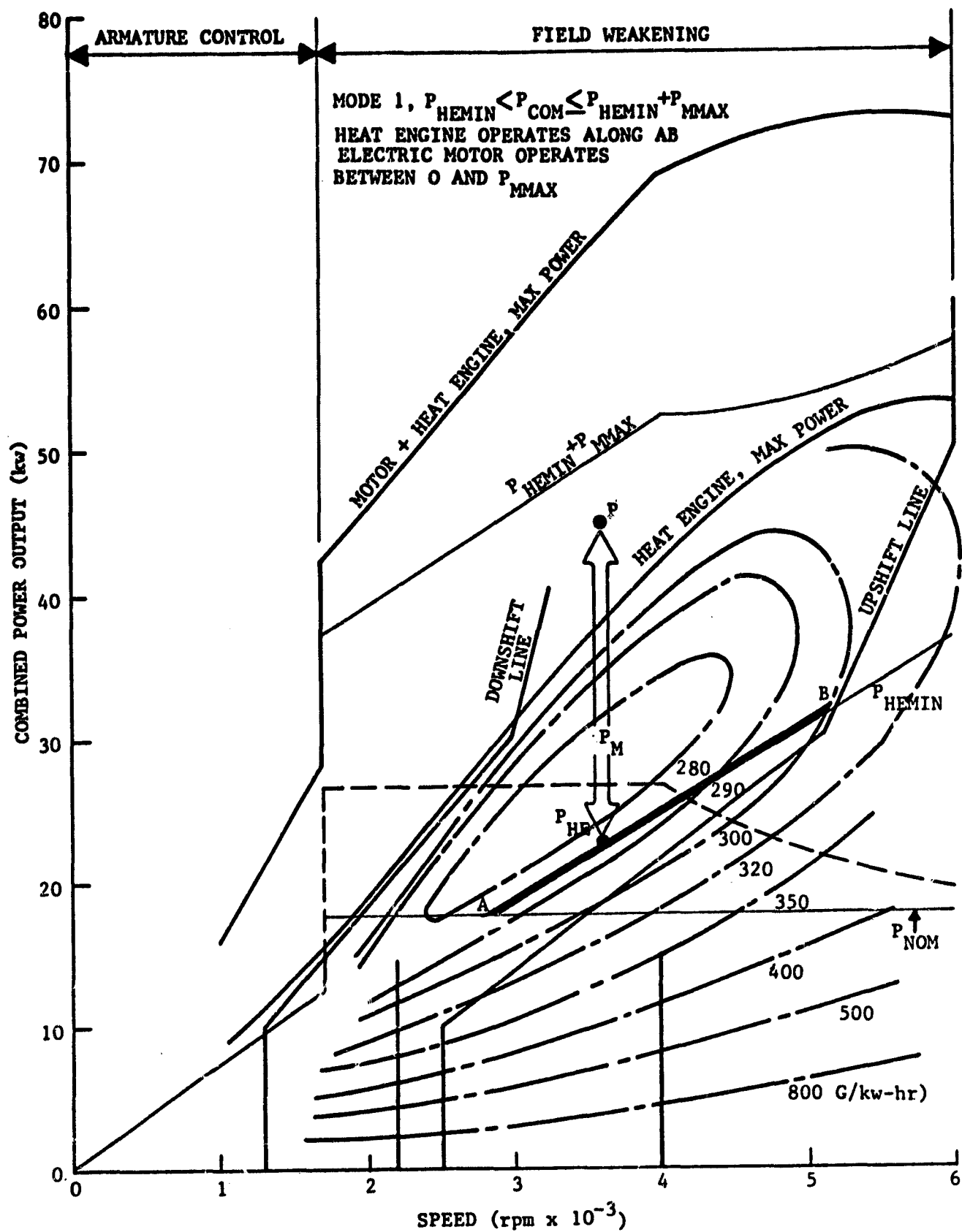


Figure 4-11 Hybrid Control Strategy (4)

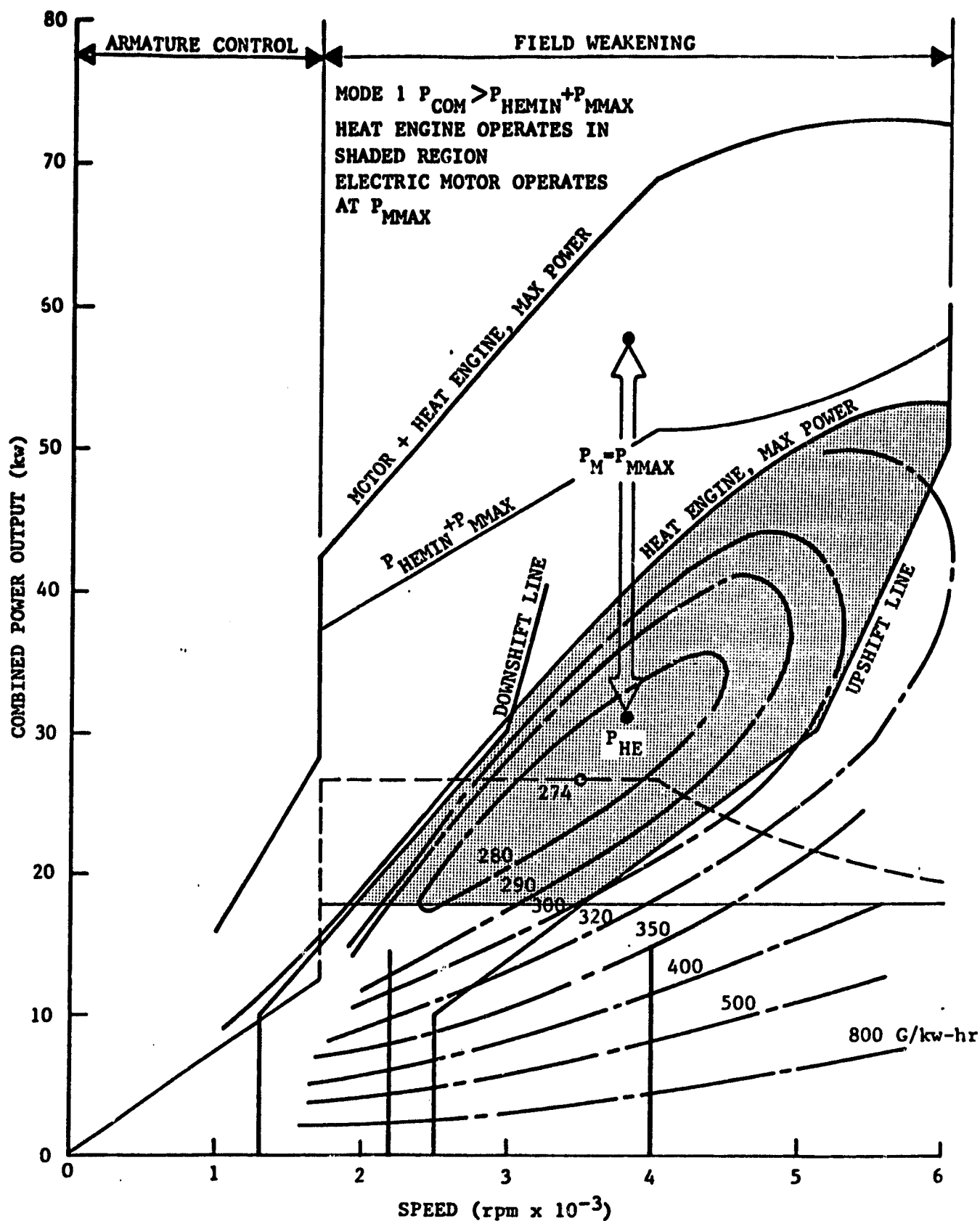


Figure 4-12 Hybrid Control Strategy (5)

or within 30% of the minimum bsfc of 274 g/kw-w. The battery sustained specific output is kept below about 52 w/kg.

Figure 4-10 illustrates what happens on Mode 1 if the system demand  $P_{COL}$  exceeds  $P_{NOM}$ . At this point, we have to introduce another control parameter  $P_{HEMIN}$ , which is the power corresponding to the torque at which it would be desirable to operate the heat engine. Note that  $P_{HEMIN}$  corresponds to about 2/3 maximum load on the heat engine, and runs quite close to the minimum bsfc region for the engine. If the power demand is between  $P_{NOM}$  and  $P_{HEMIN}$ , the electric motor idles and the heat engine picks up the total load. Normally, the heat engine will be operating within the heavily shaded region, although, in fourth gear there is the possibility of operating to the right of the region. In this region, the bsfc is below 310 g/kw-hr, or within 15% of the minimum. This region, combined with the one shown in Figure 4-9, encompasses the road load power requirement (at 0 grade) from 72 kph up to 100 kph; consequently, during normal highway travel, the heat engine will be operating continuously, even on Mode 1.

The situation which occurs if the total power demand exceeds the  $P_{HEMIN}$  line is illustrated in Figures 4-11 and 4-12. In this case, the heat engine remains on the  $P_{HEMIN}$  line; and the difference is made up by the electric motor as long as the difference does not exceed the maximum available motor power,  $P_{MMAX}$  (Figure 4-11). Along this line, the bsfc stays within 10% of its minimum value. If the difference between the power demand and the  $P_{HEMIN}$  line exceeds the maximum available motor power, then the motor operates

at its maximum and the heat engine operating point moves above the  $P_{HEMIN}$  line. (Figure 4-12 )

A question which arises, with respect to the transition between those operating regions in which the engine is off and the regions in which it is operating, concerns the amount of hysteresis or deadband which must be introduced to avoid 'hunting'; i.e., cycling back and forth between engine off and engine on under certain driving conditions. This is something which will have to be determined experimentally; however, it is clear that the  $P_{NOM}$  line and the transition speed will both have to be adjusted upward by some increment while the engine is off, and adjusted downward by an increment while the engine is on to provide the necessary deadband. The discussion we have just given, and the situation illustrated in Figures 4-8 through 4-12 , consequently, represent average conditions.

Operation in Mode 2 is a little simpler than Mode 1. In this case, the heat engine operates if the system power demand exceeds a line corresponding to a minimum motor torque. This line is shown as  $P_{HEMN2}$  , Figure 4-13 . For power demands below this line, the total system demand is supplied by the motor, as indicated in Figure 4-13 . Above this line, and provided the power demand does not exceed the maximum available heat engine power  $P_{HEMAX}$  , the electric motor idles at the same speed as the heat engine and the heat engine supplies the total requirement, as shown in Figure 4-14. If the demand exceeds  $P_{HEMAX}$  , the heat engine operates at its maximum and the motor makes up the difference (Figure 4-15 ). The

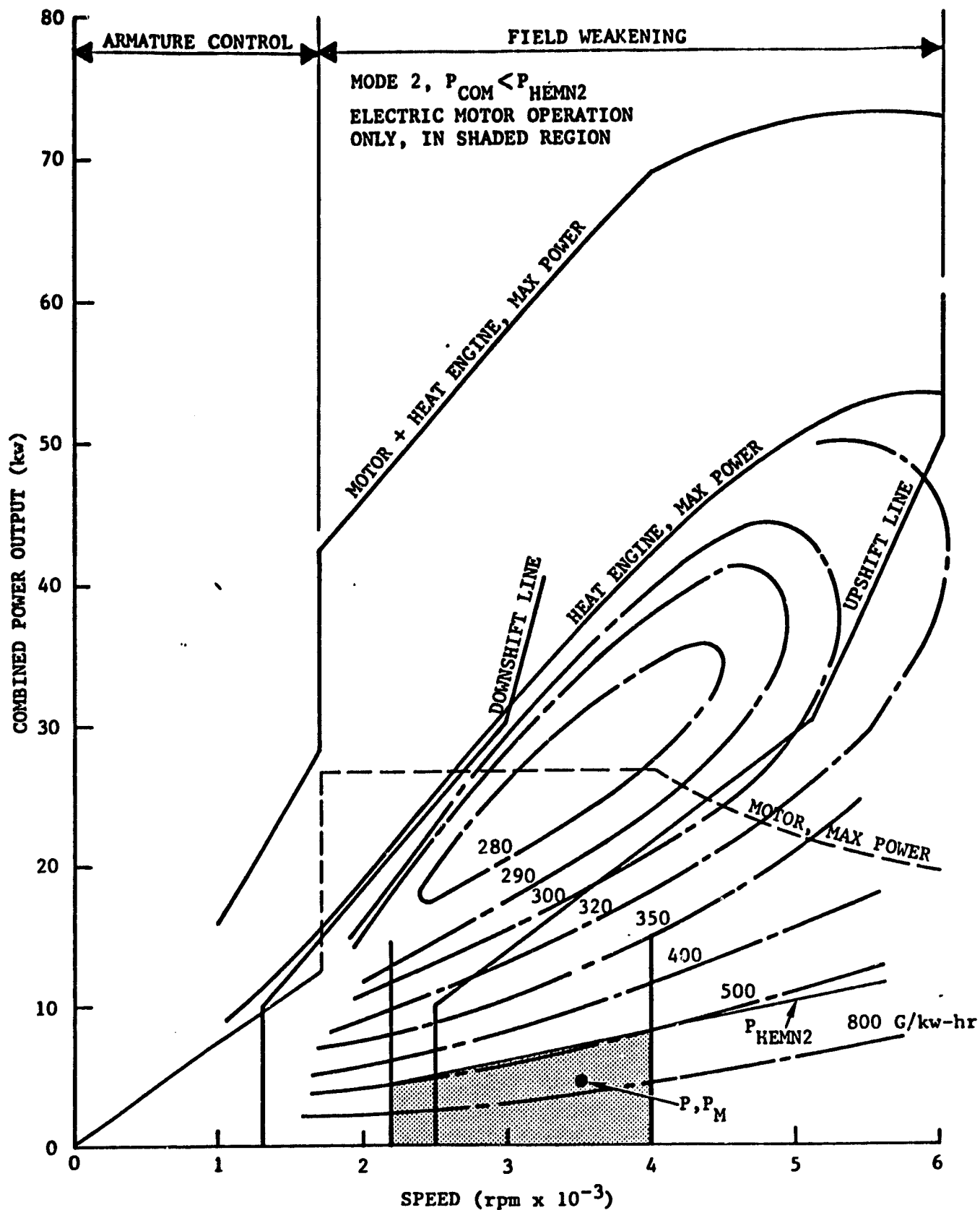


Figure 4-13 Hybrid Control Strategy (6)

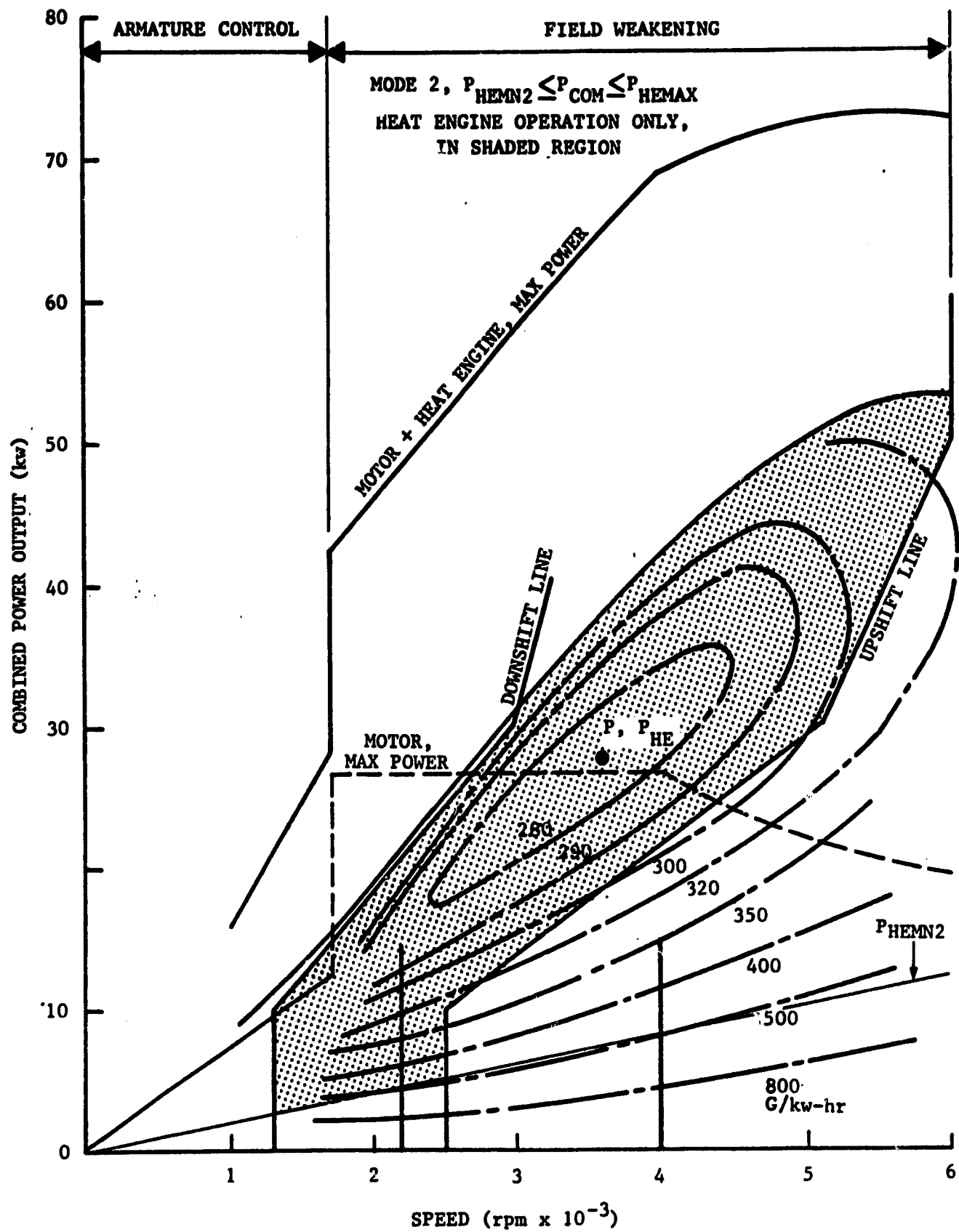


Figure 4-14 Hybrid Control Strategy (7)



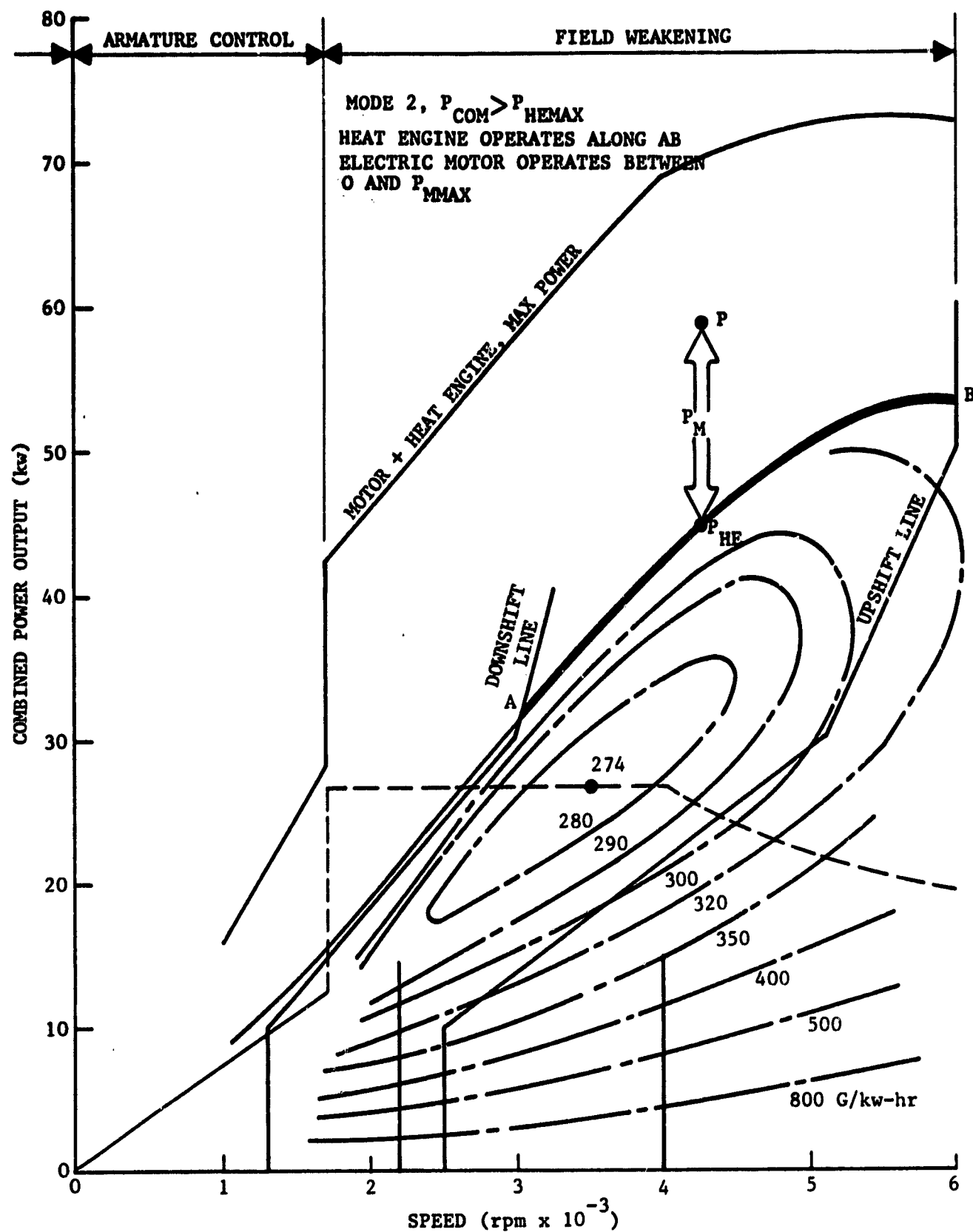


Figure 4-15 Hybrid Control Strategy (8)

PRECEDING PAGE BLANK NOT FILMED it is original missing.

above the discharge limit. Since Mode 2 operation involves more nearly continuous engine operation at fairly heavy load, except while the vehicle is idling or braking, it would provide a rapid warmup. The only difficulty with the scheme is if the average engine loading on Mode 2 is too high for warmup operation. If this is the case, it is a simple matter to adjust the engine and motor power commands in a way which is similar to the method for adjusting these commands when the battery drops below the discharge limit on Mode 2. In the case of the warmup operation, the heat engine power command would be adjusted downward from its normal Mode 2 value, and the motor command adjusted upward.

Whether such adjustments are necessary will have to be determined experimentally. Under the assumption that they are not necessary, a series of runs were made with HYBRID2 to estimate the fuel economy penalty which would result if a fixed distance were driven every day with the vehicle operating on Mode 2 during warmup. The results are summarized in Figure 4-16. They indicated a loss of about 2.5% in fuel economy for every 2 km of warmup distance, with the rate of loss increasing with warmup distance.

We must point out that this is not the loss associated with the richer mixture ratio and higher lubricant viscosities, which normally occurs when the engine is cold. This occurs with both the hybrid and a conventional vehicle; and there is not much that can be done about it in either case, apart from choosing the best available lubricants and calibrating the engine properly. The loss shown in Figure 4-16 is over and above this value and occurs as

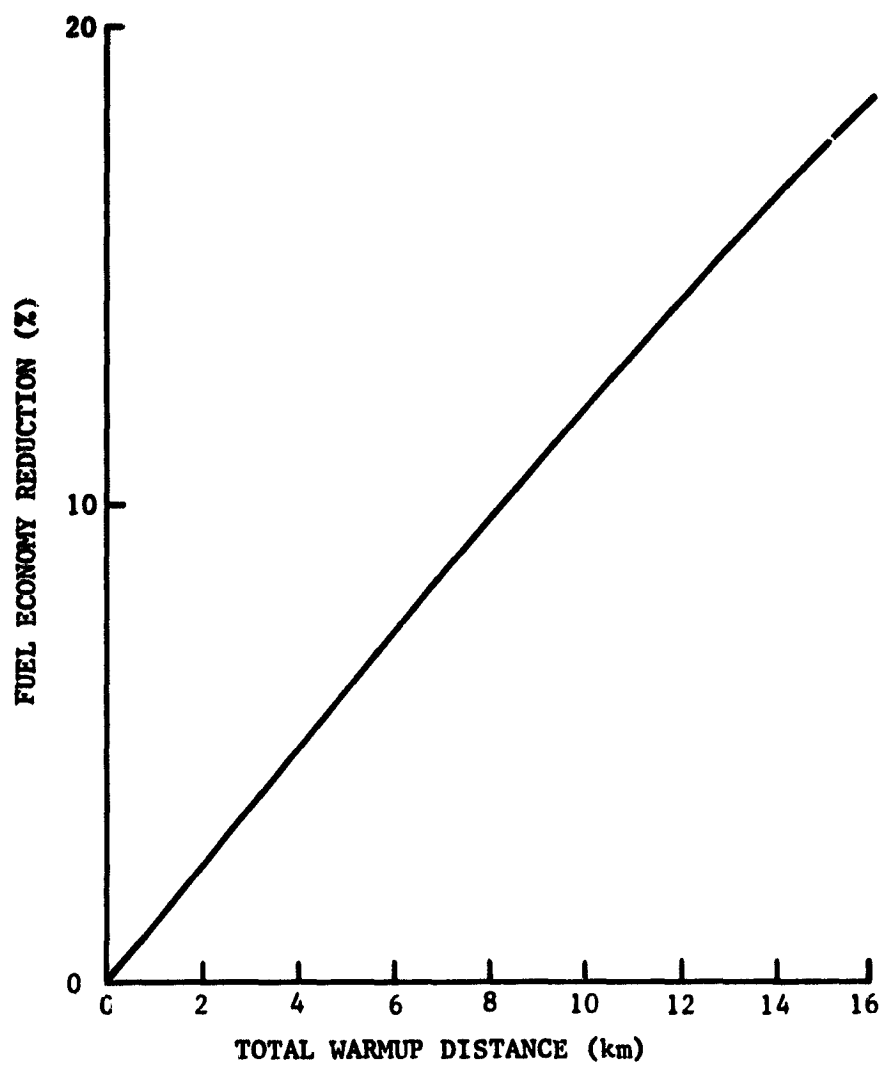


Figure 4-16 Effect of Using Mode 2 Operation  
for Warmup on Fuel Economy

a result of the fact that the amount of operation on Mode 1 is cut back on those days for which daily travel is less than the warmup distance plus the normal operating range on Mode 1.

#### Control Strategy Optimization

In this section, we shall describe the process by which we arrived at the control strategy and control parameter values just described. Optimization of the control strategy involved both modification of the strategy itself and variation of the control parameters to determine an optimum set. The starting point for this process was the control strategy developed in Task 2 and described in the Task 2 report.<sup>(1)</sup> In essence, this strategy was identical to that just described, with the following exceptions.

- There was no lower limit on heat engine power level in Mode 2.
- Transmission shift points were based only on the system power demand, and whether or not the heat engine is operating.

The first modification made to this strategy was to optimize the shift strategy so that the shift speeds are determined by the engine power command rather than the total system power command. The shift strategy was constructed by laying out upshift and downshift lines on the engine bsfc map which satisfied the following conditions:

- They followed as closely as possible the same line of constant bsfc.

- This line of constant bsfc was as close as possible to the minimum bsfc.
- They would provide the capability of attaining the maximum available engine torque, from a speed less than the peak torque point to a speed slightly greater than the peak power point.
- They would not permit the engine speed under power to drop into a region in which engine operation would not be smooth.
- Enough hysteresis or deadband would have to be provided between upshift and downshift points so that, with the maximum gear ratio gap, there would be no hunting back and forth between gears under certain loading conditions.

The lines which satisfied all of these conditions are shown in Figure 4-17. They follow the 300 g/kw-hr line fairly closely, and then deviate to provide adequate hysteresis, allow maximum torque to be attained, and prohibit lugging.

The Mode 1 control parameters  $T_{EOMIN}$  (minimum heat engine operating torque),  $P_{NOM}$  (max motor power under electric-only operation), and  $V_{MAX}$  (transition speed) were then varied systematically to determine the best combination of values.  $T_{EOMIN}$  was varied from 40 to 60 N-M. It was found that the yearly average fuel economy rose at a declining rate as  $T_{EOMIN}$  increased. It will be noted that on Figure 4-17 that 60 N-M falls very close to the minimum bsfc of the heat engine and corresponds to about 2/3 maximum load. For these reasons, and to avoid loading the engine too heavily, 60 N-M was taken as the maximum value for  $T_{EOMIN}$ . A subsequent run at 70 N-M showed a drop in fuel economy from the 60 N-M value, indicating that 60 N-M is near optimum.

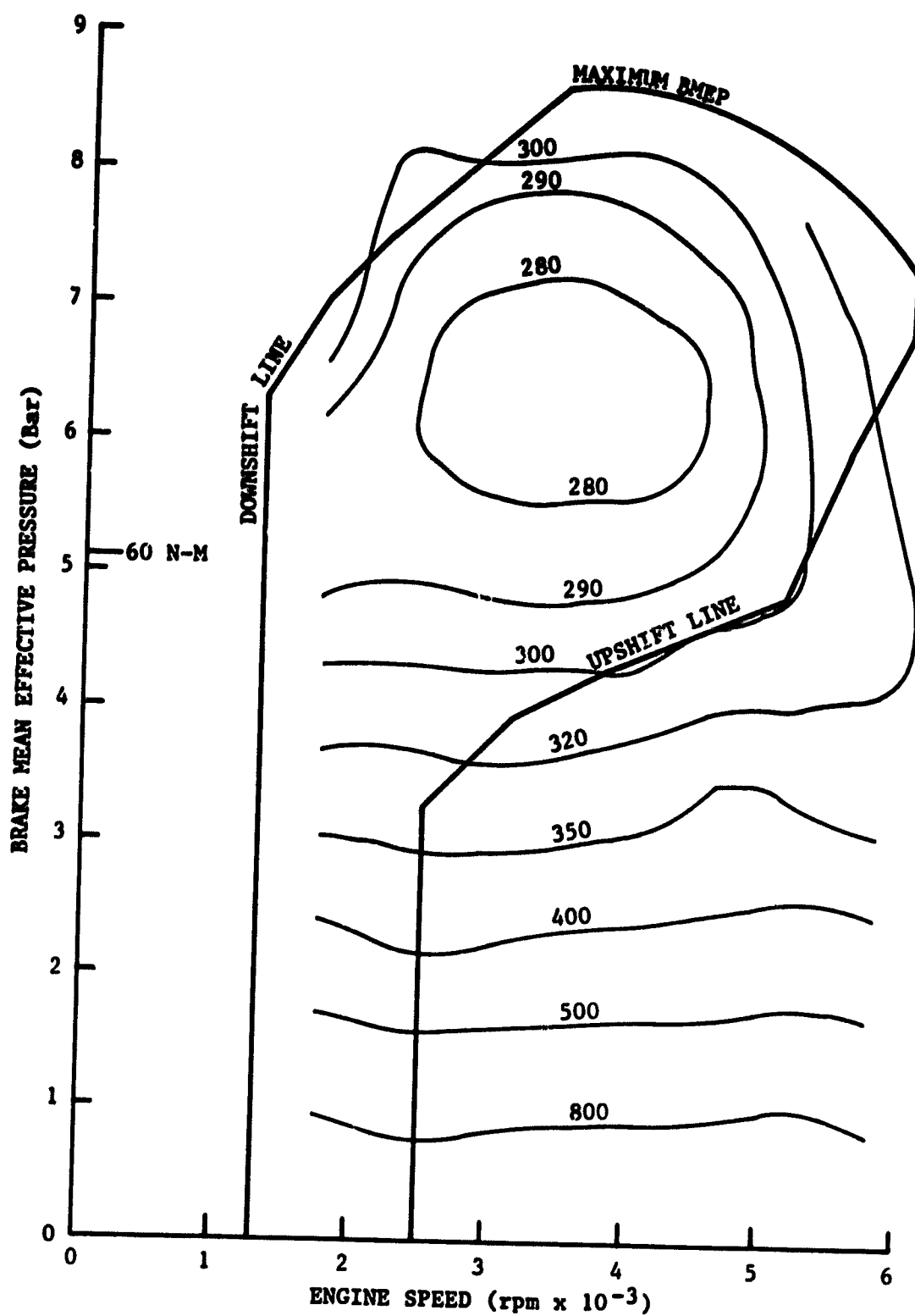


Figure 4-17 Shift Strategy

The next parameter to be chosen was  $P_{NOM}$ . This was varied from 10 to 20 kw. A maximum in fuel economy was found at about 18 kw, which is slightly over the nominal motor rating. Although it would appear that the yearly average fuel economy should continue rising as a wider range of all-electric operation is permitted by raising  $P_{NOM}$ , this is not the case. As  $P_{NOM}$  is raised, the battery works at higher specific power levels, and the available energy drops. The resultant drop in Mode 1 operating range thus eventually negates any gains in Mode 1 fuel economy due to operating the electric motor more. A side benefit of a low value of  $P_{NOM}$  is that the motor is very rarely operated beyond its nominal power rating, and consequently we would expect excellent motor life.

An effect similar to the above was noted when running variations in  $V_{MAX}$ . A maximum in fuel economy was attained somewhere in the 70-80 kph range, although the sensitivity in this range was very slight. Transition speeds below this value resulted in lower fuel economy numbers because of increasing heat engine operation in a region of high bsfc. In the 70-80 kph range, the high battery loading with consequent reductions in available energy and Mode 1 operating range was apparently just enough to cancel the fuel economy benefit resulting from a lower average bsfc.

A summary of the variation in yearly fuel economy with respect to both Mode 1 and Mode 2 control parameters will be found in Figure 4-19 following the discussion of Mode 2 operating parameters.

Before settling on the Mode 2 strategy described in the previous section, a couple of alternatives were tried, both of which were aimed

at reducing the amount of time which the heat engine spent at light load and high bsfc. The first alternative was the one described previously; i.e., the heat engine is not operated for system power demands below a value  $P_{EOMN2}$  corresponding to a torque threshold,  $T_{EOMN2}$ . During periods when it is on, an adjustment of the heat engine power level is made to compensate for the withdrawal of battery energy at system power demands below the torque threshold. The second alternative involved operation of the heat engine whenever the system power demand is positive. For system demands below the torque threshold, the excess heat engine power goes into charging the batteries. During periods when the system demand is above the threshold, a downward adjustment is made to the heat engine power level to permit the energy stored during low system demand periods to be withdrawn, thereby maintaining the battery discharge level at the discharge limit  $D_{BMAX}$ .

The first of these two alternatives turned out to be marginally better than the second. The reason for this is that the average heat engine bsfc is slightly lower in the first case. The engine operates less for the first alternative but supplies the same total amount of energy; the average loading is thus higher and the bsfc lower.

The first alternative was, consequently, selected for the basic control strategy. Variation of the threshold torque  $T_{EOMN2}$  indicated a continuous increase in fuel economy with increasing  $T_{EOMN2}$ . The value of  $T_{EOMN2}$  was, therefore, set based on keeping the upward adjustments of the heat engine power level, which are required to keep the battery state-of-charge from continuously declining, down to reasonable values. A value of 20 N-M was selected.



The selection of the final control parameter  $D_{BMAX}$ , which determines the transition between Mode 1 and Mode 2 operation, must be based on meeting gradeability requirements as well as on a trade-off between fuel economy and battery life. The variation in yearly average fuel economy with  $D_{BMAX}$ , as well as the other control parameters, is shown in Figure 4-19. Clearly, the greater the battery discharge limit, the better the fuel economy. On the other hand, the Task 2 studies indicated that the drop in battery life associated with operation to high depths of discharge outweighed, from a cost standpoint, the fuel economy gain. At this point, let us introduce the effect of gradeability. In Figure 4-20, points are plotted representing the combined engine and motor power requirements for the grades and speeds indicated in the legend. The gears shown in the legend are the normal ones in which the indicated grade would be climbed at the indicated speed for Mode 2 operation. Figure 4-20 shows that the distances that an 8% grade could be climbed at 65 kph, and 3% grade could be climbed at 90 kph, are indefinite; i.e., no net energy withdrawal is required from the battery to maintain these speeds on these grades. The 5%, 90 kph condition requires a little help from the batteries; the other two, substantially more. Assuming that the curve of specific energy vs. specific power shown in Figure 4-49 is correct for nickel-iron batteries, the additional fractional depletions beyond the battery discharge limit which would occur in climbing these grades for the distances specified in the Task 1 report<sup>(2)</sup> are as follows:

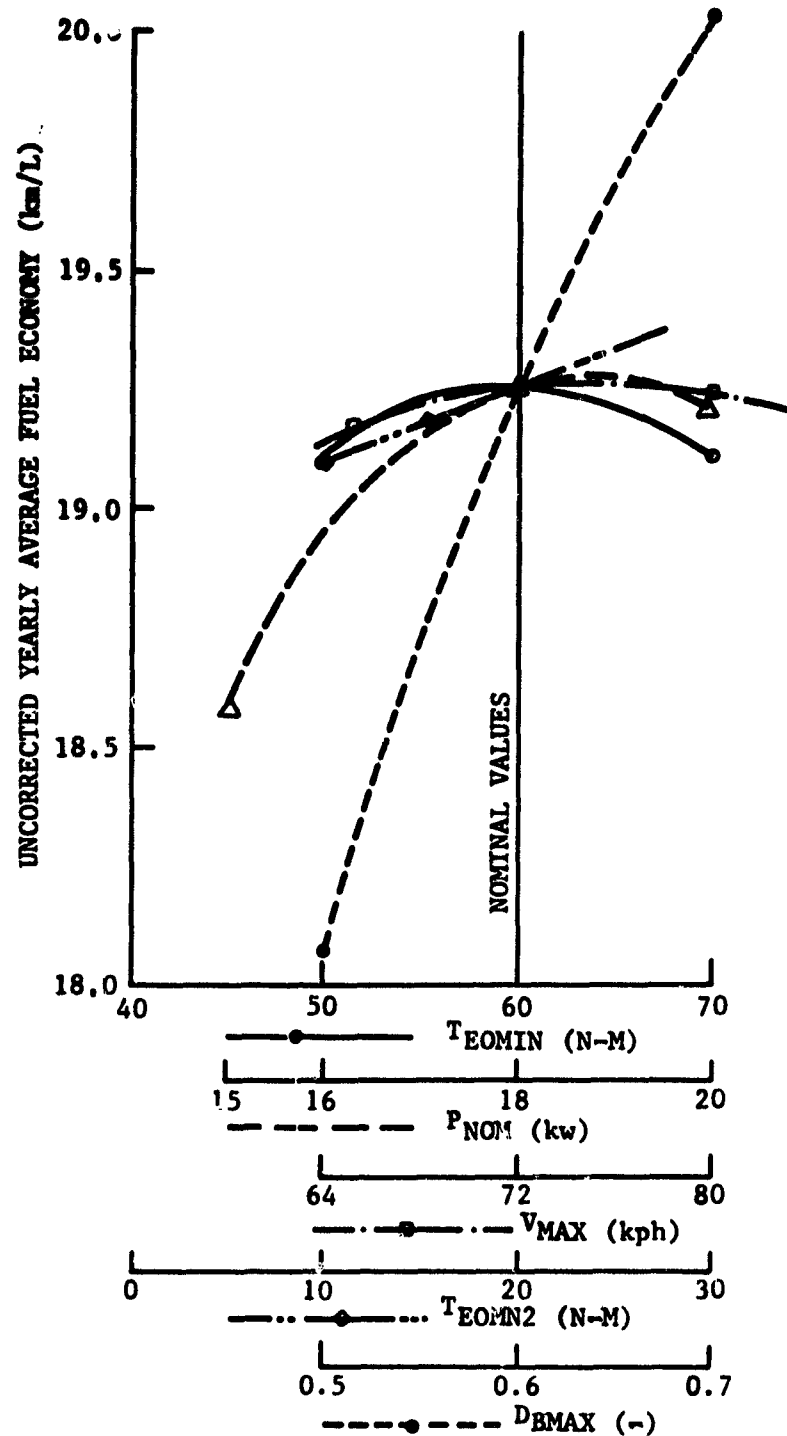


Figure 4-19 Variation in Fuel Economy with Control Parameters

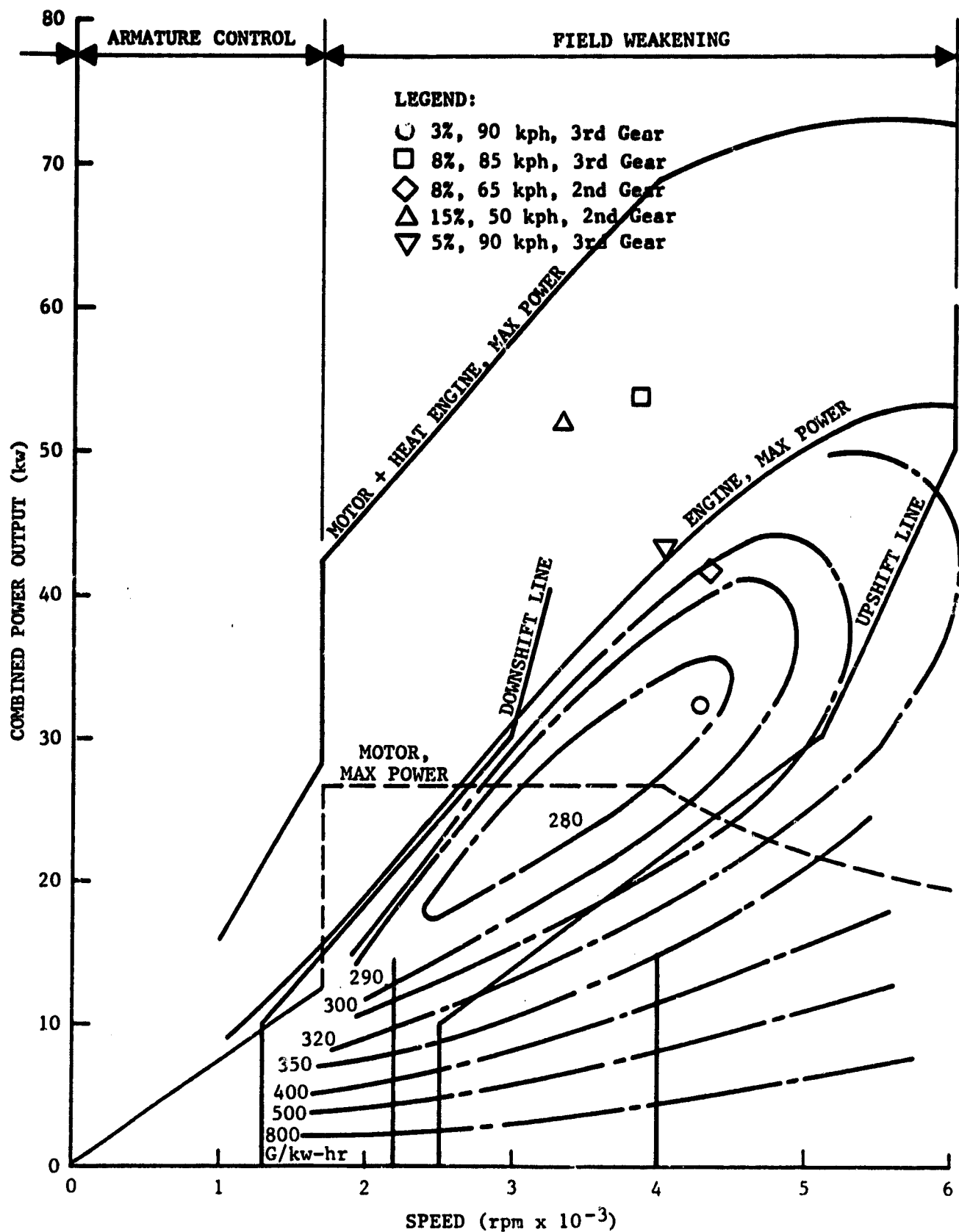


Figure 4-20 Power Requirements on Grades

5%, 90 kph, 20 km	-	.027
8%, 85 kph, 5 km	-	.134
15%, 50 kph, 2 km	-	.134

The critical conditions here are the 8%, 85 kph and 15%, 50 kph ones. In these cases, if a maximum depth of discharge of .9, say, is not to be exceeded, the batteries must start out not discharged above about .76. This fixes an absolute lower bound on  $D_{BMAX}$  if the gradeability requirements are to be met.

To summarize, the factors of life cycle cost, fuel economy, and gradeability drive the value of  $D_{BMAX}$  toward the following:

Life cycle cost	-	near 0
Fuel economy	-	1.0
Gradeability	-	.76

In view of the fact that the ISOA nickel-iron batteries are as yet uncharacterized in terms of the variation of life with depth of discharge, and little performance data is available for discharge rates other than the 3-hr rate, it is purely a matter of guesswork at this point as to what really constitutes the best overall choice for the value of  $D_{BMAX}$ . Our guess is that it would be between .6 and .7, with the .6 end of the scale being favored if the cycle life drops off with increasing depth of discharge at about the same relative rate as for lead-acid batteries, and the .7 end being favored if the drop-off in cycle life is not so rapid. A further discussion of the impact of the unknowns about batteries will be found in Section 4.1.7, Batteries and Charger.

A similar gradeability analysis was performed for lead-acid batteries, which are regarded as the best backup to the nickel-iron system. These calculations were performed for a 341 kg battery pack with the performance characteristics shown in Figure 4-49. In this case, the additional fractional depletions associated with the grade/speed/distance combinations requiring withdrawal of battery energy were as follows:

5%, 90 kph, 20 km	-	.053
8%, 85 kph, 5 km	-	.247
15%, 50 kph, 2 km	-	.269

Thus, for the case of the lead-acid battery, a maximum value which could be set for  $D_{BMAX}$ , if a DOD of .9 is not to be exceeded, would be .631. In the lead-acid case, then, the range of possibilities for  $D_{BMAX}$  is a little less; and we would select a value of .6 as a starting point for development.

If we apply the factor of .88 to the uncorrected fuel economy numbers in Figure 4-19, as discussed previously in connection with the reference vehicle, we come up with a fuel economy of the NTHV in the range from 16.9 to 17.6 km/l (40-41.5 mpg), with nickel-iron batteries, depending on what value of  $D_{BMAX}$  (between .6 and .7) is eventually used. The lower of these two values is not significantly different than the 16.5 km/l (39 mpg) projected in the Task 2 report, also for  $D_{BMAX} = .6$ . Consequently, the question can legitimately be asked, how come such a small improvement if we were continuing to optimize the control strategy? The answer to this lies primarily in the fact that the battery modelling techniques used in the computer simulation HYBRID 2 have changed considerably, as described

in Section 2; and the change is in a direction to give much more conservative results. We think, based on the fact that these techniques provide good results in modelling the SCT electric vehicle, that they are more realistic than the earlier method of just looking at the cycle average specific power to determine specific energy. Unfortunately, for nickel-iron batteries in particular, the needed data is just not there at anything but the three-hour rate; and much higher power levels are encountered in performing accelerations on the urban driving cycle. Consequently, the results that we have just given are dependent on the shape of the Ragone plot in the high power region, which is purely a guess at this point.

Surprisingly, however, this dependence is not too strong. When a run was made in which the slope of the curve was changed from  $-2.26$   $(2/\text{kh})/(2\text{-hr/kh})$  to  $-2.58$ , the increment in the uncorrected annual fuel economy was only  $.05$  km/l; rather insignificant. An alternative which was also investigated was to modify the control strategy to limit battery peak power. This change terminated the upper end of the distribution of battery power at about  $20$  kw, which compares to about  $32$  kw with the basic control strategy. However, it also meant working the heat engine harder; and the net increment in fuel economy was only  $.01$  km/l.

The fact that the variation in fuel economy is rather small when some of the system parameters are changed significantly indicates that we are pretty close to an optimum strategy. Obviously, further optimization in Phase II will be required once heat engine and battery characteristics are better defined; and the control strategy discussed previously should not be looked at as the final

word, either in terms of structure or actual parameter values. However, it is clear at this point that it has the basic elements required to achieve a highly fuel efficient vehicle, provided acceptable emission characteristics can also be achieved.

Any conclusion to be drawn regarding the in-use fuel economy of a hybrid incorporating such a strategy must be hedged with all sorts of caveats, relating to battery characteristics, warmup requirements, relationships between real world usage and the driving cycles with respect to which the optimization was done, and so forth, all of which must be obvious to the reader by now. That being said, it appears that a NTHV employing the elements of the basic control strategy just described could achieve an in-use fuel economy in the 16.9 to 17.6 km/l range, depending on the specific value of  $D_{BMAX}$  used. The corresponding wall plug energy values would be in the .177 to .187 kw-hr/km. An indication of the extent of optimization and overall efficiency which these numbers represent is given in Table 4-2. Note that the total energy consumption, as well as petroleum energy consumption, is less than the reference vehicle; also, that the minimum attainable heat engine bsfc for the assumed engine characteristics is 274 g/kw-hr, so the average values are very close to the minimum attainable.

#### Backup Control Strategy

As discussed in Section 3, the magnitude of the problems which will be encountered in attempting to control emissions is not foreseeable. That being the case, it would be well to have a backup strategy which involves fewer heat engine startups and shutdowns.

Table 4-2 . FUEL AND ENERGY CONSUMPTION FOR HYBRID  
AND REFERENCE VEHICLES (for .6 - .7 battery  
discharge limit)

	<u>Hybrid</u>	<u>Reference Vehicle</u>
1. Average Heat Engine BSFC on Urban Cycle (g/kw-hr)		
Mode 1	297	-
Mode 2	310	520
2. Average Fuel Economy (km/l)	16.9 - <u>17.6</u>	7.65
3. Average Wall Plug Energy Consumption	.117 - <u>.187</u>	-
4. Average Total Energy (1) Consumption (kw-hr/km)	1.202 - <u>1.210</u>	1.371
5. Average Petroleum Energy (2) Consumption (kw-hr/km)	.708 - <u>.688</u>	1.371

(1) Computed as the energy equivalent of the total crude oil required at the refinery input, under the assumption that all the input energy comes from crude oil, and under the following assumptions:

Refinery/distribution efficiency =	.93 (fuel oil)
	.84 (gasoline)
Electrical generation efficiency =	.36
Electrical distribution efficiency =	.91

(2) Same as (1), except the assumption is made that only 15% of the electrical energy generation comes from petroleum.



Such a strategy would still shut the heat engine down during idle and braking periods; however, it would be running at all other times. Consequently, the transition speed is no longer used as a control parameter; and Figures 4-8 and 4-9 are replaced by Figures 4-21 and 4-22. If the system power demand is less than the power  $P_{HEMN1}$ , which is the power level corresponding to a constant light torque load on the engine, then the engine operates at  $P_{HEMN1}$ , and the excess engine power developed is used to drive the motor as a generator. (Figure 4-21) If the demand is between  $P_{HEMN1}$  and  $P_{HEMIN}$ , then the motor idles and the engine takes the full load. (Figure 4-22) If the demand is greater than  $P_{HEMIN}$ , the strategy is identical to that discussed previously and illustrated in Figures 4-10 through 4-12. Similarly, on Mode 2, the heat engine would be running the motor as a generator for power demands below  $P_{HEMN1}$ . In this case, operation is identical to the Mode 1 operation for the backup strategy, illustrated in Figure 4-21. For power levels above  $P_{HEMN1}$ , operation is identical to Mode 2 operation for the basic control strategy.

With this control strategy, it was found that the uncorrected yearly average fuel economy dropped from the 19.25 km/l obtained with the basic control strategy at  $D_{BMAX} = .6$ , 13.1 km/l, or a 32% decrease. This number is still 51% better than the fuel economy achieved by the updated reference vehicle. The actual difference in fuel economy between the basic and backup control strategies is likely to be somewhat less if the warmup distance required by the basic strategy is substantial. (Note that, since the backup strategy

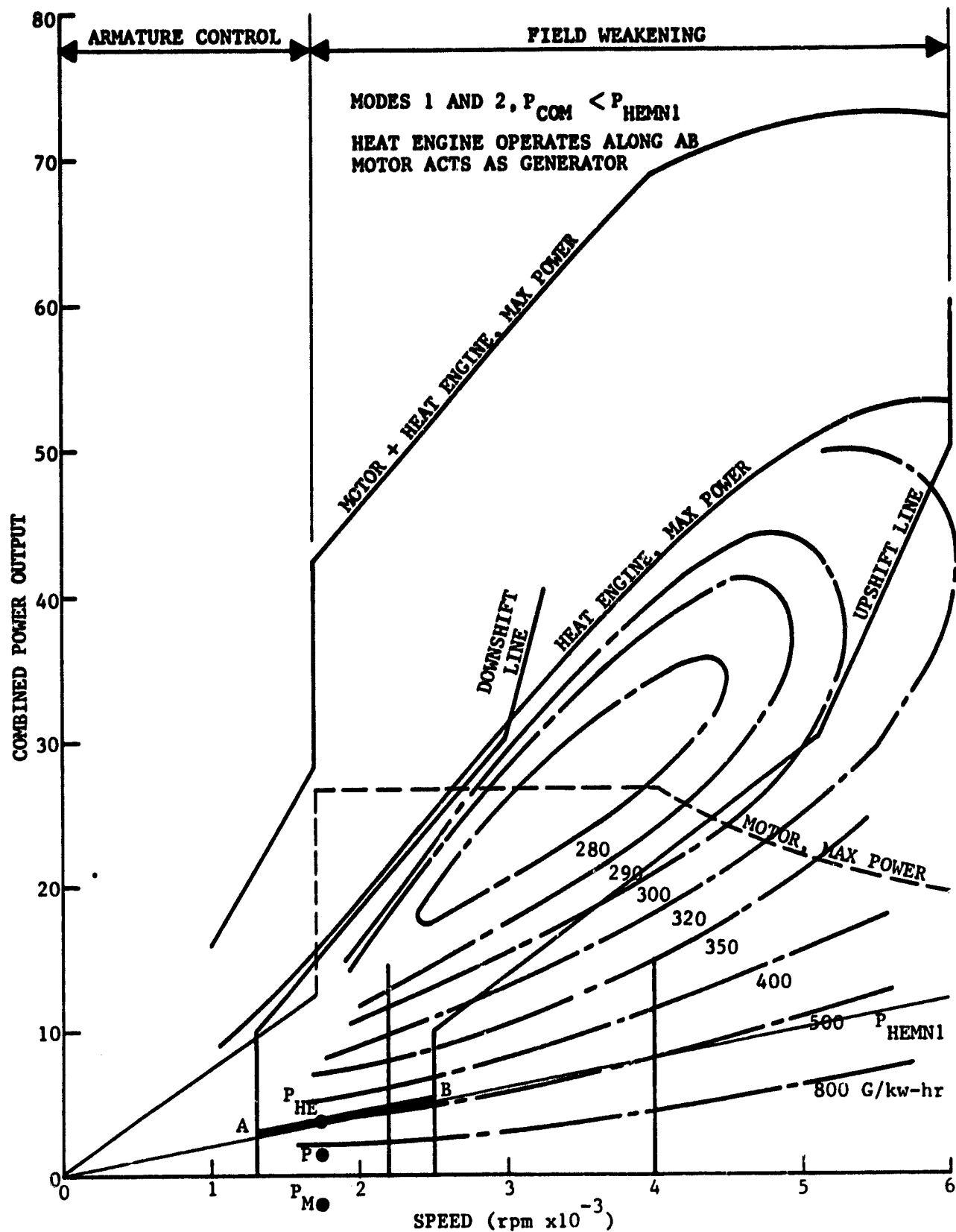


Figure 4-21 Backup Control Strategy (1)

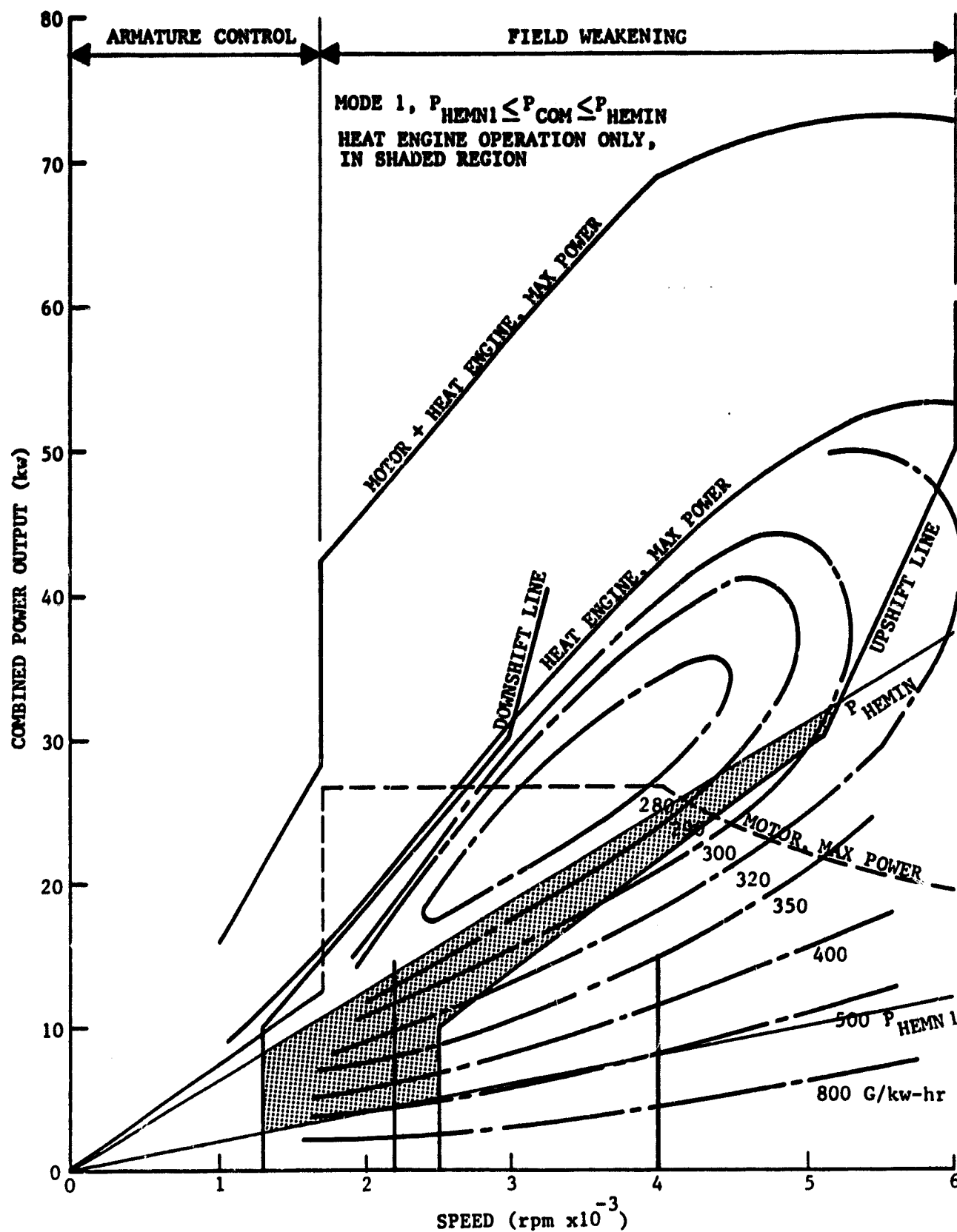


Figure 4-22 Backup Control Strategy (2)

involves nearly continuous operation of the heat engine even on Mode 1, it does not require a warmup period in which the mode of operation has to be different from its normal Mode 1 operation.) For example, if a typical warmup distance of 6 km per day is required, a reduction in uncorrected fuel economy to about 17.8 km/l is expected for the basic strategy; and the fuel economy penalty associated with the backup strategy would then be about 26%.

One area in which the backup strategy would offer a definite advantage over the basic strategy is in improved battery life, as a result of a lower average depth of discharge. (The fact that the fuel economy with the backup strategy is lower, is a simple corollary to this lower average depth of discharge, and hence, lower utilization of wall plug energy.) The Mode 1 operating range on the various composite driving cycles which comprise the yearly driving pattern is almost constant at about 275 km. The Mode 1 range, in fact, exceeds the corresponding daily travel on most days of the year; about 92 % of the annual driving is done on such days. In contrast, with the basic control strategy, the Mode 1 range varies from about 38 to 128 km; and only about 18% of the annual travel occurs on days for which the battery discharge limit is not reached. As a by-product of the consistency with which a vehicle operating on the basic control strategy reaches the battery discharge limit, it is easy to estimate the battery life for the basic control strategy (provided the cycle life vs. depth of discharge characteristics are known). Because of the variation in depth of discharge with the backup strategy, we have not attempted to quantify the improvement in battery life; however, it is clear that there is some.

### Strategy Modifications for Cold Weather Operation

Either of the strategies described previously will have to be modified somewhat for cold weather operation for two reasons. The first is to provide for passenger compartment heating and defrosting. Unless an auxiliary gasoline heater is provided, which seems like a needless waste of space and money, the engine will have to be operated enough to bring up the temperature of the passenger compartment reasonably and, more importantly, meet FMVSS defrost specifications. The second reason involves the possibility that the battery temperature might be very low as a result of previous storage conditions. Under such conditions, the propulsion battery could probably be depended on to start the engine but not provide propulsive power until its temperature was raised, which would have to be accomplished by using the heat engine to run the motor as a generator.

Under such conditions, the engine will have to be operated at a fast idle or lightly loaded by the motor when the vehicle is at rest, rather than being shut down. Under braking, fuel (but not ignition) would probably be shut off and restarted before the vehicle reached some minimum speed. Under conditions of positive system power demand, the cold weather strategy would be identical to the backup strategy, either on Mode 1 or Mode 2 depending on the battery temperature and state-of-charge.

No attempt has been made to quantify the effect on fuel economy of such a strategy modification. Obviously, it would vary widely depending on climatic conditions.

Importantly, the proposed basic control strategy and its related hardware and control mechanisms offers the flexibility to handle unique driving conditions without need for revising the strategy. Ambient temperature sensors and a sensor monitoring passenger compartment climate control functions can change or modify engine and motor operating cycles to provide occupant comfort with optimum fuel economy.

### Microprocessor Selection

As discussed in the Task 2 report, <sup>(1)</sup> implementation of the control strategy will require a microprocessor-based system controller. An overall functional block diagram of the system controller is shown in Figure 4-23. In the following paragraphs, we shall examine the key criteria on which the selection of a  $\mu$ P must be based and provide a list of available components which would satisfy the requirements of the NTHV.

#### 1. Technology Selection

Microprocessors are presently being produced by several different integrated circuit manufacturing processes. This section will briefly discuss the limitations/capabilities and tradeoffs between the major technologies. Points to bear in mind are:

- a) Is the inherent speed of the process (gate delay) fast enough?
- b) Is the logic density high enough to economically produce complex microprocessors?
- c) Is the inherent noise immunity adequate?
- d) Is the process capable of operating over an extended temperature range (-40 to +90 degrees C)?

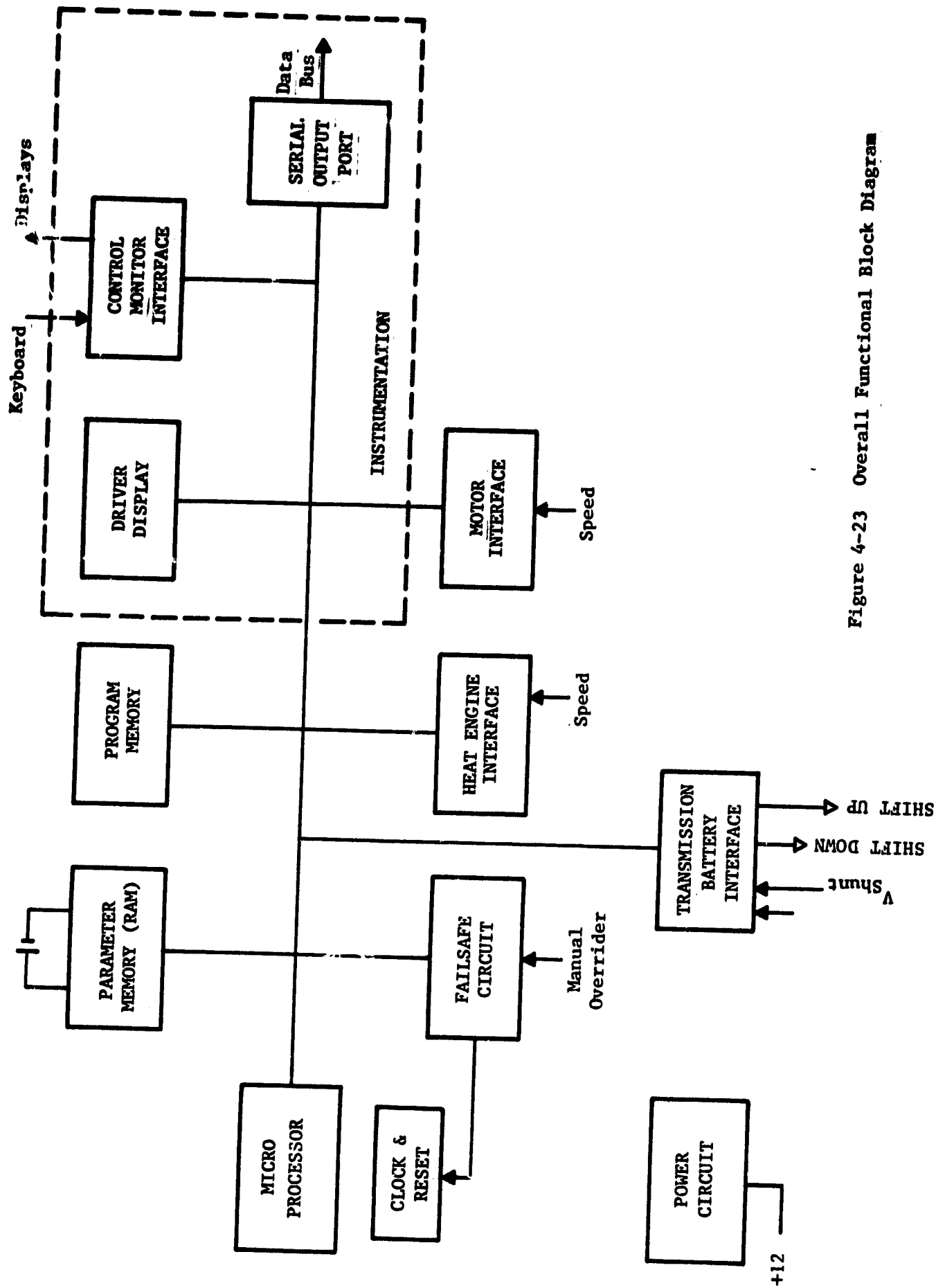


Figure 4-23 Overall Functional Block Diagram

e) Is the process mature and will it still be competitive in the next five years?

f) Are there any abnormal price considerations?

#### Bipolar Technology

Standard (Gold dope TTL). Gold dope ttl has been the standard discrete logic technology for the last seven years. Although there are many standard logic functions available in gold dope, there are no gold dope processors (except bit slice) available. Most new designs, especially LSI and processor circuits, requiring bipolar technology, utilize the other technologies described below. Although a processor could be built out of standard gold dope parts (i.e., 7400 family), the final design would not be price competitive.

Schottky(S TTL). The utilization of a Schottky clamping diode in the standard TTL structure produces a family of parts that are significantly faster than gold dope TTL. The penalty for the faster speed is higher power dissipation, a disadvantage for an automotive application. Presently, Schottky speeds greatly exceed the needs of most automotive applications. Schottky processors, such as the Signetics 8X300 are extremely fast, require expensive high speed memory, and would be a definite overkill for this application.

Low Power Schottky (LS TTL). Low power Schottky has a lower power dissipation and slower speed than the preceding two processes. Today it is one of the most popular standard logic family technologies available (74 LS Family). For



automotive applications, LS would be suitable. Power dissipation, speed, noise immunity, and operating temperature ranges are all acceptable. Today, the deficiency is that there are no suitable microprocessors utilizing this technology. Most of the presently available processors are aimed at the bit slice market and are not economical for an automotive controller.

Integrated Injection Logic ( $I^2L$ ). The  $I^2L$  process is a seven year old technology that expands on the capabilities of the standard bipolar processing. It is ideally suited for an automotive controller for several reasons: First,  $I^2L$  can achieve gate densities comparable to those of MOS circuits. Texas Instrument is presently manufacturing a 16 bit microprocessor (sbp 9900) which contains 6000 gates and 8000 bits ROM. Another major advantage of  $I^2L$  is its inherent capability of manipulating the speed/power ratio over a range of several decades. In one mode or the other,  $I^2L$  can operate faster than N channel MOS or can consume less power than CMOS. In some existing circuits today, the operating point can be selected as easily as varying the injector current into the circuit. Further speed enhancements (less than 5 nsec) will soon be realized by combining processing techniques such as ion implantation and Schottky clamping.

Environmentally,  $I^2L$  again is superior to other technologies. Tests have proven that  $I^2L$  to be more than twice as resistant to damage by spark discharges as an equivalent MOS/LSI circuit. Further,  $I^2L$  has been found to operate reliably at extended temperature ranges without additional restrictions.

The disadvantages of  $I^2L$  are few. First, although  $I^2L$  circuits have good noise margins internally, the internal levels must be translated (usually to TTL levels) to communicate outside the actual chip. This generally limits practical  $I^2L$  circuits to be self contained (all on one chip). Most  $I^2L$  circuits today are LSI. The second disadvantage at the present time is the non-availability of an 8 bit  $I^2L$  processor. Sixteen bit processors are presently being manufactured by TI (SBP 9900) and Fairchild (9440). Other  $I^2L$  vendors include Signetics and General Instrument.

In summary,  $I^2L$  technology is an ideal process that is mature and will continue to be enhanced in the foreseeable future. Unfortunately, there are no 8 bit  $I^2L$  processors today.

**Emitter Coupled Logic (ECL):** ECL is a bipolar process strictly oriented towards extremely fast speeds (less than 700 psec). Because of the extremely high power dissipation, low noise immunity, and very low circuit density (complexity), ECL would be inappropriate for an automotive controller.

#### MOS Technology

P Channel MOS (P MOS). P channel MOS is a process that was widely utilized in the early 70's. Today P channel usage is steadily declining, giving way to the advantages of N channel MOS. Disadvantages of P MOS include limited speed, multiple power supply requirements (3) and difficulty in meeting extended temperature requirements.

N Channel MOS (N MOS). N channel MOS today is by far the most widely utilized technology for the manufacturing of microprocessors and RAM circuits. Fabrication enhancements (HMOS, VMOS, 3  $\mu$  line width, etc.) have steadily broadened the capabilities of the N channel process. Both gate and memory densities are doubling every two years. Speed (gate delay) presently rivals that of bipolar technologies. Forecasts of future N channel capabilities predict continual improvements.

Because of this immense technological advancement and research in N MOS, most of the potential disadvantages for automotive usage have been removed. Speed is presently more than adequate. Power dissipation in most devices remains well under one watt. Circuit complexity is presently unmatched by any other technology. Extended temperature ranges do require special efforts in the design of the IC and are not standardly available for all products. Noise immunity is fair assuming adequate shielding and protection.

In summary, because of the popularity and lack of major disadvantages, N MOS is probably the prime choice for an 8 bit microprocessor.

Complementary MOS (CMOS). CMOS technology is a MOS process that utilizes both n- and p+ channel transistors connected in parallel. Because of the many advantages gained by using complementary logic, CMOS would definitely be suitable for an automotive application.

One of the major advantages of CMOS is its extremely high noise immunity. Its guaranteed noise margin of 1.5 volts makes it superior to any other technology. Another advantage is the low power dissipation. Although power dissipation increases with speed, power dissipation at normal operating speeds (usually slower than N MOS) is still considerably lower than other technologies.

Extended temperature ranges in CMOS can be met by additional testing and engineering.

The one disadvantage to CMOS that is often mentioned is its susceptibility to damage caused by static discharge. This can usually be overcome with proper protection and circuit design.

Processors presently in production include the Intersil 6100 (12 bit), RCA 1802 (8 bit), and the Motorola 14000 (1 bit). Manufacturers of CMOS include Solid State Scientific, RCA, Fairchild, Intersil, Motorola, Harris and National.

## 2. Execution Speed Requirements

The selected processor must execute a given software program to accomplish all the tasks required by the system. The time required to perform these tasks is called the processor execution time or speed. Figure 4-24 outlines all the tasks that are required by the system. These tasks must be accomplished 20 times per second or once every 50 msec. In addition, it is strongly recommended that a 40% speed improvement be specified to allow for actual software estimation tolerances, unforeseen problems, and future expansion or modification capability. The

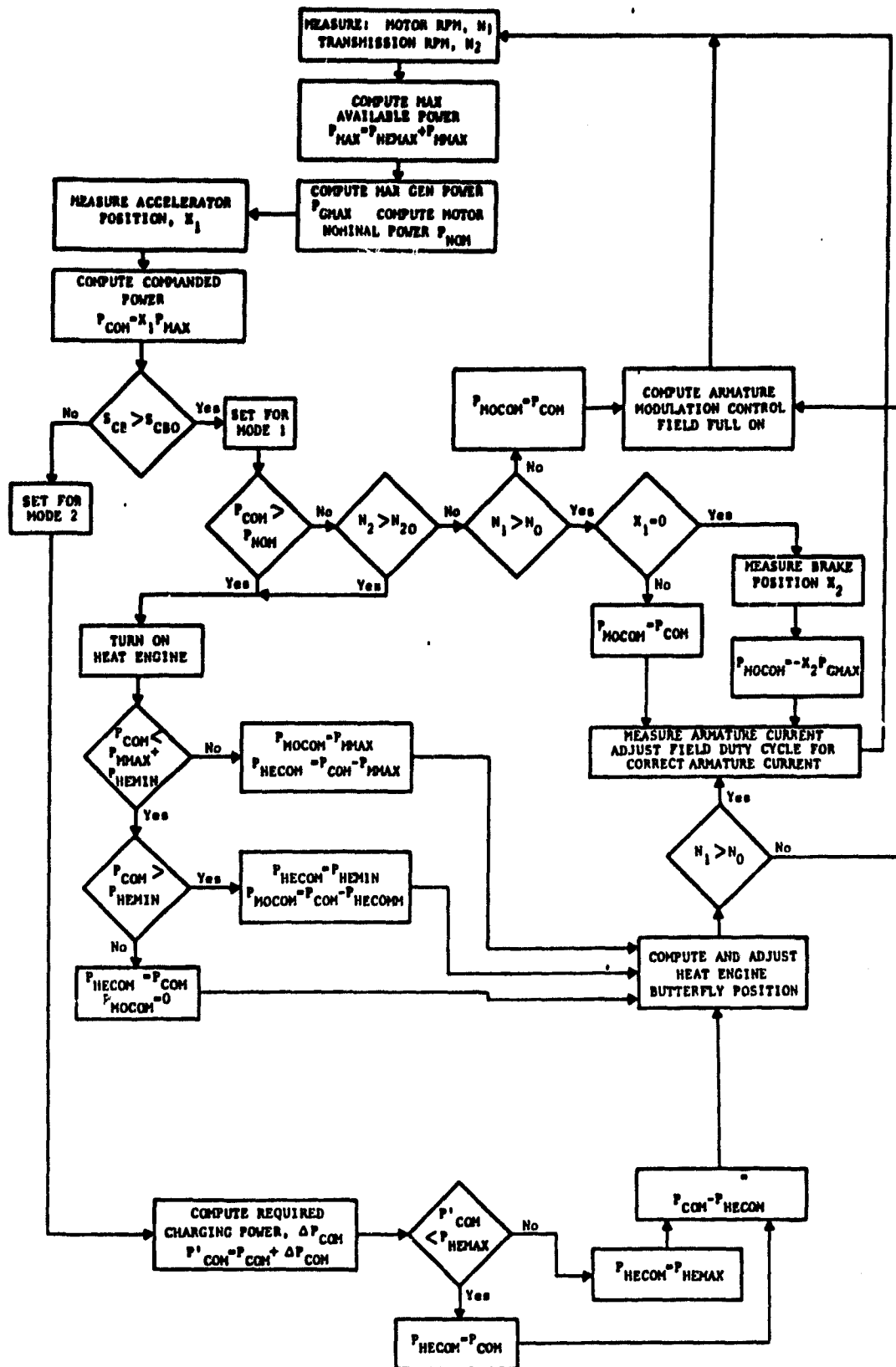


Figure 4-24 Power Control Flow Diagram

foregoing execution time requirement must be accurately predicted. Execution speed is one of the most important parameters in the selection of a suitable microprocessor.

Although most processors are generally rated by instructions/sec (or  $\mu\text{sec/instruction}$ ), this is not a reliable measure due to variations in instruction mix, internal processor architecture, data width, etc. (discussion of processor differences is included elsewhere.) To insure that the selected processor will execute to the given requirement, a benchmark program must be written and tested. The penalty for underestimating speed requirements is high. Once a processor is selected and the software completed, it is often very difficult and time consuming to reorganize the hardware or rewrite the software for a faster processor.

### 3. Memory Requirements

The size of both the program memory and the Random Access Memory (RAM) are again dependent on the flow diagram in Figure 4-24 . The number of instructions is a function of both the outlined procedure and the instruction set and data width size of the selected microprocessor. Similarly, the number of changeable RAM locations is also defined.

The program memory for the controller should be implemented using EROM technology to allow rapid programming changes during debugging. The present program memory requirement is between 2 and 4K bytes.

Data Storage Memory: The memory for the parameters should be non-volatile to prevent memory loss during power outages and transients.

The best approach is to use a CMOS RAM with battery backup. Present data memory estimates are 256 x 8.

#### 4. Input/Output Requirements

The total number of digital and analog input lines must be evaluated to determine the number of memory addresses required. In most applications outside of single chip microprocessors, this is not a critical specification.

#### 5. Life Cycle

Presently, most microprocessors have an average marketing period of 5-9 years. Selecting a processor that is nearing obsolescence will greatly limit the amount of support that can be obtained for problems and questions. Similarly, selecting a processor that has been just introduced leads to the same problem of lack of support and "the learning curve" experience.

#### 6. Single Chip Processors vs. Standard Processors

Today, there are several single chip microprocessors that contain both the CPU and memory required to implement an automotive controller. The first major disadvantage to the single chip solution is that the program memory is generally ROM based. This does not allow for program changes or debugging and is, therefore, unacceptable for a test bed application. Secondly, the input/output lines on these chips are generally limited. Since the test bed will require many more I/O lines due to instrumentation demands, extender chips would be required. The advantage of a single chip processor disappears. Single chip microprocessors that employ erasable EROM memory are also unsuitable due to the limited size of the program memory. It appears that a standard bus oriented microprocessor would be the best solution.

## 7. Data Width

The data width of a microprocessor refers to the width of the data path; i.e., how many bits are transferred in a parallel move. Present microprocessors are available in 4, 8, 12 and 16 bits. In general, the wider the word width, the greater the throughput of the processor will be. A key factor in the choice of data path is the width of the arithmetic data that is to be manipulated. If most of the data are 8 bit values, then a 16 bit processor does not improve the throughput significantly (some improvement due to faster program fetches). In all processors, arithmetic operations greater than their word width can be accomplished using software techniques at the expense of time utilization. Some processors have double precision instructions to further enhance double precision arithmetic. Some processors also have multiply/divide instructions.

For the automotive controller application, an 8 bit microprocessor appears to be the best choice.

- a) A majority of the parameters are 8 bit integers.
- b) The speed requirements can be easily met by current 8 bit processors.
- c) An 8 bit processor board generally requires less real estate.

## 8. Architectural Differences

When comparing two microprocessors with the same instruction execution speed, one must consider the power of the instruction set. One processor can have a superior instruction set which can handle a given application in fewer instructions than another, therefore,



affording a higher throughput rate. Addressing schemes utilized by the processors should also be compared. By using relative addressing, some processors can squeeze more instructions into a given memory size.

The last consideration that should be evaluated is the amount of external hardware support the microprocessor will require. Some require fancy clock drivers, status latches, multiple power supplies or demux latches.

#### 9. Development Aids and Support

A very high percent of the total engineering effort required to prototype the controller will be directed at hardware debugging and software development. The availability of a dedicated microprocessor development system for the selected processor is an economic necessity.

A complete development system should contain the following:

- Program storage capability such as floppy or rigid disk.
- CRT terminal
- Resident text editor/assembler and debugging software.
- An in-circuit emulator module with suitable hardware.
- Preferably, a printer of TTY for hard copy output.
- An EROM programmer for immediate updating of the controller's program memory for actual operation.
- Possibly a higher level language to support the data reduction effort.

#### 10. Qualified Microprocessors

The list of microprocessors below all meet the conditions and specifications outlined above. The list is not in priority of qualifications.

- Intel 8085
- Motorola 6800 family
- Rockwell 6500
- Zilog Z 80
- Signetics 2650
- Intel 8035
- Fairchild F8
- RCA 1800 family

The following list of microprocessors were deemed inappropriate for this application:

Bit Slice

AMD 2901 family

Fairchild Macrologic

Intel 3000 family

Motorola 10800 family

Monolithic 6700 family

16 bit Processors

TI 9900

Fairchild 9940

National IMP 16

GI 1600

Intel 8086

Zilog Z8000

Motorola 68000

Bipolar

Signetics 8x300

1 bit Processors

Motorola 14100

12 bit Processors

Intersil 6100

Single Chip Processors

Intel 8048/8021

Fairchild 3870

Zilog Z8

AMI S2000 family

Other 8 bit Processors

Intel 8008

Intel 8080

National SC/MP

#### 4 bit Processors

Intel 4004

Rockwell PPS -4

TI TMS1000

A final selection from among the qualified microprocessors will be deferred until early in the Phase II program.

#### Software Implementation of Control Functions

In this section, implementation of the basic control strategy discussed earlier is illustrated. Refinements such as the use of a threshold heat engine torque in Mode 2, or strategy modifications to limit peak motor power in normal operation, are not included. Obviously, the system controller capacity must be adequate to handle modifications and refinements.

The basic control strategy, exclusive of such additions, is given in the flow diagram of Figure 4-25. Tradeoffs and implementation of the various control functions follow a brief description of this overall control sequence.

Motor RPM,  $N_1$ , and transmission shaft RPM,  $N_2$  are measured on a pulse by pulse basis. Maximum available power,  $P_{MAX}$  is computed as a function of motor RPM by adding the available heat engine power,  $P_{HEMAX}$  to the maximum available motor power  $P_{MMAX}$ . Also computed is the maximum motor generation capability  $P_{GMAX}$  and the motor's nominal rating  $P_{NOM}$ .

Accelerator position  $X_1$  is next measured and the commanded power  $P_{COM} = X_1 \cdot P_{MAX}$  is computed. Also measured is the battery voltage,

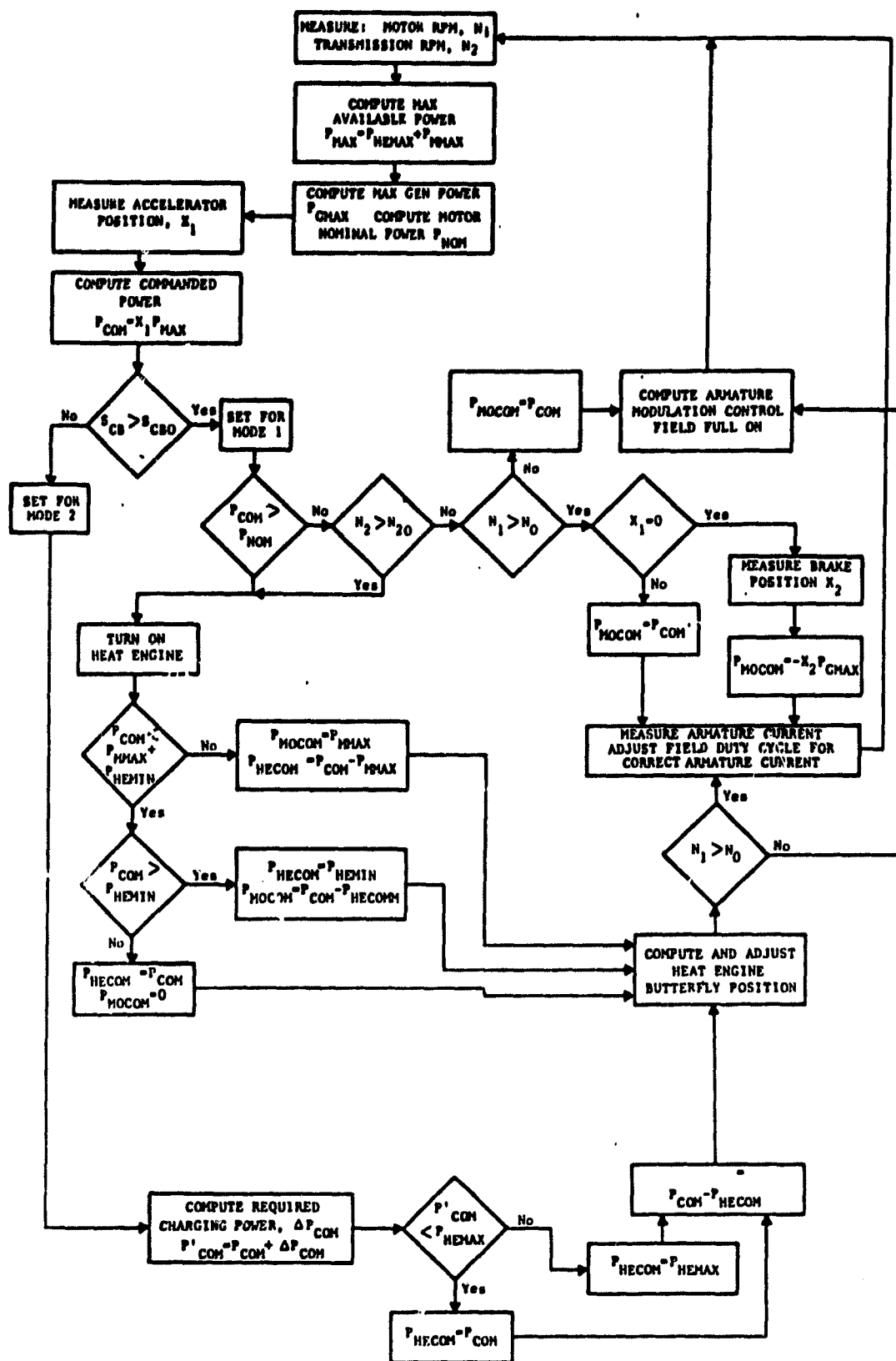


Figure 4-25 Power Control Flow Diagram

current, and temperature which allows computation of the battery state-of-charge,  $S_{CB}$ . The state-of-charge parameter,  $S_{CBO} = 1 - D_{BMAX}$ , is used for mode selection.  $S_{CB}$  greater than  $S_{CBO}$  results in operation on Mode 1.  $S_{CB}$  less than  $S_{CBO}$  results in Mode 2 operation.

Assuming we are in Mode 1 operation ( $S_{CB} > S_{CBO}$ ), the decision to turn the heat engine on depends on whether the commanded power level  $P_{COM}$  is greater than the nominal rating  $P_{NOM}$ , or the transmission shaft RPM  $N_2$  is greater than  $N_{20}$  which corresponds to the transition speed defined previously. If that is the case, the heat engine is turned on and a power split between the motor and heat engine is computed.

The power split is predicated on keeping the heat engine operating at its most efficient torque (if possible) and supplying the rest of the power with the electric motor. This is possible only if the commanded power  $P_{COM}$  is less than the maximum motor power  $P_{MMAX}$  plus the most efficient heat engine power  $P_{HEMIN}$ . ( $P_{COM} \leq P_{MMAX} + P_{HEMIN}$ .)

Also, the commanded power must be greater than  $P_{HEMIN}$ . Given that these conditions are satisfied, the commanded power split is as follows:

$$P_{HECOM} = P_{HEMIN}$$

$$P_{MOCOM} = P_{COM} - P_{HECOM}$$

If the commanded power is greater than  $P_{MMAX} + P_{HEMIN}$ , then the motor commanded power is set at  $P_{MMAX}$ , and the heat engine supplies the rest of the required power.

$$P_{MOCOM} = P_{MMAX}$$

$$P_{HECOM} = P_{COM} - P_{MMAX}$$

If the commanded power is less than  $P_{HEMIN}$ , then the heat engine supplies all the commanded power and the motor power is set to zero.

$$P_{HECOM} = P_{COM}$$

$$P_{MOCOM} = 0$$

Once the power split is computed, the heat engine butterfly position is adjusted for the required power level, and the motor power is set by adjustment of either the field or armature duty cycle depending on whether the motor is running above or below base speed.

If in the previous computation, it turned out that  $P_{COM} < P_{NOM}$  and  $N_2 < N_{20}$ , the heat engine would not be turned on and the motor would supply all the power. For both these situations, i.e., motor only and power split, regenerative braking will occur if the accelerator pedal  $X_1$  is zero, the brake pedal  $X_2$  is depressed, and  $N_1 > N_0$ . At this time,

$$P_{MOCOM} = -X_2 P_{GMAX}$$

Mode 2 operation is initiated if the battery state-of-charge  $S_{CB}$  drops below  $S_{CBO}$ . The commanded heat engine power is incremented by a value  $\Delta P_{COM}$ , which depends on how far  $S_{CB}$  is below  $S_{CBO}$ . This modified command,  $P_{COM}^1$ , is then checked to determine if the heat engine can supply this demand. The motor is commanded a regenerative power level equal to  $\Delta P_{COM}$  if  $P_{COM}^1 < P_{HEMAX}$  or some fraction of  $\Delta P_{COM}$  if  $P_{COM}^1 > P_{HEMAX}$ . This fraction could be zero.

#### 1. RPM Measurement

Motor RPM must be measured in order to compute motor and heat engine maximum power levels, maximum power generation capacity as well

as the translation of commanded power levels to heat engine butterfly positions and motor armature and field control signals.

Transmission shaft RPM must also be measured. This gives a direct indication of vehicle speed and is used for several logic decisions in the overall control strategy.

There are basically two ways of measuring RPM from a pulse train which reflects the rotation of a shaft: a frequency or a period measurement. Frequency measurement requires the generation of a gate for a fixed period of time during which the incoming pulses are counted. Frequency measurement generally yields an ambiguity of  $\pm 1$  pulse count since it is not known when the first pulse arrived with respect to the start of the timing gate.

In order to keep this  $\pm 1$  count ambiguity error to acceptable levels, the width of the timing gate must be chosen such that a large number of pulses fall within it. Having 10 pulses fall within the gate, for example, will generate a peak to peak error of 10%, while 100 pulses will yield an error 1%. Since at 300 RPM the shaft rotates at five revolutions per second, either a very large timing gate must be used or a large number of pulses must be generated during one revolution of the shaft. Neither solution is acceptable, so the frequency measurement must be dropped.

Period measurement requires a time measurement from the edge of one pulse to the edge of an adjacent pulse. Based on estimates of expected RPM rates of change, it is felt that it is sufficient to sample RPM at a rate of 10 per second. As an added margin of safety, 20 samples per second will be used. Assuming the lower RPM bound to

be 300 (five revolutions per second), 4 pulses per shaft revolution are required to get 20 samples per second (50 milliseconds between pulses).

Four pulses per shaft revolution implies 2 milliseconds between samples at 7000 RPM. This is quite a bit more samples than necessary and will require higher than necessary timing resolution in order to keep quantization errors to acceptable levels. It also unnecessarily loads up the processor.

An acceptable compromise between these two requirements might be to perform a period measurement for every incoming pulse until a period of 12.5 milliseconds is reached, after which the period measurement is done on every fourth pulse. This allows the minimum measured period to be greater than 8 milliseconds, thereby lowering the timing resolution requirements and decreasing the processor loading. The relationship between measured and actual period is shown pictorially in Figure .

The period measurement should be performed by a hardware timer so as not to tie up processor time. The processor should be interrupted only when necessary to service the period measurement hardware.

Since two RPM measurements are to be made, a separate timer can be used for each. This in itself does not inflict a hardware penalty because microprocessor-compatible timers come in a package of three or four anyway. In order to start and stop the timer, however, some additional hardware would be required to generate a gate. Also, the RPM sample rate would be cut in half since the gate would be on half the time and off the rest of the time.



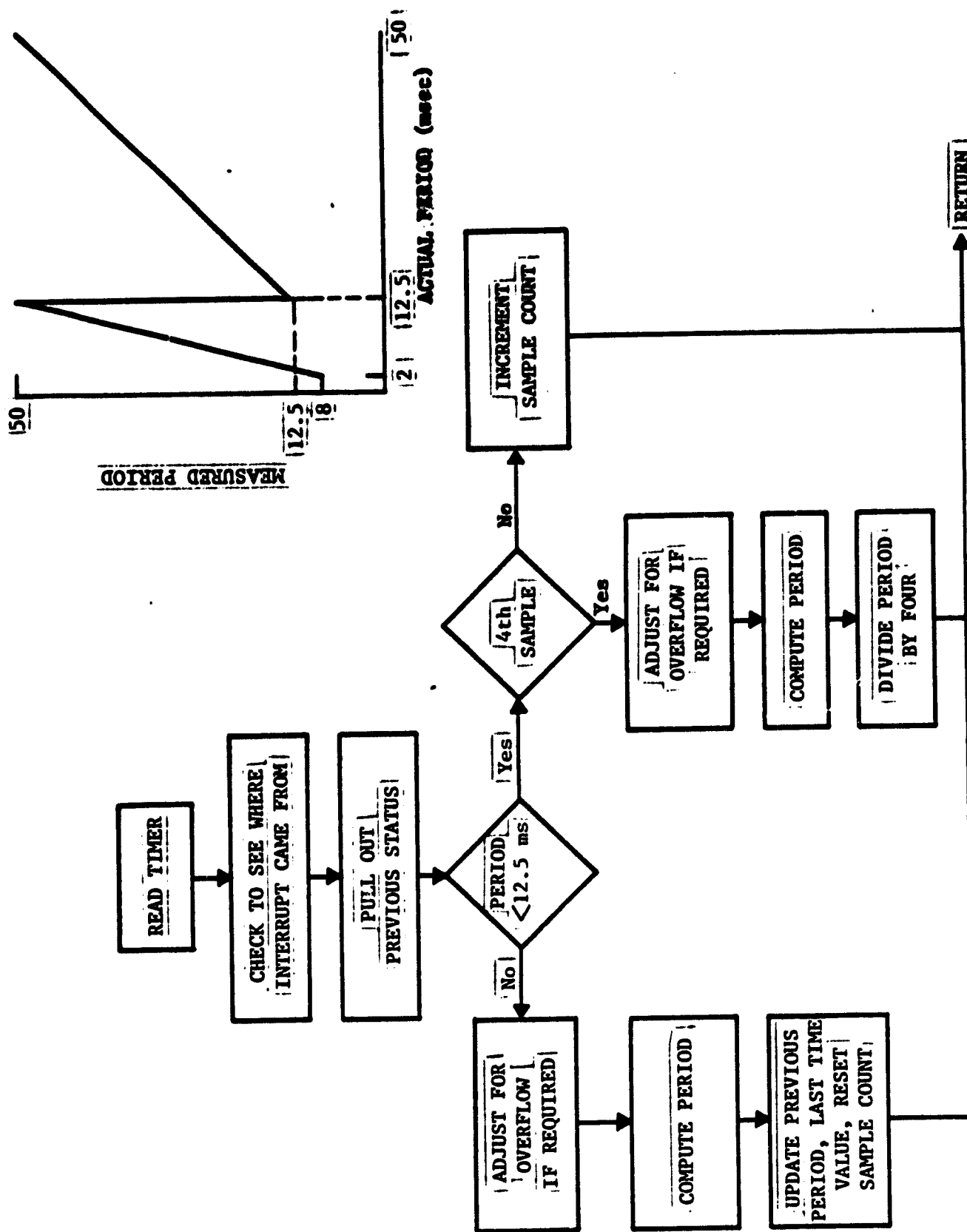


Figure 4-26 RPM Interrupt Service Routine

In order to get around this, a single free running timer can be used. The software interrupt routine required to service this timer is shown in Figure 4-26. The processor gets interrupted each time a pulse from either shaft is received. The processor reads the value of the free running timer, checks to see which shaft caused the interrupt via an input port. The processor then pulls out the appropriate timer value stored from a previous interrupt as well as a previously measured period and sample count. If the previous period is below 12.5 milliseconds and the sample count is less than 4, then the sample count is incremented and the processor returns from interrupt. If, on the other hand, the previous period is greater than 12.5 milliseconds or it is the fourth sample, then the timer value is adjusted for overflow (if required) and a new period is computed and stored. Adjustment for overflow is required since the timer is free running and may recycle during two adjacent pulses.

In order to keep the quantization error below 1%, a timing resolution of 50 microseconds is required. A 50 microsecond resolution will require a 10 bit counter to measure periods up to 50 milliseconds. Since the transmission shaft requires the measurement of a period longer than 50 milliseconds, a 16 bit timer (standard for microprocessor systems) will be used.

## 2. Maximum Power Tables

Maximum heat engine power and maximum electric motor power tables are used to compute maximum usable power at a given RPM. Typical curves are shown in Figure 4-27. Since typical values are used, the tables are not required to be extremely accurate. Very

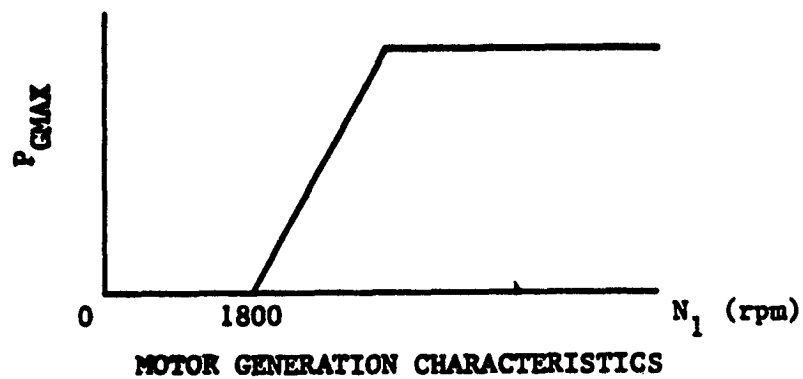
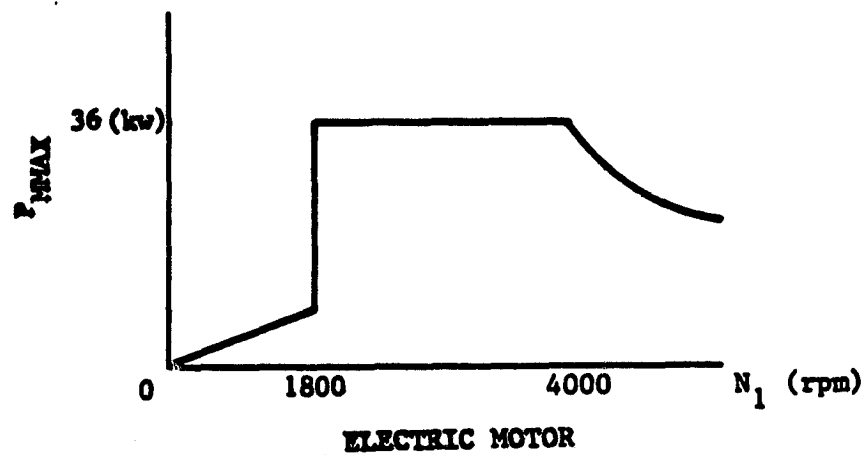
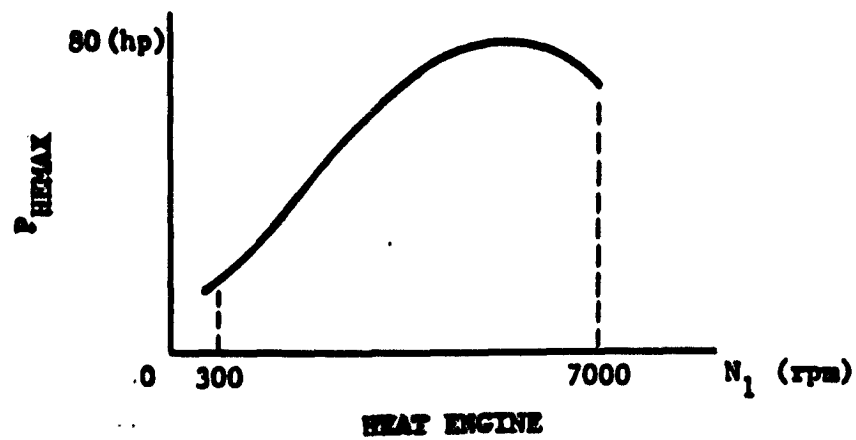


Figure 4-27 Maximum Power Tables

large, high resolution data storage is, therefore, not necessary. A piecewise linear approach will allow for small tables and still provide the required accuracy. Sixteen breakpoints are estimated to be adequate.

The interpolation computation required when using the tables can be speeded up somewhat at the expense of some additional storage space by storing not only the breakpoint value but also the slope to next breakpoint. This will make each table 32 bytes long, still quite short. Using 8 bits to store each value in the table will yield a resolution of approximately one HP. This should be adequate for maximum power calculations.

Since the RPM is actually measured as period of a quarter rotation of the shaft, there is no reason why the power tables should not be stored as a function of period rather than actual RPM. This will save a division which would otherwise be required to convert the period measurement to RPM.

### 3. Maximum Generation Characteristics

Maximum generation characteristics require another table (Figure 4-27 ). Note that advantage could be taken from the fact that a good portion of the curve has a fixed value. This, however, would decrease the overall flexibility of the design and would not save much in storage capacity anyway.

It is recommended that a table similar to the maximum horsepower tables be used. This will allow a single subroutine to be used for extracting data from the various tables. Also, all tables which pertain to motor and engine physical characteristics can be stored in a

single memory chip, separate from the program memory so that any changes in these characteristics can be easily accomplished by plugging in a newly programmed chip without impacting the control program.

#### 4. State-of-Charge Computation

State-of-charge is computed from a family of curves similar to that shown in Figure 4-28. The curves represent battery voltage at various battery current levels. From previous work done at SCT, it has been shown that a good approximation to the state-of-charge is obtained using a single piecewise linear curve translated in the horizontal axis to the correct operating point. This will allow two 32 byte piecewise linear tables to be used for the state-of-charge computation.

Figure 4-28 also shows the state-of-charge algorithm. The battery current  $I$  is first measured. Next, the battery voltage  $E_{vo}$  at a reference state-of-charge  $S_{cb1}$  is computed from Table 1 on Figure 4-28. Next, the battery voltage  $E_v$  is measured, and the voltage difference  $\Delta E_v = E_v - E_{vo}$  is computed. The state-of-charge  $S_{cl}$  is computed from Table 2 as a function of  $\Delta E_v$ .

The battery temperature is also measured and will be used to modify the translation (Table 1) as well as the slope of the curve in Table 2. Both tables should physically be located in the same memory used for the engine and motor parameters.

#### 5. Heat Engine Control Algorithm

Once the heat engine commanded power is computed, it is only necessary to compute the required butterfly position and output the necessary signals to adjust a stepper motor which drives the butterfly for the appropriate output.

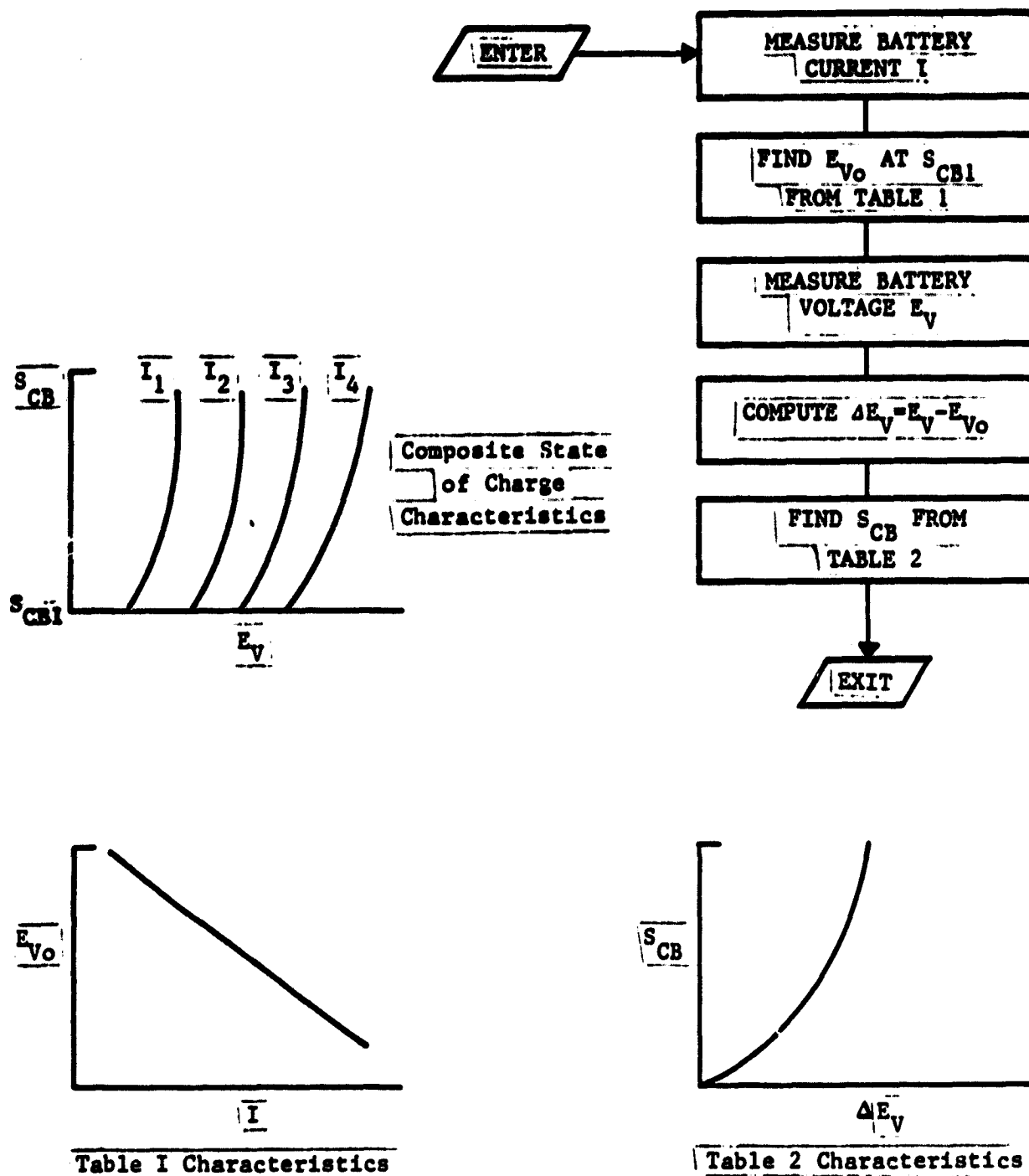


Figure 4-28 Battery State of Charge Computation

Typical heat engine commanded power as a function of butterfly position at various RPM levels is given in Figure 4-29 . Thirty-two byte piecewise linear tables can be used for each of the curves with linear interpolation between 2 RPM values. Ten tables (320 bytes) would be sufficient.

Another approach which would require less storage, but would increase processor loading somewhat and would not be as accurate, would be to store a single curve at an RPM  $N_1$  and multiply that curve by a factor based on RPM (another table) which would change the slope of the stored curve to the proper value. More work is required to determine whether the accuracy of this approach is adequate. A flow diagram of the algorithm is also given in Figure 4-29 .

#### 6. Transition from Motor to Heat Engine Power

Engaging and disengaging the heat engine in Mode 1 operation during peak power demands represents a design problem which will have to be thoroughly investigated during the hybrid vehicle test program. The transitions will have to be smooth enough to be barely noticeable. The hybrid vehicle control system should, therefore, be capable of a lot of experimentation in this area.

One way to implement a smooth engagement is to monitor the motor RPM and armature current while adjusting the field for constant RPM operation. As the engage command is sent out, the commanded motor power can start to increase in anticipation of increased drag from cranking the heat engine. The RPM should be continually monitored, and the motor field control should be "fine tuned" to avoid a drop in RPM. As the heat engine comes on line, the armature current will drop.

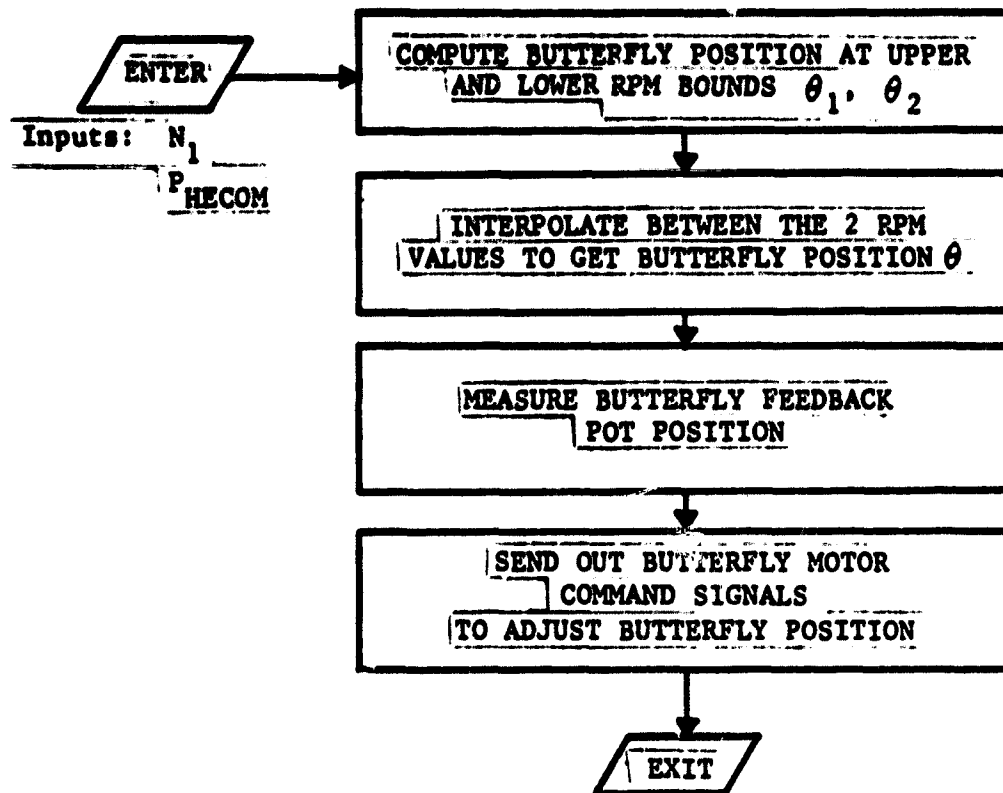
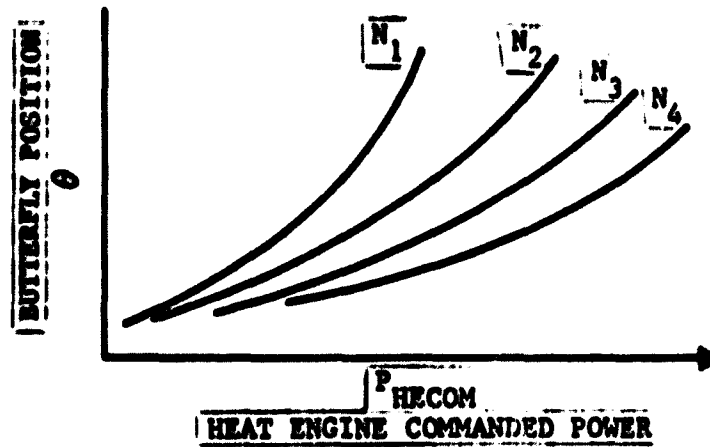


Figure 4-29 Heat Engine Control



This is sensed by the processor which is still adjusting the field for the proper RPM. Normal operation resumes once the heat engine is completely on line.

Heat engine disengagement follows a similar process. As the disengagement command is sent out, the motor commanded power starts increasing while using armature feedback to prevent a change in RPM.

All time constants used for the engage and disengage functions will be made programmable parameters allowing for adjustment during the test phase.

#### 7. Motor Control Functions

Armature Control: The function of armature control of the electric motor is to provide useful motor output at speeds below base speed. That is the minimum speed achievable with full field current. Armature control consists of switching the battery voltage at the armature to reduce the average armature current. Armature chopper operation is very simple in theory. The inputs to the armature chopper are the armature current sense voltage developed from the armature shunt and externally commanded current level. (Really commanded power since the motor is operated at nearly constant armature voltage) A comparator senses the relative currents and switches the armature "on" whenever the armature current falls below the command level. When the armature current rises above the reference, the armature is switched "off."

Parameters of interest in the design of an armature chopper are the switching rate, and maximum switching current. For tight regulation of the armature current, high switching rates are desirable.

It is desirable to maintain a high switching rate since mechanical resonances will develop at rates of less than 5 KHZ. Maximum switching current is an important parameter because it determines the maximum load under which the motor is able to operate below base speed. Since the switching speeds are, of necessity, high, and large amounts of power are being switched, it is advantageous to have armature control being performed in hardware. The microprocessor then presents the armature chopper with a command corresponding to desired power level. The processor need then only monitor the average armature current.

If the processor were required to monitor the instantaneous armature current, it would be at significant processor overhead. In addition, the tight timing requirements would be incompatible with the stated objective of software flexibility of the test bed. Increases and decreases in commanded power should be converted to an analog voltage to command the armature chopper. The minimum control voltage corresponds to the motor idling with no load at approximately 300 RPM. As the accelerator is depressed, the average armature current and motor speed are gradually increased. Average armature current should be sensed and used to trim the measured power to match the commanded power output. When the motor reaches base speed, the armature chopper should provide an output to the processor informing it that the chopper is on 100%. The processor will then bypass the armature chopper, and the field controller function will then take over. Alternatively, if maximum acceleration is called for, the chopper can be bypassed before 100% duty is reached at a speed at which the maximum motor current of 300 A would not be exceeded at max field.

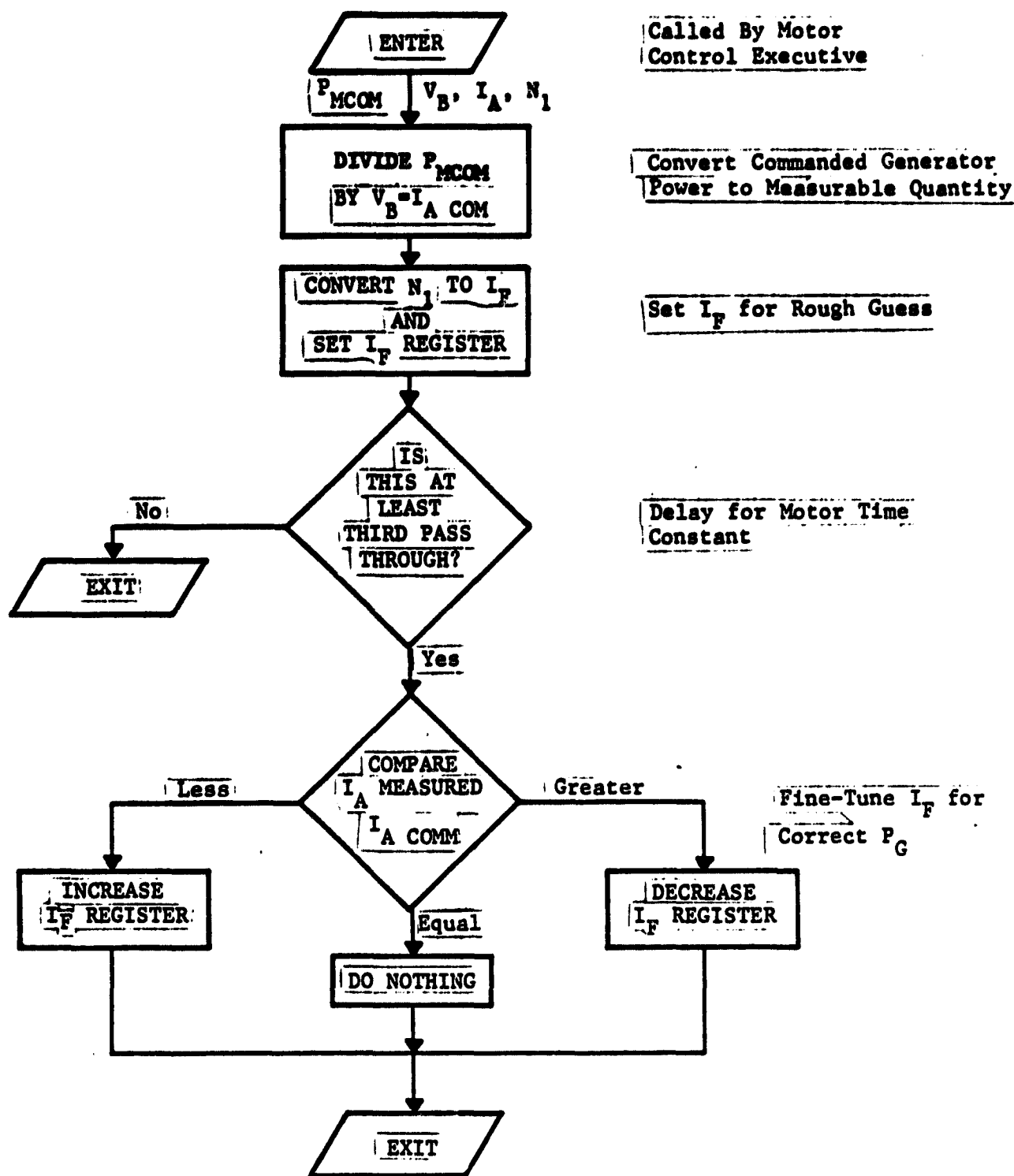


Figure 4-30 Field Control Routine

Field Control Output: Field control is used to control both generated and commanded power above base speed. To minimize power dissipation in the field control circuit, pulse width modulation (PWM) is used to control the average field current. In order to minimize the field control circuit complexity, the switching rate is kept intentionally low. 20-100 HZ is adequate considering the average time through the control loop (50 ms) and the response time of the motor (.1 to .3 sec.). Pulse width modulation can be implemented in hardware or software with equal ease. In this case, no significant penalty is associated with requiring the processor to update a hardware timer on an interrupt scheduled basis.

Processor control of commanded (or generated) power is performed in four steps, which are illustrated in Figure 4-30 . First, the processor converts  $P_{COM}$  to  $I_{A COM}$  (commanded armature current) by dividing  $P_{COM}/E_v$ . Second, the field current corresponding to the no-load RPM is found from a look-up table containing 64 entries from 1800 RPM to 7000 RPM. This produces a coarse approximation of the correct operating point. The 8 bit entry in the table corresponds to the number of clocks of the PWM "high" time. Third, a utility routine then converts the table value to a preset for the PWM timer. This value is stored in a register. Successive interrupts to the processor will preset the timer to the table value and then its complement. This process will be repeated until the table value is updated. Fourth, the processor waits for three passes through this loop before it compares the actual armature current to the commanded value. Each modification to the field current PWM wave form is delayed

to allow for the motor to respond. The delay time parameter should be stored in the CMOS RAM so that it may be adjusted during testing.

Transition from Armature to Field Control: Transition from armature to field control and the reverse is quite straightforward. As the motor speed is gradually increased towards base speed, the duty cycle of the armature chopper reaches 100%. The switching elements within the chopper detect this and report it to the discrete input port of the processor. The processor detects this and bypasses the armature chopper. This transition is inherently smooth since there is no step change in the field current or armature current, as long as the commanded armature current is less than the current limit in the armature control regime. On deceleration, in transition from field control to armature control, the processor monitors the armature current and the gear position. When in first gear at the instant that the armature current passes from negative through zero, the processor opens the armature contactor and commands a current level to the chopper to continue the deceleration.

Motor Generation Control: Control of the motor generation capability is employed for two reasons. The first is to utilize the power of the motor to assist in vehicle braking. The second is to utilize the motor for charging the vehicle battery. Although these two features are frequently combined into one in conventional field control electric vehicle, the hybrid vehicle presents interesting opportunities to employ either one by itself. For instance, in Mode 2, the heat engine may be used to charge the vehicle batteries when the command power of the heat engine is less than maximum.

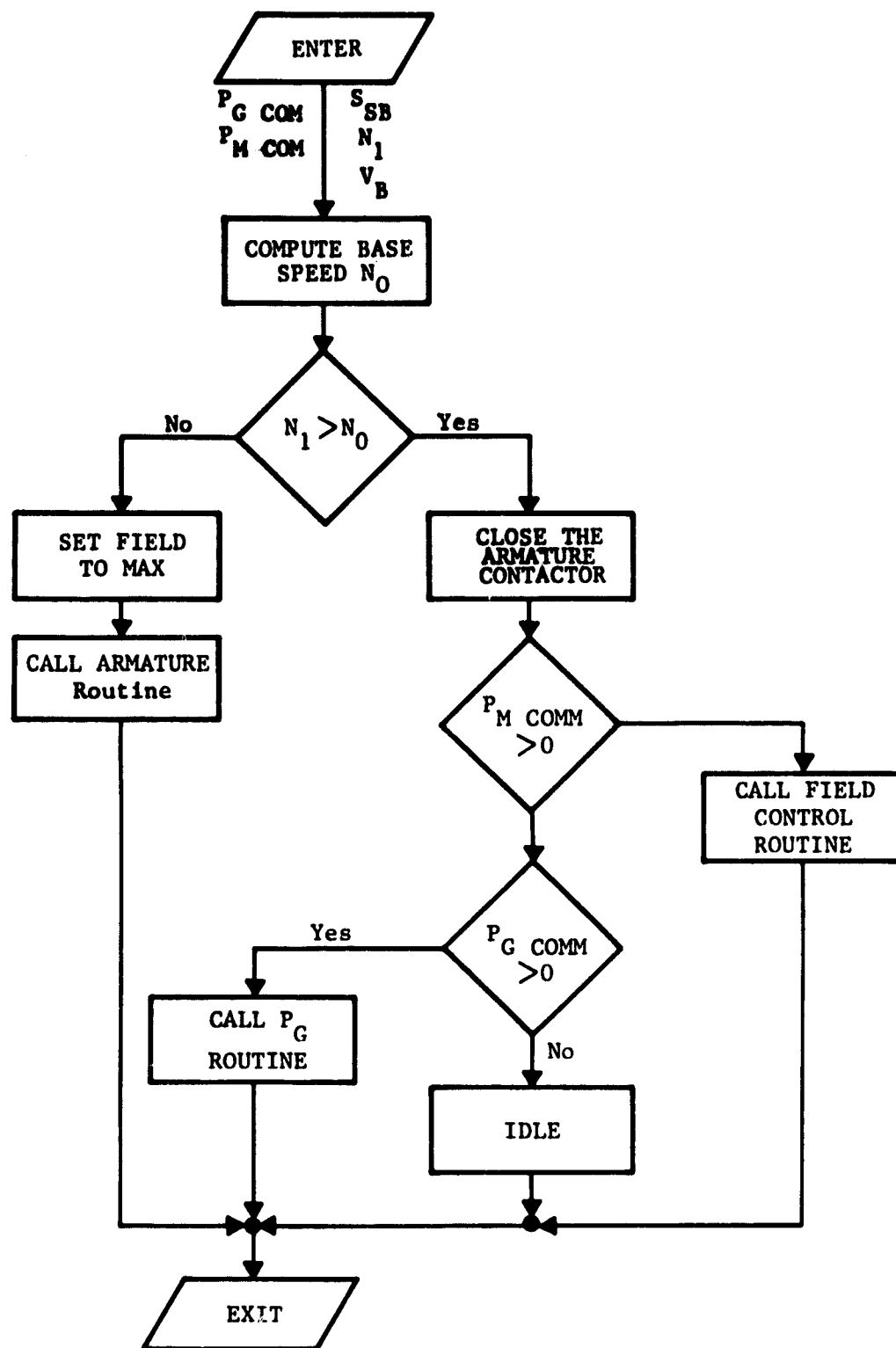


Figure 4-31 Motor Control Flow Diagram

Due to the characteristics of the electric motor, generated power rises rapidly from zero as applied torque to the motor increases. Microprocessor control of the motor generation can use this fact to good advantage. The field control commanded power routine stores a curve of no-load speed versus field excitation. The processor then need only compute coarsely the field current required for whatever the present speed is. A second routine (in fact, the same routine used for field commanded power) then monitors the armature current and battery voltage to set the generated power exactly. This technique is both hardware and software efficient since no additional table space is required. Only a driver routine utilizing the no-load field characteristics and the fine adjustment routine is needed. The nature of the motor characteristics make the exit from the power generation mode at base speed smooth since the motor output is constrained to go to zero as base speed is approached.

During the testing phase,  $P_{GMAX}$ , the maximum generated power should be an adjustable parameter to evaluate different levels of regenerative braking and its effect on vehicle efficiency.

Figure 4-31 shows the logic to be implemented in controlling the motor generation characteristics.

#### 8. Transmission Shift Control

The gear selection for the hybrid vehicle transmission will be directly controlled by the processor via two output lines (shift up, shift down). The gear selection is based on the following description.

If the heat engine is inactive and the transmission is not in high gear, the next higher gear will only be selected when the motor

speed exceeds 4000 RPM. If the transmission is not in low gear, shifting to the next lower gear will only occur if the engine speed is below 2200 RPM.

If the heat engine is active, the criteria for gear shifting is based solely on the heat engine. Two methods were considered. Method 1 involves estimating heat engine power based on speed and an input from a heat engine vacuum sensor and basing the shift points upon this power, according to logic shown previously in Figure . The second method involves basing the shift points on the heat engine power command  $P_{COM}$ , rather than the actual power. The second of these methods is the simpler, and is preferred.

Parameters that should be modifiable during the test program are:

- a) electric motor shift up speed
- b) electric motor shift down speed
- c) heat engine shift up power
- d) heat engine shift down power
- e) shift pulse duration
- f) minimum shift time

#### Hardware and Interface Implementation

##### 1. Input Interfaces

To provide lowest eventual user cost as well as provide hardware simplification, the following ground rule should be observed. "Minimize hardware by shifting the burden to software when possible." In evaluating the input/output requirements of the hybrid controller, that guideline is used to evaluate alternate I/O structures. However,



design flexibility is also a constraint. Table 4-3 lists the parameters to be measured with regard to possible implementation, accuracy requirements, and update rates.

RPM Measurements can be implemented in a number of ways. The principal constraint on the various implementations is the system update rate of 20 times per second (discussed elsewhere). Pulse counting schemes (essentially frequency measurements) are an acceptable and accurate solution at high RPM's where many pulses can be expected to occur in the 50 msec period between updates. However, with the motor running at 300 RPM with a 4 pulse/rev rate, only one pulse will occur in 50 msec. Clearly, this is unsatisfactory in making accurate measurements.

Counting schemes which measure the time interval between pulses with a high speed clock, however, can measure the motor or transmission speed quite accurately. At high RPM, the period measurements can be averaged over several successive periods for additional (although not required) accuracy.

To accommodate a 300-7000 RPM motor range, a 10 bit counter is required. For transmission shaft RPM, the counter must be somewhat larger to accommodate the fact that the shaft may be turning at a near zero rate, such as when stopping. A 16 bit (typical configuration) can handle a .22 RPM shaft rate.

In practice, pulse period measurements are implemented with a free running 16 bit counter being clocked at the 20 KHz rate. Lower clock rates increase the time between updates; faster clocks limit the lower RPM range in drive shaft measurements. The outputs of the

<u>Inputs to be Monitored</u>	<u>Range</u>	<u>Resolution/Accuracy</u>
Battery Voltage	90-140	.5 V
Battery Current	-150 - +400	3 amps
Motor RPM	300-7000	5% of measurement
Transmission RPM	0-7000	5% of measurement
Temperature (battery)	-40° - +70°C	2°C
Motor Temperature	-40° - +70°C	2°C
Engine Temperature	-40° - +130°C	2°C
Accelerator Position	0-100%	64 steps minimum
Brake Position	0-100%	64 steps minimum
Contactor Closure Sense	Discrete Signal	N/A
Engine Oil Pressure	Discrete Signal	N/A

<u>Outputs to be Controlled</u>	<u>Range</u>	<u>Resolution/Accuracy</u>
Field Control	0-10 A	64 steps
Armature Control	0-150 A	Continuous control
State of Charge	0-100%	32 steps
Butterfly	0-90°	64 steps
Shift Up/Down	Discrete Signals	N/A
Engine On/Off	Discrete Signals	N/A
Contactor	Discrete Signals	N/A
Clutch	Discrete Signals	N/A
Fan Hi/Low	Discrete Signals	N/A
Field Contactor	Discrete Signals	N/A

Table 4-3

counters are connected to the microprocessor bus. Incoming pulses from the tachometer pickups interrupt the processor and identify themselves to the processor. In response to the interrupt, the processor reads the time of the interrupt. Internally, the processor performs all calculations on a period basis rather than frequency, primarily to avoid performing the reciprocal calculations.

Accelerator and brake controls require a sufficient number of steps to appear continuous. A low cost 8 bit analog to digital (A/D) converter can provide 256 discrete steps and can be shared among the other analog inputs. Using a linear potentiometer, an analog to digital converter provides a cost effective solution which shifts the burden of accurate pedal position measurement to the processor.

In practice, the processor will read in an analog voltage by selecting the appropriate input to an analog multiplexer through its address lines (see Figure 4-32 ), and then reading the output of the A/D converter connected to the processor data bus.

The accuracy required for these measurements is not very high. The principal constraint on these measurements is that the pedal appear to operate smoothly and repeatably within 5%. The quality of the potentiometer is the pacing parameter here since A/D accuracy is about .5%. The system update rate of 20/sec is adequate for the expected rates of change of the pedal position.

Battery voltage is measured for the state-of-charge and base speed calculations. Since state-of-charge is to be used for driving a coarse indicator such as a fuel gauge with resolution of 1/32 of full scale at best, and also for mode switchover, the voltage

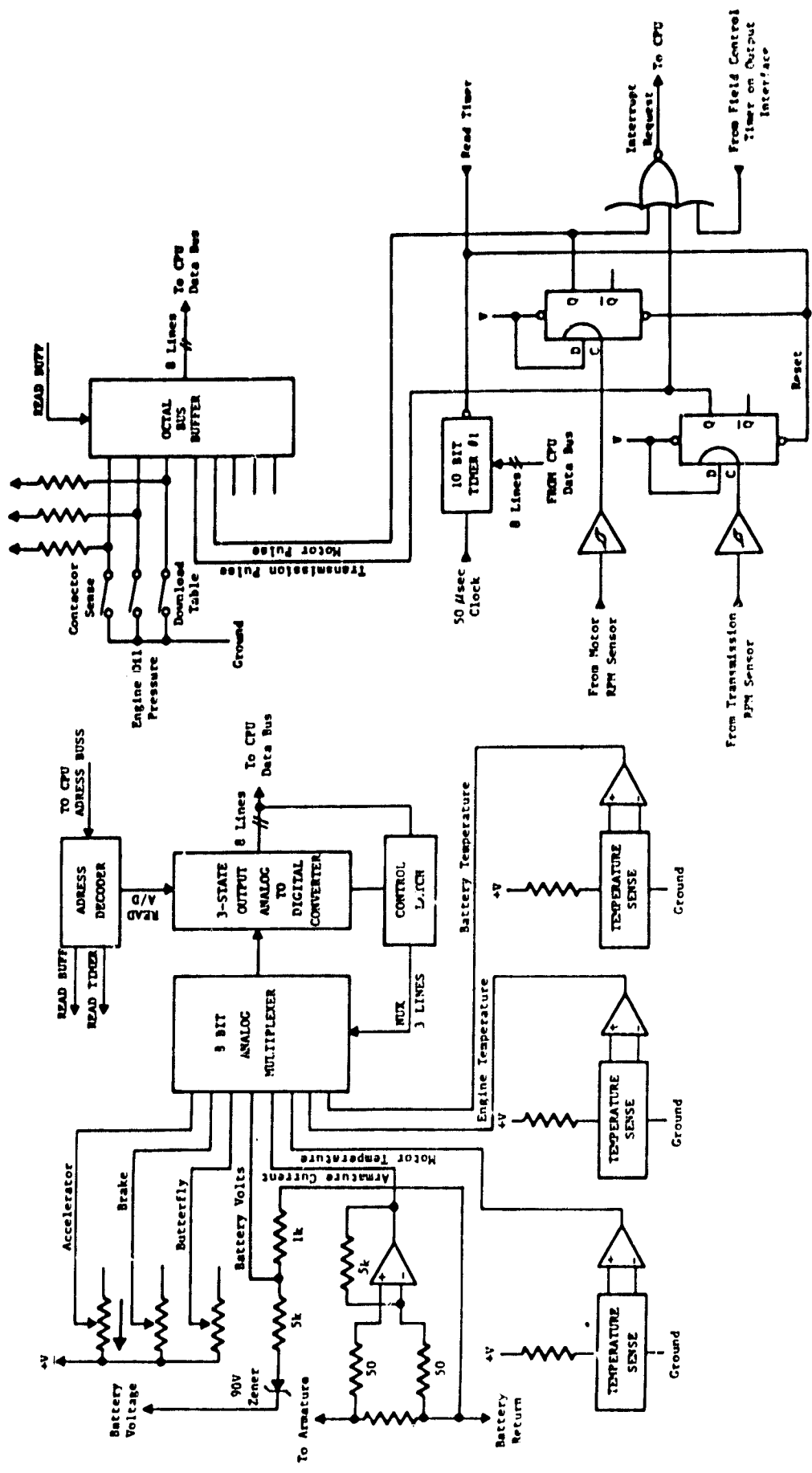


Figure 4-32 Hybrid Vehicle Input Interface

measurement accuracy need only be 1/64 of the expected range of variation. Since A/D conversion is already provided, battery voltage can be measured with 8 bit accuracy at almost no additional cost. Voltage can be measured to .13 volts in the operating range. To achieve this accuracy, the battery voltage could also be measured to within .8 volts across an expanded range of 0-200 volts without level shifting the battery voltage.

The battery voltage can be updated continuously if desired. However, since the state-of-charge is expected to change slowly (over a period of minutes), the system update rate of 20 times/sec is more than adequate.

Battery current is also measured for the state-of-charge calculation. In that regard essentially, the same remarks as above apply to it. This can be done by monitoring the increase or decrease in armature current at a fixed speed to determine the status of the heat engine. The speed requirement to monitor the armature current is determined by the maximum change rate of the heat engine. The mechanical moment of inertia of the heat engine requires the armature current to be measured at least five times per second.

Armature current is also useful to determine when the heat engine has started, and then to provide for smooth engagement of the heat engine to the power train.

The hybrid vehicle requires measurement of the motor and heat engine temperature as well as battery temperature. Motor temperature is monitored for an overload condition. If motor temperature rises past a first limit, the cooling fan will be switched from low to high.

If the temperature continues to rise, the maximum output power available will be reduced. Both of these limits should be allowed to be varied during testing to arrive at meaningful limits. Heat engine temperature is monitored for both high and low extremes, and to provide a basis for selection of a warmup mode. Maximum heat engine power will not be commanded when the engine temperature is outside either extreme. Battery temperature is monitored in order to apply corrections to the state-of-charge computations.

Without discussing temperature sensor implementation in detail, it is appropriate to mention that solid state temperature sensors are available at low cost, capable of measuring absolute temperature without calibration. Using such a sensor would permit measuring  $2^{\circ}\text{C}$  increments when connected to a five volt full scale analog to device converter. In addition to the above continuous signals, the following discrete signals need to be monitored:

- An armature and field contactor closure monitor will verify contactor closure. This will reduce the likelihood of damaging the armature chopper or motor.
- Also, heat engine oil pressure should be monitored to protect the heat engine.

## 2. Output Interfaces

As a general rule, all outputs will be digital signals to make them less sensitive to external noise.

Field Control: The philosophy of field control by the micro-processor is discussed elsewhere in this report and will not be dealt with here. This section only discusses the implementation of the field control interface.

Field control, as it is currently being implemented in electric vehicles, is done by some form of switched control rather than linear implementation. The reason for this is simple: to minimize the size, weight, and power dissipation in the control elements. Switched control elements operate with typically 80-90% efficiency compared to 30-40% efficiencies of rheostat or linear amplifiers.

Typically, pulse width modulation is used to control the average field current. The pulse period is usually 10-40 msec to minimize the active power dissipation in the switching elements and the induced ripple and power dissipation in the armature. Higher switching rates only raise the power dissipated in the control circuits. Slower rates limit the rate of change of motor speed.

Implementing this pulse width modulation scheme under processor control is relatively straightforward. The processor first calculates the duty cycle required for the field current. The processor then sets the PWM control high and presets a timer to a time corresponding to the "high" pulse time. When the timer times out, it interrupts the processor, which then sets the PWM control line low and presets the timer with the corresponding "low" time. This process is then continuously repeated with new PWM characteristics. The pulse period is controlled by the timer clock frequency and the timer preset.

Armature Control: The discussion on armature control is similar to the one on field control in some respects. PWM is again preferred because of the high efficiency. Armature control below base speed involves switching up to 150 amps.

However, switching speeds of 25-50 times/sec are wholly inadequate. Chrysler Corporation reports that at switching speeds of up to 5 KHz, objectional resonances are transferred from the drive train throughout the car. This requirement for high pulse repetition rates switching would be difficult for a microprocessor to achieve in conjunction with its other control functions. In addition, if due to logic error, noise or processor failure, the PWM characteristics were not accurately controlled, the chopper could be damaged by commanding an excessive armature current. For this reason, it is recommended that the processor only command an armature chopper level but have hardware self-monitoring and limiting within the chopper module. In this way, the processor will be relieved of monitoring the armature current at high rates. Armature control of this type is implemented by supplying the armature chopper with voltage from a digital to analog (D/A) converter. This D/A converter is connected to the processor data bus. Armature current can be adjusted in .6 amp steps across the control range of 0-150 amps with an 8 bit D/A converter. Above base speed, the armature current is controlled by the field. The processor calculates the base speed using the state-of-charge indication. Above base speed, the processor closes the armature contractor by setting a bit in its discrete output port. Contact closure is verified by reading the state of the sense switch at the discrete input port.

State-of-Charge Output Display: The function of the state-of-charge output display is to provide the operator with an indication of remaining battery capacity. As such, its function is similar to an automotive fuel gauge. Resolution of fuel gauges is generally limited to 1/32 of fuel scale.



The question of display type, i.e., digital readout or analog meter, is resolved by noting that airlines prefer analog outputs for their ability to convey meaningful information with a minimum of interpretation time. Digital readouts, while offering greater precision, take significantly longer to interpret. It is felt that an analog meter driven by a D/A converter represents the most effective low cost output.

Heat Engine On/Off, Cooling Fan Low/Hi, Shift Control, Contactor Controls: These outputs are naturally digital control functions. The processor, by setting or resetting individual bits of a discrete output port, can control these functions with little additional hardware.

The philosophy of transmission control is discussed elsewhere. We only note that its control is easily accomplished by two discrete output control lines.

Butterfly Control: In having microprocessor control of the butterfly, it is important that the processor does not get tied up performing as part of a servo loop in order to maintain the butterfly position. The processor should only set the throttle position, and then periodically verify it.

A stepper motor is a natural for this application, since it can be digitally controlled. A follow pot mounted on the butterfly shaft monitors the commanded throttle position. Four-phase stepper motors are commonly available which can provide  $1.8^{\circ}$  steps. The processor moves the stepper by applying commands from its output port to the stepper motor driver I.C. Typical stepper motors can be programmed

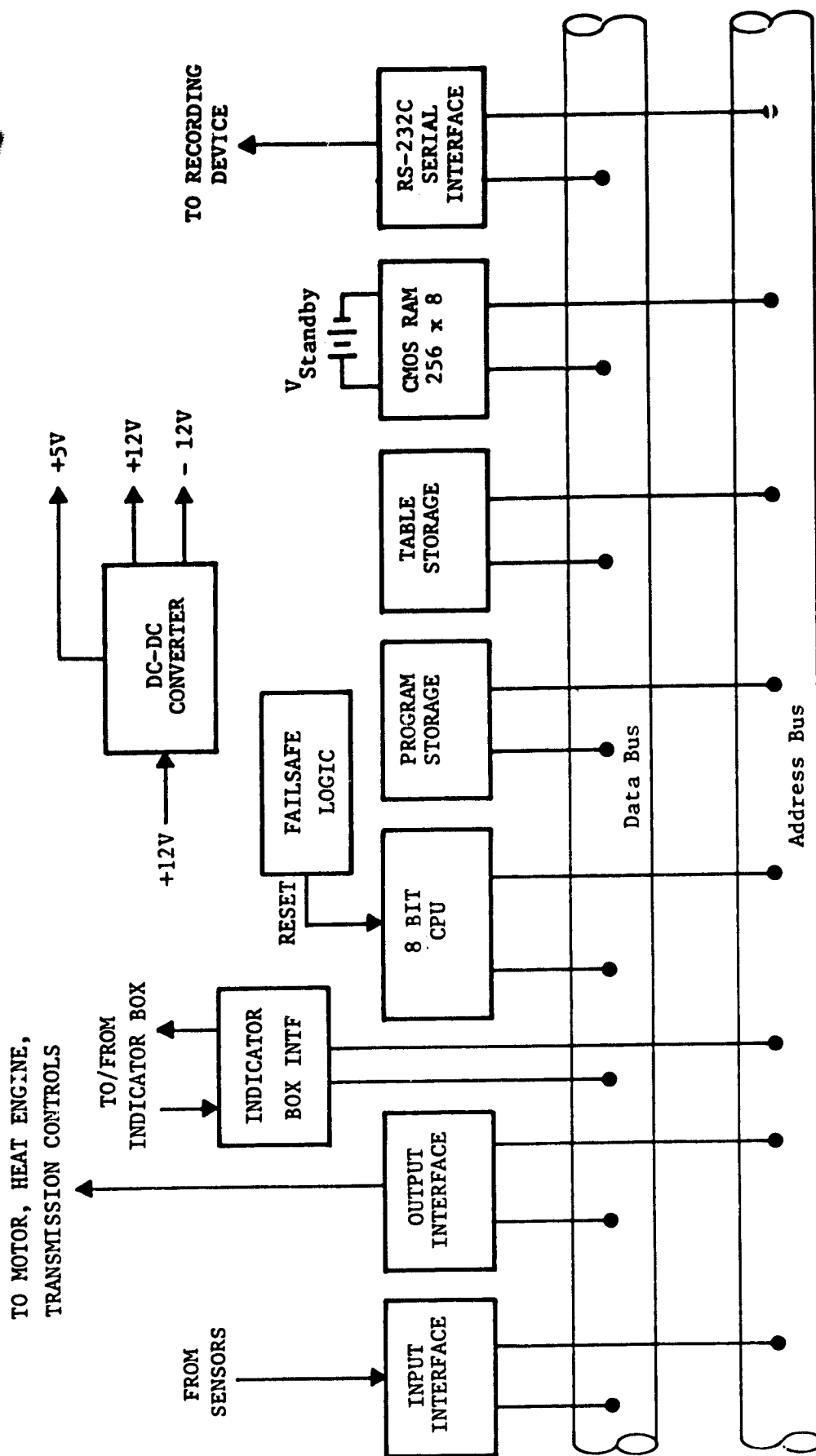


Figure 4-33 CONTROL SYSTEM HARDWARE

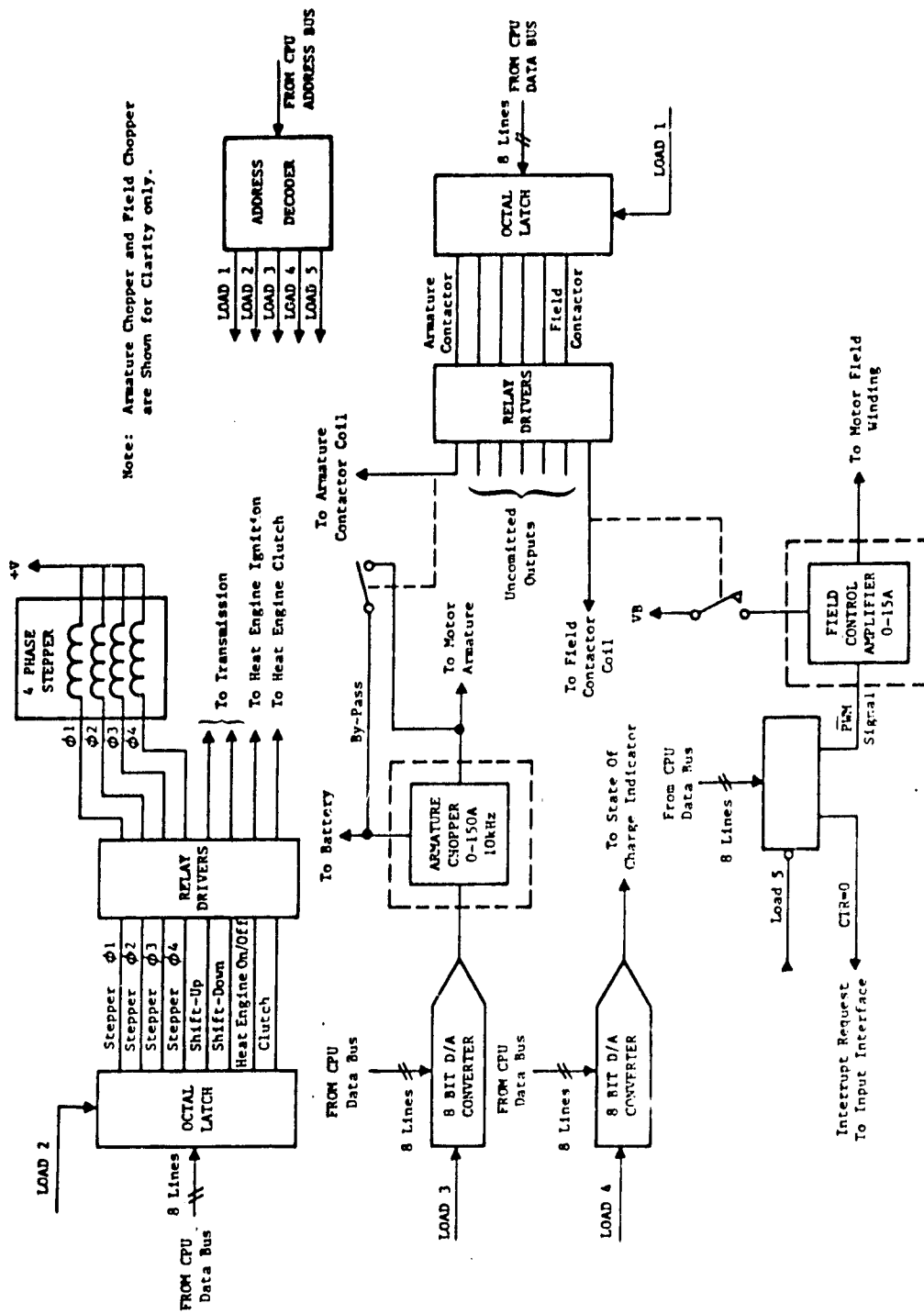


Figure 4-34 Hybrid Vehicle Output Interface

to drive the  $90^{\circ}$  throttle rotation in 30 milliseconds. This is certainly more than adequate.

Clutch Control: The operation of the heat engine clutch is discussed elsewhere. We will only say that the processor controls clutch engagement using its discrete output port.

### 3. Overall Hardware Block Diagrams

Figure 4-33 presents the system level block diagram. Preliminary sizing of the control program indicates that 2K bytes of memory is required; 256 bytes of volatile Random Access Memory (RAM) is expected to be adequate. Figure 4-33 shows a 256 byte CMOS RAM with battery backup. This area is envisioned as the area where constants of the control algorithms will be stored between tests. By implementing this area in RAM rather than ROM, these constants may be varied during testing but still retained between power downs.

Figures 4-32 and 4-34 present the input and output interface block diagram. The functional performance and requirements of the components has been covered in the preceding discussion.

Also shown in the overall block diagram is an RS232 interface port operating at 9600 baud. Measured and calculated parameters will be transferred to an external data recording device for possible subsequent data reduction. This feature is discussed in more detail elsewhere. An operator interface is also provided. This interface allows the operator to examine, monitor, or change parameters in the CMOS RAM.

The final point to note is that a hardware reset timer has been provided. The time out period for this one-shot is selected to be

slightly longer than the control loop pass time. If the processor should "bomb out" due to noise, the one-shot will time out and reset the processor before damage can be done.

#### Fail Safe Logic

Like all other electronic circuits, a microprocessor and its supporting circuitry are susceptible to operating faults from a variety of sources (i.e., power supply transients, induced noise, power outages, and component failures). In addition, errors such as design errors, programming errors, procedural errors, and unforeseen situations or combinations complicate the detection of errors in a microprocessor-based system. Since a microprocessor is, in reality, a sequential state machine, the occurrence of a single temporary error condition may permanently disrupt the proper operation of the controller until the processor is reset.

Because of this possibility of failure and the concern for human safety and protection of the vehicle's equipment, it is strongly recommended that two separate defeat circuits be included in the controller specification.

The first circuit should be a direct operator-invoked override of all controller operations. A switch on the driver's display console and the monitor panel could be utilized by an operator who detects an unsafe or abnormal condition.

The second circuit would be a fail safe circuit. The function of this circuit is to continuously monitor the processor for proper operation. If a fault is detected, the controller is gracefully turned off and the processor is reset.

Processor fail safe circuits are usually implemented by two different means. In the first method, the fail safe circuit demands the attention of the processor for a short duration of time. The processor is required to perform this test at a fixed time interval to insure that the processor has not stopped or fallen out of sequence. During the short interval, the processor is required to perform a self-test. If the processor fails to respond within the allocated time period or fails a self-test, a fault is declared and the processor is restarted. Total processor loading should not exceed 1-2% of the processor's available time.

The other method of fault detection is to monitor the processor's address, data, and control busses to detect illegal addresses or op codes and illegal timing combinations.

In addition to the methods above, the power supply to the controller should also be monitored for out of tolerance conditions. For any abnormal condition, the processor should be considered potentially non-operational and immediately be halted and restarted.

#### Instrumentation

Since the main objective of constructing a hybrid test vehicle is to provide a means to critically evaluate and analyze system performance and tradeoffs, it is of paramount importance to incorporate into the controller the necessary flexibility and instrumentation capabilities. The instrumentation module permits the operator this flexibility by allowing him to directly modify the operating parameters of the controller. In addition, the operator can observe any of the

current controller parameters (programmed or calculated) via a display. Parameters are also available at a serial output port for data collection.

The three separate submodules of the instrumentation module are discussed below.

#### 1. Driver's Display Console

The primary function of the console is to provide the driver with the standard vehicle information and an indication of proper operation. The following information would be displayed on the console:

- a) Vehicle speed
- b) Engine speed
- c) Battery state-of-charge
- d) Mode and controller status
- e) Temperature alarms

Also contained on the console are:

- Start/stop key
- System override switch
- Standard automotive controls and indicators

#### 2. Control Monitor

The control monitor provides the flexibility of modifying the operating of the controller. The monitor contains a keyboard entry and a display (Figure 4-35 ) and is located on the passenger's dashboard. The functions of the control monitor include:

- a) The ability of directly modifying all operating parameters via the keyboard entry. Since most operating parameters

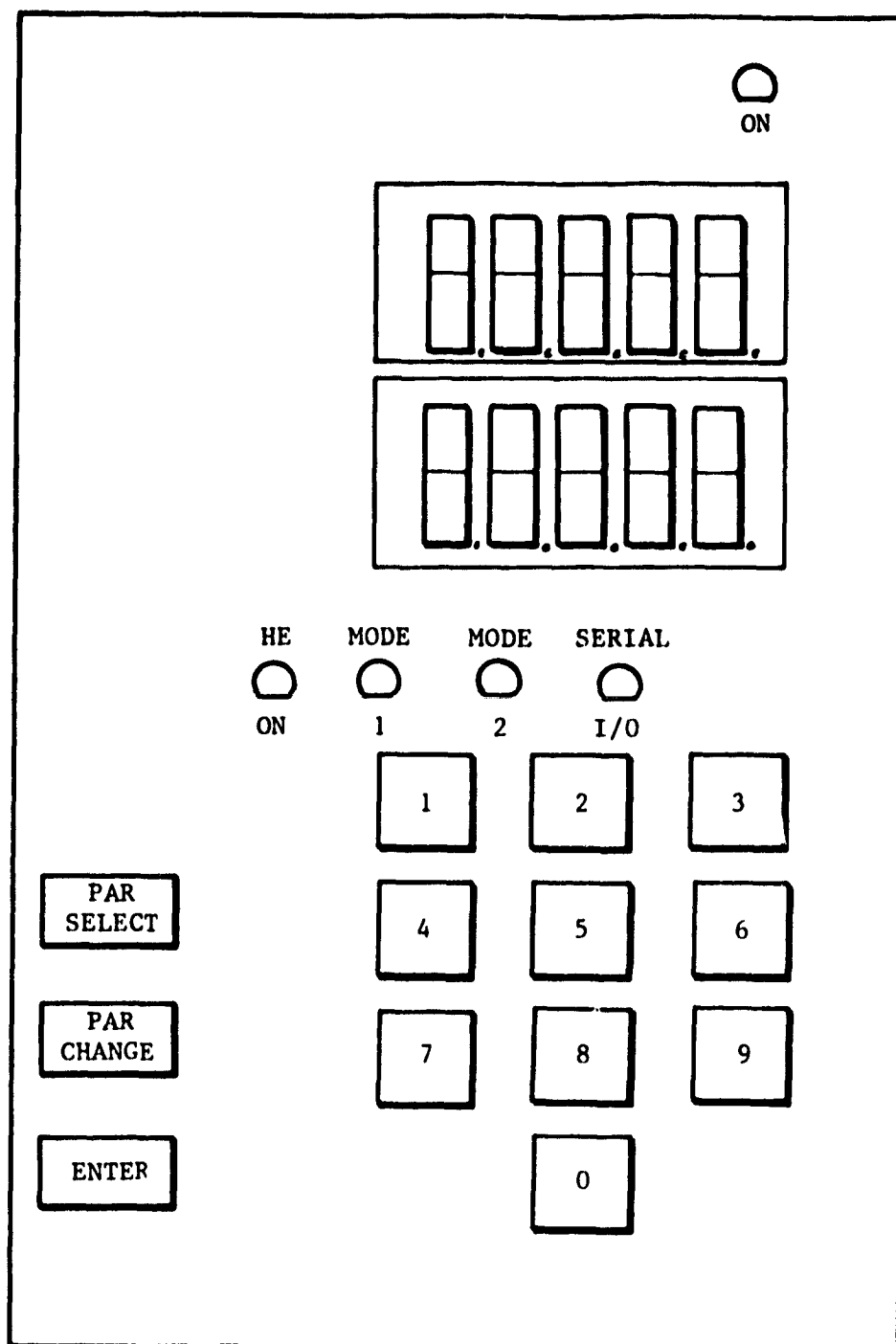


Figure 4-35 Indicator Box



and decision points will be stored in RAM, the operator has the ability to change operating characteristics instantaneously.

- b) Observe any parameter(s) that are monitored by the controller in real time. The display panel should contain two separate 5-digit displays that can be programmed to indicate any pair of processor parameters (i.e., commanded power, butterfly setting, power split, etc.).
- c) Control the serial output port.

### 3. Serial Output Port

The serial output port provides the means for an external device to monitor or record the dynamic operating parameters of the controller during actual operation. A recording device such as a digital cassette recorder can be utilized to store the raw output data for further analysis.

Some related requirements for the serial port and related equipment are discussed below.

Sampling Rate: The serial port should be capable of outputting a full set of operating parameters 20 times per second.

Maximum Transfer Rate: The maximum transfer rate (bits/sec) of the serial port must be capable of transferring at least 32 8 bit values 20 times per second, or roughly 5120 bits/second. Due to inefficiencies in the serial protocols and limited processor response times, a bit rate of 9200 baud should be specified.

Recording Device: Since most of the collected data will be reduced and formatted using an external minicomputer, computer service or desk top calculator, the recording device and media should

be compatible with the reducing processor. Magnetic digital recording would be an ideal candidate because of its adequate transfer rate, acceptable data storage density, low error rate, economical price for both recorder and media, and the availability of many compatible versions.

Data Reduction Equipment: A significant portion of engineering manpower will probably be directed towards formatting, plotting, and evaluating the data supplied by the vehicle controller. Since the vehicle controller has a relatively slow processor, all data produced by the controller will be in a raw format. The data reduction equipment must be programmed and utilized to perform the necessary formatting to create plots and curves from the actual performance data. Possible candidates for this job include desk top calculators (such as the HP 9830), minicomputers, computer services, or even the micro-processor development system. Desired features would include:

- a) A high level language for programming time efficiency  
(such as Basic, Fortran, PL/1, etc.).
- b) The ability of connecting a plotter for printout of curves and graphs.
- c) Adequate program storage such as floppy disks or mag tape.

#### 4.1.3 Heat Engine and Controls

The basic choice for the heat engine is the VW 1.5 l. four cylinder gasoline engine as used in the Rabbit. In 49 state form, this engine delivers 53.3 kw at 5800 RPM, with a peak torque of 99 N-M at 3500 RPM. It is a fuel-injected engine, and this offers the potential for fuel control during the engine start-up and shut-down transients. We project that this engine will probably have closed loop fuel and spark control by 1985 using a 3-way catalyst and oxygen sensor; whether the hardware required to implement such a closed loop system will be available in time for use on the Phase 2 NTHV program is not known at this time.

As discussed in Section 3, availability of hardware to facilitate changes in engine calibration may dictate the use of an alternative engine whose fuel and electrical systems have been developed by a U.S. manufacturer and use components from U.S. suppliers. Such an alternative is the Omni-Horizon engine. This is a 1.7 l., longer stroke version of the VW engine, which delivers 50 kw at 5200 RPM, with a peak torque of 110 N-M at 2800 RPM. It uses a Holley 2 barrel carburetor; ignition system is by Essex or Prestolite. Dimensionally, the basic engine is externally identical to the Rabbit engine except for manifolding and the fuel distribution system. The potential difficulty with this engine is the lack of control over fuel flow during startup and shutdown transients. Consequently, the choice between these two engines will be based on where the emissions problems are, and this will require Phase 2 testing

to determine.

Because of the unknowns involving emissions characteristics, we are not in a position, at this point in time, to define precisely the engine fuel, spark, and emissions controls to be used on the NTHV engine. The alternatives for fuel control with the injected Rabbit engine include the following:

- 1) Unmodified (mechanical control of fuel metering from air flow sensor).
- 2) Same as (1) with separate solenoid valves at each injector to provide fuel shutoff during start-up and shut-down transients.
- 3), 4) Same as (1) and (2), respectively, but with fuel metering controlled by a  $\mu$ P based on signals from an air flow sensor and/or exhaust oxygen sensor.

Alternatives for fuel control of the carbureted Omni-Horizon engine are similar to (1) and (3) above. Likewise, alternatives for control of spark advance and EGR rate for either engine may be based on the existing engine controls or may utilize the system  $\mu$ P.

Whether or not fuel shutoff during startup and shutdown is used, it will be necessary to ensure that the ignition is turned on before the cylinders receive fuel. With the carbureted engine, it would be necessary, of course, to shut the engine down by turning the ignition off, and there is not much that can be done about burning the fuel which is inducted between the time the ignition is turned off and the time the engine comes to a complete halt. With the injected engine, if individual fuel

shutoff valves are used upstream of the injectors, engine shut-down could be accomplished by fuel shutoff, with the ignition being turned off after fuel is shut-off. Emissions resulting from residual unburned fuel during shut-down would therefore be reduced.

When the start-up of the engine is called for, its speed is brought up to operating speed by engaging a clutch between the engine and transfer case (Figure 4-6 ). This is a normal plate and disc automotive clutch, actuated hydraulically. With proper adjustment, there would be negligible drag when the clutch is released. In addition, it must be noted that there is no power loss in the throwout bearing when the clutch is released, since the engine is not rotating under these conditions; that is, the throwout bearing is under load when the clutch is released, but the races are not rotating relative to each other, and so there is no power loss. As a result, the clutch does not represent an added load of any significance on the electric motor when the heat engine is not operating.

The rate at which the engine can be brought up to speed and power is a critical factor in the driveability of the vehicle. The engine must get up to speed and develop power fast enough to provide a reasonable approximation to the throttle response of a conventional vehicle. In order to understand the relative importance of various factors in this startup process, a parametric study was made, using the programs VSYS and VSYS2 described in Section 2 and Appendix C1 of this report. The parameters of

interest, in terms of their effect on the system, were the following:

- . Clutch engagement rate, in N-M/sec. (This is the rate at which the clutch picks up torque)
- . The point at which engine torque buildup begins, in engine revolutions from the start of clutch engagement. (It was assumed that, once the torque buildup started, the engine would come up to its steady state torque within one engine revolution)
- . Torque converter status (locked up or not)
- . Engine moment of inertia
- . Motor moment of inertia
- . Vehicle speed

The influence of these parameters on the following system variables was investigated:

- . Time for full clutch engagement,  $t$  (i.e., time at which engine speed reaches motor speed). This is the point in time at which the net power flow from the engine becomes positive; i.e., the engine starts delivering power instead of absorbing it to overcome its inertia.
- . Peak motor torque,  $T_{mx}$
- . Peak clutch torque,  $T_{clx}$
- . Peak vehicle acceleration,  $a_x$

Of these variables,  $t$  is important in terms of how the power response feels to the driver, and  $a_x$ , is a measure of how much the car lurches when the clutch is engaged; these are the variables which are directly related to driveability. The maximum torques

$T_{mx}$  and  $T_{clx}$  are important in terms of component sizing and durability.

The results of the study may be summarized as follows. First, the clutch engagement time  $t$  varies inversely as the .47 power of the clutch engagement rate (or, roughly the square root of the clutch engagement rate). This time is essentially independent of the status of the torque converter, but varies strongly with the engine moment of inertia. The variation of  $t$  with these parameters is shown in Figure 4-36. In Figure 4-37, the variation of the peak vehicle acceleration with several parameters is shown. As expected, it is a strong function of the torque converter status. With the torque converter active, the peak acceleration is only about  $-.02G$ , a value which changes only slightly with engagement rate and engine inertia. With the torque converter locked up,  $a_x$  varies approximately as the .62 power of engagement rate, with engine inertia also being a strong influence.

The variation in peak clutch and motor torques are shown in Figures 4-38 and 4-39, respectively. Torque converter status has very little influence on peak clutch torque; it varies approximately as the .54 power of the engagement rate and, again, the influence of engine inertia is strong. Peak motor torque, on the other hand, is strongly affected by the torque converter status on peak vehicle acceleration. Essentially, what happens is that with torque converter locked up, most of the energy required to get the engine up to speed comes from a reduction in vehicle kinetic energy. The associated speed change is very

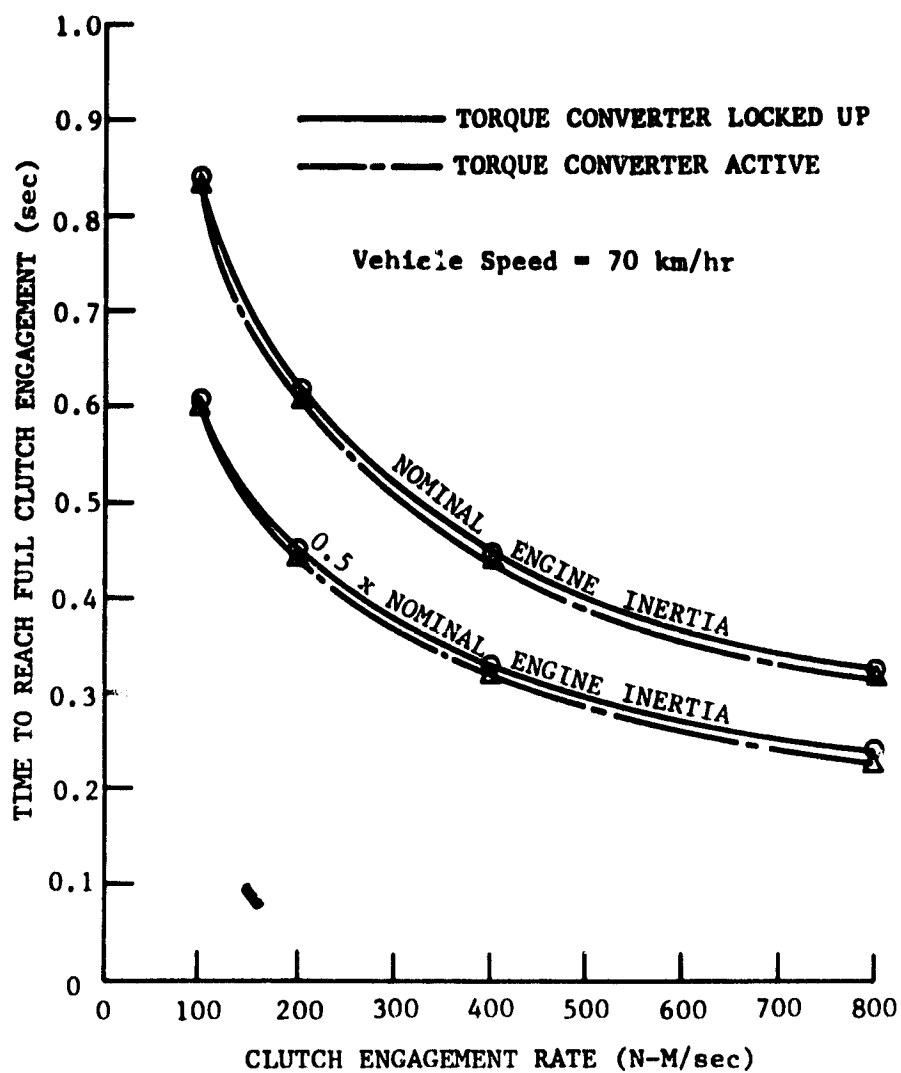


Figure 4-36 Variation in Clutch Engagement Time



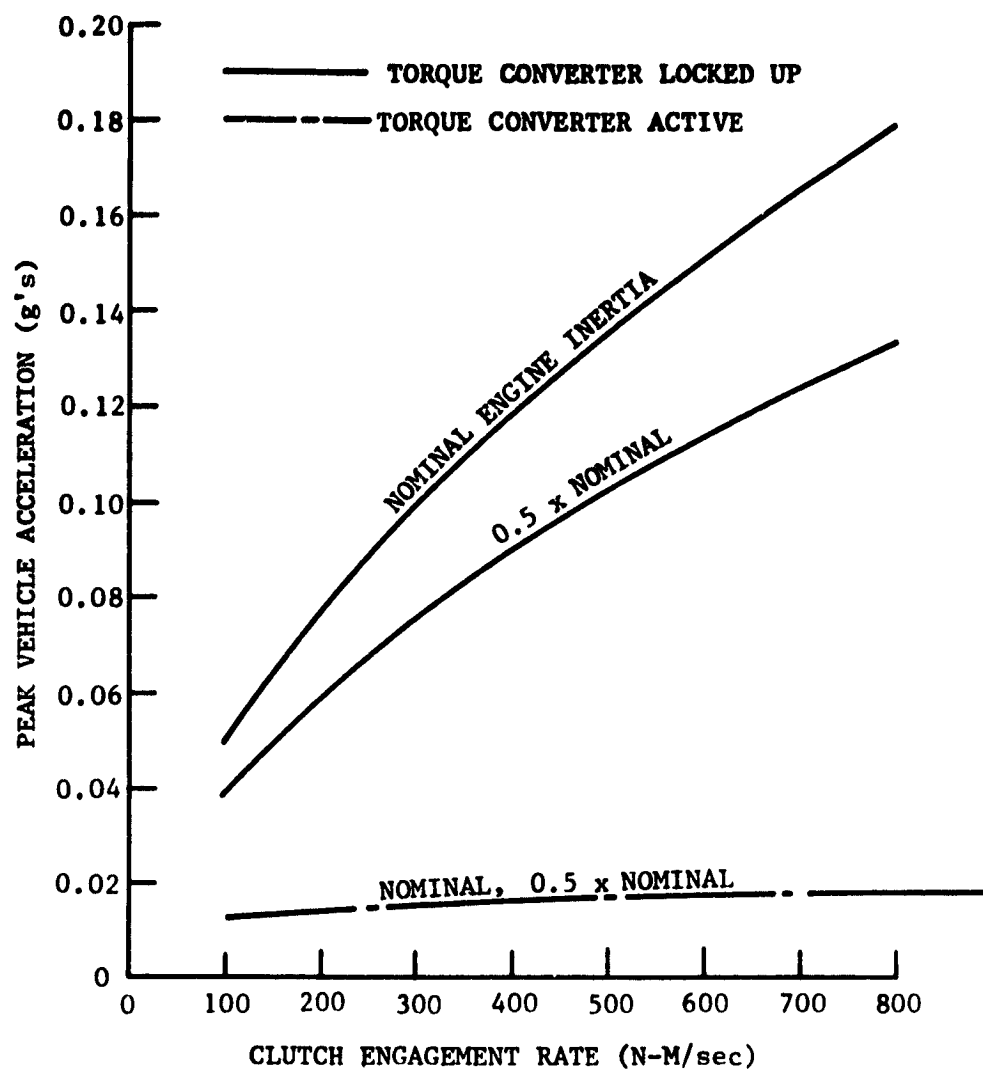


Figure 4-37 Variation in Peak Vehicle Acceleration

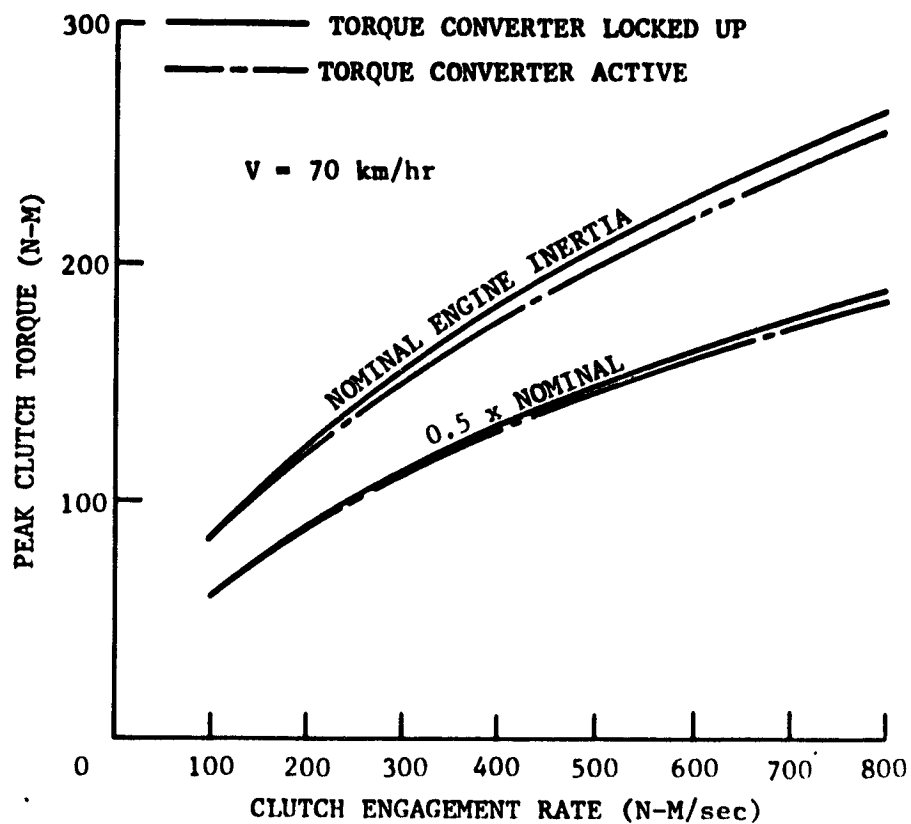


Figure 4-38 Variation in Peak Clutch, Torque with Clutch Engagement Rate

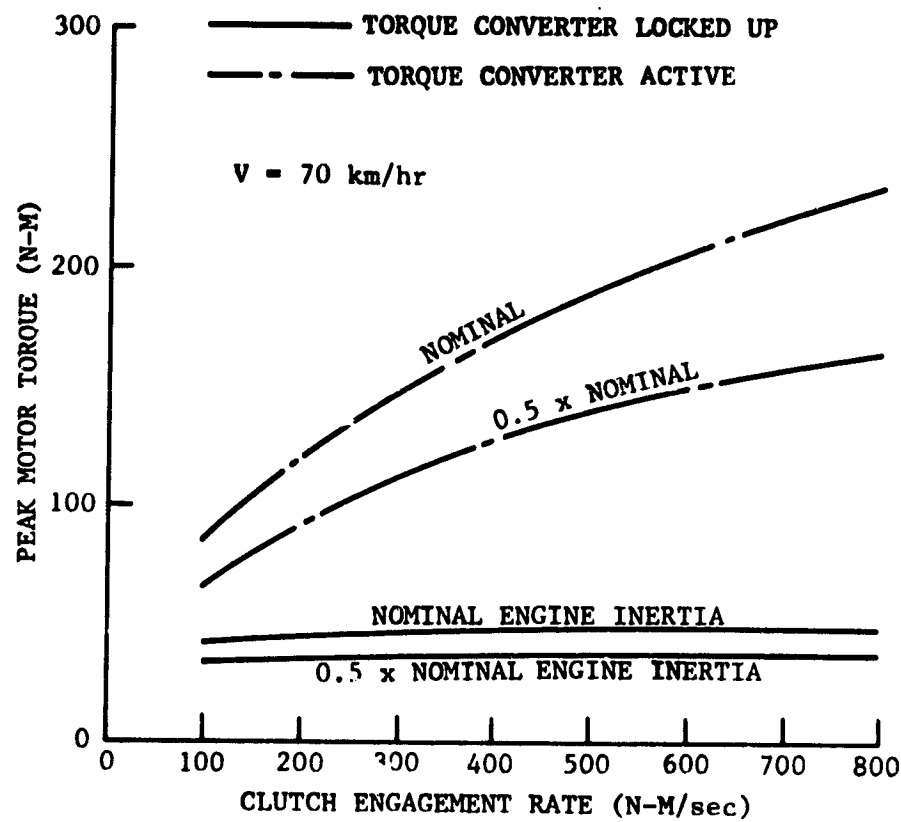


Figure 4-39 Variation in Peak Motor Torque

small, and hence so is the associated motor torque increase. On the other hand, with the torque converter active, most of the energy required to speed up the engine is supplied by the motor, since the torque converter acts to isolate the vehicle mass from the engine/motor combination. Consequently, the torque increase, and speed change, of the motor is much higher in this case. As would be expected, the engine inertia has a much stronger influence on the peak motor torque in the active torque converter case.

Thus far, we have made no mention of motor inertia, for the simple reason that it has very little effect on anything. The only case for which it could be expected to have an effect is the active torque converter case, in which increased motor inertia would aid the motor in starting the engine. However, if the inertia increase was held within reasonable bounds, the influence was very small.

Somewhat more surprising than this was the fact that the time required for the engine to start developing torque on its own had little effect on the engagement time or on the peak motor and clutch torques. Figure 4-40 shows the variation in these three variables for an active torque converter case with a vehicle speed of 20 km/hr., and a clutch engagement rate of 200 N/M sec. Not plotted was the effect on vehicle acceleration, since it was nil.

The effect of speed on the system variables for the active torque converter case is summarized in Table 4-4. Engine moment of inertia is nominal and the clutch engagement rate is 200 N-M/sec.

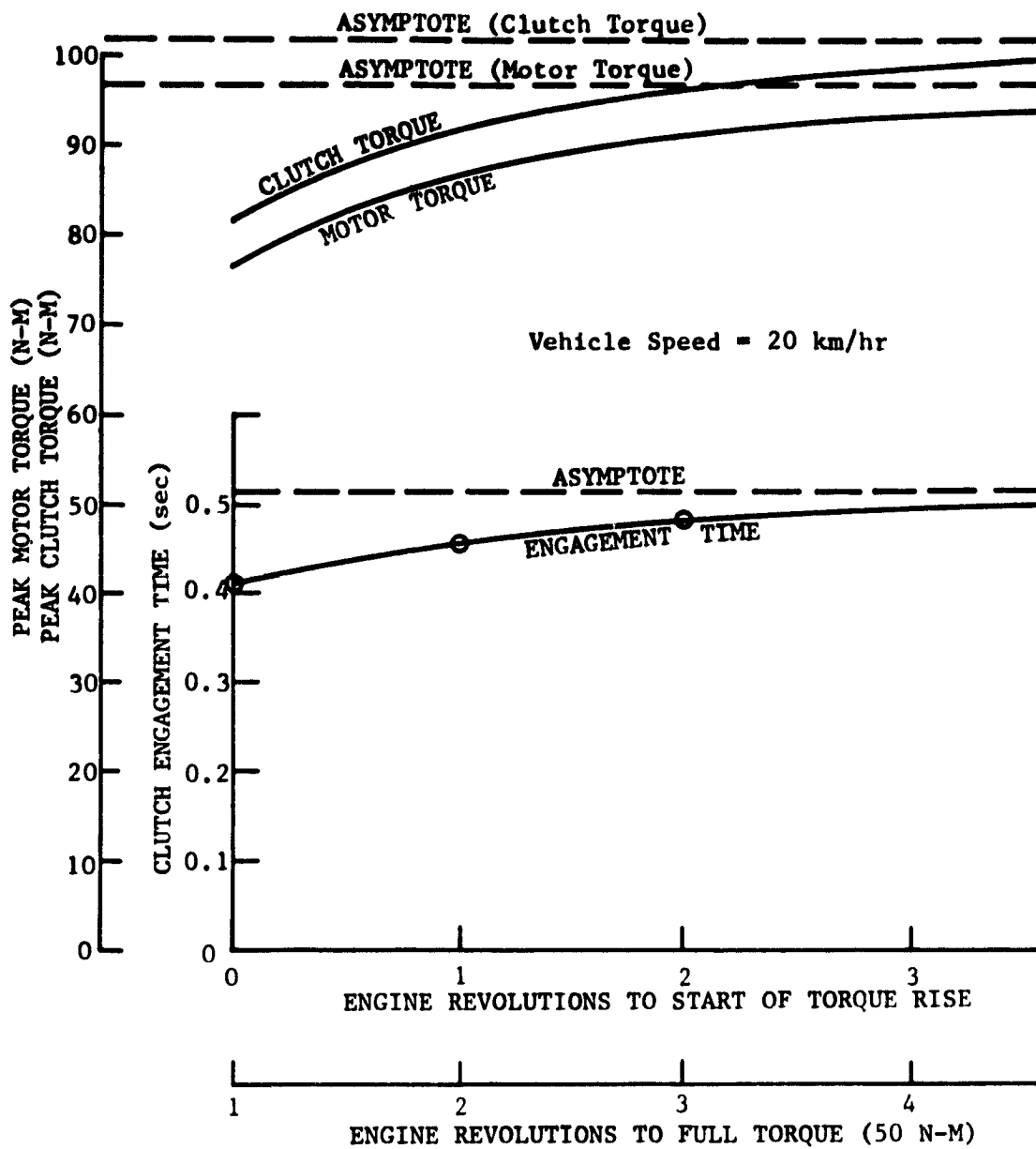


Figure 4-40 Variation in Several Parameters with Engine Startup Period

TABLE 4-4  
EFFECT OF VEHICLE SPEED ON SYSTEM VARIABLES

Vehicle Speed	20 kph	70 kph
Clutch Engagement Time (sec)	.46	.61
Peak Acceleration (G)	.010	.017
Peak Clutch Torque (N-M)	92	122
Peak Motor Torque	87	120

The conclusions drawn from this study are the following:

- . Engine inertia should be minimized. A practical lower limit to this inertia will be set by the inertia of the crank, con rods, pistons, etc., combined with the inertia of the clutch plate. Most of the engine flywheel, which is integral with the clutch plate, should be cut back to minimize the flywheel moment of inertia (normally an order of magnitude higher than that of the internal engine parts). Once the clutch is engaged, the engine will have plenty of flywheel, since it is coupled to the motor and the torque converter pump. Another consideration involves the dynamic loads on the engine/motor coupling chain. In the final design stage, a careful dynamic analysis will have to be done to see how much flywheel has to be retained at the engine to avoid severe load excursions in this chain.
- . With the engine inertia cut back to about 50% of nominal, it should be possible to achieve clutch engagement and engine startup times on the order of .3 - .4 sec. without exceeding the limiting motor torque (160 N-M for the Siemens motor) in the active torque converter case. Under these conditions, the clutch should be sized to handle a dynamic load of about 150 N-M. Clutch engagement rate would be about 400 N-M/sec.
- . It would be highly advantageous from a driveability standpoint to have the torque converter active when engine

startup occurs, due to the much lower effect on the vehicle as compared to the case in which the torque converter is locked up. Thus, if the torque converter is locked up when engine startup is called for, it would be desirable to release the torque converter lock-up clutch and then re-engage after the engine startup is complete. Whether all of this action can be squeezed into a time span of something less than .5 sec. will have to be determined experimentally.



#### 4.1.4 Motor and Motor Controls

##### Motor

The motor selected for the NTHV is the Siemens IGV1 separately excited machine. It was originally designed for application in an electric version of the VW transporter, with a nominal 144 V battery pack. The design center of the motor is 130 V, at which voltage its nominal (1 hr) rating is 17 kw and its peak 33.5 kw. SCT has used this motor with great success in its electric conversion of the VW Rabbit. In that application, a nominal 108 V battery pack is used, and the peak motor power is limited to about 24 kw by current limiting. In the hybrid, the motor will be used with a nominal 120 V battery pack; to achieve the maximum power of 27 kw required with the nickel-iron batteries, about the same current limit will be required as is used in the SCT electric (300 A). Approximately a 10% higher limit will be required with the lead-acid battery pack. These limits are consistent with the motor's maximum current rating of 320 A. The projected maximum and minimum torque curves for the hybrid application are shown in Figure 4-41 .

Efficiency maps in both the driving and braking (generating) modes are shown in Figures 4-42 and 4-43 . The motor characteristics are given for the design center of 130 V; the braking characteristics for 165 V. Time has not permitted the running of dynamometer tests to ascertain the characteristics at the off-design voltage the motor will actually operate at; however, experience with the SCT electric has indicated that the drop-off in efficiency

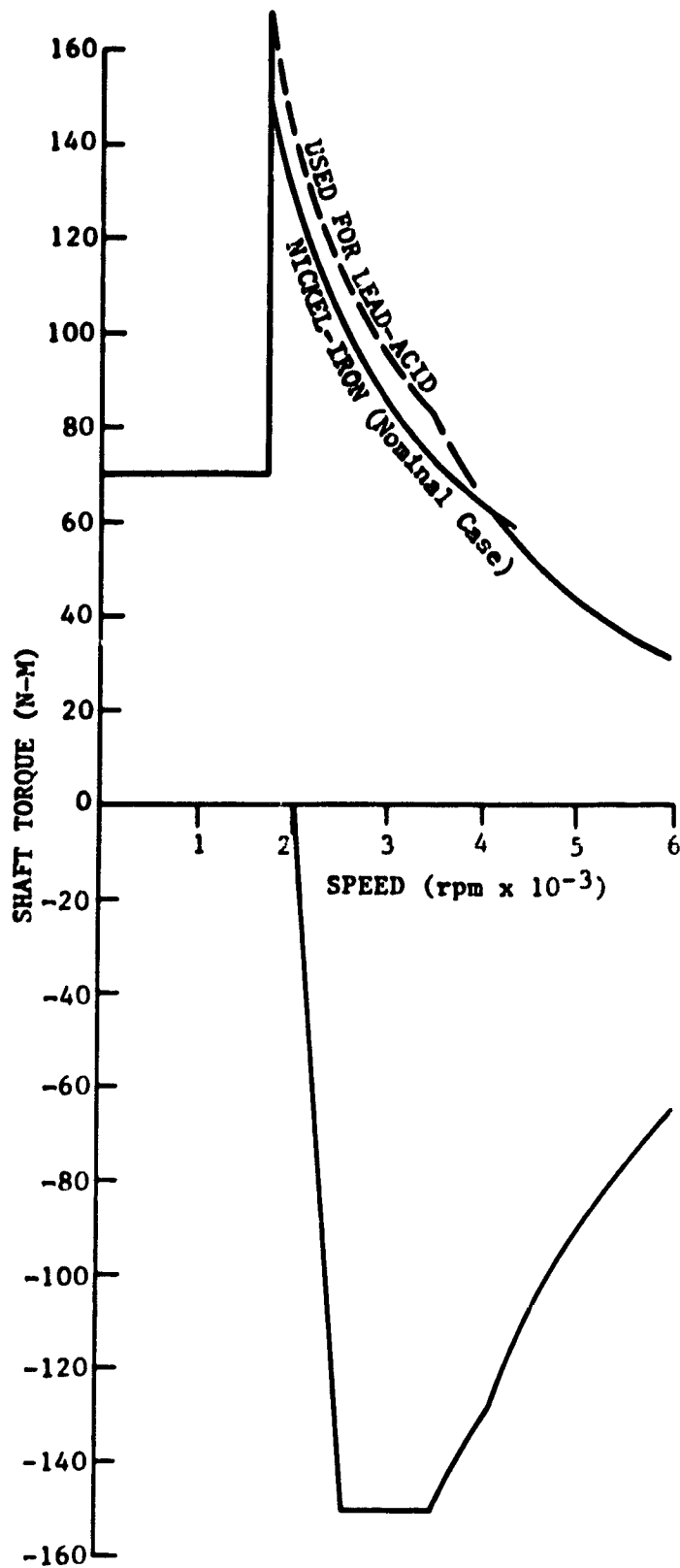


Figure 4-41 Motor/Generator Characteristics

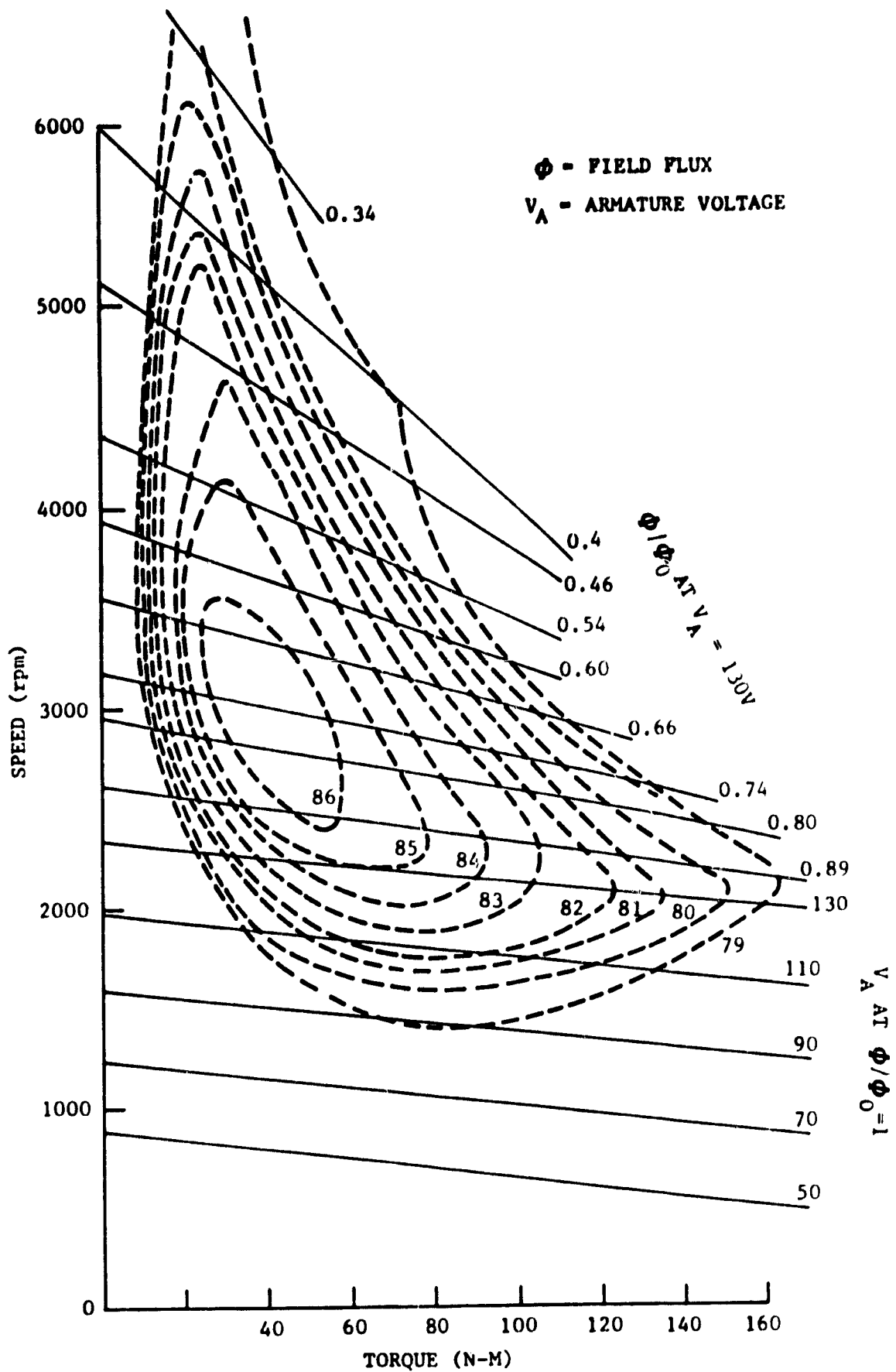


Figure 4-42 Motor Characteristics in Driving Mode

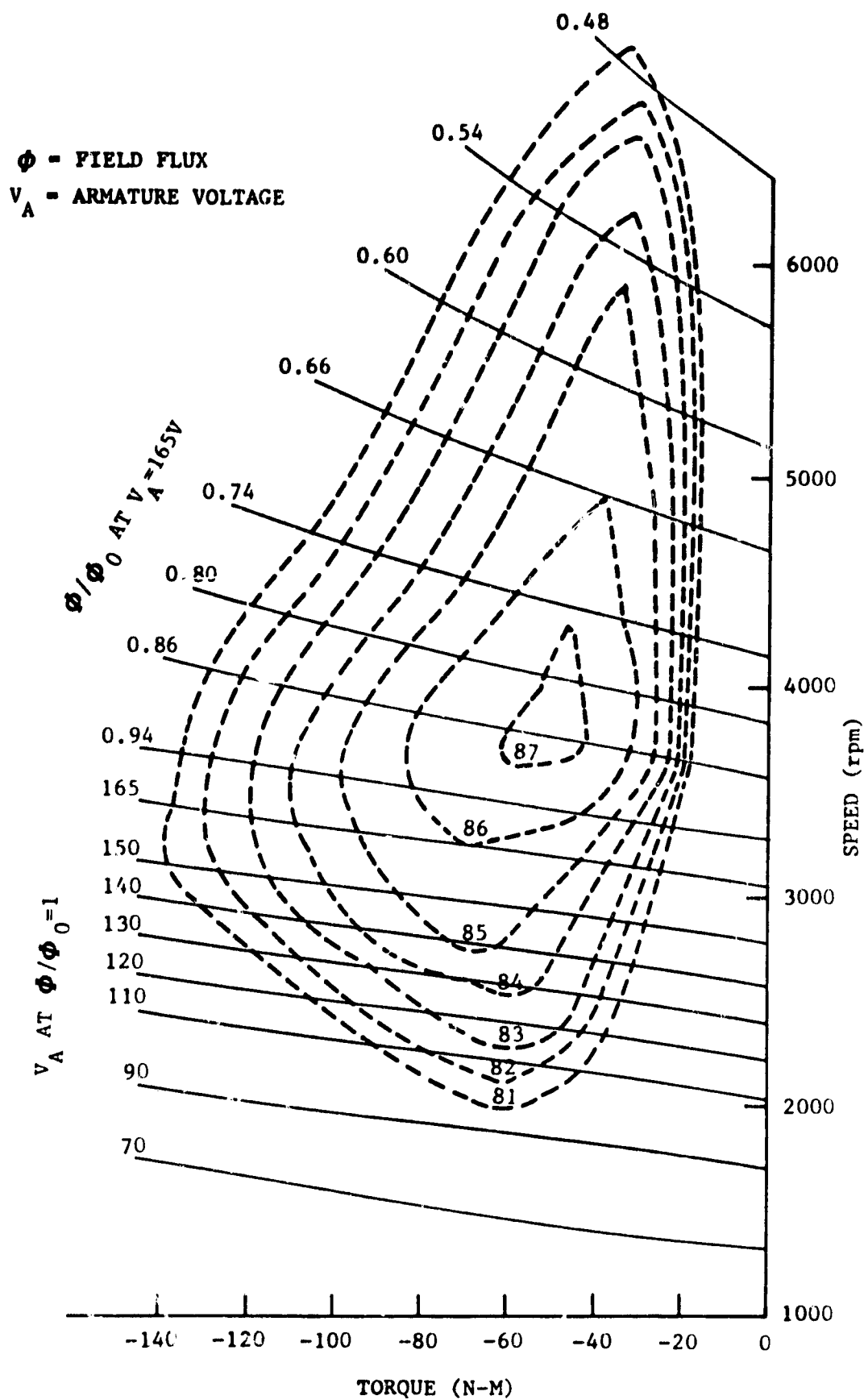


Figure 4-43 Motor Characteristics in Braking (Generating) Mode

is not great from the indicated curves. For example, analysis of full-throttle acceleration traces in 2nd gear for the SCT electric indicated overall drive train efficiencies of about 75%, which implies a motor efficiency of about 80% at the 300 A current limit. This is not significantly different than the Siemens data in the vicinity of the 320 A current limit at the higher voltage. Consequently, within a couple of percentage points, we would expect the efficiency maps of the motor used in the hybrid to look similar to those in Figures 4-42 and 4-43 , with the vertical (speed) scale compressed by the ratio of the nominal battery voltages (120/144, or .833).

The reasons for selecting this motor and using it in essentially its present form, rather than extensively modifying it or attempting to get something new designed specifically for this application, are simple. The motor, as it stands, is so close to what is needed for the hybrid that the time, effort, and cost which would be required for a new or modified design would be better spent addressing the real development problems of the hybrid: controls, emissions, and batteries.

### Armature Chopper

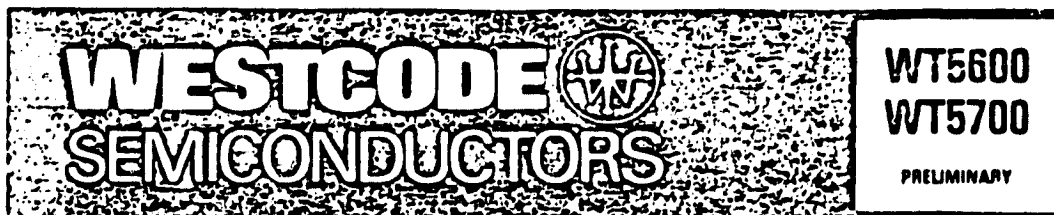
The armature chopper performance requirement has been defined by various computer simulations.

The chopper must supply 140 AMPS of armature current to accelerate the vehicle until the motor reaches base speed. The Siemens motor has an armature inductance of approximately .8 MH. This results in a time constant of approximately .93 ms. In order to reduce the peak-to-peak ripple current to about 10% of the operating current, a chopping frequency of approximately 10.7 KHZ is required. Lower chopping frequencies would require additional inductance in series with the armature.

Switching transistors capable of operating at 10 KHZ and 150 AMPS are not common, but in recent months, several manufacturers have introduced new transistors capable of very high current operation. Several of these are large enough to be used in a single transistor output configuration. Figure 4-44 shows the important operating characteristics of these transistors.

A single transistor output stage would eliminate the need for emitter balancing resistors or other balancing techniques which either waste power or force compromises in the design.

However, these transistors are still considered developmental devices, and their suitability for a particular application must be tested. The final chopper design will be determined only after testing the various devices in a chopper circuit such as those of Figures 4-45 and 4-46. The only difference between Figures 4-45 and 4-46 is the output transistors. Figure 4-45 shows the simplification



## NEW TRANSISTORS to over 550V, 350A

### WT5600 and WT5700 Series HIGH VOLTAGE TRANSISTORS

Westcode Semiconductors have developed the WT5600 and WT5700 Transistors which are the first of a new generation of high voltage, high current transistors, using a single-chip construction. They consist of a triple-diffused  $n-pn-p$  structure, having the advantage of being readily adaptable to a variety of performance levels by adjustment of the internal diffused layers and selection of the appropriate silicon material.

An interdigitated emitter-base structure is incorporated to ensure uniform current distribution and particular attention has been paid to achieving a low saturation voltage at high current levels. The transistor is encapsulated in a hermetic ceramic housing, utilising well proven internal compression bonding techniques to ensure a high tolerance to thermal cycling under arduous duty cycles.

These high current transistors are finding widespread military and commercial applications in high-speed inverters, traction motor drive systems, electric vehicle propulsion, welding sets, spark erosion machines and regulated power supplies.

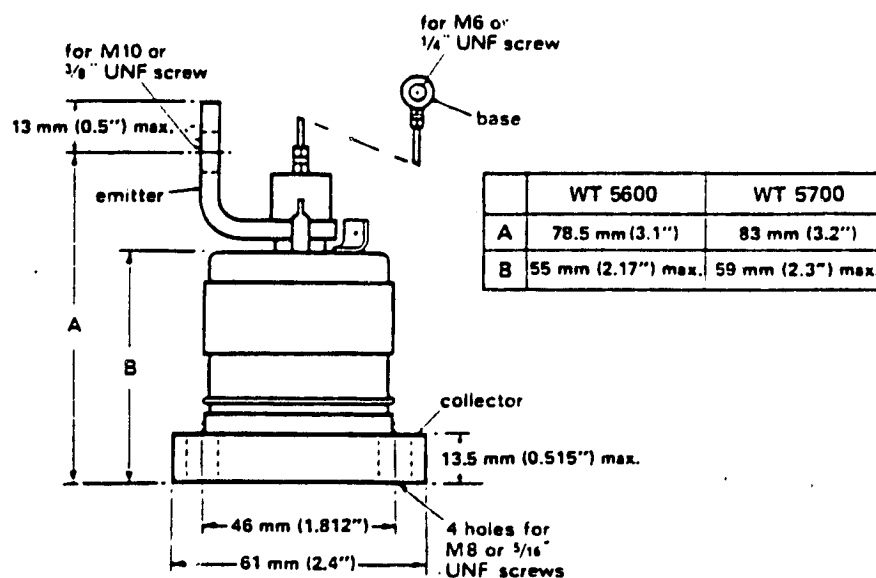


Figure 4-44a Typical Power Transistor Data

**WT5600 Transistor Series – representative data**

Collector-Base Voltage:	( $V_{CBO}$ )	550V
Collector-Emitter Sustaining Voltage:	( $V_{CEOSUSI}$ )	450V
Collector Current:	( $I_C$ )	200A
D.C. Gain at $I_C$ 100A and only $V_{CE}$ 2V:	( $h_{FE}$ )	10
Collector-Emitter Saturation Voltage, at $I_C$ 100A, $I_B$ 15A:	( $V_{CEISAT}$ )	1.0V
Emitter-Base Voltage:	( $V_{EB0}$ )	10V
Collector Current fall time at $I_C$ 100A, $I_B$ – 15A, $V_{EB}$ 5V Clamped Inductive load, $V_{CE}$ 450V:	( $t_f$ )	0.75 $\mu$ s
Total Device Dissipation:	( $P_T$ )	1.25kW

**WT5700 Transistor Series – representative data**

Collector-Base Voltage:	( $V_{CBO}$ )	550V
Collector-Emitter Sustaining Voltage:	( $V_{CEOSUSI}$ )	450V
Collector Current:	( $I_C$ )	350A
D.C. Gain at $I_C$ 200A, $V_{CE}$ 2V:	( $h_{FE}$ )	10
Collector-Emitter Saturation Voltage, at $I_C$ 200A, $I_B$ 30A:	( $V_{CEISAT}$ )	1.0V
Emitter-Base Voltage:	( $V_{EB0}$ )	10V
Collector Current fall time at $I_C$ 200A, $I_B$ – 30A, $V_{EB}$ 5V Clamped Inductive load, $V_{CE}$ 450V:	( $t_f$ )	1.5 $\mu$ s
Total Device Dissipation:	( $P_T$ )	1.5kW

**Westcode Semiconductors**  
P.O. Box 159,  
Richford, Vt. 05476  
Telephone (514) 263-1028  
Telex 05-24218

or, in Canada  
108 Buzzell Street,  
Cowansville, Quebec  
J2K 2N5

Figure 4-44b Typical Power Transistor Data



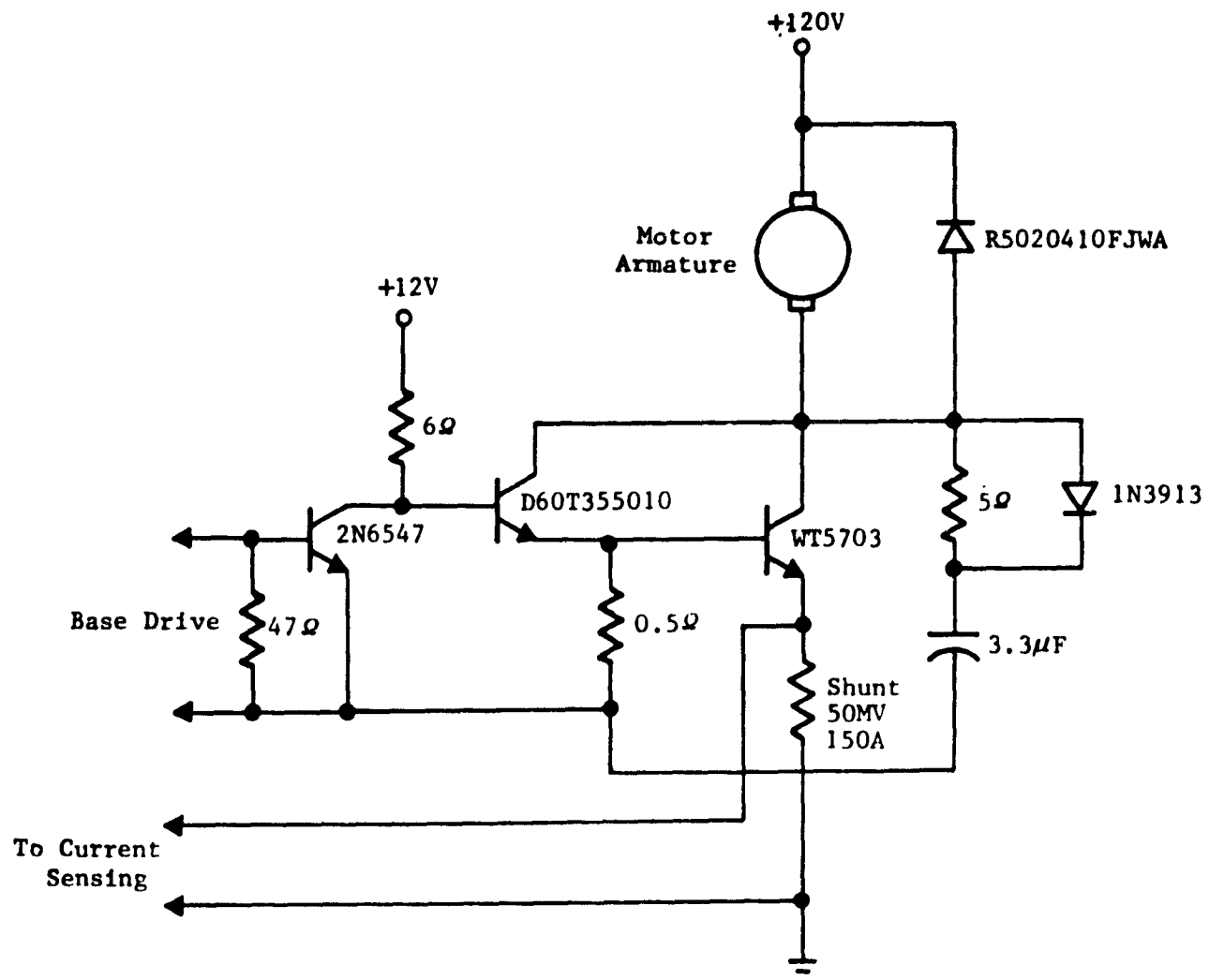


Figure 4-45. Single Transistor Armature Chopper Circuit  
(Shown with WT5703 Transistor)

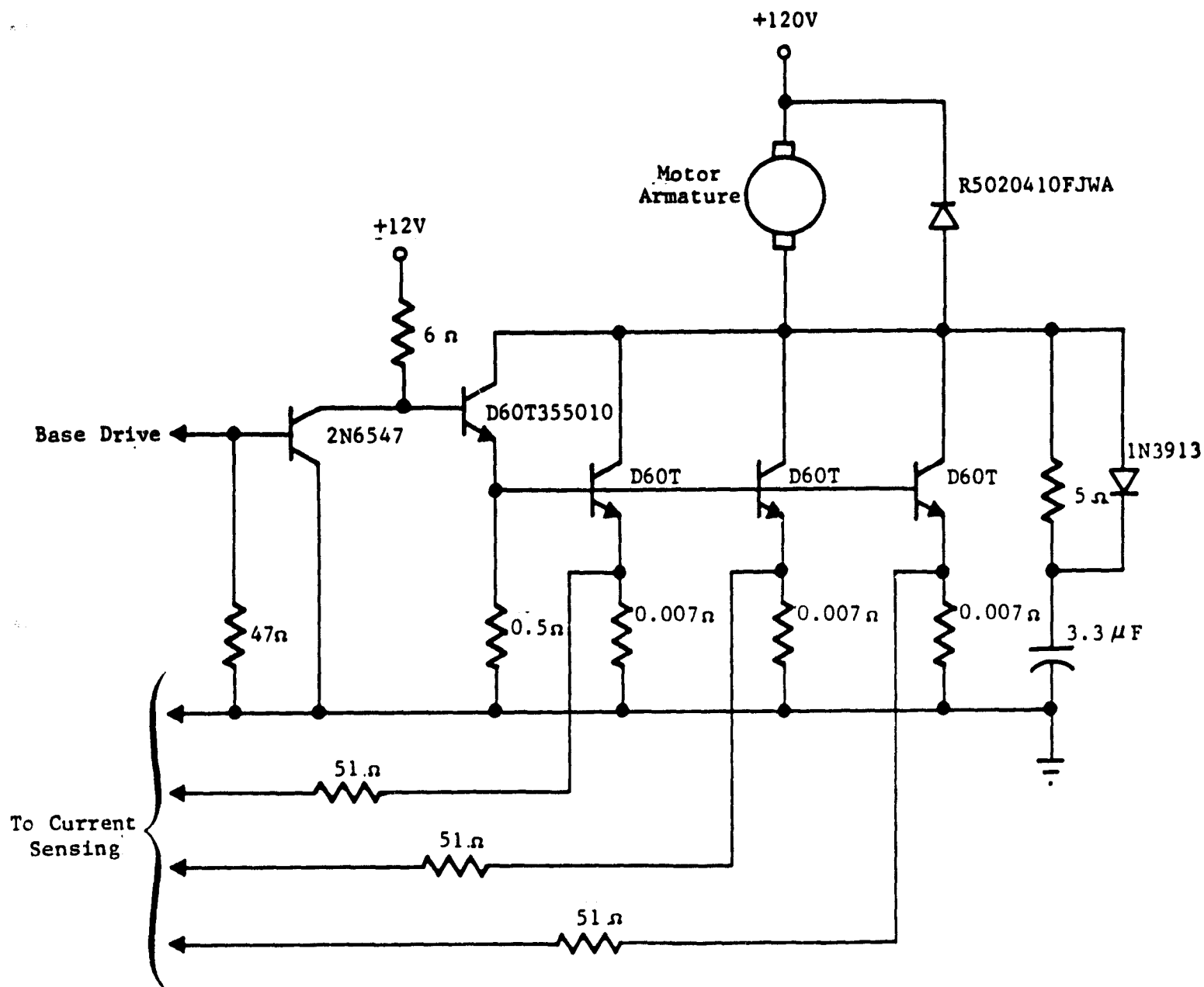


Figure 4-46. Multiple Transistor Armature Chopper Circuit  
(Shown with D60T Transistors)

of the single transistor design.

However, there are other, more subtle differences in these designs. One of the most critical is the turn-off snubber network comprised of the 5 resistor, 3.3 uF capacitor, and the 1N3913 diode. The purpose of this network is to share the current load during transistor turn-off, providing load line shaping. Turn-off is the most critical period of transistor switching, because the collector current flows for a substantial length of time during turn-off, after collector voltage has risen to nearly its peak value. A simple series RC is effective in some cases, but if the collector voltage must be held very low for any appreciable length of time, the value of the required resistor becomes very small, resulting in excessive current on turn-on also. The addition of a diode, as shown, causes the resistor to be bypassed during transistor turn-off, allowing the use of a relatively large resistor which spreads the capacitor discharge time out over a chopper cycle. The use of the diode also cuts resistor power dissipation.

The power dissipated in the snubber network can be substantial. For instance, the snubber network shown in Figures 4-45 and 4-46 will dissipate 150 watts at 10 KHZ. Although this is not a terribly significant amount of power at the overall power levels involved, it is often 20 to 30% of total chopper losses. The hardware required to remove this excess heat is non-trivial and might require forced air cooling which would influence the packaging configuration.

The switching speed of the power transistor is obviously very critical, as well as the safe operating area. Slower switching speeds (long rise times and fall times) increase power dissipation,

and small safe operating areas, which require extensive load line shaping, also waste power in the snubber network.

Since all of the transistors under consideration are newly developed, state-of-the-art devices, they have not been fully characterized for the various operating modes being considered. Therefore, a certain amount of testing, under guidance of the transistor manufacturers involved, will be necessary to arrive at a final, optimized circuit configuration.

Since the final chopper design is still, to some extent, undetermined, the drive circuits are shown in block form in Figure 4-47. The final circuit implementation will be similar to the drive circuits for the battery charger. (Section 4.1.7)

As shown in Figure 13, the input control signal for the armature chopper will be a voltage from 0 to 10 volts which will correspond to 0 to 140 AMPS of armature current. Since the transistors cannot be left in the "ON" state for much more than 100  $\mu$ s at a time, direct microprocessor control was not considered. The control signal commands an average current, and the chopper control logic produces the required waveform. The control logic is similar to the battery charger logic. When the rising current (because of armature inductance) reaches the commanded value, the transistors turn off for a short period of time. They then turn on again to repeat the cycle.

Overall circuit efficiency will be approximately 90 to 95%. The entire chopper, including power circuits and drive circuits, will be contained in a box approximately 12" X 20" X 8" weighing approximately 25 pounds. This box will also include the field chopper.

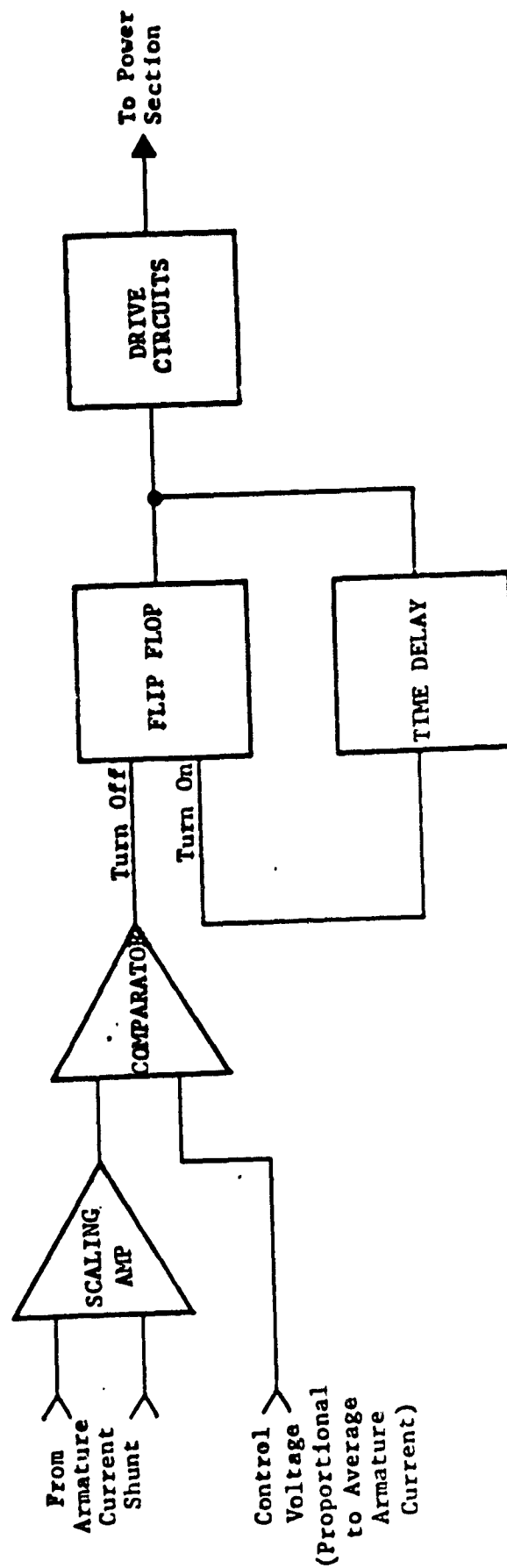


Figure 4-47 Armature Chopper Control Circuits

### Field Chopper

The field chopper power section will be very similar to the one used on the Electric Rabbit SCT and the basic design is illustrated in Figure 4-48 . Pulse width modulation control signals will be generated by the microprocessor. The chopper frequency will be selected so that induced armature current ripple is minimized. Experience has shown that a frequency in the range of 25 to 100 Hz would accomplish this. This low a frequency is possible since the field inductance is high, on the order of 1.5 H. One transistor is used in the output stage, a Kertron U675, which is gain rated at 15 A with a 200 volt breakdown rating. The field winding resistance is on the order of 10  $\Omega$  so this single device is well suited for this application. SCT's present controller uses three 2N6259 transistors in parallel for this purpose because the U675 or a similar device was not available at the time of that controller's development.

The circuit of Figure 4-48 also illustrates the use of the turn-off snubber network described previously in the armature chopper section. It accomplishes the objective of holding the collector voltage low during turn-off while still allowing a reasonable turn-on time with the R and C shown.

This circuit will be appropriately tested prior to arriving at the final design configuration.

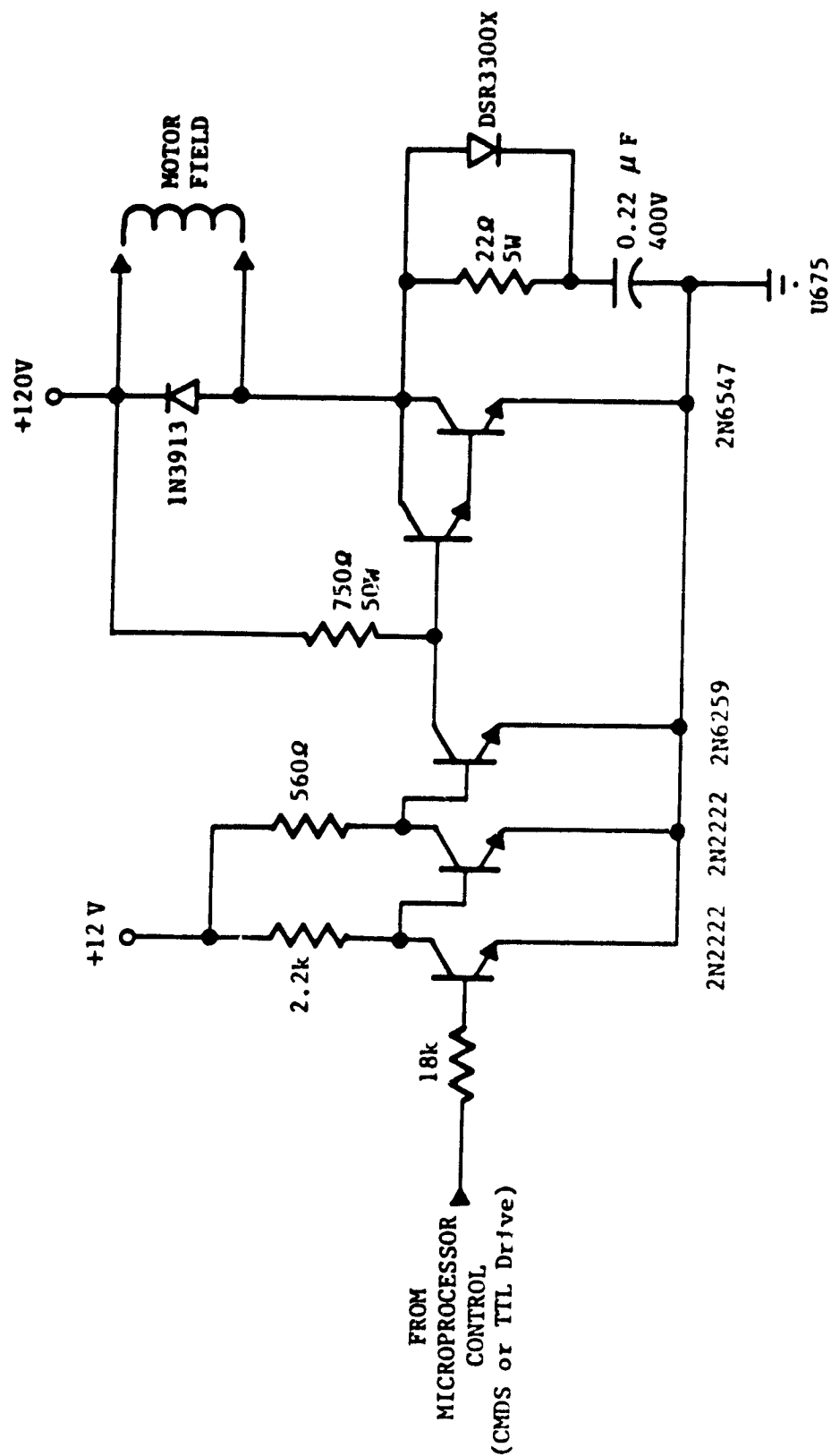


Figure 4-48 Field Driver

#### 4.1.5 Batteries and Battery Charger

##### Batteries

As an introduction to this section, it appears worthwhile to mention that all of the design and development work on the near-term, or improved state-of-the-art (ISOA), batteries has been carried out for cell and battery configurations tailored to pure electric vehicles. Nothing of substance (i.e., something built and tested) has been done relative to the hybrid application. Moreover, the different states of development of the three near-term battery types are such that no hard conclusions can be drawn yet as to which would be best for the electric vehicle application in the mid-80's. If this were possible, then there would not be any reason for ANL to continue to pursue multiple lines of battery development. Consequently, it is very clear that there is no clean, demonstrably accurate method for selecting the 'best' battery for the hybrid application. The best that can be done is examine the status of the three battery systems relative to the ANL goals, together with their performance in the hybrid system, assuming these goals are attained, and make a judgement as to which system or systems to work with within the constraints of the NTHV program.

The latest results presented by ANL regarding the progress of the three battery systems have been examined; based on these results, and on communication with the battery developers, we have not seen anything to change the conclusions stated in the Task 2 report (1). These were: that the nickel-iron system



had the highest overall potential because of a good combination of relatively high specific energy and specific power and a low cost/life quotient, with lead-acid and nickel-zinc a fairly close second and a distant third, respectively. However, it must be recognized that the nickel-iron system has not had the same amount of development applied to it as the other system, and consequently there are more unknown areas. To guard against this being an application of the law that the more unknowns there are about a system, the better it looks, good judgment would dictate carrying along an alternative into the development program. Consequently, we have selected as a preferred system a nickel-iron system designed by Eagle-Picher, with a lead-acid system by ESB as a backup.

1. Nickel-Iron Battery. This battery pack is comprised of 102 cells of the same height (264 mm) and width (178 mm) as those being developed by Eagle-Picher for ANL on the Improved State-of-the-Art Battery Program. The cell thickness is reduced to 28 mm to get the required number of cells to provide a nominal 120 V battery at the relatively low weight of approximately 270-280 kg. The cells are arranged in three rows of 34 cells each, with the overall package fitting behind the vehicle's rear axle. Having all of the cells in a single package like this simplifies the problems of thermal management and ventilation.

A decision has not yet been made with respect to the physical connection of the cells. Whether the battery will

be built up from individual cells with all external connections, or from a smaller number of modules with through-cell wall connections within a module, will be decided during Phase II.

The specific energy density projected by Eagle-Picher at the C/3 rate is 54 w/kg. The projection for peak specific power is that 130 w/kg. is readily attainable, with 150 w/kg possibly attainable. These numbers agree with the following information presented by ANL at the 3rd EHV Program Contractor's Meeting: on a cell basis, 58 W-H/kg C/3 specific energy is being obtained and 150 W/kg 15 sec peak specific power at 50% depth of discharge. Battery performance is expected to be 10-20% lower. Based on these numbers, we have assumed a Ragone plot for nickel-iron batteries of the form shown in Figure 4-49. This curve may be too conservative, at least at the upper end. However, although the progress of this system relative to the ultimate goals is extremely encouraging, there is no hard data available to characterize it under conditions other than the C/3 rate, and the best we can do at this stage is examine the sensitivity of our results to variations in the assumed characteristics. The results of such an examination were discussed in Section 4.1.2.

The same data availability problem exists, to a greater degree, with respect to life data. Life testing has only started recently in this program, and there has not been time to accumulate the needed data (and probably won't be for some time to come, if the life goals come anywhere close

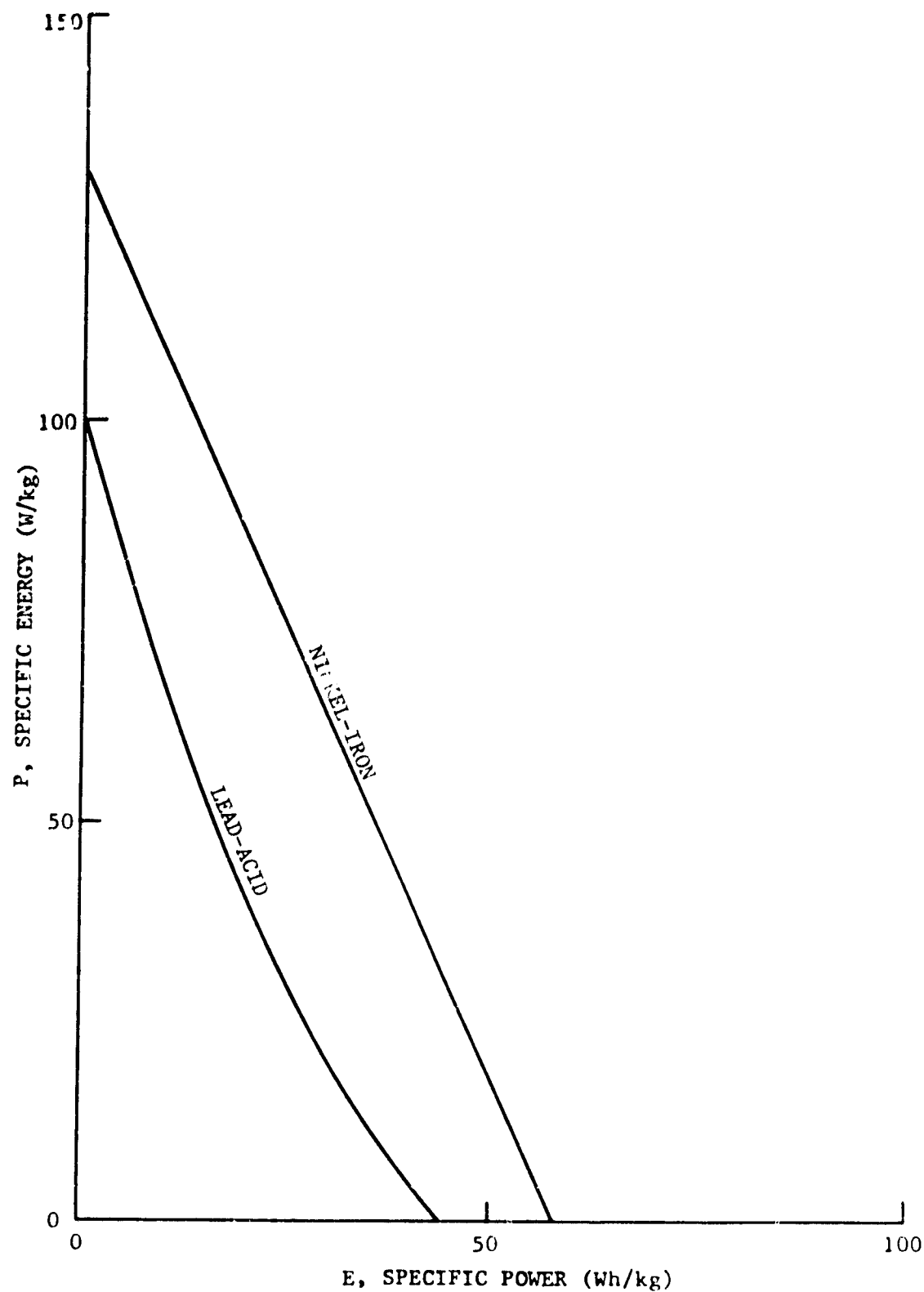


Figure 4-49 Assumed Battery Performance Characteristics

to being obtained).

The Eagle-Picher design utilizes the iron electrode technology developed by the Swedish National Development. This is a relatively low gassing electrode, which obviates one of the historical disadvantages of the nickel-iron system, and provides a relatively low maintenance battery. Batteries which would be provided initially in the Phase II program would require normal service, with the goal of providing a reliable, single-point watering system eventually. Single-point watering would, of course, be a necessity on a production vehicle.

Apart from the gassing problem, other disadvantages which the nickel-iron system has had include high stand losses (i.e., a relatively high rate of self-discharge), and low temperature problems. The former might impact the maximum period of time for which the vehicle can be stored unserviced. Tests to determine stand losses would have to be performed during Phase II, and an evaluation made at that time of their effect on storage requirements. In either the nickel-iron or lead acid cases, battery heating for low temperature storage and forced air cooling for high temperature operation, will be required. As long as such systems must be provided under any circumstances, the relative merits of the two battery systems with respect to thermal management are not particularly relevant. It must also be recognized that the hybrid does have the advantage of having a heat engine

available. In extremely cold weather, all that is really necessary is to have enough energy available from the propulsion battery to get the heat engine started. Once it is started, a portion of its output can be diverted to charging the battery. This would require implementation of a separate, low-temperature control strategy which would permit the engine to run at all times, even when the vehicle is stopped or decelerating. Reversion to the normal strategy would occur when the battery temperature rises to an acceptable value.

2. Lead Acid Battery. The lead-acid battery is comprised of ten 12 V modules to be designed and developed by ESB. Module dimensions are 31.8 cm. high x 17.9 cm. wide x 27.4 cm. long. and the total battery weight is estimated at 341 kg., or 71 kg more than the nickel-iron system. This module size does not correspond to the case size on any existing production battery, and new case tooling would be required. Battery performance characteristics would be similar to the XPV-23 (EV 130), adjusted for size weight, etc. The energy density is estimated at 36.1 w-hr/kg, which corresponds to a usable energy at the three hour rate of 12.3 kw-hr. As in the case of the nickel-iron system, normal maintenance would be required on test-and-development batteries; eventually, however, a single-point watering system would be required.

With the module configuration described above, the lead-acid

battery pack can be accommodated in essentially the same overall package as the nickel-iron battery; overall dimensions for the lead-acid pack are 90 m long x 56 m wide x 32 m high, vs. 96 m long x 55 m wide x 33 m high for the nickel-iron battery. Packaging in the vehicle for both battery types is shown in Figure 4-50.

#### Battery Charger

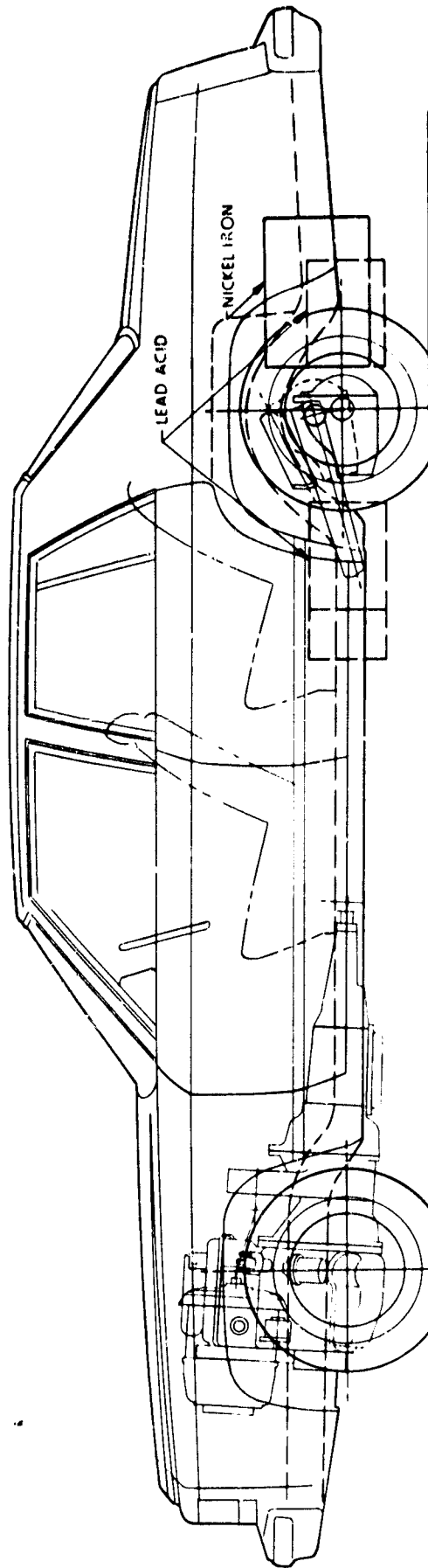
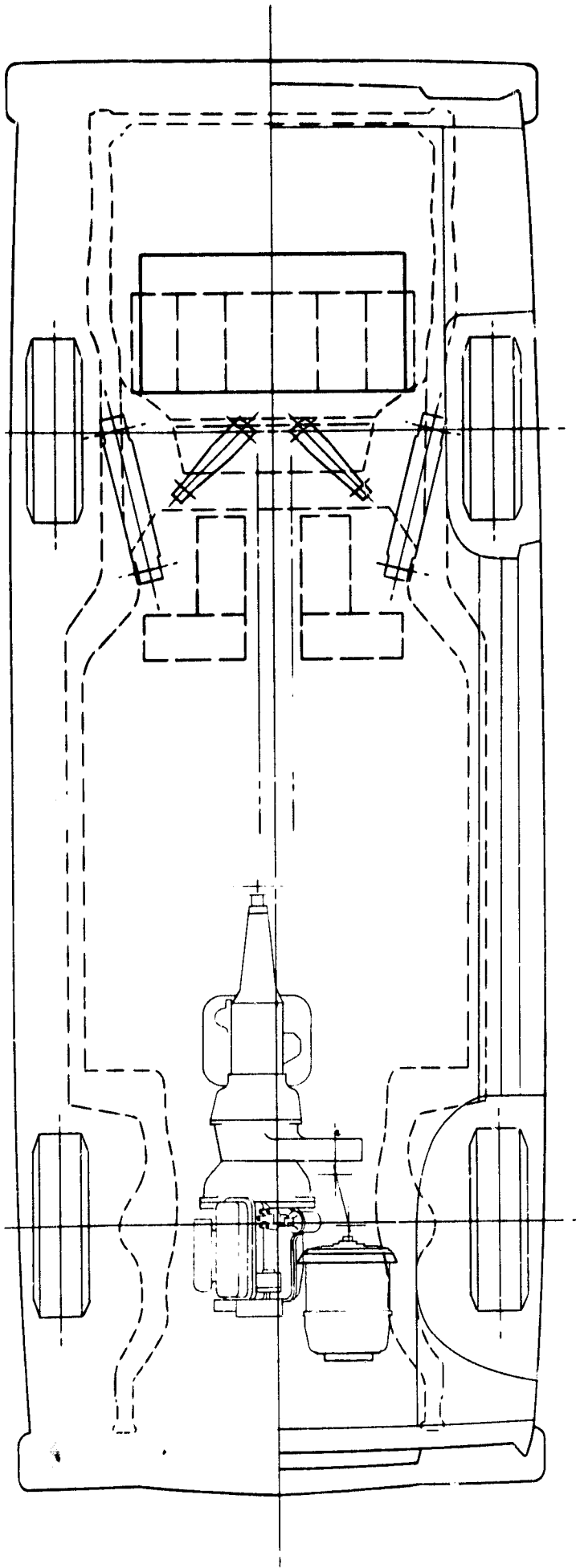
The battery charger design began with a survey of possible techniques. Three basic types of chargers were considered:

- (1) Ferroresonant
- (2) SCR switching series inductor
- (3) Transistor switching series inductor

The ferroresonant design, although quite common, was rejected because of its size and weight.

The SCR/series inductor was a very promising design because of the simplicity of the SCR bridge operating directly off the AC line. Its major drawback was the size of the required series inductor. This inductor became extremely large if 220V operation was required. Although not required by the original design goals, it was decided that the higher battery currents available from 220V operation were highly desirable.

This left the transistor chopper. A transistor chopper can operate at relatively high frequencies, thus proportionately reducing the



SOUTH COAST TECHNOLOGY	
2214 BEEBEAR CA 93117	
HYBRID-1979 LTD PACKAGE	
DATE: 11	DRAWN BY: J. W. JONES
	CHECKED BY: J. W. JONES

Figure 4-50. BATTERY PACKAGING

size of the series inductor. Since an inductor for 220 volt operation would have weighed close to 40 pounds, the transistor chopper became the obvious choice. The inductor for the transistor chopper will weigh about 2 pounds.

The following features were to be designed into the charger:

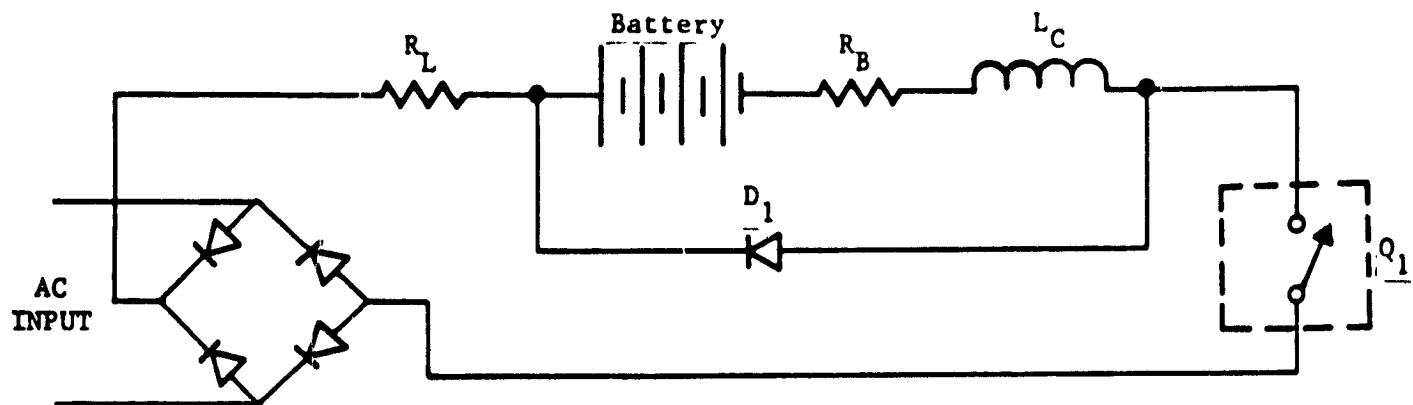
- . 20/30 AMP line select
- . 115/230 volt operation
- . current cutback at gassing point
- . automatic shutdown at voltage
- . automatic startup
- . equalize mode (finish and 24 hour trickle)
- . blower air flow interlock
- . thermal shutdown for high heatsink temperature

With these features in mind, a computer simulation was run on the power section of the charger. Figure 4-51 shows the equivalent circuit used in the simulation. The model is relatively simple, since its main purpose was to determine the inductor size and transistor ratings. The simulation assumed the following control strategy:

- (1) If current through  $Q_1$  is less than  $I_{max}$ , and if  $Q_1$  has been off for at least time  $T$ , then turn on  $Q_1$ .
- (2) If  $Q_1$  is on, stay on until the current through  $Q_1$  exceeds  $I_{max}$ .
- (3) As the current through  $Q_1$  exceeds  $I_{max}$ , turn off  $Q_1$  for time  $T$ .

This control strategy prevents the transistor current rating from being exceeded, while maintaining average battery current at its





$R_L$  = Resistance of AC Line  
 $R_B$  = Combined Resistance of Battery and Inductor  
 $L_C$  = Inductance of Series Inductor  
 $Q_1$  = Idealized Transistor Switch  
 $D_1$  = Ideal Diode

<u>INPUT:</u>	BATTERY VOLTAGE
	PEAK CURRENT
	INDUCTANCE
	OFF TIME
	BATTERY RESISTANCE
	LINE RESISTANCE
	AC LINE VOLTAGE
	INTEGRATION STEPS
<u>OUTPUT:</u>	RMS BATTERY CURRENT
	RMS LINE CURRENT
	AVG BATTERY CURRENT
	AVG LINE CURRENT
	PLOT OF CURRENT WAVEFORM
	PLOT CHARGING CURRENT vs
	BATTERY VOLTAGE

Figure 4-51 Equivalent Circuit Used in Simulation

highest possible value.

Figure 4-52 shows the waveform of battery current produced by the simulation for 108 volt AC input (1/2 of AC cycle plotted). No current flows until the line voltage rises above battery voltage. Current then begins rising. When the transistor's maximum current rating is reached, the transistor turns off for a preset length of time, allowing the inductor to discharge through the battery. The transistor then turns on again, causing the inductor to begin charging again. This cycle continues as long as line voltage remains above battery voltage. Figure 4-53 shows the average battery current as a function of battery voltage for 117 volts input.

Circuit efficiency is expected to be about 92% with 115 volt input, and 94% with 230 volt input. All components could be mounted in a box approximately 14 X 14 X 7 weighing approximately 15 pounds.

A preliminary schematic diagram of the charger logic board and power circuits is enclosed with the Preliminary Design Drawing Package (Appendix B).

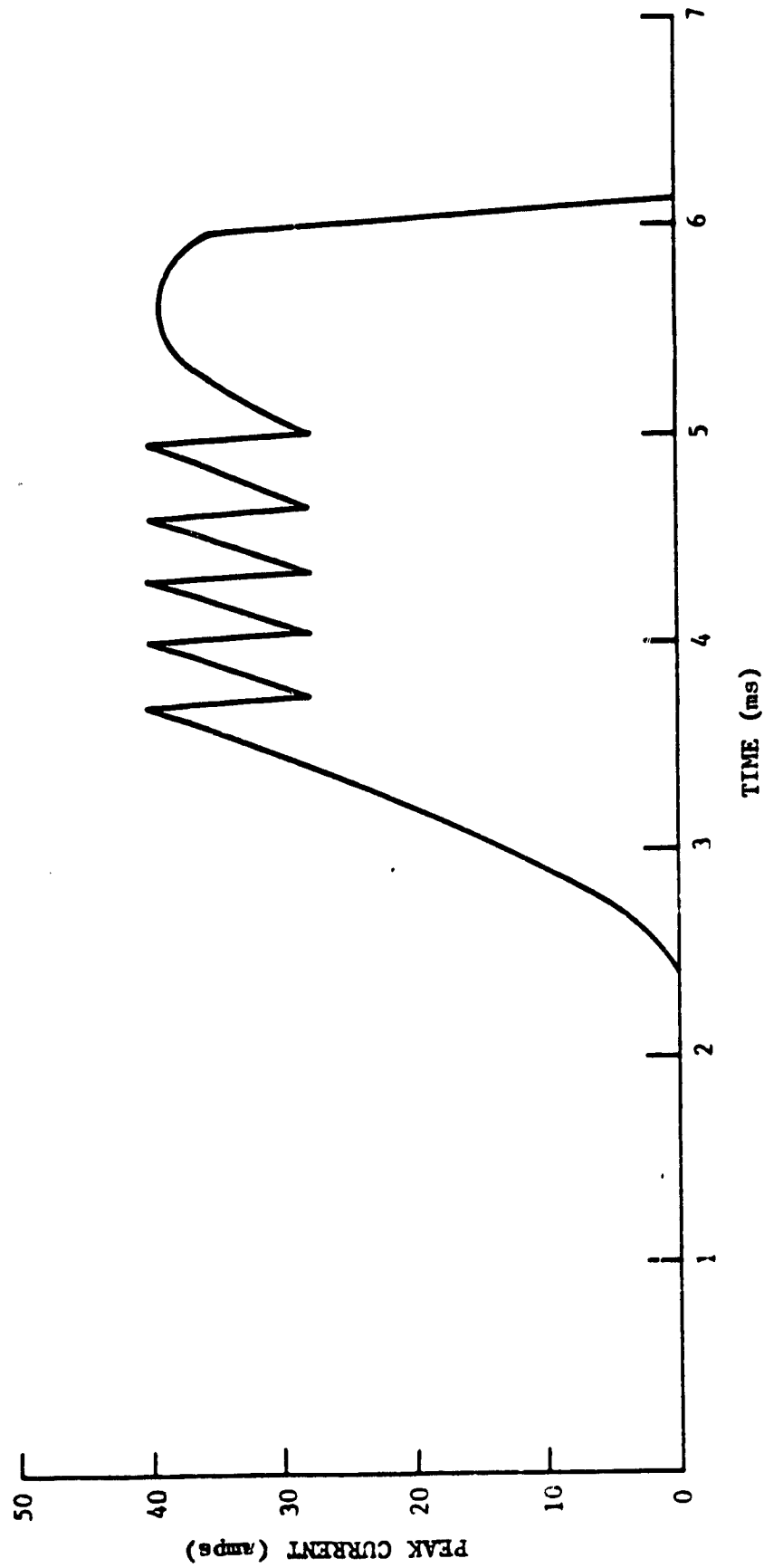
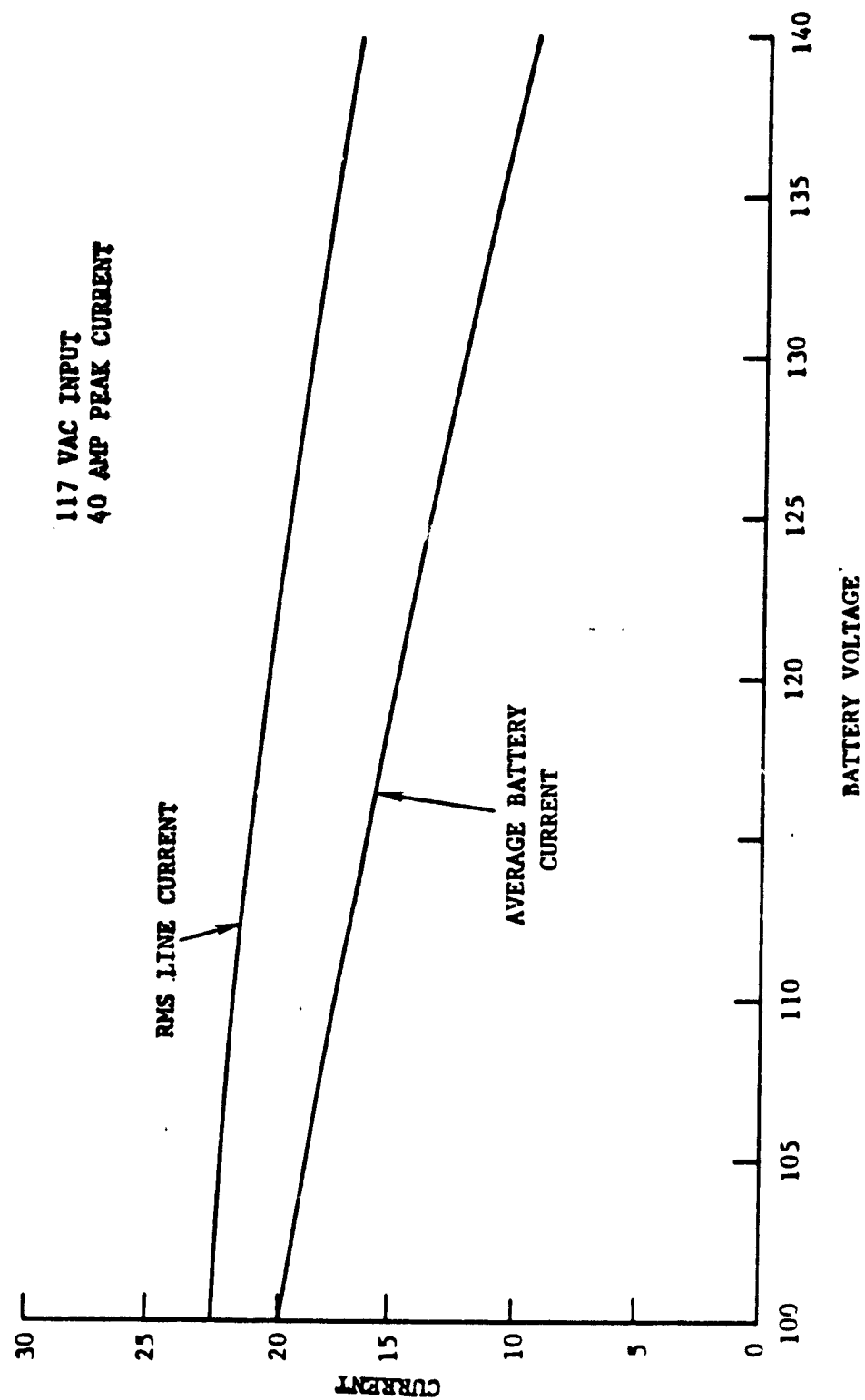


Figure 4-52 Current Waveform During Charging



#### 4.1.6 Transmission and Rear Axle

##### Transmission

The transmission for the NTHV is a four-speed overdrive automatic transmission with torque converter lockup on the top two gears. Originally, we were looking for lockup on the top three gears; however, deleting the second gear lockup had very little effect on fuel economy (about 1%), so it was dropped from the requirements. The specifications developed for transmission are shown in Table 4-5. Unfortunately, there is no production transmission which meets precisely the specifications needed for this transmission. The three production transmissions which come closest are the following:

- . Chrysler A904 Torqueflite, as used on the 3.7 l Aspen/Volare model. This is a 3-speed transmission with lockup on third. The gear ratios are identical to those specified in Table 4-5, but it lacks the overdrive fourth gear. The torque converter is a 273 mm dia. unit with a stall torque ratio of 2.01. Input torque capacity is in excess of 300 n-m. Apart from the lack of a fourth gear ratio, the only deficiency might arise from the fact that the power plants with which the transmission is normally used have a speed range which does not extend past about 4500 RPM. The hybrid power plant operates in a higher average speed range, so front pump losses might be higher than normal.

TABLE 4-5

NTHV TRANSMISSION SPECIFICATIONS

Number of speeds:	4
Ratios:	1st 2.45
	2nd 1.45
	3rd 1.00
	4th 0.75
	Reverse 2+
Input Speed Range:	0-6000 RPM
Input Torque Range:	0-220 N·M
Lockup Provisions:	3rd and 4th gears, minimum
Stall Torque Ratio:	2.1
Normal Torque Converter Dia.	276 mm.

- . Ford F10D. This is a 4-speed overdrive transmission which will become available as an option on 1980 Ford products with 5 liter and 5.8 liter engines. It has full lockup in overdrive and a split torque path in direct 3rd in which only 40% of the engine torque flows through the torque converter. The gear ratios in are 2.4, 1.47, 1.0, and .67; close to the specification with the exception of the overdrive 4th, which is a little lower (numerically) than is desirable. The basic problem with this transmission for the hybrid application is that it is designed for a higher torque, lower speed power-plant than the hybrid. Speed reduction on the order of 33% would be required at the torque converter input before it would be suitable.
- . Toyota A40D. This is a 4-speed overdrive with the right ratios, except for the overdrive 4th which is a little low (.69 vs. .75), and the right speed range (0-6000 RPM). It is a little short of torque capacity (rated at a maximum of 196 n-m), but it would probably be adequate for development purposes. The torque converter is also on the small side for the hybrid application. The major problem which inhibits its use for the hybrid is the lack of lockup capability.

The closest approximation to the specifications derived for the NTHV transmission would be the Toyota 4-speed equipped with a lockup torque converter. Developing a lockup converter for this transmission would be, however, outside the scope of a program such as this. The approach which appears to simulate

the desired transmission characteristics most closely is to use the Chrysler A904 3-speed in conjunction with an electrically controlled overdrive. This may not represent the approach that Ford, GM, or Chrysler would use (although American Motors would be likely to do something like it); however, it is preferable to work with an acceptable simulation of the optimum transmission which can be put together at reasonable cost, rather than turn the Phase II NTHV Program into a transmission development program. A backup possibility is to use the Toyota transmission and forego the lockup capability. This alternative would be used only in the event that development testing indicates that the vehicle transients during engine startup are excessive with the torque converter locked up, and that the technique of unlocking the torque converter during the startup transient is not workable. The combination of a shift to a smaller torque converter and the loss of lockup capability would probably mean about a 5% drop in fuel economy.

In any event, a substantial amount of development work will be required to adapt the transmission to control by the system  $\mu$ P. The simplest way of doing this will probably be to implement a minimum of internal modifications to the transmission, and develop an external program and interface hardware whose function is best described by the following example:

Suppose the operating conditions are such that the  $\mu$ P decides an upshift is called for; say the transmission output speed is 3000 RPM at this point. The external program would have stored



the transmission's normal shift logic (i.e., shift points as a function of speed and throttle opening), and it would decide what throttle opening would normally provide an upshift to the 3000 RPM output speed. In place of the normal linkage from the carburetor to the 'throttle' valve in the automatic, a small servoactuator would move the throttle valve to the appropriate position, based on the program output.

A simpler scheme would be to just shift the transmission throttle valve full stroke in one direction (closed throttle) when the  $\mu P$  calls for an upshift and full stroke in the other direction when it calls for a downshift. This, however, is unlikely to be satisfactory without making substantial internal modifications to the transmission, since all upshifts would then take place like a light throttle upshift (i.e., 'soft' and slow), and all downshifts would take place like a full throttle downshift (harsh and fast).

Internal modifications will be necessary in any case on the Chrysler transmission to raise the full throttle shift points of the transmission to the 6000 RPM maximum speed of the hybrid power plant.

#### Rear Axle.

The rear axle needed for the hybrid is also non-standard. The standard LTD axle ratio is 2.26; the hybrid requires something on the order of 5.12. Consequently, a custom ring and pinion set will be needed.

#### 4.1.7 Accessory Power

##### Mechanical

Mechanically driven accessories are limited to the power steering pump and air conditioning compressor. For computer simulation purposes, the front pump of the transmission is also lumped in with these; however, these two are the only ones which are belt-driven from the engine/motor package. The power steering pump also supplies hydraulic pressure to the Hydroboost power brake; it is the stock Ford LTD unit. The air conditioning compressor, for packaging reasons, is a General Motors unit as used on the X-body cars. Both of these are belt driven from the motor input side of the transfer case.

Consideration was given to two alternative methods of driving these components other than by a fixed ratio belt drive, in order to reduce their power consumption. The first alternative was to use a separate DC motor, operating off the battery pack and driving these accessories at constant speed. This was quickly rejected because of the cost involved; something on the order of a 5 HP motor would be required, and it would be an expensive, bulky and heavy addition to the system. The second alternative considered was a variable-ratio belt drive. Such drives are currently under development by Morse Chain Division of Borg-Warner and AiResearch Manufacturing Company of Garrett Corporation. Because of the wide variation in speed of the hybrid propulsion system, ranging from 200-300 RPM at idle on up to 6000 RPM, using such a unit to limit the range

of operating speeds of the accessories would be desirable to cut accessory losses. It does, however, require some additional evaluation with regard to the production economics of these drives and the amount of development which would be required to incorporate one in the NTHV. If extensive additional development is required, it would probably not be worth diluting the main thrust of the hybrid development effort in controls, emissions, and batteries, with a large effort in a secondary area. For this reason, the preliminary design for the NTHV shows a fixed ratio belt drive; however, developments in this area should be monitored in the Phase II program and, if the production economics and development effort issues can be resolved favorably, it would enhance the fuel economy of an already fuel-efficient vehicle.

#### Electrical

12 V electrical power is required by the system controller, logic sections of the motor controls, heat engine ignition system, lights, engine fan, motor cooling blower, battery compartment cooling and ventilation blower, heater/defroster motor, radio, and other optional power driven accessories. There are basically two alternatives for supplying these needs: the first is a DC/DC converter operating off the main propulsion battery together with a small accessory battery and the second is an engine-driven alternator, again with an accessory battery. With the second alternative, the accessory battery would have to supply the system needs by itself during periods when the engine is not running. The first alternative is a little cleaner solution, and this is what we have assumed for

the NTHV. However, this is another peripheral area which has not been investigated in detail in this phase, and warrants further evaluation, particularly from a cost standpoint, in Phase II.

## 4.2 Chassis Systems

### 4.2.1 Brakes

The major modifications required to the braking system of the current production LTD are the use of a hydraulic assist instead of vacuum assist at the master cylinder, and modifications to either the rear wheel cylinder size or the valve which governs front-to-rear brake effort proportioning to accommodate the larger rear weight bias of the hybrid. It should be noted that the regenerative braking provided by the traction motor, which is applied at the rear wheels since the drive layout is rear wheel drive, automatically compensates to some extent for the rearward weight bias. Consequently, the change in hydraulic proportioning will be less than would be expected solely on the basis of the change in weight distribution. The hydraulic assist unit is the Hydroboost system by Bendix, which had been used on large Ford and Mercurys prior to downsizing, and is in current use on diesel powered GM products.

The weight increase of the hybrid over the present LTD is only about 156 kg, distributed -67 kg front and +222 kg rear. The relatively small increase, coupled with the presence of regenerative braking, makes physical increases in the size of the brakes unnecessary. The stock LTD front disc, rear drum system is retained with slightly higher line pressure, or larger diameter wheel cylinders for the rear brakes.

### 4.2.2 Suspension

The situation with the suspension is similar to the brakes. No modification is required to the front suspension, while at the

rear, higher rate (by about 20%) springs and heavier duty shocks will suffice. Because of the low CG of the added battery mass in the rear, and the high rear suspension roll center, it is not necessary to introduce a rear anti-roll bar.

#### 4.2.3 Tires and Wheels

The hybrid requires tires and wheels with a load rating of at least 670 kg (1473 lbs) per wheel; this is the rear wheel loading at the maximum payload of 520 kg. (Total weight at max payload is 2384 kg, distributed 43.8% front, 56.2% rear.) The current standard tires on the LTD are Firestone 721 steel belted radials, size FR78-14. This tire has a maximum load rating of 1500 lbs at 32 psi inflation pressure, so it would be adequate for the job; however, to achieve lower rolling resistance, an advanced version of this tire will be utilized. This will be a development of an existing experimental tire, size P195/75R14, which has a rolling resistance about 20% less than a regular production Michelin X tire of comparable size.

The current OEM Ford wheel is a 14" diameter, 5.5" wide steel wheel, weighing 19.0 lbs each. The wheel material is .1335 hot rolled low carbon steel.

When considering material substitution for weight reduction, design of a basic rim contour must meet industry standards set by the Tire and Rim Association. A styled molded composite wheel has proven, in initial testing, a potential weight savings versus a comparable mild steel styled wheel of 40-50%. Wheel uniformity becomes greatly improved with minimum balancing problems, since radial and lateral run-out characteristics are excellent if the mold

has been built to specification. If dimensional shrinkage is uniform or non-existent, the wheel produced will be in balance every time the press opens.

A one-piece wheel can be molded, with only the bolt holes and valve hole required as post-finishing operations. This terminates the many stamping, rolling, assembling, and welding operations in the manufacture of a steel wheel. Styling is another obvious advantage to wheel design; but as with any new steel wheel, design changes will result in different stress locations, which all have to be analyzed in detail.

Until composite wheel laboratory testing attains the same confidence level as that of steel wheels, very exhaustive testing will be required for each new wheel design before it reaches the marketplace.

Properties such as Poisson's ratio, interlaminar shear strength, compressive strength, flexural and tensile properties, impact resistance and fatigue resistance for temperatures ranging from  $-40^{\circ}\text{C}$  to  $177^{\circ}\text{C}$  are needed for many of the glass or carbon reinforced materials that are available. Data generation is now in progress for many materials; but even after the data is available, a wheel will have to be molded and subjected to long term fatigue testing.

Currently there are three major suppliers developing composite wheels: Firestone, Owens Corning, and Motor Wheel Corporation. All three are reporting excellent results. Selection of a supplier will be made early in the Phase II effort.

As a backup, aluminum wheels will be considered. Kelsey Hayes, working in cooperation with Reynolds Aluminum and Alcoa have each announced their ability to form aluminum wheels by means similar to those used in fabricating steel wheels. These fabricated wheels have a potential for reducing vehicle weight by approximately 50 lbs.

The final consideration will be the cost effectiveness of one material to another and the ability to select wheels that do not introduce major design risks during the NTHV program.

The potential weight savings for the hybrid 14 x 5.5 rim are summarized below:

	<u>Weight/Wheel</u>
HRLC Steel (standard)	19.0
HSLA Steel	17.8
Fabricated Aluminum	12.0 - 14.0
Molded Composite	11.0 - 12.0



#### 4.3 Body

The proposed SCT hybrid vehicle is predicated on the use of a high volume six-passenger vehicle as both the reference vehicle and as the actual hardware basis for the design and build of the hybrid.

The Ford LTD was selected as being representative of a weight efficient down-sized full-size car. This car will undergo considerable design changes and resultant weight reductions between now and the 1981-2 model year when the ITV deliverable prototypes would be built. The hybrid vehicle requires certain modifications being made to package the new propulsion system and its associated batteries, controller, and charger. In addition, it would be desirable to make other limited, cost effective changes to reduce aerodynamic drag and to reduce vehicle weight to be more representative of the anticipated weight of the 1985 model year baseline program.

Changes not directly related to packaging hybrid components, to improved aerodynamic drag, and to weight reduction will not be made to the LTD body. While it is certainly true that a greater weight savings could be achieved by incorporating changes to the central body, greenhouse, and frame, the improvements to the hybrid fuel economy could not, in our judgment, justify the expenditure of funds and manpower that would be needed to do a completely new and unique body. As stated above, it is very likely that Ford will make changes to the LTD that will result in the availability of lighter weight body components in some of the body components that will be used, unchanged, in the ITV vehicles.

#### 4.3.1 Structure and Materials

The unique body components that will be incorporated in the SCT hybrid are made up of three groups. These are: 1) The vehicle front end which consists of the bumper system, hood, and fenders; 2) rear end changes consisting of the deck lid and rear bumper system; 3) other surface panel changes to reduce weight such as door outer panels; and 4) changes related to packaging batteries and propulsion system components.

An analysis of material properties has been conducted by SCT and Sheller-Globe, our planned ITV body detailed design, prototype tooling, and prototype part source. Material selections are based on an analysis of structural and other special vehicle requirements, and represent the direction most likely to be followed by the major U. S. auto manufacturers for the 1985 model year.

Our limited use of plastics and aluminum is essentially assumed equivalent to what Ford would do to the reference vehicle. Published data and recent studies combined with the knowledge available to SCT through Sheller-Globe support our assumptions. Detailed part by part assumptions on the 1985 Ford LTD are not available or known even to Ford Motor Company, but the level of change planned is reasonable. It should be noted that the question of cost of the plastic and aluminum parts is not included in the hybrid vs reference vehicle cost as the increase applies to both vehicles. Sheller-Globe, as a major developer and supplier of plastic materials and as a fabricator of sheet metal bodies for buses, trucks, and vans, is in a position to provide meaningful, realistic direction to our program. The bottom line of our relationship to Sheller-Globe is

that the EV vehicle unique prototype parts are to be detail designed and built by them.

Structurally, all materials selected will provide components that are the functional equivalent of their current steel counterparts. As shown on the summary below, extensive use will be made of plastic components for exterior surface parts of the car. The one exception is the hood, in which an aluminum outer panel would be used to preclude problems that may be encountered with a plastic hood over the high engine compartment temperatures. Modifications to the floor, engine, and motor mounts will use high strength steel to the maximum extent possible.

Unique SCT Hybrid Vehicle Body Components

<u>Part Name</u>	<u>Current Material</u>	<u>Hybrid Material</u>	<u>Remarks</u>
Front bumper	Steel	Polypropylene or Urethane	Entire soft front end or skin only
Hood outer	Steel	Alu or HSLA	
Front fender outer	Steel	RIM Urethane	
Door outer panels	Steel	RIM Urethane	
Decklid inner & outer	Steel	RIM Urethane	
Rear bumper	Steel	Polypropylene cover	
Propulsion system mounts	Steel	HSLA	
Battery compartment & Other control compartments	-	HSLA	
Seat frames	Steel	Molded plastic	

A general discussion of some of the plastics to be used in the hybrid vehicle follows:

#### Polypropylene

Polypropylene is a thermoplastic which is combined with EPDM modifier for molding. It is used primarily in injection molding and is one of the lowest specific gravity materials available. It exhibits a high modulus with strength (tear resistance) and flexibility for severe wear applications. It is one of the lowest cost polymers and affords good paintability (special primers or flame treatment).

#### Urethane

By 1985, urethane will be competitive with SMC in pricing. It has a low density with a wide range of modulus flexibility of approximately 20,000 psi to 500,000 psi for rigid parts. By 1985, the industry expects to offer a reinforced rigid material with a modulus of 1,000,000 psi, excellent weatherability with no finishing problems.

#### ABS

ABS offers excellent elongation and heat distortion qualities. It is one of the lower cost automotive application plastics. Parts may be formed in a variety of methods - injection, molded, extruded, or thermoformed.

#### Mica

Mica is a structural organic additive that when added to a resin, significantly affects its modulus (increases). Mica has less of an effect on surface finish than adding glass fiber or graphite fiber. Mica would be used as a urethane filler.

#### 4.3.2 Design Improvements

In designing the unique body components that are required for the SCT hybrid, major attention will be focused on achieving two objectives that will contribute toward minimizing vehicle energy usage. These objectives are to reduce vehicle aerodynamic drag and to reduce vehicle weight.

Aerodynamic drag: By having the flexibility to change all the front end sheet metal, it should be possible to achieve a measurable gain. A design program supported by analysis and the use of wind tunnel testing will be used to optimize the vehicle front end. Concurrently, spoiler design and the vehicle underbody will also be pursued as avenues to reduce drag.

Vehicle weight: As shown on Table 4-6 , the changes over which SCT can accept and maintain weight reduction control total a weight reduction of 248.5 pounds. In addition, on a conservative basis, we would anticipate that Ford would make weight reduction changes that we could incorporate in the ITV vehicles that would amount to 51.5 pounds, for a total weight reduction of 300 pounds.

Table 4-6a - MATERIAL SUBSTITUTION HYBRID PROGRAM

PART	EXISTING MATERIAL	EXISTING WEIGHT	GA THKSS	SUBSTITUTION MATERIAL	WEIGHT PROJECTION	GA THKSS	POTENTIAL WT. REDUCTION	COMMENTS
FRONT BUMPER	STEEL	70.5 ASSY.	.103	XMC AND URETHANE	45.0 ASSY.	-	25.5	ENTIRE SOFT FRNT.
HOOD	STEEL	54 ASSY.	.028	ALU.	46. ASSY.		8.0	OUTER SKIN ONLY
FRONT FENDER L.H. OUTER SKIN	STEEL	18.5	.035	RIM URETHANE	10.2	0	8.3	OUTER SKIN ONLY
FRONT FENDER R.H. OUTER SKIN	STEEL	18.5	.035	RIM URETHANE	10.2	-	8.3	OUTER SKIN ONLY
REAR DECK INNER & OUTER	STEEL	43.0	.035/.028	ALUCOBOND	19.0	-	24.0	ELIMINATES MOST OF INNER PANEL
REAR BUMPER	STEEL	64.750 ASSY.	.103	POLYPROPYLENE	34.750 ASSY.	-	30.0	SKIN WITH XMC IMPACT BEAM
FRONT DOOR R & L	STEEL	12.5 EACH	.030	RIM URETHANE	8.26/SKIN	-	8.48/PAIR	OUTER SKIN ONLY
REAR DOOR R & L	STEEL	8.0 EACH	.030	RIM URETHANE	6.32	-	3.36/PAIR	OUTER SKIN ONLY

Table 4-6b - MATERIAL SUBSTITUTION HYBRID PROGRAM

PART	EXISTING MATERIAL	EXISTING WEIGHT	GA THKNSS	SUBSTITUTION MATERIAL	WEIGHT PROJECTION	GA THKNSS	POTENTIAL WT. REDUCTION	COMMENTS
WHEELS	STEEL	19.0	10 GA	VINYLESTER	9.0	-	40 lbs/VEH.	MOLDED STRUC. PLASTIC
FRONT SEAT FRAME	STEEL FRAME	83.5 ASSY.	MISC.	STR. RIM URETHANE	53.5	-	30 lbs	STRUCTURAL PLASTIC
DOOR TRIM PNLS FRONT	UPHOLS. & TRIM	5.25 EA	-	THERMOPLASTIC	7.5/PAIR	-	3 lbs/PAIR	NONSTRUCTURAL PLASTIC
REAR	UPHOLS. & TRIM	3.50 EA	-	THERMOPLASTIC	5.0/PAIR	-	2 lbs/PAIR	NONSTRUCTURAL PLASTIC
FUEL TANK & LINES	STEEL	25.750	14 GA.	BLOW MOLDED PLASTIC	12.75		13 lbs	

SUBTOTAL DESIGN CONTROLLABLE BY SCT

203.94

OTHER ANTICIPATED WEIGHT SAVINGS (FORD DESIGN CHANGES) INCLUDES HARDWARE SUCH AS DOOR HINGES (4) AXLE HOUSING (10) FRAME AND SUSPENSION (30) WINDOW CHANNELS (7.5) ADDITIONAL FORD AND SCT HARDWARE (44.56)

96.06

TOTAL WEIGHT REDUCTION PROJECTED

300.0

#### 4.4 Vehicle System Characteristics

In this section, the NTHV characteristics are summarized in terms of performance, fuel and energy consumption, costs, and so forth; these characteristics are related, where appropriate, to the vehicle performance specifications derived in Task 1 and described in Section 5 of the Task 1 report (2).

##### 4.4.1 Acceleration Gradeability and Maximum Speed

The acceleration characteristics projected for the NTHV are shown in Figure 4-54 . These data are given for fully charged, nickel-iron batteries; they are also representative of acceleration performance with lead-acid batteries. They are computed for a test payload of 140 kg and without air conditioning operating. The acceleration times can be expected to be on the order of 4% longer when operating on mode 2 with the batteries at a discharge limit in the .6-.7 range. An acceleration curve for the reference vehicle is shown for the purposes of comparison. The acceleration specifications of 0-50 kph in 6 sec., 0-90 kph in 15 sec., and 40-90 kph in 12 sec. are all met.

A graph of the maximum instantaneous gradeability with fully charged batteries is shown in Figure 4.54 ; again, the reference vehicle characteristics are shown for comparative purposes. The maximum grade requirement of 30% is met easily. Gradeability over extended distances is summarized in Table 4.7 ; again, there appears to be no problem meeting these specifications when a battery discharge limit of .6 to .7 is used, for nickel-iron batteries. With lead-acid batteries, a discharge limit not in



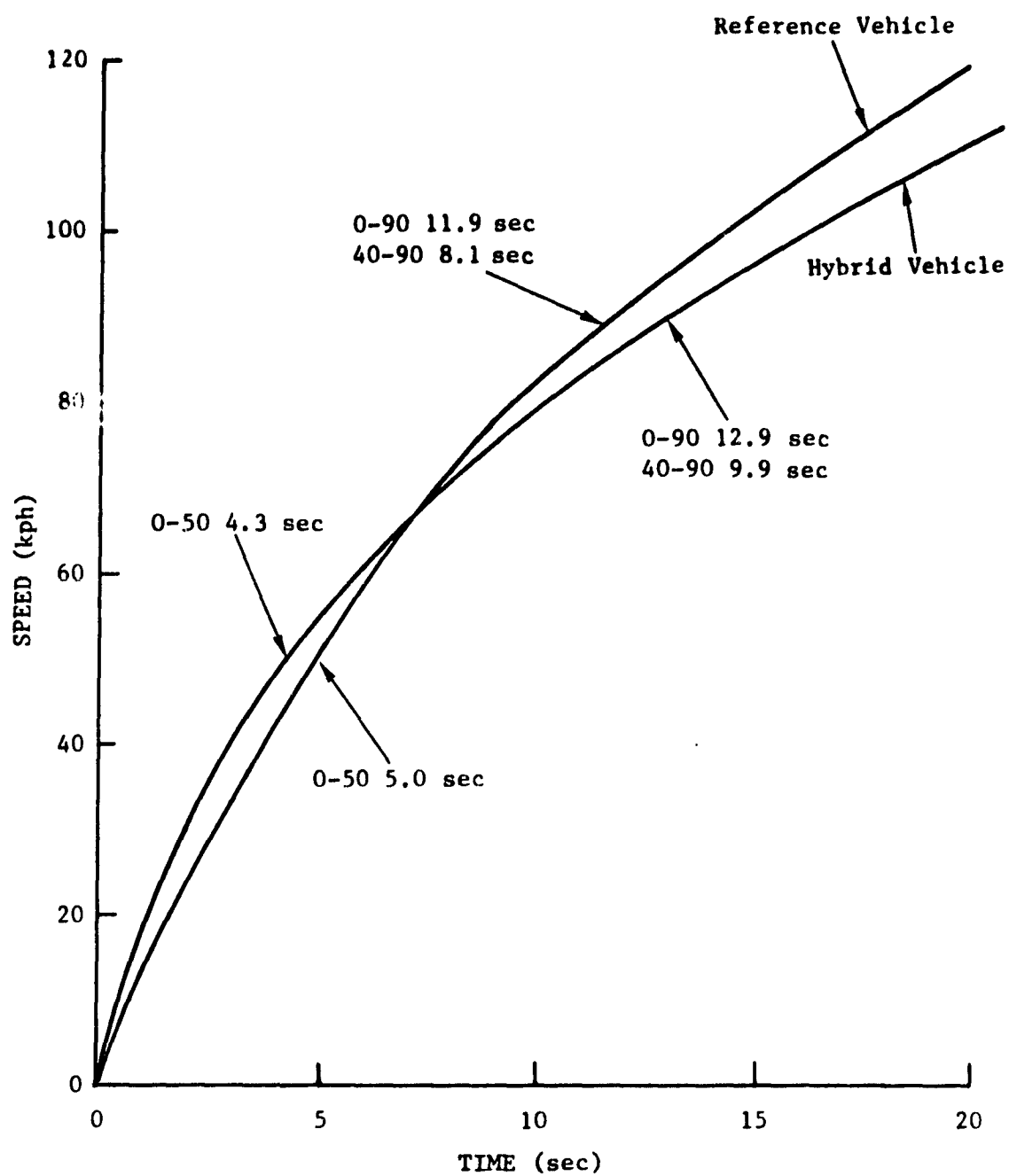


Figure 4-54 Acceleration Characteristics

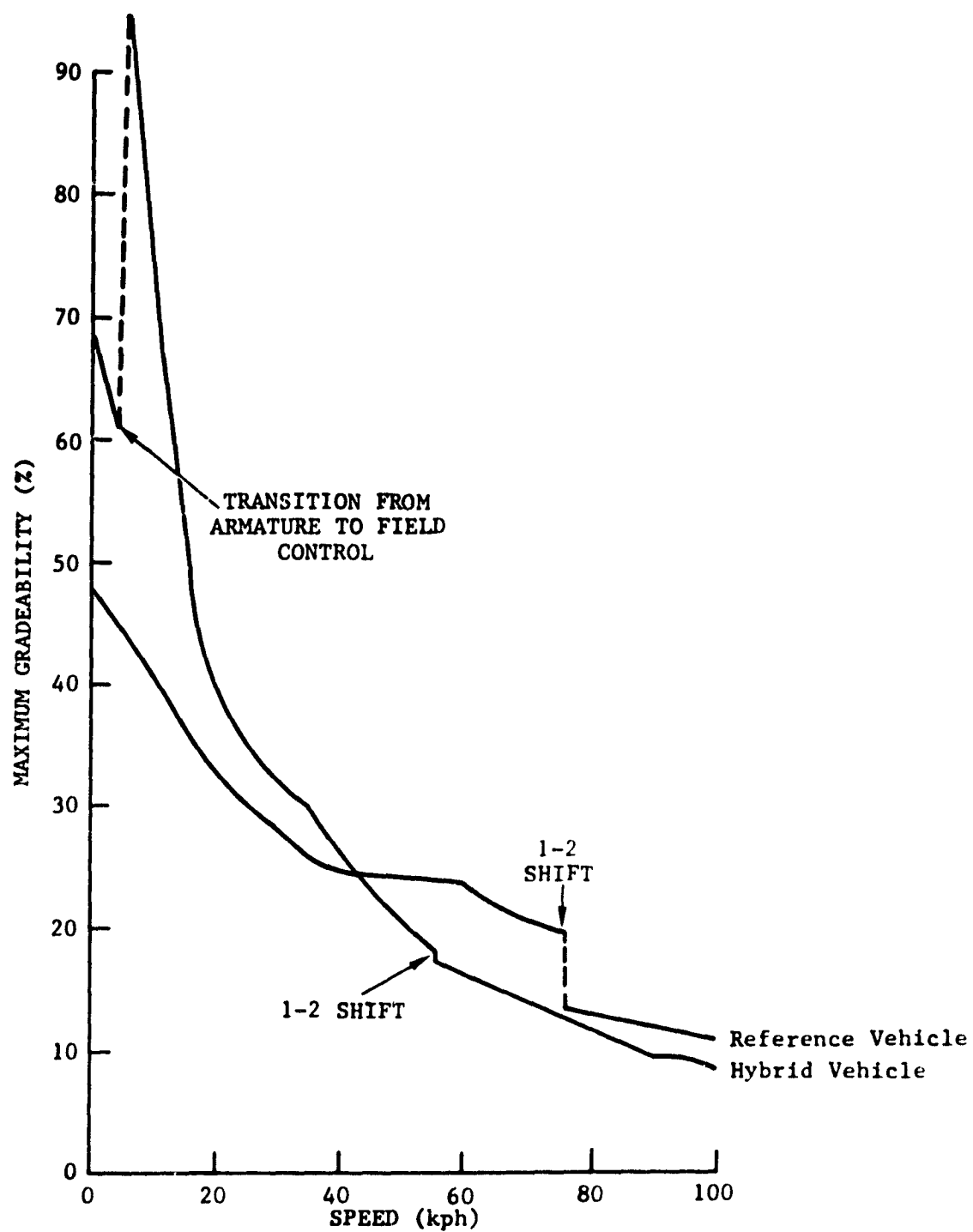


Figure 4-55 Maximum Gradeability SPEED (kph)

excess of .6 would be used.

Table 4-7 - Gradeability of Hybrid Vehicle with Nickel-Iron Batteries

<u>Grade</u>	<u>Speed</u>	<u>Specification</u>	<u>Distance (km)*</u>	
			<u>Projected</u> (Nickel-Iron)	(Lead-Acid)
3	90	Indef.	Indef.	Indef.
5	90	20	148	99
8	85	5	7.5	6.9
8	65	Indef.	Indef.	Indef.
15	50	2	3	2.6

\* Assumes battery discharge limit is such that an additional 20% depletion is feasible (i.e., discharge limit is in the 60-70% range) for nickel-iron batteries, 30% for lead-acid batteries.

The system power requirements at 130 kph are only about 38 kw at 4340 RPM in overdrive, which is well within the available system power of 70.5 kw at this speed. Consequently, the vehicle top speed will be well in excess of the specified 130 kph. A detailed analysis of the high speed pass requirement has not been carried out; however, such a maneuver generally takes on the order of 25 sec. Assuming the motor operates at maximum power for this period, a maximum of .25 kw-hr would be withdrawn from the batteries. This can be totally replaced in the 4½ minutes or so which occurs between the high speed pass maneuvers by incrementing the engine power upward by only about 4 kw., which is still well within the engine's capabilities at a 90 kph cruise. Consequently, we can

conclude that the repetitive high speed pass requirement can be easily met with the proper adjustment of the heat engine power command as the battery drops below the discharge limit.

#### 4.4.2 Fuel and Energy Consumption

The average annual fuel consumption of the NTHV is projected at 16.9 to 17.6 km/l with nickel-iron batteries, for battery discharge limits in the .6 to .7 range. The corresponding wallplug energy consumption ranges from .117 to .187 kw-hr/km. Fuel consumption, battery output energy, and mode 1 operating range for the three component driving cycles are summarized in Table 4-8. Wallplug output energy can be assumed to be battery output energy divided by .54.

Table 4-8 - Fuel and Energy Consumption on Component Driving Cycles

	SAE J227a (B)	FUDC	FHDC
Mode 1			
Fuel Consumption (l/km)	.0029	.0336	.0637
Battery Energy Consumption (kw-hr/km)	.2876	.1616	.0427
Range to .7 DOD (km)	29.6	50.3	204.8
Mode 2			
Fuel Consumption (l/km)	.1067 (.1883)	.0881 (.1350)	.0764 (.0862)

Reference vehicle values are given in parenthesis. These numbers are representative of what the vehicle would be expected to do on a dynamometer test. The distributions of battery output on Mode 1 for the urban and highway driving cycles are shown in Figure 4-56.

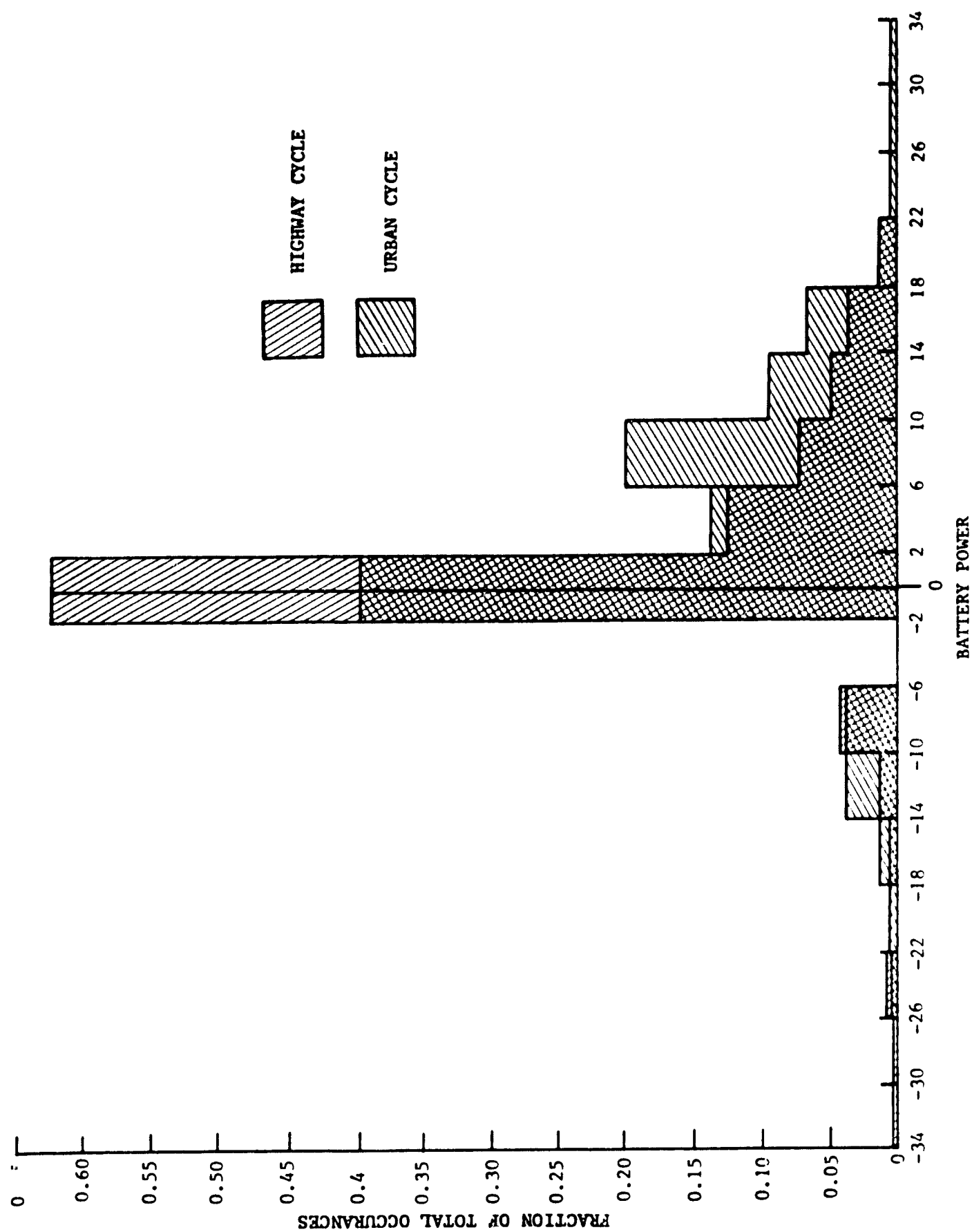


Figure 4-56 Battery Power Distribution

The energy consumption measures E1-E9 requested by JPL are summarized in Table 4-9 and Figures 4-57 to 4-59. It must be recognized that the measures E5-E8 are dependent on the size of the fuel tank; the numbers are for a 40 liter tank, which provides the following operating ranges, starting with a full tank and fully charged batteries:

SAE J227a (B)	404 km
FUDC	485 km
FHDC	557

These satisfy the specifications developed in Task 1.

The energy measures have been computed both in terms of input to the vehicle and refinery input, under the following assumptions:

Refinery efficiency - .84 for gasoline

.93 for fuel oil

Electrical generation efficiency - .36

Electrical distribution efficiency - .91

In other words, for the 'vehicle input' numbers, petroleum-based fuel energy consumption ( $E_{pv}$ ) is computed as the heat equivalent of the gasoline consumption, and total energy input ( $E_{TV}$ ) is computed as  $E_{pv} + E_{ev}$ , where  $E_{ev}$  is the wallplug output energy. The 'refinery input' numbers are computed as follows:

Petroleum-based:  $E_{pr} + E_{pv}/.84$

Electrical:  $E_{er} = E_{ev}/(.93 \times .36 \times .91)$

Total:  $E_{Tr} = E_{pr} + E_{er}$ .

The energy measure  $E_g$ , of course, is computed only on a total energy basis.

Note that all of the energy consumption measures have been computed on the basis of a .7 battery discharge limit, and do not

include allowances for changing the control strategy during vehicle warmup. Consequently, they correspond to the upper limit of what is achievable in terms of petroleum energy savings.

Table 4-9 - Energy Consumption Measures

Measure	Reference Vehicle		Hybrid Vehicle	
	Vehicle Input	Refinery Input	Vehicle Input	Refinery Input
E 1 MJ/Vehicle yr.	81300	96700	35200	41900
E 2 MJ/Vehicle yr.	0 <sup>(1)</sup> 81300 <sup>(2)</sup>	96700	13200 <sup>(1)</sup> 48400 <sup>(2)</sup>	85200
E 3 MJ/Vehicle yr.	(2.63x10 <sup>12</sup> ) 0 <sup>(3)</sup>	(3.13x10 <sup>12</sup> ) 0	(1.14x10 <sup>12</sup> ) 1.49x10 <sup>12</sup>	(1.35x10 <sup>12</sup> ) 1.78x10 <sup>12</sup>
E 4 MJ/yr.	0 2.63x10 <sup>12</sup>	3.13x10 <sup>12</sup>	.43x10 <sup>12</sup> 1.56x10 <sup>12</sup>	2.76x10 <sup>12</sup>
E 5 MJ/yr.				
E 5.1	0 2.73	3.25	.104 2.38	3.06
E 5.2	0 4.28	5.09	.112 2.73	3.48
E 5.3	0 5.97	7.11	.140 3.28	4.20
E 6 MJ/km				
E 6.1	2.73	3.25	2.28	2.71
E 6.2	4.28	5.09	2.62	3.11
E 6.3	5.97	7.11	3.14	3.74
E 7, E 8	See Figures 4-57	to 4-59		
E 9 MJ/Vehicle				
E 9.1		131x10 <sup>6</sup>		153x10 <sup>6</sup>
E 9.2		961x10 <sup>6</sup>		869x10 <sup>6</sup>
E 9.3		4x10 <sup>6</sup>		4x10 <sup>6</sup>

(1), (2) Where 2 numbers are given, the first represents vehicle electrical energy input, the second total energy input.

(3) Number in parenthesis is total; other is savings.

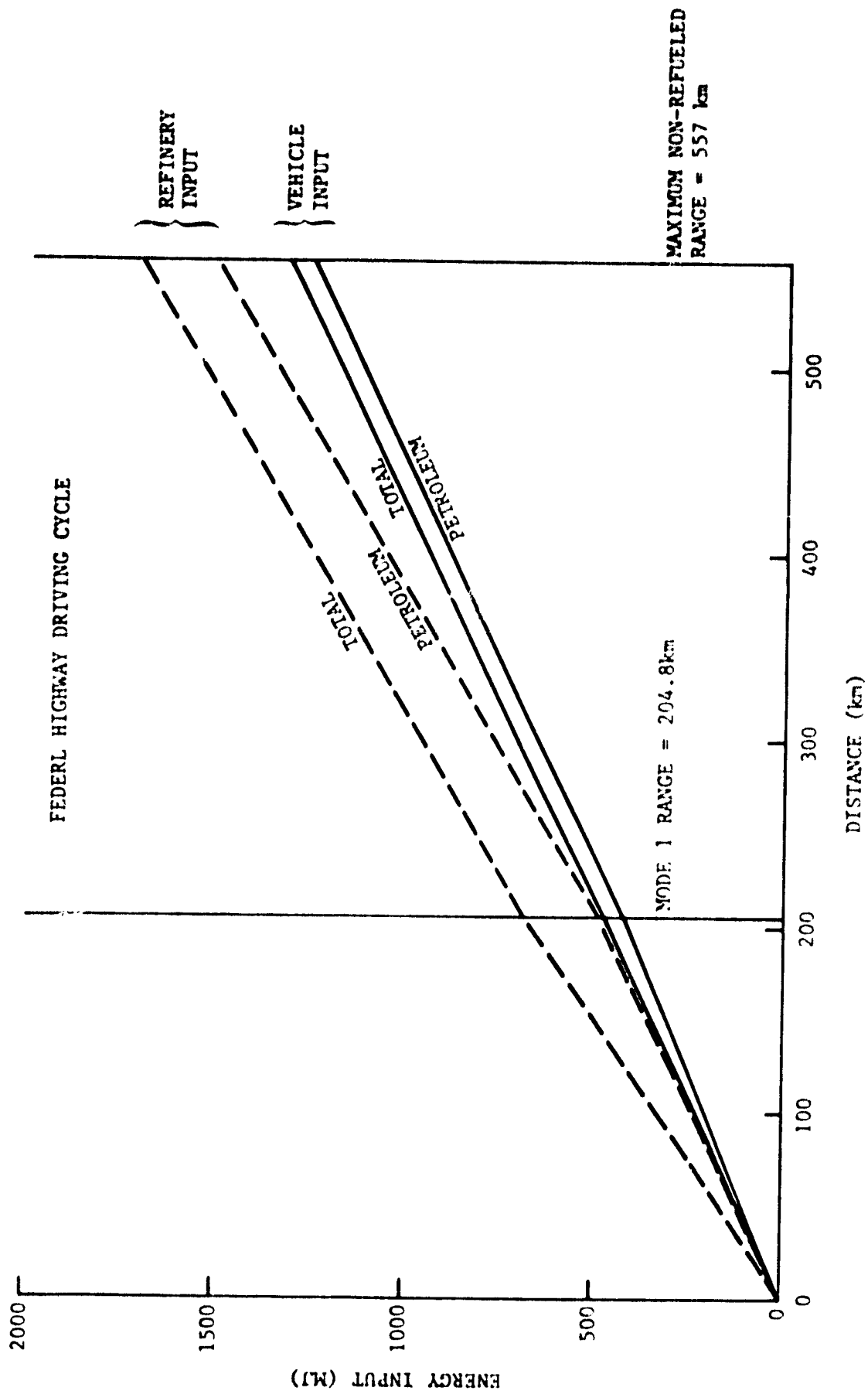


Figure 4-57 Energy Consumption Measures E7.1, E8.1



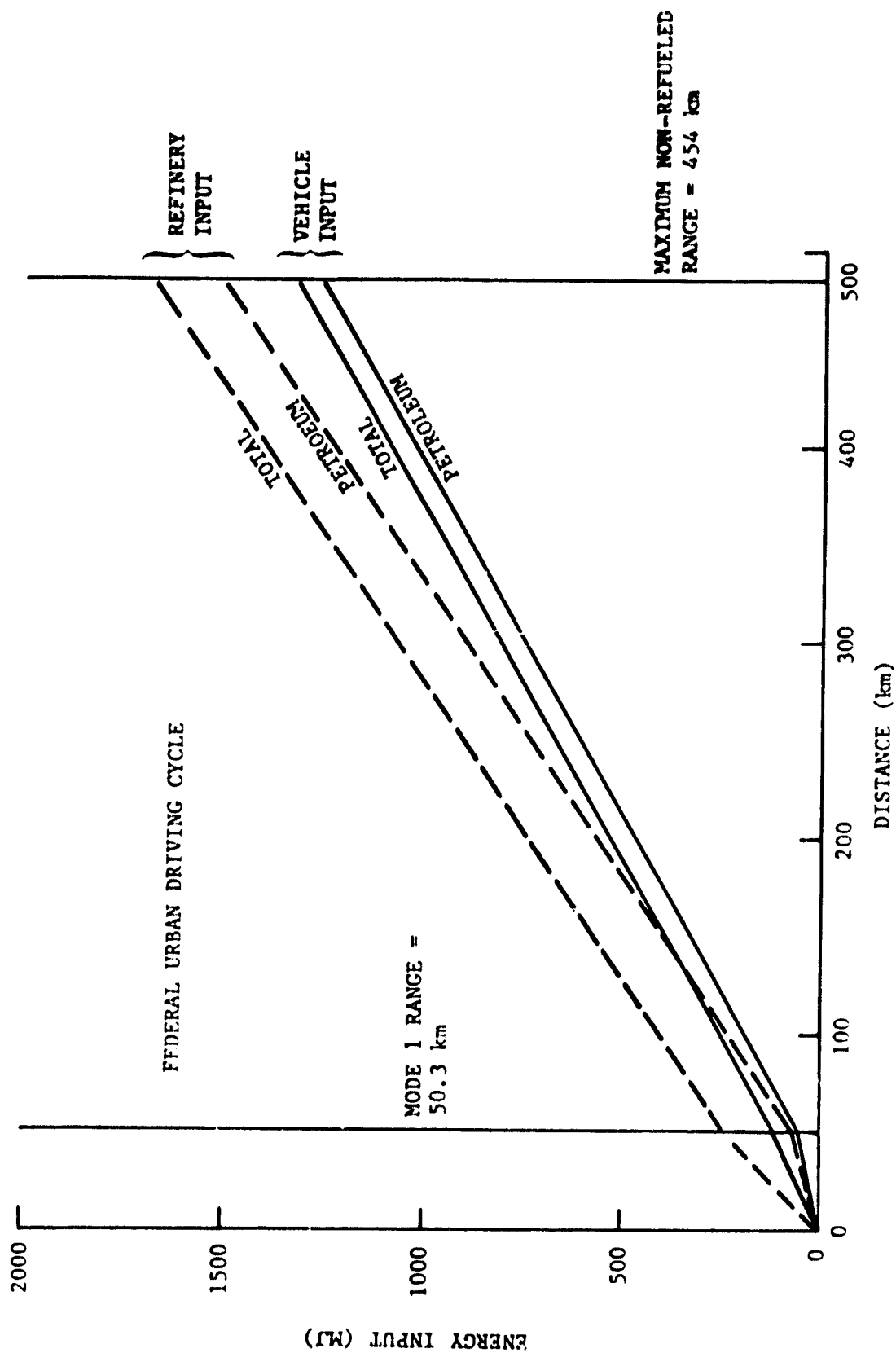


Figure 4-58 Energy Consumption Measures E7.2, E8.2

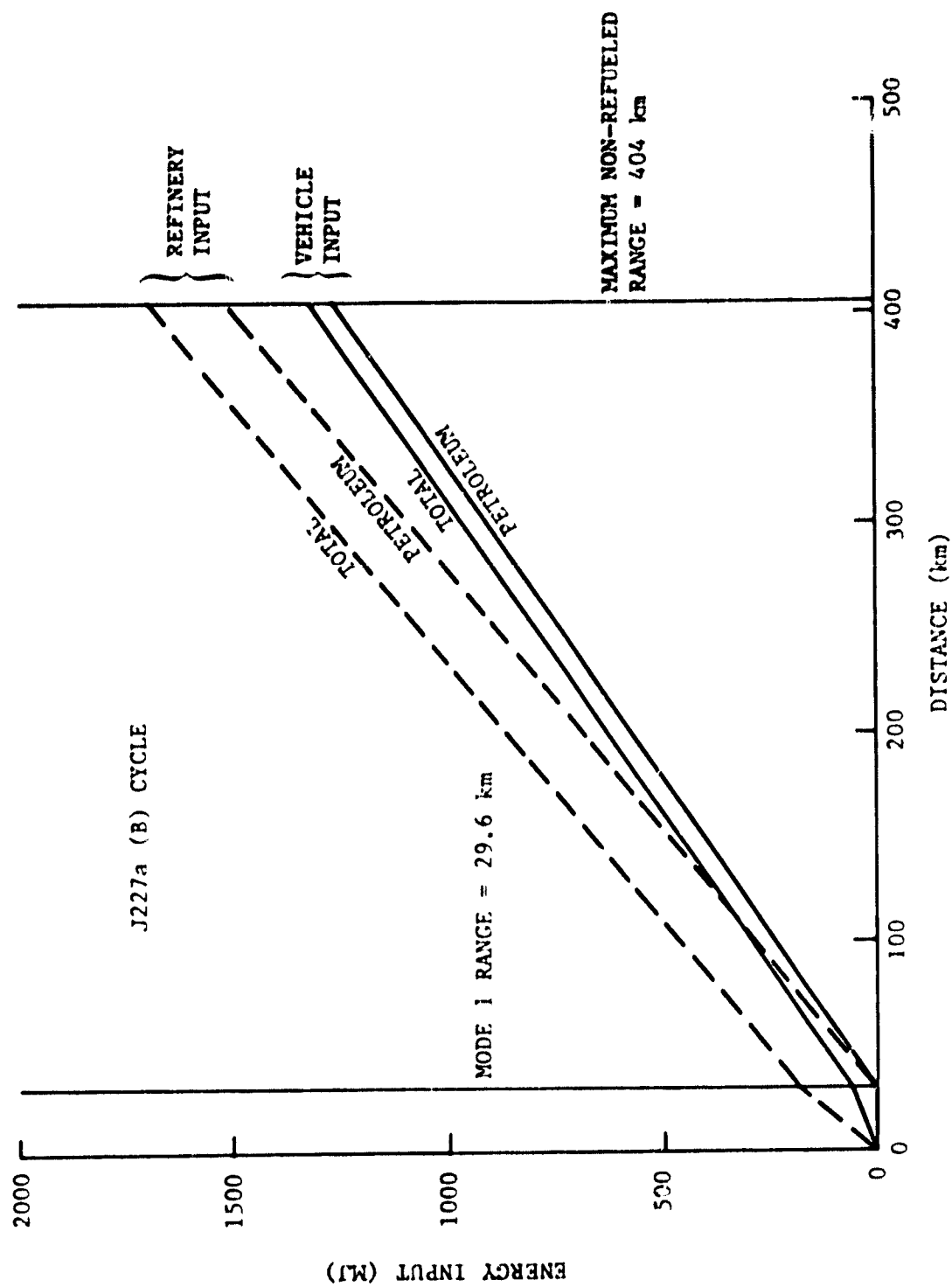


Figure 4-59 Energy Consumption Measures E7.3, E8.3

Life cycle energy consumption per vehicle compared to the reference vehicle (E9.1 through E9.3) have been developed as follows.

A literature survey was conducted which provides a basis for deriving a value for vehicle fabrication energy requirements and a basis for determining the energy cost of vehicle disposal. A copy of the study conducted for South Coast Technology by Roy Kenner is included in this report as Appendix C3 .

After reviewing this report it is clear that accurate data do not exist for projecting the energy used to fabricate or dispose of any particular vehicle. Thus, we have chosen to simplify the comparison of our proposed hybrid vehicle and its reference ICE vehicle counterpart by considering both vehicles to be equivalent except for the engine/motor and battery pack requirements of the hybrid. Other changes that might be made to reduce vehicle weight etc., could and should apply to both the hybrid and reference vehicle.

With respect to vehicle operation and maintenance energy, the data for vehicle operation is based on fuel and energy usage data projections for the hybrid and baseline vehicles.

Lifetime replacement part energy requirement has been estimated by Berry and Fels to amount to only 665 kwh, or only 1.8% of the total free energy required to manufacture a new car. Thus, with the exception of the battery replacement energy requirement we will assume no significant difference between the hybrid and baseline vehicles.

#### 4.4.3 Costs

An updating of the manufacturing costs has been completed based on the latest design level that is incorporated in this Preliminary Design Report.

These costs are summarized below:

	<u>Costs (over)/under Reference Vehicle</u>
Four cylinder engine vs. V-8	\$ 250
Parallel system hardware costs	(146)
Added clutch hsg & clutch pkg.	(32)
Axle ratio-low volume	(5)
Suspension & tire upgrading	(9)
Frame & motor mounting provisions	(12)
Battery packaging & cooling	(60)
Engine exhaust & emission control	150
Engine cooling system	(20)
Motor cooling system (blower motor)	(14)
Accessory drive	(15)
Hydroboost brakes	(13)
Motor	(800)
Controller/charger, actuators, & mounts	(311)
Batteries and cables (nickel-iron batteries)	(1200)
Instrumentation	<u>(120)</u>
TOTAL HYBRID (OVER) REFERENCE	<u><u>\$( 2357)</u></u>

It should be noted that these costs do not assume any penalty associated with the planned material substitution as these same or equivalent costs would be incurred by the manufacturer of the reference

vehicle in order to achieve weight reductions. In comparison to the costs included in our Design Tradeoff Studies Report, these manufacturing costs have increased by \$557. The major factor responsible is the decision to include nickel-iron batteries in our base cost. Use of lead-acid batteries at their estimated cost for the ISOA batteries would reduce this initial cost penalty for the hybrid vehicle by \$250. Cost information on any battery system cannot be regarded as particularly firm at this point in time due to unknowns concerning the relationship between future production batteries and current developmental cells and batteries. The situation is further complicated in the lead-acid case by the recent volatility of the price of lead. Eagle-Picher recently performed a cost and design study for ANL in which the cost of batteries in quantities of 100,000/year were estimated at \$79/kw-hr. ESB's most current estimate for production costs for lead-acid batteries for the hybrid is \$75/kw-hr. This yields OEM prices of \$1152 for the nickel-iron battery and \$900 for the lead-acid battery, the values used in this comparison of the hybrid and reference vehicles.

Other cost increases vs. the prior report include a better definition of propulsion system mounts, battery charger, and controller mounts, hydroboost brakes, and the cost penalty for a unique, and therefore low volume, rear axle ratio.

#### Retail Price

If one were to assume that the entire cost of the hybrid system must be recovered in the vehicle's retail price, the price would increase in an amount of \$2950 to \$4714, depending on whether one assumes a minimum markup cost passthrough or a maximum 2 x manufacturing

cost formula. This price range is based on nickel-iron batteries and would be reduced by \$315 to \$500 if lead-acid batteries were used.

The current turmoil in auto industry sales would support the likelihood that the industry would be conservative in the delta price for hybrids in order to move buyers into purchasing new full-sized cars. In addition to taking a reasonable approach to pricing the hybrid, it would be likely that the issue of battery pricing would be studied and addressed by the auto industry. In our cost structure, the nickel-iron batteries account for over half the total increase in manufacturing cost over the reference vehicle. This not only accounts for a major new car pricing problem, but also could present a maintenance cost shock to the owner of a hybrid when he must pay to replace a complete set of batteries at a retail price level.

A solution to both problems would be to sell the car less batteries and lease the batteries to the car owner. This would spread the costs out more evenly over the life of the car and would provide the car owner with expert service support and the manufacturer with a supply of batteries for recycling when they are trucked in, thus reducing battery costs. This issue should be addressed in Phase II.

#### Life Cycle Costs

Life cycle costs have been updated to reflect the changes in the cost of the hybrid vehicle discussed above which include the use of nickel-iron batteries, and to incorporate changes in the life cycle cost, LYFECC.

Two changes have been made in LYFECC since its use in the Mission Analysis and Performance Specification Studies Report. First, the method of computing the discount factor now matches the one described in Hybrid Vehicle Potential Assessment Interim Progress Report, Appendix C, Electric and Hybrid Cost Handbook, R. Left, S. Heller, Draft #5030-162, Jet Propulsion Laboratory, Pasadena, California.

The second change involves the inclusion of replacement batteries down payment. This was inadvertently omitted from operating and life cycle costs in the first version of the program.

A comparison of life cycle costs (¢/km) is summarized below:

	Reference Vehicle	Hybrid	
		Nominal Pricing	2 x Manufacturing Cost Pricing
Nominal	9.4	10.6	11.9
Fuel + 30%	10.3	10.9	12.2
Fuel - 30%	8.6	10.2	11.5
Electricity + 30%	9.4	10.8	12.1
Electricity - 10%	9.4	10.5	11.8

The relative life cycle cost of the hybrid vehicle vs. the reference are not significantly different from the Task 1 and Task 2 reports. Not considered in the life cycle cost of the hybrid is the likelihood that its residual used car value at the end of 10 years may be significantly higher than a conventional, non-fuel efficient large car.

#### 4.4.4 Handling

The results of a computer analysis of steady-state handling are shown in Figure 4-60 . The same analysis was run for the existing production LTD and for the hybrid vehicle. The LTD, as expected, understeers throughout the operating speed range, with the understeer getting stronger at high speed. The hybrid shows slight oversteer up to about 16 m/sec (58 kph, or 36 mph), and then becomes understeering. The small amount of oversteer, coupled with the fact that the fully loaded (worst case) weight distribution does not put more than 56% of the weight on the rear wheels, leads us to the conclusion that acceptable steady-state characteristics can be achieved by proper tire selection, suspension tuning, and, if necessary, use of higher rear tire pressures. Except for the slight oversteer at low speeds, the characteristics lie within the specifications published for the intermediate ESV.

The plotter output from the HYSIM program showing the response of the hybrid to a step in steer angle is shown in Figures 4-61 to 4-63 . Again, the runs were also made for the LTD; and these are shown to provide a basis for comparison. The reduction in response time is very slight and remains well within the intermediate ESV specifications. The traces also show the characteristically higher damping associated with the response of the nearly neutral hybrid vs. the overshoot of the understeering LTD.

In summary, with the proper suspension tuning, we expect the hybrid to be a neutral to slightly understeering vehicle, with slightly slower transient response and higher damping than the current production LTD.



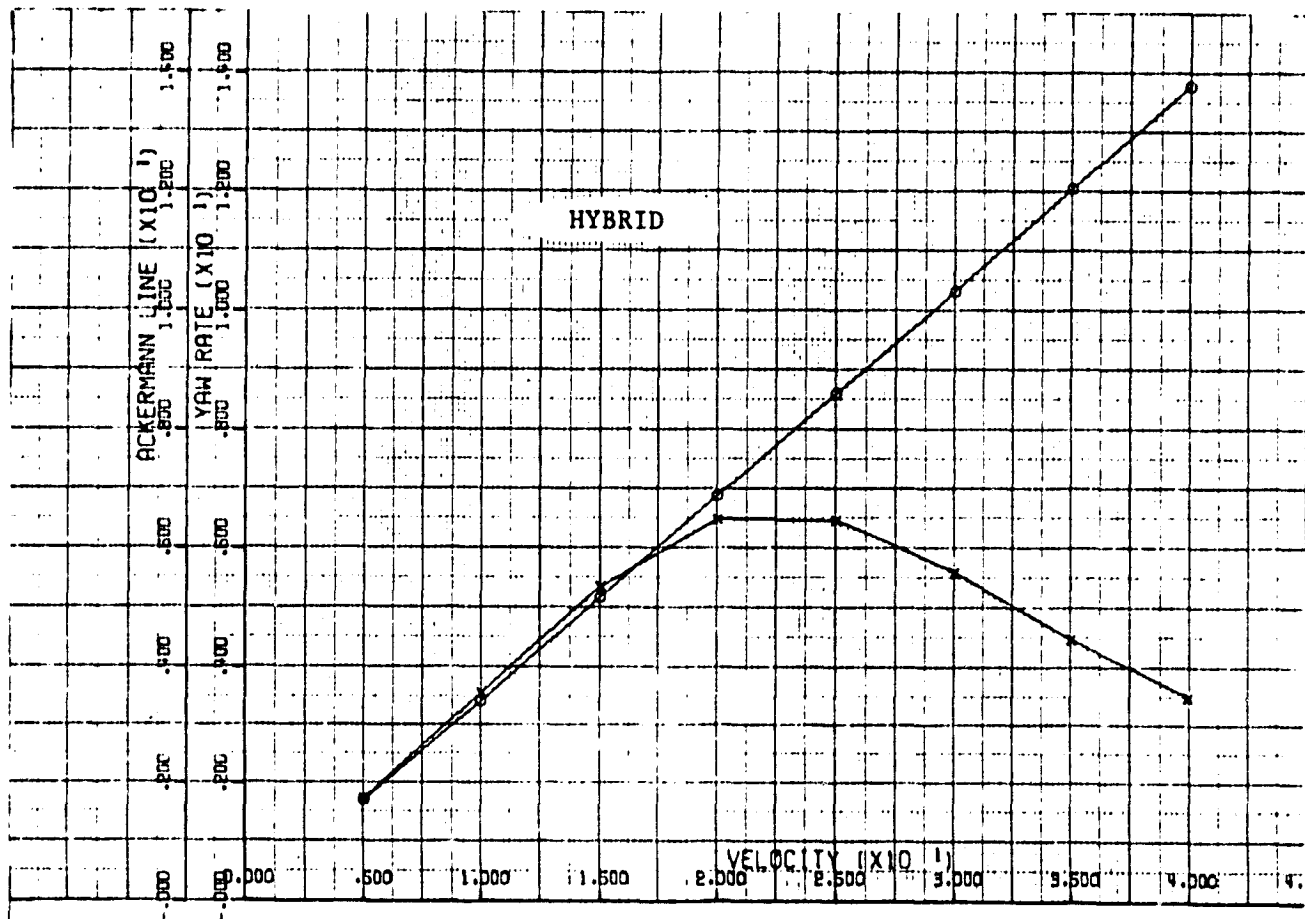
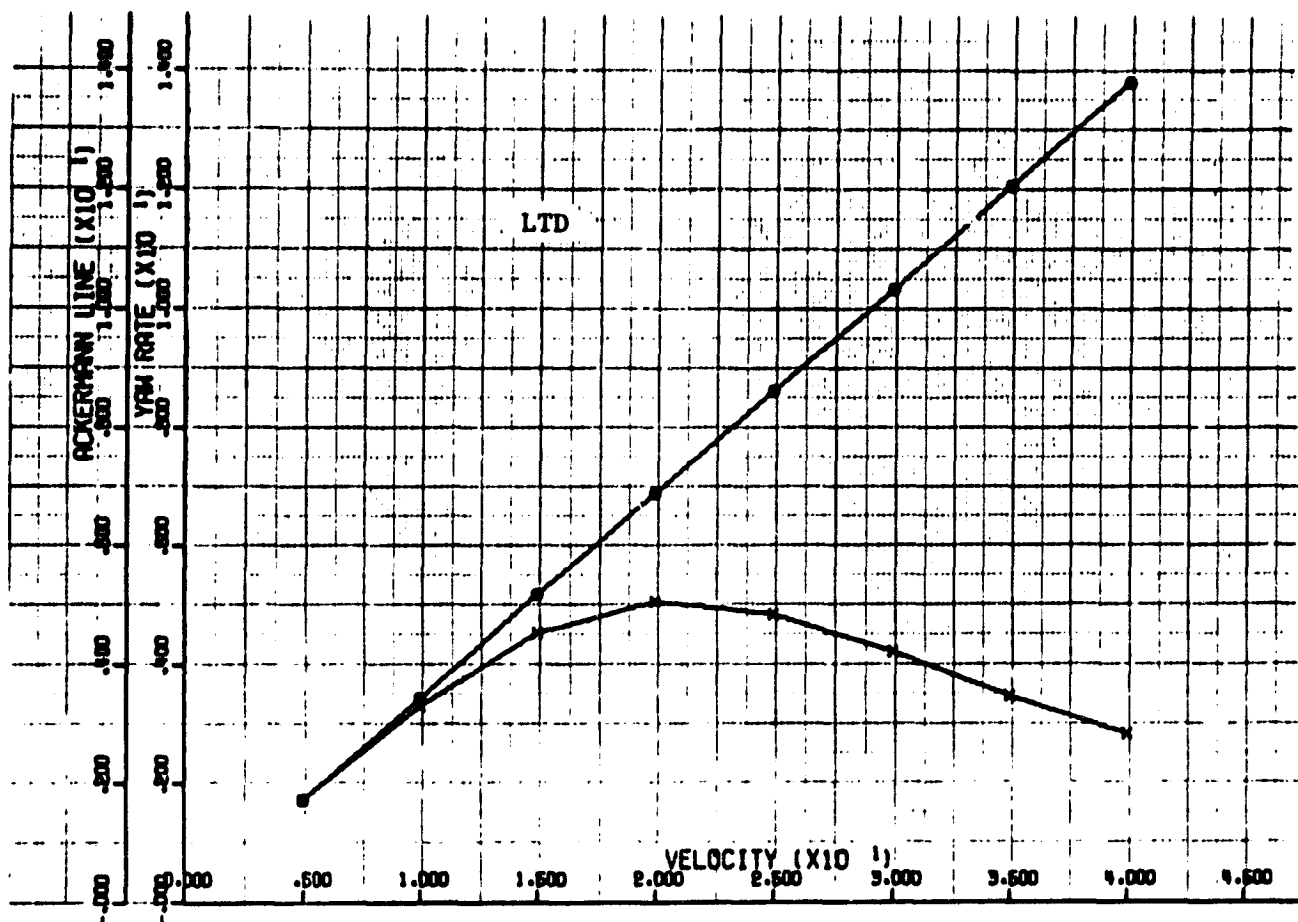
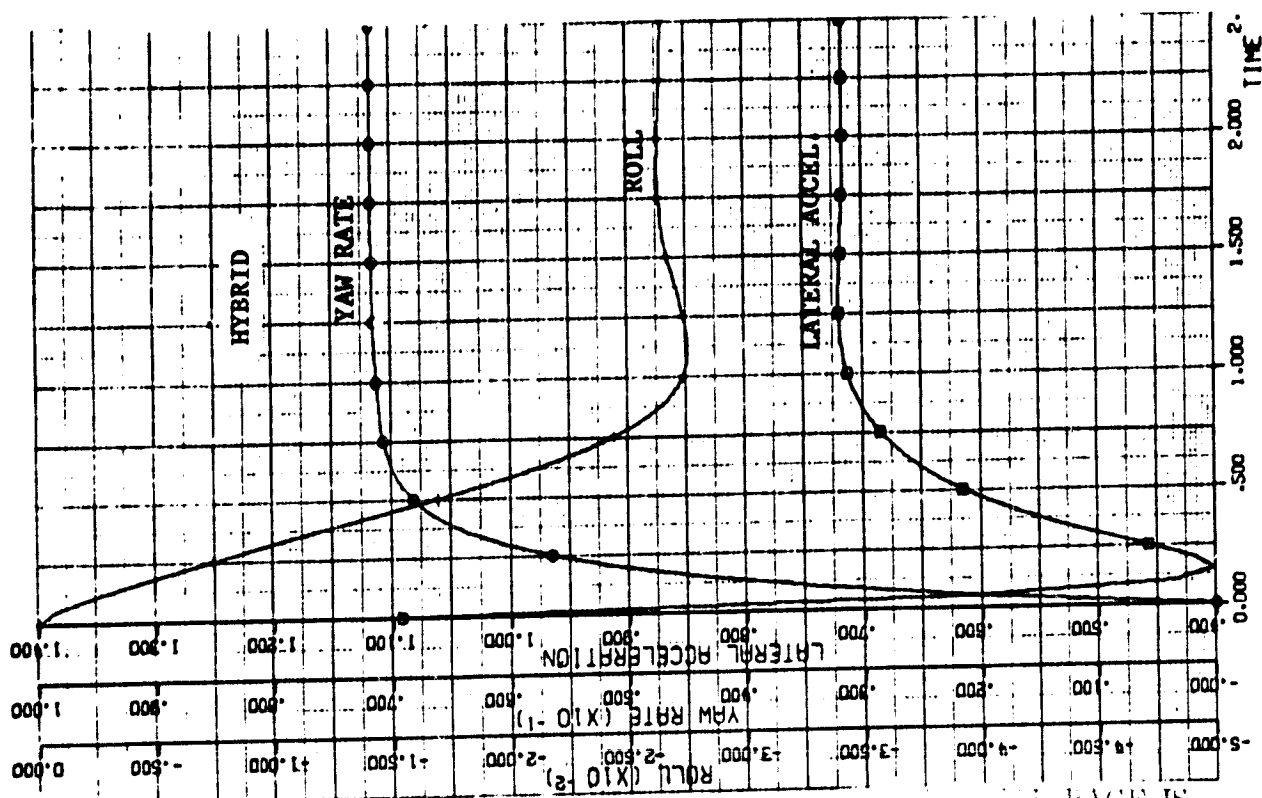


Figure 4-60 Steady State Yaw Response



THIS PAGE IS  
OF POOR QUALITY

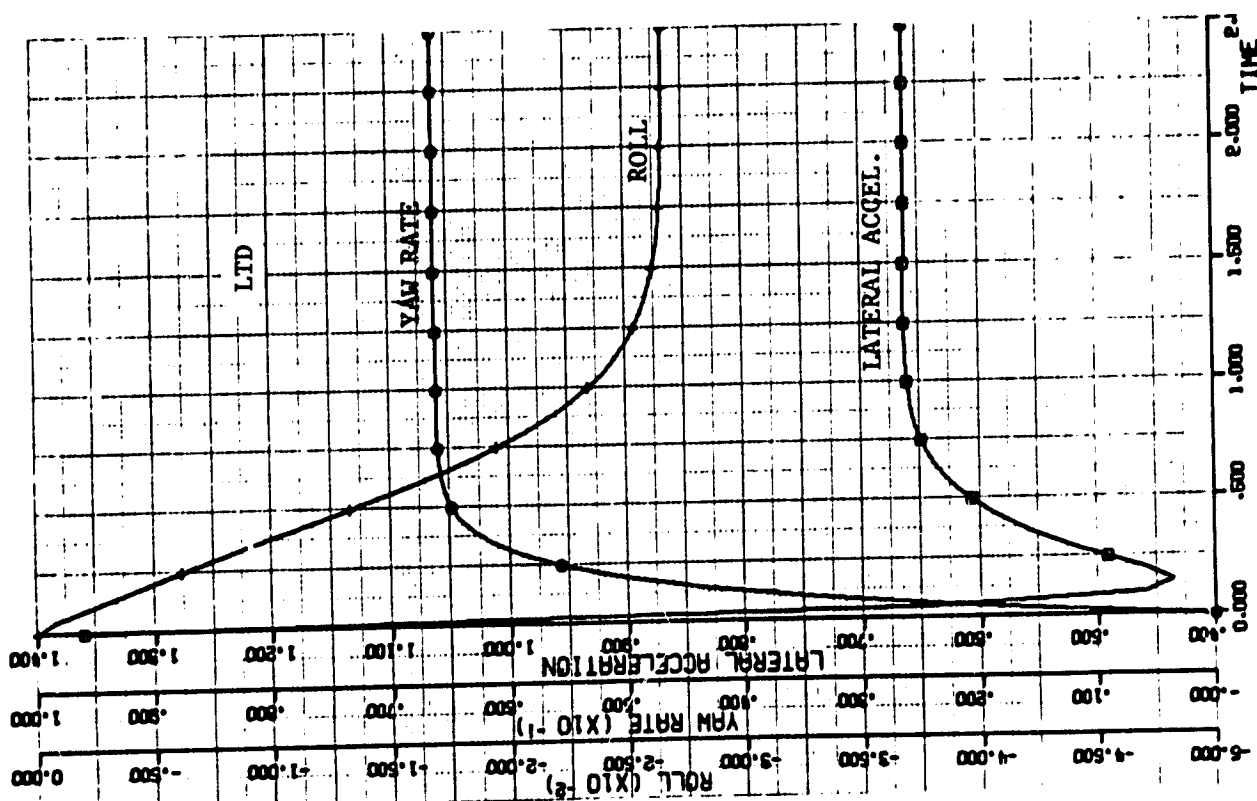
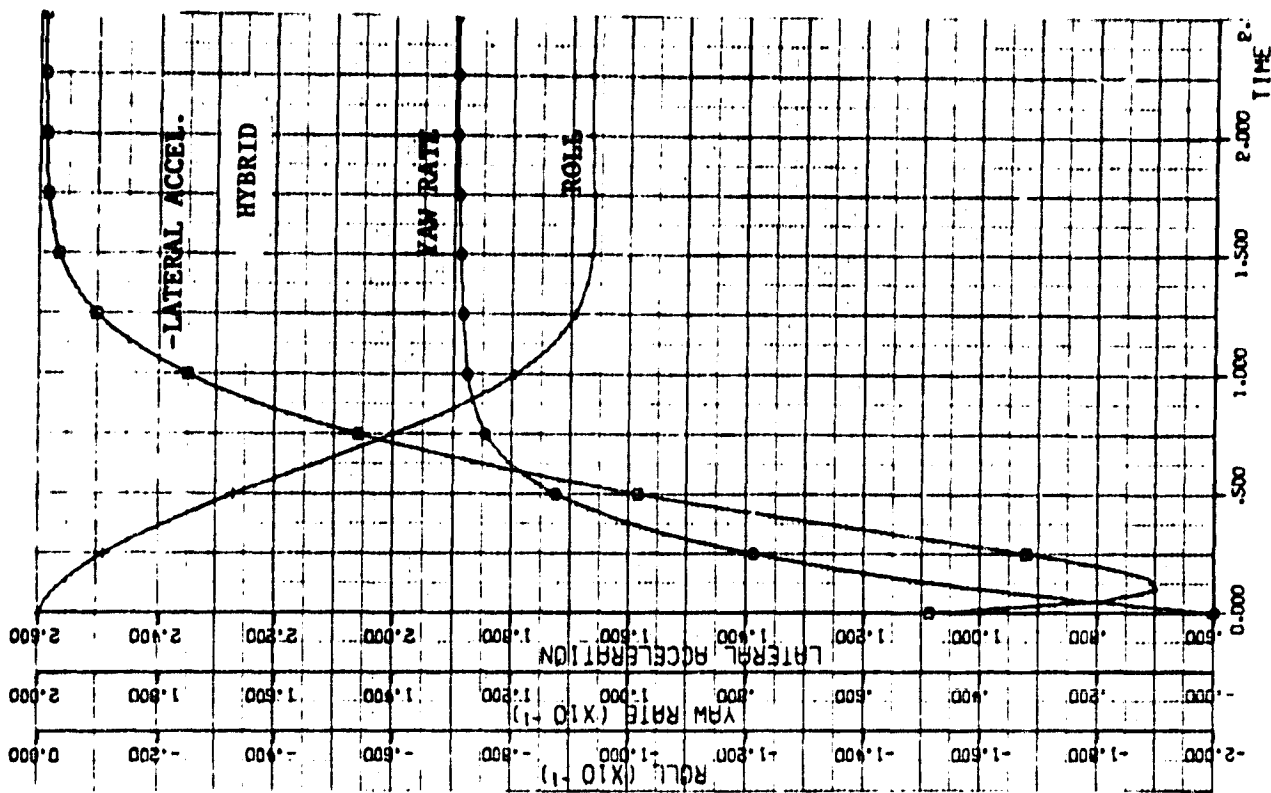


Figure 4-61 Transient Response at 10 m/sec



ORIGINAL PAGE IS  
OF POOR QUALITY

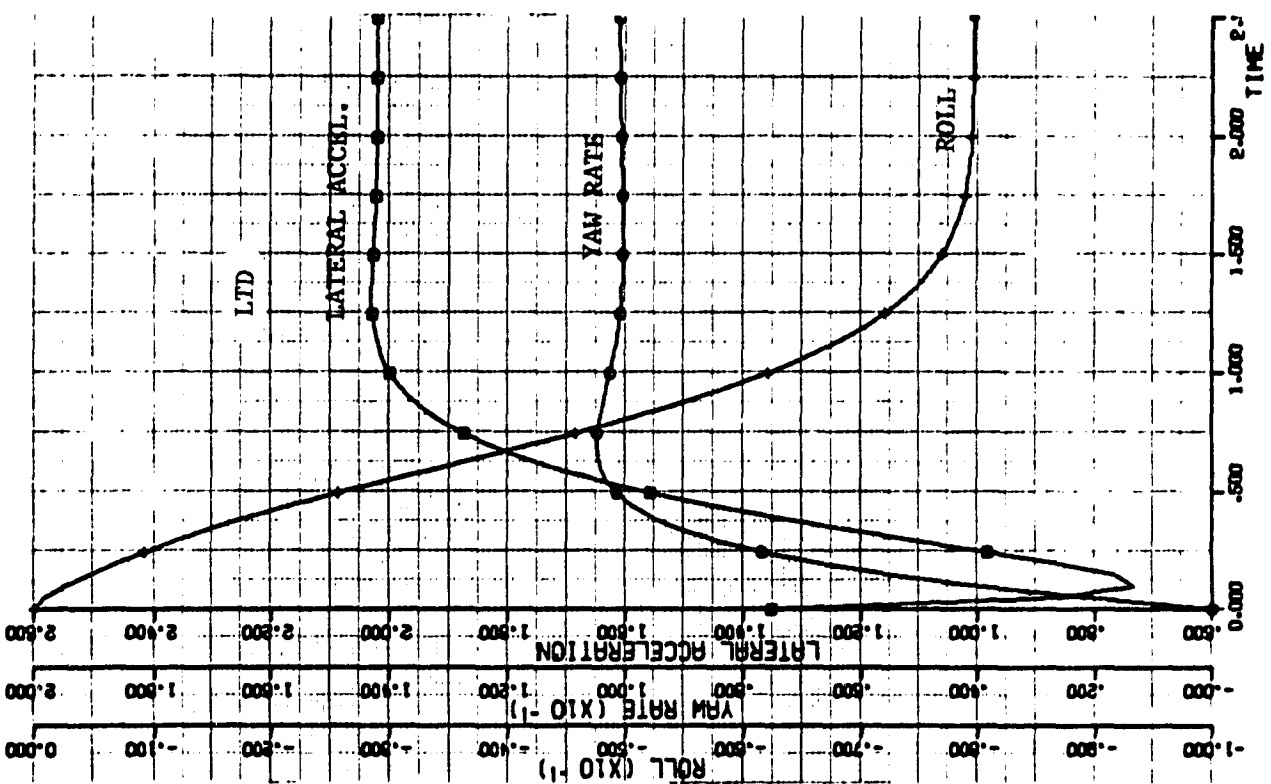
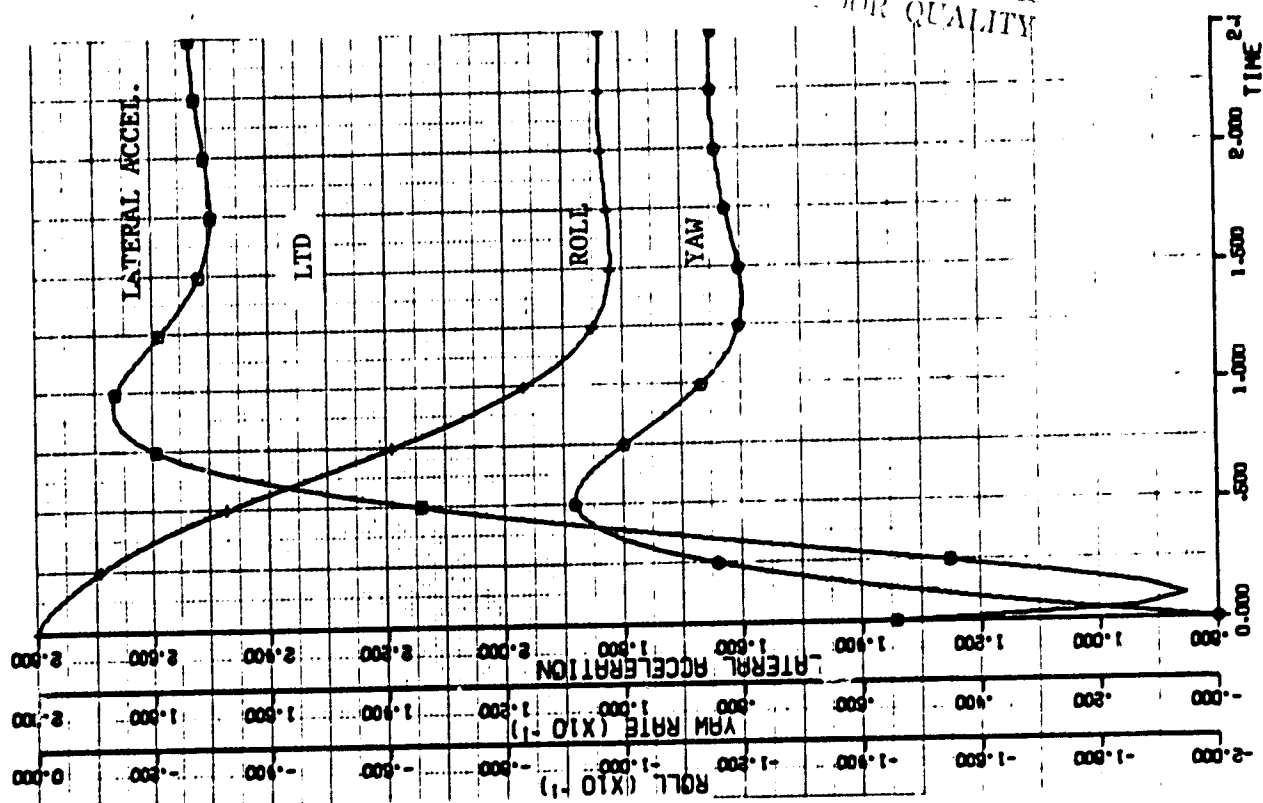
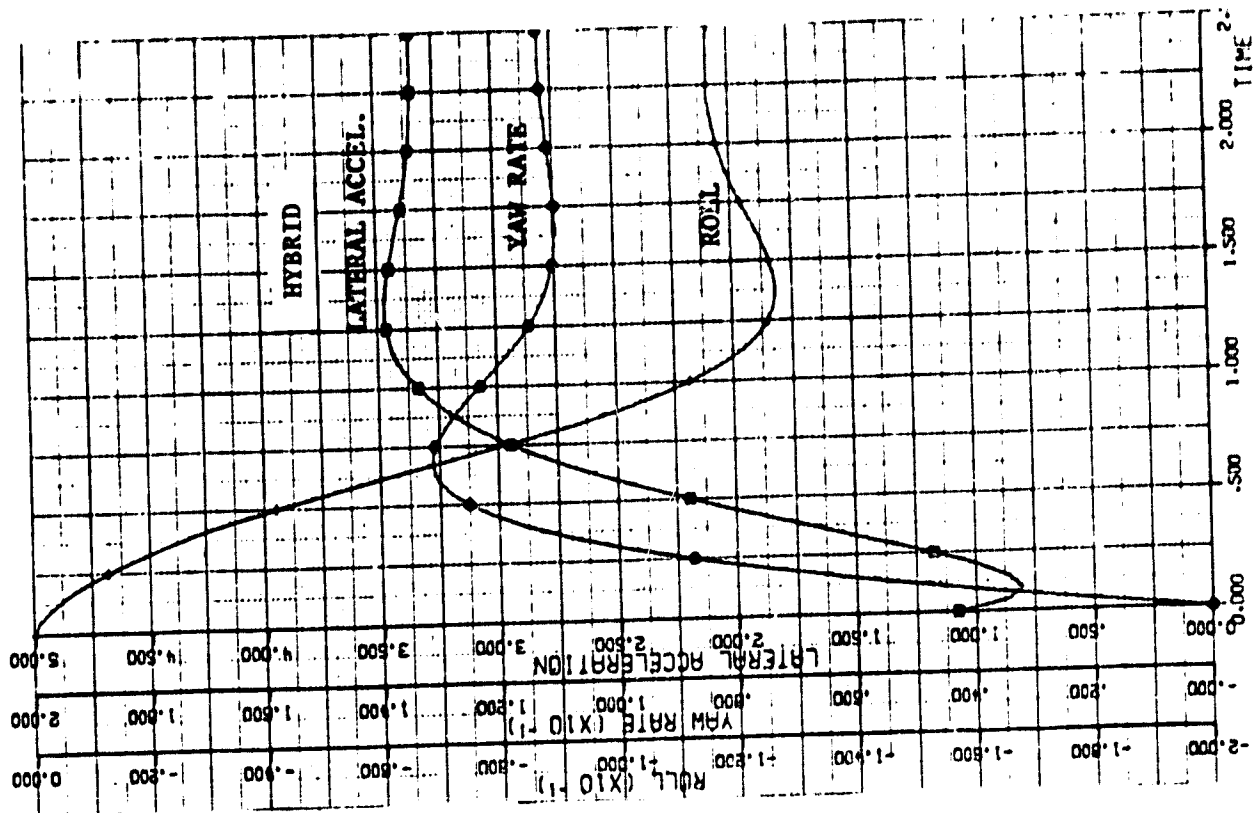


Figure 4-62 Transient Response at 20 m/sec



ORIGINAL PAGE IS  
OF POOR QUALITY

Figure 4-63 Transient Response at 30 m/sec

#### 4.4.5 Crashworthiness

After constructing a model of the existing LTD and adjusting it so that the CRASH program gave a realistic crush value of about .5 m in a 48 kph barrier impact, the same model, with appropriate adjustments to the component masses and addition of the batteries and support structure, was run for the hybrid. The results indicated an increase in front end crush of about .013 m (.5 in.). In short, there should be no problem in meeting barrier crash requirements of 48 kph, and even somewhat beyond with the hybrid. The key factors here were the modest weight increase of the hybrid over the current LTD (only 156 kg with the nickel-iron battery pack), combined with the retention of the present LTD steel frame for the hybrid. This frame provides on the order of 90% of the total energy absorption in a barrier crash. The plotter output of the CRASH program is shown in Figure 4-64 for the hybrid vehicle.

#### 4.4.6 Weight Breakdown

An estimate of the NTHV weight has been prepared based on a careful analysis of the changes being made to the Ford LTD. Accurate weights on key components were obtained by actually weighing components such as the heat engines and electric motor. Other weights were obtained by analysis and prior design experience (charger, controller, microprocessor). Battery weights were provided by their developers.

With a solid basis for determining the weight of selected Ford LTD, VW Rabbit, and Electric by SCT weights, we are confident that the NTHV weight is achievable. If anything, changes that Ford would make to the baseline vehicle that would be used to build the

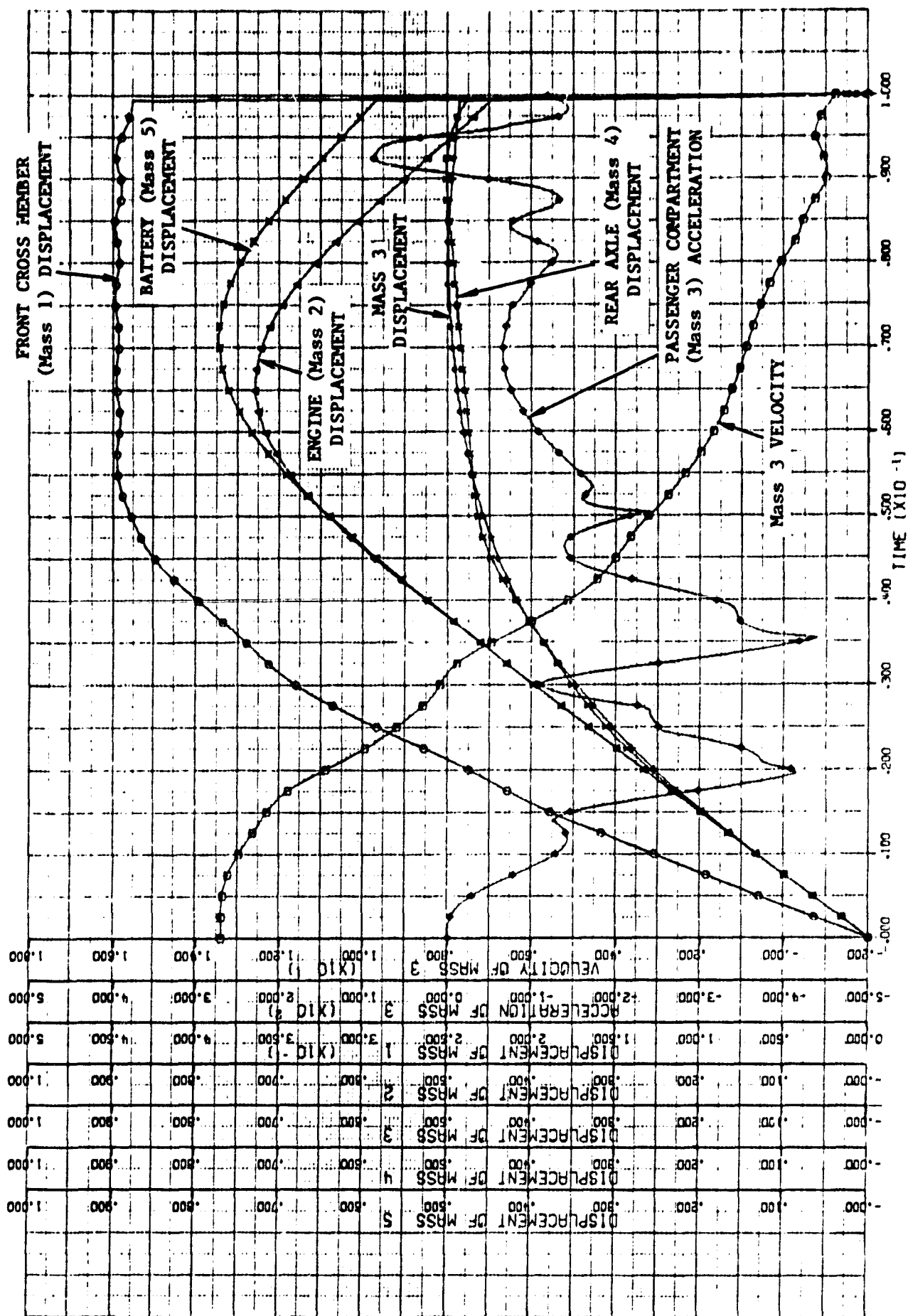


Figure 4-64 Projected Hybrid Crash Response

ITV vehicles would reduce our current estimate. The weight reductions discussed in Section 4.3 are considered in the weight shown for the NTHV.

A table summarizing the weight of the NTHV (1864 kg) vs. the weight of the Ford LTD (1708 kg) is shown in Table 4-10 .

Table 4-10 . ESTIMATED WEIGHT SUMMARY

<u>Item</u>	<u>Mass (kg)</u>	<u>Items Retained from LTD</u>	<u>Mass (kg)</u>
Fuel storage	74.0	Transmission	84.6
Coolant system	18.2	Drive shaft	10.0
Exhaust system	21.2	Brakes (4)	61.8
Engine	220.0	Brake hydraulics	15.1
Transmission	84.6	Steering system	28.8
Drive shaft	10.0	Air conditioner	36.3
Rear axle	52.6	Battery	<u>11.8</u>
Suspension (4)	75.8		248.4
Brakes (4)	61.8	<u>Item Replaced or Added</u>	
Brake hydraulics	15.1	Transfer case	29.5
Steering system	28.8	Batteries	270.0
Catalytic converter	12.7	Motor controls	30.0
Emission control	16.7	Charger	9.07
Tires and wheels (4)	98.0	Microprocessor	2.3
Tire & wheel (spare)	17.6	Engine	118.5
Air conditioner	36.3	Coolant system	9.18
Battery	11.8	Tire & wheel (spare)	18.5
Body	789.0	Exhaust system	18.8
Seats (2)	<u>64.0</u>	Rear axle	48.1
		Suspension (4)	67.8
TOTAL VEHICLE	<u>1708.0</u>	Seats (2)	45.9
		Body	737.6
		Motor	87.0
		Fuel storage	38.3
		Tires & wheels (4)	<u>84.8</u>
		TOTAL VEHICLE	<u>1864.0</u>



#### 4.5 Drawing Package

A drawing package (Appendix C2) is enclosed with this report.

A summary description of the contents of this package follows:

##### Drawing No.

HV80010 - 2 sheets full size

Propulsion system layout, showing reference to Ford LTD body lines and chassis and suspension. Complete cooling system and accessory mounting and drive with all interface and propulsion mounting and clearances.

HV80011 - 2 sheets full size

Propulsion system assembly, reference drawing showing relationship of heat motor and electric with mechanical interface and mounting.

HV80012 - 1 sheet full size

Battery pack layout, references nickel-iron and lead-acid in package determined best in tradeoff studies and subsequent development work. Shown in side elevation with rear view and sections thru critical areas. Details blower and ventilation, sealing, battery restraint and cable routing. Interfaces with Ford master body layout of body structure, chassis, and suspension.

HV80013 - 1 sheet full size

Clutch and transfer assembly drawing, details drive from heat engine clutch into transfer case.

HV1000 - 2 sheets full size

Sheet 1: Design stack up, details drive from heat engine crank through clutch and chain drive to rear face of output shaft.

Sheet 2: Design stack up, from output shaft of electric motor through universal joints and drive shaft to and including transfer case with shaft and chain drive.

HV1001 - 1 sheet full size

Shaft - input drawing, detail part showing input shaft.

HV1002 - 1 sheet full size

Shaft - output drawing, detail part showing output shaft.

HV1003 - 1 sheet full size

Output shaft assembly drawing.

HV1004 - 1 sheet full size

Crankshaft machining, showing crankshaft modification for snout of input shaft indexing.

HV1005 - 1 sheet full size

Adaptor plate, for mounting heat engine to clutch housing.

HV1006 - 1 sheet full size

Flywheel assembly drawing, showing modification to existing flywheel.

HV1007 - 1 sheet full size

Sprocket - chain drive, detail drawing showing sprocket for output shaft at heat engine.

HV1008 - 1 sheet full size

Sprocket - chain drive, detail drawing showing sprocket for chain drive from electric motor.

HV1009 - 1 sheet full size

End yoke - electric motor, detail drawing showing modifications to Dana Spicer end yoke 2-4-2003 for drive shaft at electric motor.

HV1010 - 1 sheet full size

End yoke - transfer case details modifications to Dana Spicer  
end yoke #2-4-783 for drive shaft at transfer case.

HV1011 - 1 sheet full size

Shaft output, detail drawing of output shaft for chain sprocket  
in transfer case at electric motor.

HV1012 - 1 sheet 2X actual size

Key detail, drive for electric motor drive.

## 5. REFERENCES

1. "Design Tradeoff Studies and Sensitivity Analysis Report," Appendix B (Task 2 Report for Phase I of the Near Term Hybrid Vehicle Program), JPL Contract No. 955189, South Coast Technology, May, 1979.
2. "Mission Analysis and Performance Specification Studies Report," Appendix A (Task 1 Report for Phase I of the Near Term Hybrid Vehicle Program), JPL Contract No. 955189, South Coast Technology, January, 1979.